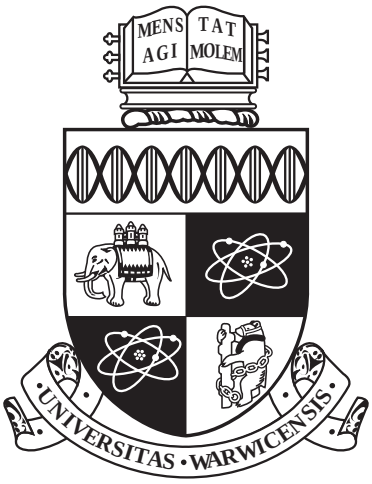

Rational Maps with Clustering and the Mating of Polynomials

by

Thomas Joseph Sharland

Thesis

Submitted to The University of Warwick

for the degree of

Doctor of Philosophy

Mathematics

December 2010

THE UNIVERSITY OF
WARWICK

Contents

List of Figures

Acknowledgments

First of all I would like to thank my parents, Cheryl Sharland and Andrew Sharland, for all the support they have shown me and for always lending a sympathetic ear whenever I need it. I am very grateful for the many sacrifices they have both made in order for me to have the opportunity to study for a PhD.

I would also like to thank my supervisor, Dr Adam Epstein whose patience and guidance has been extremely helpful during the course of this research. His willingness to discuss not just complex dynamics but also many other area of mathematics, as well as provide encouragement throughout the course of my research has been invaluable. I would also like to thank my examiners, Professor Anthony Manning and Professor Mary Rees, for agreeing to read the thesis and for providing a number of useful corrections and suggestions for improving the final document.

Furthermore I would like to thank all the people in the Mathematics Institute at the University of Warwick that have helped me in any way, whether by useful discussions on the mathematics or by aiding my sanity by providing welcome and interesting conversation when my mind required rest. In particular I would like to thank Professor Anthony Manning who provided a number of useful discussions and in particular pointed me towards the power of symbolic dynamics in describing quadratic polynomials. I would like to thank James for his good humour and many enjoyable conversations. Finally, a special mention to Ayşe'm for her love and support.

This research was funded by a grant from the Engineering and Physical Sciences Research Council.

Declarations

I declare that this thesis and the work presented in it are my own and represent my own original research. Wherever contributions of others are included, I have endeavoured to ensure that this is stated clearly and attributed with explicit references. No part of this thesis has been submitted for a degree or any other qualification at Warwick University or any other institution.

Abstract

The main focus of this thesis is the study of a special class of bicritical rational maps of the Riemann sphere. This special property will be called clustering; which informally is when a subcollection of the immediate basins of the two (super-)attracting periodic orbits meet at a periodic point p, and so the basins of the attracting periodic orbits are clustered around the points on the orbit of p. Restricting ourselves to the cases where p is fixed or of period 2, we investigate the structure of such maps combinatorially; in particular showing a very simple collection of *combinatorial data* is enough to define a rational map uniquely in the sense of Thurston. We also use the language of symbolic dynamics to investigate pairs (f, g) of polynomials such that $f \perp\!\!\!\perp g$ has a fixed or period two cluster point. We find that that the internal addresses of such maps follow very definite patterns which can be shown to hold in general.

Chapter 1

Introduction

1.1 Overview

Complex dynamics emergence as a popular subject for mathematical research came about as a result of the rediscovery of the early 20th Century works of Fatou [Fat19, Fat20] and Julia [Jul18]. After a comparably quiet period, the subject was given a new life in the 1980s. Perhaps the most notable contributions were supplied by A. Douady and J. Hubbard, whose "Orsay lecture notes" [DH84, DH85] provide a number of enlightening and amazing results about the behaviour of such systems. A lot of the work has been motivated by the many pictures of the various objects found in this topic, not least the Mandelbrot set.

The focus of this thesis is the study of rational maps which have a cluster cycle. Clustering is a property found in some bicritical rational maps - that is, rational maps with precisely two critical points. We define clustering informally below and more formally in Chapter 3. One way of constructing maps with this property is by mating together monic unicritical polynomials (polynomials with only one finite critical point) of the form $z^d + c$. We outline the general structure of the thesis, and emphasise some of the main results found during the research. We will use some terms and notions which are defined more formally in the main body of the thesis, but we will endeavour to outline these notions in this overview.

The first chapter contains standard results and definitions from complex dynamics. Many of the results are stated without proof, since they are general folklore, or references are provided. A lot of the notation and terminology that will be used in the thesis is introduced here. One particular feature of this chapter is the discussion of external rays. External rays are an important tool in the construction of matings of polynomials (see Chapter 2), and we discuss in this section some of

the properties we require for the definition of a mating (as defined in the thesis) to make sense. We also introduce some notions from symbolic dynamics - for example, the internal address - since we will be making use of this theory throughout the thesis.

Let Ω_F be the set of critical points of a map. Recall that a map is postcritically finite if the set

$$P_F := \bigcup_{n>0} F^{\circ n}(\Omega_F)$$

is a finite set. P_F is called the postcritical set of the map F. In Chapter 2, we focus on the study of postcritically finite branched self-coverings of a topological sphere. A map $f\colon X \to Y$ is called a branched covering if there exists a finite set $Z \subset Y$ such that the restricted map $f\colon X \setminus f^{-1}(Z) \to Y \setminus Z$ is a covering map. The branched coverings in this chapter will, in the main, be constructed by "mating" two degree d (the degree of a branched covering is the number of pre-images - including multiplicity - of each point in the image) monic polynomials f_1 and f_2. There are actually a number of different definitions of mating, and we endeavour in Chapter 2 to outline the differences and connections between them. We also discuss some properties of matings that will be useful in later chapters.

One of the most important results in the theory of branched coverings is the notion of *Thurston equivalence*. It gives a condition for checking whether or not two branched coverings are, in some sense, the same. Furthermore, *Thurston's Theorem* realises the full power of this equivalence, by showing that each equivalence class contains only one rational map, up to Möbius transformation. We will find two uses of the theorem in the thesis. Firstly, it will allows us to discuss, in general, when a branched self-covering of the sphere constructed by a mating is equivalent to a rational map. Secondly, we will use it in the chapters on clustering to discuss the equivalence of rational maps which have clusters of the same period; more on this later.

Suppose F is a type D rational map, that is, the two critical orbits belong to (super)attracting orbits with the same period. We will define a cluster point to be a point in $J(F)$ which is the endpoint of the angle 0 internal rays of at least one critical orbit Fatou component from each of the two critical cycles, see Figure 1.1. We split the theory of clustering into three separate chapters, though one of these, Chapter 3 is quite short and contains only the results which are applicable to clusters of arbitrary period. However, this chapter will contain results which apply for all periods. In particular, it focuses on the actual structure of a cluster: how the Fatou components are arranged around the cluster point. We also outline in this

chapter the notion of *combinatorial data* of a cluster, which will be made up of a pair (ρ, δ), where ρ is the combinatorial rotation number and δ will be called the critical displacement.

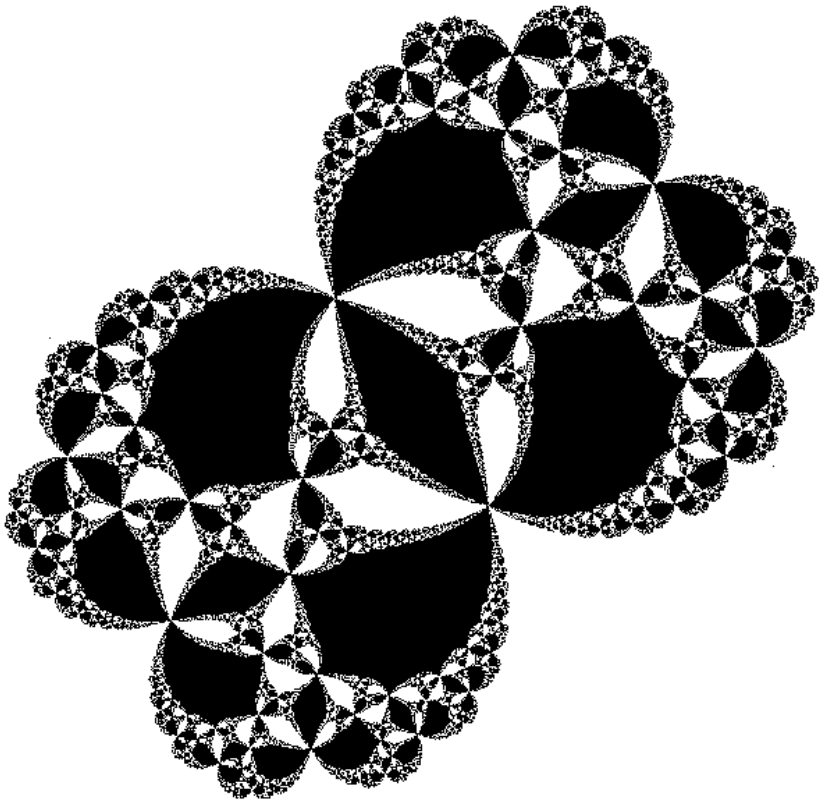

Figure 1.1: An example of a map with a cluster point.

We then consider the case when the cluster is fixed (Chapter 4). Some of the content of this chapter is perhaps already known by those who have studied matings in some detail. However, many of the techniques in this chapter will be useful when considering the period two cluster case, and it is often easier to understand the methods when applied to the simpler, fixed cluster case. Furthermore, it has been found that comparisons with the two cluster case draw up some interesting contrasts, and so it was felt necessary to include this case to aid the discussion in the following chapter. We investigate which combinatorial data are actually obtained by rational maps. The main theorem in this chapter is Theorem 4.3.5. We show that the combinatorial data of a fixed cluster is enough to classify a degree d rational map in the sense of Thurston.

The other focus of this chapter is on the properties of polynomials f_1 and f_2, such that the mating $F \cong f_1 \amalg f_2$ has a fixed cluster cycle. We will show that we able to be quite specific about one of the maps: precisely one of them has to be an n-rabbit; that is, a map which belongs to a hyperbolic component that bifurcates off of the unique period one component in parameter space. This is unsurprising; when one looks at the Julia set of a map with a fixed cluster cycle, one can often "see" the Julia set of an n-rabbit inside it. For example, one notices the shape of the rabbit polynomial in Figure 1.1. The properties of the "complementary" map - the f_i which is not an n-rabbit - are a little more difficult to study. However, we are still able to carry out a classification to some extent. To do this, we take advantage of the fact that the combinatorial rotation number of the α-fixed point of the n-rabbit in the mating will force an ordering of the angles of the rays landing at the root point of the critical orbit Fatou components of the complementary map. We then show that the maps that have the "correct" angular ordering are precisely those that create a rational map with a fixed cluster point when mated with an n-rabbit. Combined with the result on Thurston equivalence, we get the following theorem.

Theorem 4.0.3. *Suppose that F is a bicritical rational map with a fixed cluster point and the combinatorial rotation number is p/n. Then F is the mating of an n-rabbit with angled internal address $1_{p/n} \to n$ and another map h. In the degree 2 case, h has an associated angle with angular rotation number $(n-p)/n$.*

Finally the case where the cluster is of period 2 is discussed in Chapter 5. This case, unsurprisingly, is more complicated than when the cluster is fixed, and a number of the results found were perhaps *a priori* unexpected after one has considered only the fixed cluster case. In this chapter we will compare and contrast the two cases. In Appendix F we will also discuss some examples with clusters of higher period, showing why an increase in period beyond two creates a number of complications that makes studying this phenomenon much more involved. Again, the main theorem of this chapter (Theorem 5.3.2) shows that the combinatorial data is once again enough to classify the rational map in the sense of Thurston, at least in the quadratic case. We also discuss the difficulties of extending this result to the general case for degree d bicritical maps with a period two cluster cycle.

As with the previous chapter, we also investigate the properties of f_1 and f_2 under the assumption that $F \cong f_1 \amalg f_2$ is a rational map with a period two cluster cycle. In this case we restrict ourselves to the quadratic case. It is simple to show that precisely one of the maps must belong to the $(1/3, 2/3)$-limb of the

Mandelbrot set. The results in the one cluster case may lead us to conjecture that the map belonging to the $(1/3, 2/3)$-limb would have to be a map belonging to a hyperbolic component which bifurcates off of the period two component of the Mandelbrot set. However, in the two cluster case, we are no longer able to make out the shape of these "double rabbits" (maps which belong to hyperbolic components which bifurcate off of the period two component of the Mandelbrot set) in the Julia sets of these maps (see Figure 1.2). Indeed, we will show it is no longer true that one of the maps has to belong to a bifurcation component. There is a secondary component of period $2n$, which belongs to the limb of the Mandelbrot set beyond these bifurcation components of $2n$. It turns out that, in certain cases, this secondary map can be mated with another polynomial to create a map with a period two cluster cycle.

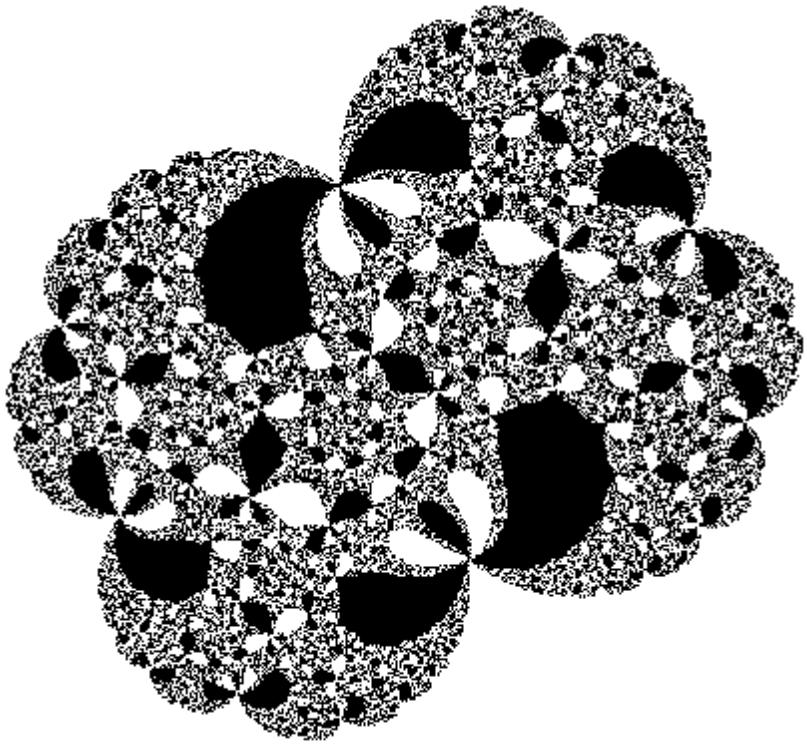

Figure 1.2: An example of a map with a period 2 cluster cycle.

This increase in complexity outlined above means there is now much more to investigate with regards to the matings. Firstly, assuming that one of the maps

is a double rabbit, we can ask what we can say about the properties of the map h if we know that h mates with a double rabbit to form a rational map with a period two cluster cycle. A similar technique as that used in the fixed cluster case again yields a necessary condition on the complementary maps. Furthermore, we can ask what conditions are needed on the complementary map h in order for this secondary map to be able to create a rational map with a period two cluster cycle when mated with h? Again, we discuss this problem combinatorially, and see that there is a very simple restriction on the combinatorial data of the rational maps constructed in this way.

The other aspect of this thesis is the study of progressions of internal addresses and Hubbard trees. For example, in the fixed cluster case, we know from the work of Chapter 4 that one of the maps is an n-rabbit. Therefore, most of the study into the properties of the maps in the matings that create maps with fixed cluster cycles is into the properties of the complementary map. In the appendices, we have given the internal addresses of these complementary maps for given combinatorial data. It turns out that there are a number of progressions which seem to follow some sort of set pattern. We prove these progressions - in simple cases - hold for arbitrarily large periods. The author is confident that more patterns in the progressions could be found in more complicated cases.

As well as cataloguing these complementary maps, the appendices also include the Hubbard trees of the complementary maps in cases of low degree. Though not necessarily vital to the exposition, these trees give the raw data that was used in the formulation of a number of the results and again, in some cases, the reader will see that in some sense there are patterns followed by the Hubbard trees as the period increases, at least in simple cases. Finally, we include an appendix discussing the increased complexity found as the period of the clusters goes from two to three, and towards even higher periods. There is very little formal discussion in this final appendix, but conjectures are made as to what the author expects to happen for higher periods.

A standard reference for complex analysis may be useful. For this purpose, the author heartily recommends either [Ahl78] or [Con78].

1.2 Preliminaries

In what follows, we will use the standard notation $\mathbb{C} = \{a + bi : a, b \in \mathbb{R}\}$. A lot of the time we will want to consider the one point compactification of $\mathbb{C}$ by adding a point at infinity. We call $\mathbb{C} \cup \{\infty\}$, given an appropriate analytic structure, the

Riemann sphere and denote it by $\overline{\mathbb{C}}$. When we wish to use the complex numbers with the circle of directions at infinity, we will write $\widehat{\mathbb{C}} = \mathbb{C} \cup \{\infty \cdot e^{2\pi i s} : s \in \mathbb{R}\}$; this space is homeomorphic to the closed unit disk.

1.2.1 Notation and terminology

If, for some $n \geq 1$ and $w \in \overline{\mathbb{C}}$ we have $f^{\circ n}(w) = w$, then we say w is a *periodic* point. If, furthermore, n is the smallest such integer satisfying this property, we say the period of w is n. If w has period 1 we call it a *fixed point* of f.

Now suppose w is a periodic point of period n. Then the *multiplier*, μ, of f at w is defined to be

$$\mu = (f^{\circ n})'(w) = \prod_{k=0}^{n-1} f'(f^{\circ k}(w)).$$

We can now classify periodic points according to the modulus of their multipliers.

Definition 1.2.1 (Classification of periodic points)**.** A periodic point is called

- superattracting if $\mu = 0$.
- attracting if $|\mu| < 1$.
- rationally indifferent (or parabolic) if $\mu = e^{2\pi i\theta}$, $\theta \in \mathbb{Q}$.
- irrationally indifferent if $\mu = e^{2\pi i\theta}$, $\theta \in \mathbb{R} \setminus \mathbb{Q}$.
- repelling if $|\mu| > 1$.

It is reassuring to note that the definitions given above (using the multiplier to describe the behaviour of a periodic point) agree with the usual dynamical (or topological) definition of attracting. That is to say, a fixed point p is (topologically) attracting if there exists a neighbourhood U of p such that the iterates $f^{\circ n}$ are all defined in U and they converge to the constant map $z \mapsto p$. A similar equivalence holds for repelling points.

Given any point z, the *orbit* of z is defined as the set

$$\mathcal{O}(z_0) = \{z, f(z), \ldots, f^{\circ n}(z), \ldots\}.$$

Now, given an attracting cycle (we use the terms "cycle" and "periodic orbit" interchangeably) a natural question to ask is, which points are attracted to it? We define the *basin of attraction* of an attracting cycle $\mathcal{O}$ of period n to be the open set $\mathcal{A} = \{z : f^{\circ kn}(z) \to p \text{ for some } p \in \mathcal{O}\}$. The *immediate basin* (of attraction) is the connected component of $\mathcal{A}$ which contains a point p in the orbit $\mathcal{O}$.

Definition 1.2.2. Let $z \in \overline{\mathbb{C}}$. If in any neighbourhood of z, f is not a homeomorphism onto its image, then we say z is a critical point of f. In other words, z is a critical point precisely when the local degree of f at z is greater than 1.

Indeed, in a neighbourhood of a critical point, it is possible to conjugate the map to a dth power map $z \mapsto z^d$, and so a neighbourhood of the critical point maps in a d-to-1 way onto its image. Conversely, if z is not a critical point then there is a neighbourhood of z on which f is a homeomorphism.

Note that in the case where $f(z) = z^d + c$, 0 is the only finite critical point (∞ is a superattracting fixed point) and the critical value is c.

1.2.2 Fatou and Julia Theory

We now outline the basic definitions and results needed in the rest of this thesis. First of all we restate a standard definition from complex analysis. A good reference for background material required from complex analysis can be found in, for example [Ahl78] or [Con78]. We will generally avoid stating well-known results from complex analysis, except where we deem it relevant or if the statement is required for emphasis. In what follows, we assume that the function f is rational.

Definition 1.2.3 (Normal Family of Functions)**.** Let $U \subset \overline{\mathbb{C}}$. A family $\mathscr{F}$ of holomorphic functions $f : U \to \overline{\mathbb{C}}$ is normal in U if each sequence in $\mathscr{F}$ has a subsequence which converges to a holomorphic function $g : U \to \overline{\mathbb{C}}$.

Note that the function g does not have to be in $\mathscr{F}$. In some sense, normal families of functions are "well-behaved". Indeed, if we take $\mathscr{F} \subset \mathrm{Hol}(U, \overline{\mathbb{C}})$ then a family is normal precisely when it has compact closure in the function space $\mathrm{Hol}(U, \overline{\mathbb{C}})$.

Definition 1.2.4. Let $f \colon \overline{\mathbb{C}} \to \overline{\mathbb{C}}$ be a rational map on the Riemann sphere, of degree at least 2. Consider the family $\mathscr{F} := \{f^{\circ n} : n \in \mathbb{N}\}$. We now split the Riemann sphere into two disjoint sets. Let $z \in \overline{\mathbb{C}}$. If there exists a neighbourhood $U \ni z$ so that the family $\mathscr{F}$ is normal in U, then we say z belongs to the *Fatou set* of f, $F(f)$. If z does not belong to the Fatou set, then we say it belongs to the *Julia set* of f, which we denote by $J(f)$.

The connected components of $F(f)$ will be called Fatou components. Note in particular that attracting basins of attracting periodic orbits belong to the Fatou set, since all orbits in a small neighbourhood of the orbit converge to the orbit. A similar argument shows that repelling periodic points must belong to $J(f)$. The Fatou

components which contain points on the critical orbit will play an important role in the discussion of clustering, and these are given more attention in Definition 3.1.1. At certain points, especially when we are dealing with the dynamics of polynomials, it will be important to consider the set of points with bounded orbits. This set is called the *filled Julia set*, $K(f)$. Note that we have $\partial K(f) = J(f)$, and the components of $K(f) \setminus J(f)$ are the bounded Fatou components. Alternatively, we can define $K(f)$ as

$$K(f) \colon = \{z : f^{\circ n}(z) \nrightarrow \infty\}$$

The sets $F(f)$, $J(f)$ and $K(f)$ are all completely invariant under iteration of f.

Remark 1.2.5. The definition given above is the original one given by Fatou [Fat19, Fat20]. Gaston Julia gave a different but equivalent definition: the Julia set is the closure of the set of repelling periodic points [Jul18] . The proof of this equivalence can be found in [Mil06].

Remark 1.2.6. It can easily be seen that $F(f)$ is an open set in $\overline{\mathbb{C}}$. It therefore follows that $J(f)$ is a closed set. Indeed, under the assumption that f is a non-linear polynomial, $J(f)$ is a closed, compact set with no isolated points. Similarly, $K(f)$ is closed.

We find that the behaviour of the critical points of a map are very important in studying the general behaviour of the map.

Theorem 1.2.7 ([Mil06], Theorem 8.6)**.** *Suppose f is a rational map of degree $d \geq 2$. Then the immediate basin $\mathcal{A}_0$ of every attracting periodic orbit of f must contain a critical point.*

We have the following very important theorem. The (sharp) bound was found first by Shishikura [Shi87] and a refinement using a different method was given by Epstein [Eps99].

Theorem 1.2.8. *A rational map can have only a finite number of attracting or indifferent cycles. Indeed, if the degree of the rational map is $d > 1$, then the number of attracting or indifferent cycles is at most $2d - 2$.*

This theorem, in particular, gives us a bound on the number of attracting cycles that a polynomial can have. The bound is called the *Fatou-Shishikura inequality*. In the case of rational maps with precisely two critical points, which is the type we will be creating in Chapters 4 and 5, there can only be two attracting periodic orbits. Since we will be assuming further that both critical orbits will be periodic, this means the only attracting cycles will be the orbits of the critical points.

1.3 External rays

An important aspect of dynamical systems is the ability to conjugate the dynamics of two systems under a change of variable map. In this section, we will use a conjugacy between the dynamics of f on $\overline{\mathbb{C}} \setminus K(f)$ and the map $z \mapsto z^d$ on $\overline{\mathbb{C}} \setminus \overline{\mathbb{D}}$ to construct external rays. These rays are an important component in defining the notion of mating of polynomials in Chapter 2.

We begin with a theorem due to Böttcher [Böt04]. The statement below is as found in [Mil06], Theorem 9.1.

Theorem 1.3.1 (Böttcher's theorem)**.** *Let f be a holomorphic germ of the form*

$$f(z) = a_d z^d + a_{d+1} z^{d+1} \cdots$$

with $d \geq 2$ and $a_d \neq 0$. Then there is a holomorphic change of co-ordinates $w = \phi(z)$ with the properties that

- $\phi(0) = 0$,
- *ϕ conjugates f to the map $w \mapsto w^d$ in a neighbourhood of 0.*

The map ϕ is also unique up to multiplication by an $(d-1)$st root of unity. In particular, it is unique in the case where the local degree is 2.

Now suppose that we have a monic degree d ($d \geq 2$) polynomial $f \colon \overline{\mathbb{C}} \to \overline{\mathbb{C}}$, given by

$$f(z) = z^d + a_{d-1} z^{d-1} + \cdots + a_1 z + a_0.$$

By considering the local behaviour at infinity (by using the change of co-ordinates $z \mapsto 1/z$), we see that this map has a superattracting fixed point at infinity, and so we can apply Böttcher's theorem there.

The following appears as Theorem 9.5 in [Mil06].

Theorem 1.3.2. *Let f be a monic polynomial of degree $d \geq 2$. If the filled Julia set $K = K(f)$ contains all of the finite critical points of f, then both K and $J = \partial K$ are connected and the complement of K is conformally isomorphic to the exterior of the closed disk $\overline{\mathbb{D}}$ under an isomorphism*

$$\hat{\phi} \colon \mathbb{C} \setminus K \to \mathbb{C} \setminus \overline{\mathbb{D}},$$

which conjugates f on $\mathbb{C} \setminus K$ to the dth power map $w \mapsto w^d$. On the other hand, if at least one critical point of f belongs to $\mathbb{C} \setminus K$, then both K and J have uncountably

many connected components. Moreover, the map $\hat{\phi}$ is asymptotic to the identity at infinity.

From the function $\hat{\phi}$ defined above (which we relabel with ϕ) we get the *Green's function* for K, which is defined as

$$G(z) = \begin{cases} \log|\phi(z)|, & z \in \mathbb{C} \setminus K; \\ 0, & z \in K. \end{cases}$$

G is strictly positive and harmonic on $\mathbb{C} \setminus K$ and continuous everywhere. Trivially, it is asymptotic to $\log|\phi(z)|$ at infinity and since ϕ conjugates f to the map $w \mapsto w^d$, G satisfies the identity $G(f(z)) = dG(z)$.

Let $\rho > 0$. Then the pre-image $G^{-1}(\rho) = \{z \in \mathbb{C} : G(z) = \rho\}$ is a closed curve which we call the *equipotential curve* of order ρ (Figure 1.3). Perhaps of more importance than these equipotential curves (at least in terms of our applications) are their orthogonal trajectories, known as *external rays*.

Definition 1.3.3. The *external ray of angle θ* for a map f, R_θ^f, is defined as

$$R_\theta^f := \{z \in \mathbb{C} : \arg(\phi(z)) = 2\pi\theta\}$$

where ϕ is the Böttcher co-ordinate at ∞ from Theorem 1.3.1.

We will sometimes omit the function f from the notation if it is arbitrary or clear in the context.

It should be noted that the external rays are the pre-images of points of the form $re^{2\pi i\theta}$ for $r > 1$. A sensible question is therefore to ask: when does $\lim_{r \searrow 1} \phi^{-1}(re^{2\pi i\theta})$ exist? In fact, the limit exists for all rational θ and when the Julia set is locally connected then it is known that this limit exists for all θ (see Proposition 1.3.7 below). It is clear from the definition that if $\lim_{r \searrow 1} \phi^{-1}(re^{2\pi i\theta}) = z$ then $z \in \partial K(f) = J(f)$; we say the external ray R_θ^f *lands* at z.

Theorem 1.3.4. *Assume that $K(f)$ is connected. Then every periodic external ray lands at a periodic point which is either repelling or parabolic. Conversely, every repelling or parabolic periodic point z_0 is the landing point of (at least) one external ray, which itself must be periodic, with period divisible by the period of z_0.*

In order to say more than the above, we need to introduce a further condition, that of local connectivity.

Definition 1.3.5. A Hausdorff topological space X is locally connected if every point $x \in X$ has arbitrarily small connected neighbourhoods.

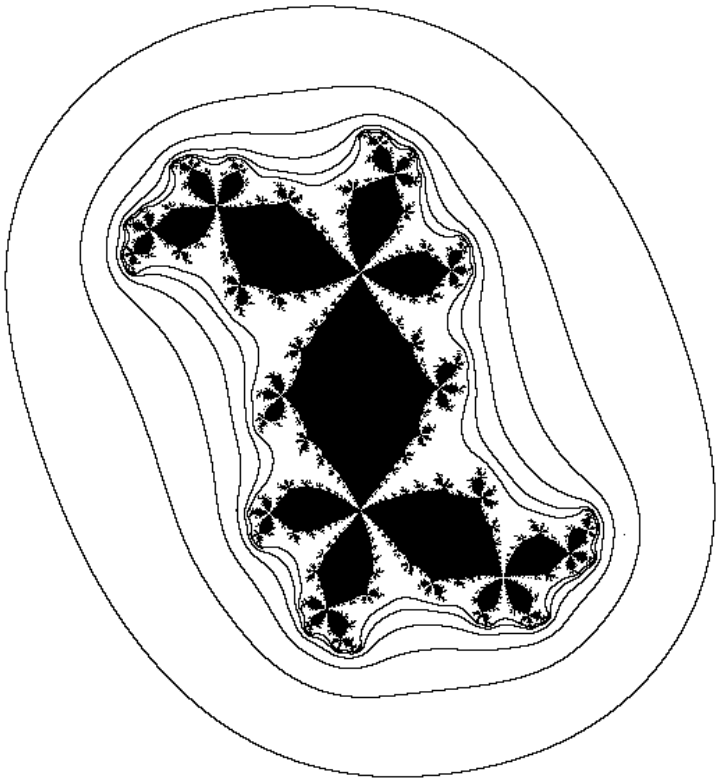

Figure 1.3: A "period 4 rabbit", or 4-rabbit, Julia set with some equipotential curves.

The following result was originally proved in [Car13], and is stated as found in [Pom92].

Theorem 1.3.6 (Carathéodory's theorem)**.** *Let f map $\mathbb{D}$ conformally onto the bounded domain G. Then the following three conditions are equivalent:*

1. *f has a continuous injective extension to $\overline{\mathbb{D}}$;*
2. *∂G is a Jordan curve;*
3. *∂G is locally connected and has no cut points.*

In our setting, local connectivity is what is required to ensure that all the rays will land.

Proposition 1.3.7. *Suppose f has a connected Julia set. Then the following are equivalent.*

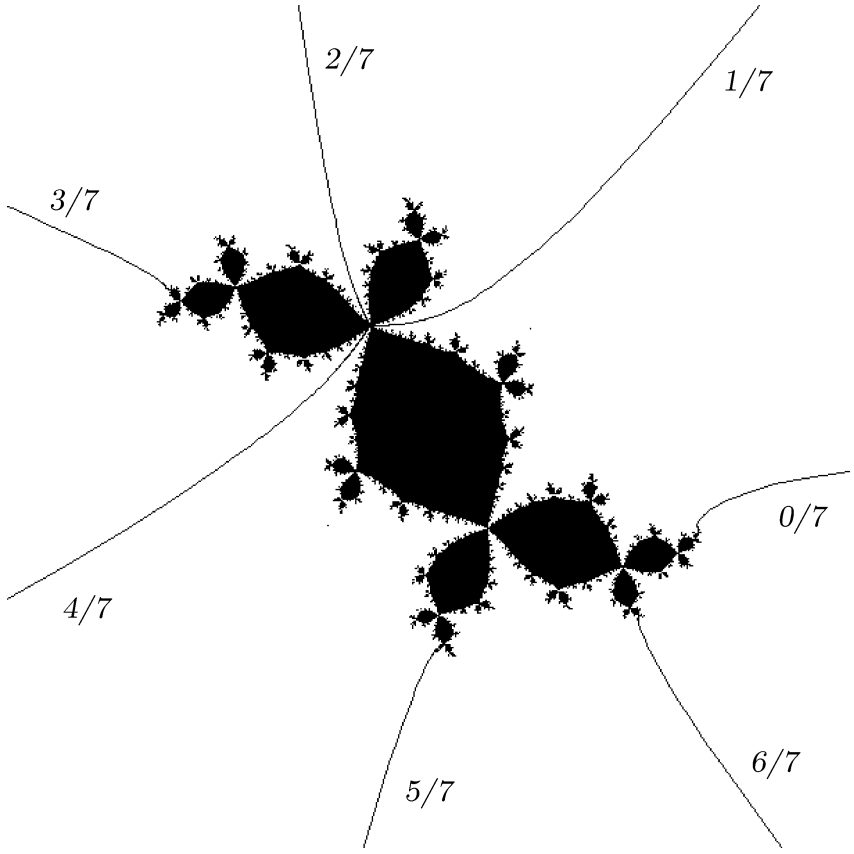

Figure 1.4: The Douady's rabbit Julia set ($z \mapsto z^2 + (-0.1225\ldots + 0.7448\ldots i)$ with external rays of the form $\theta = p/7$, $0 \leq p \leq 6$

1. *The Julia set, $J(f)$ is locally connected.*
2. *The filled Julia set $K(f)$ is locally connected.*
3. *For every θ, the external ray R_θ^f lands at a point (which we denote by $\gamma^f(\theta)$, or sometimes $\gamma(\theta)$ if f is clear in the context) on the Julia set. This point $\gamma^f(t)$ depends continuously on the angle θ.*
4. *Furthermore, the inverse Böttcher map ϕ^{-1} can be extended continuously over the boundary of $\partial\mathbb{D}$, and $\phi^{-1}(e^{2\pi i\theta}) = \gamma(\theta)$ for all θ.*

In this thesis, we will be assuming that the Julia set is connected, and so we can apply the above proposition. Suppose that the conditions in the above proposition are satisfied. Then the newly defined map $\gamma\colon \mathbb{R}/\mathbb{Z} \to J(f)$ is called the *Carathéodory semiconjugacy*. As the name suggests, it is a semiconjugacy. It maps

the circle $\mathbb{R}/\mathbb{Z}$ onto the Julia set $J(f)$ and satisfies

$$\gamma(d\theta) = f(\gamma(\theta)), \tag{1.1}$$

where d is the degree of the polynomial f. The following is well-known, for example see [Mil00b].

Proposition 1.3.8. *Suppose the external ray R^f_θ lands at $z \in J(f)$. Then $R^f_{d\theta}$ lands at $f(z)$. Furthermore, suppose that there are at least three rays $R^f_{\theta_1}, R^f_{\theta_2}, \ldots, R^f_{\theta_k}$ landing at some $z \neq 0$, then the cyclic ordering of the angles θ_j on the circle is the same as the cyclic ordering of the angles $d\theta_j$ on the circle.*

1.3.1 Properties of External Rays

The following two results tell us about the behaviour of external rays with respect to points in the Julia set. Again they can be found in [Mil00b], and are general folklore.

Proposition 1.3.9. *Assume $K(f)$ is connected. If a periodic ray lands at z_0, then only finitely many rays can land at z_0 and all rays landing at z_0 are periodic of the same period. In particular, if the period of each ray is p, the denominator of the angle of the rays is $2^p - 1$.*

In general, we will be dealing with hyperbolic polynomials, which means there are no parabolic cycles. In that case, the previous theorem says that all periodic rays land on repelling periodic points.

We now discuss some of the elementary properties of the external rays. First we take advantage of (1.1) to mark some special points on $J(f)$.

Definition 1.3.10. The point $\gamma(0)$, the landing point of the ray R_0 is a fixed point of f, called the β-fixed point of f, or β for short. In the case of quadratic polynomials, the other (finite) fixed point is called the α-fixed point. If $f_c(z) = z^d + c$, then the rays $R^f_{k/(d-1)}$ $(k = 0, 1, \ldots, d-2)$ land at fixed points. We will label the point $\gamma^f(k/(d-1))$ by β_k in this case. If there is another finite fixed point of the map f_c, then it will be called the α-fixed point.

For example, the α-fixed point for the Julia set in Figure 1.4 is the landing point of the external rays of angle 1/7, 2/7 and 4/7. The β-fixed point is the landing point of the ray of angle $0 = 0/7$.

A rational map of degree d has at most $d + 1$ fixed points. Note that for polynomials on $\overline{\mathbb{C}}$, infinity is a superattracting fixed point and so along with the $d-1$

β_k fixed points and the α-fixed point, these make up all the possible fixed points for the polynomial f_c. We restrict our attention to degree 2 below, but similar results can be proved in the more general degree d case. Since our applications of these results will only be in the degree 2 case, it was deemed unnecessary to include the general result here.

Lemma 1.3.11. *Suppose the degree of f is 2. Then the pre-images of $\beta = \gamma(0)$ are itself and the point $\gamma(1/2)$.*

Proof. This is a simple application of equation (1.1). We see that $f(\gamma(1/2)) = \gamma(0)$ and $f(\gamma(0)) = \gamma(0)$. Since β has two pre-images (counting multiplicity), these are the only pre-images. □

1.4 The Mandelbrot Set

We now shift our attention to the parameter plane for degree 2 polynomials and discuss a very important set in the field of complex dynamics. Consider the family of maps given by $z \mapsto f_c(z) = z^2 + c$. The Mandelbrot set is defined as

$$\begin{aligned} \mathcal{M} &= \{c \in \mathbb{C} : f_c^{\circ n}(0) \text{ is bounded}\} \\ &= \{c \in \mathbb{C} : J(f_c) \text{ is connected}\}. \end{aligned}$$

The Mandelbrot set is connected, but it is an open problem (and a very famous one) as to whether it is locally connected. In the sequel we give a quick tour of the Mandelbrot set, laying out some terminology and describing some well known results which will be of use later on when we handle matings of quadratic polynomials of the form $z \mapsto z^2 + c$. There are degree d generalisations of the Mandelbrot set (known as Multibrot sets) which have similar properties to the Mandelbrot set.

It turns out that there is an analogue to external rays (which exist in the dynamical plane) in the parameter plane. We call these rays *parameter rays*. To do this, we simply note that we can map the complement of the Mandelbrot set onto the unit disk by using the Riemann Mapping Theorem (there is no dynamics in the parameter plane, and so no need to use Theorem 1.3.2). Furthermore, this Riemann map Φ can be chosen so that $\lim_{z\to\infty}(\Phi(z)/z) = 1$. Furthermore, if we denote the Böttcher map for the parameter $c \in \mathbb{C} \setminus \mathcal{M}$ by ϕ_c, it was shown by Douady and Hubbard that this uniformisation is given by $\Phi(c) = \phi_c(c)$. Hence there exists a Green's function for $\mathcal{M}$, and thus we can construct parameter rays in an analogous way to how we constructed the external rays for K. We use the notation $R_\theta^{\mathcal{M}}$ for

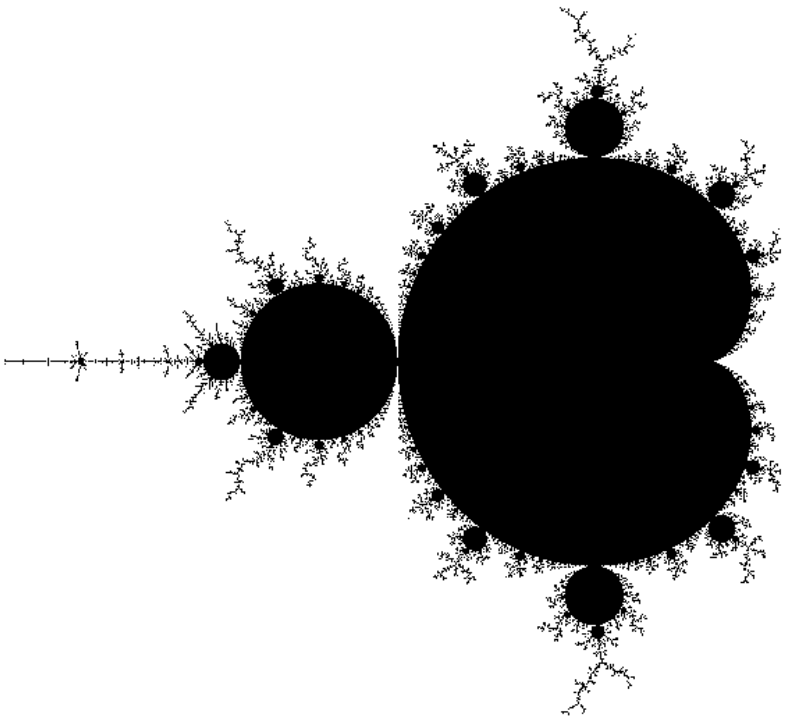

Figure 1.5: The Mandelbrot Set, $\mathcal{M}$

the parameter ray of angle θ. The landing points of these rays are also important, being the *root points* of the hyperbolic components of $\mathcal{M}$, as we will describe below.

1.4.1 Structure of the Mandelbrot Set

The Mandelbrot set is contained in the parameter plane for the polynomials $z \mapsto z^2 + c$. The interior of the Mandelbrot set contains an infinite number of connected components, and it turns out that these connected components have properties shared by all maps contained in them (by which we mean, given one of these connected components $\mathcal{H}$, each map $f_c\colon z \mapsto z^2 + c$ with $c \in \mathcal{H}$ has some properties shared by all the others). The most obvious of these connected components is the main cardioid, which contains all the parameters c for which $z \mapsto z^2 + c$ has an attracting fixed point. We will discuss these components in more detail in this section. A map will be called hyperbolic if the closure of its post-critical set is disjoint from the Julia set.

Definition 1.4.1. A period n (hyperbolic) component $\mathcal{H}$ of $\mathcal{M}$ is a connected component of the interior of $\mathcal{M}$, for which the set of parameters c are such that the map f_c has a period n attracting orbit.

The term hyperbolic is used since any parameter c belonging to some hyperbolic component $\mathcal{H}$ must have f_c is a hyperbolic map; that is, all critical orbits converge to an attracting cycle. There is a canonical way of parameterising these hyperbolic components using the multiplier of the map f_c for $c \in \mathcal{H}$.

Proposition 1.4.2. *Given a hyperbolic component $\mathcal{H}$, there exists a conformal isomorphism $\mu\colon \mathcal{H} \to \mathbb{D}$, and this can be extended to a homeomorphism on the closures. The value $\mu(c)$ is the multiplier of the attracting periodic orbit.*

We will call the point $c_0 = \mu(0) \in \mathcal{H}$ the *centre* of the hyperbolic component. We remark that c_0 is the unique parameter in the hyperbolic component such that the map f_{c_0} has a periodic superattracting cycle.

We will sometimes abuse notation and refer to a function f_c as belonging to a hyperbolic component. By this we mean that the associated parameter c is in the interior of $\mathcal{H}$. An important feature of the hyperbolic components of $\mathcal{M}$ is that the maps belonging to them are structurally stable.

Definition 1.4.3. Let f be the germ of a local homeomorphism such that $f(z_0) = z_0$. Suppose further that there is an invariant family of arcs $\Gamma = \{\gamma_1, \gamma_2, \ldots, \gamma_n\}$ (with labelling in terms of the cyclic ordering and γ_1 being chosen arbitrarily) such that each γ_i has z_0 as an endpoint. Then, since cyclic ordering of the rays is maintained by the homeomorphism, there exists an integer p such that $f(\gamma_i) \subset \gamma_{i+p \mod n}$. We then define the combinatorial rotation number at z_0 to be p/n.

We remark that this is well-defined, and that any system of arcs provides the same combinatorial rotation number. The following result is folklore.

Proposition 1.4.4. *Suppose $\Gamma_2 \subset \Gamma_1$ are two families of invariant arcs. Then the combinatorial rotation number defined for Γ_1 is the same as that defined for Γ_2.*

We can naturally use this definition to define the notion of combinatorial rotation number for periodic orbits under homeomorphisms, by considering the first return maps to each point. With this in mind, suppose that $z \in J(f)$ is a periodic point which is the landing point of at least one external ray. Then the set of external rays are invariant arcs which meet at a common endpoint, z, which is fixed under some iterate of the polynomial f. We see that we are in precisely the case where we can use Definition 1.4.3, and so this point will have a well defined combinatorial

rotation number. Furthermore, we notice that, since f will be (locally) a homeomorphism at f (since we are assuming that the critical points of the polynomial are contained in the Fatou set), the combinatorial rotation number is the same for each point in the orbit of z. Thus it makes sense to talk about the combinatorial rotation number of the orbit of z, $\mathcal{O}(z)$.

We now describe the components of the Mandelbrot set in a very natural way using parameter rays following the construction found in [Mil00b]. Fix $c \in \mathbb{C}$ and suppose that z_1 is a periodic point of f_c of period n, so that $\mathcal{O} = \mathcal{O}(z_1) = \{z_1, z_2, \ldots, z_n\}$. Suppose that one of the points of this orbit has a rational external ray $R_{p/q}$ landing on it. It can easily be shown that each point z_i in $\mathcal{O}$ has a finite, non-empty set of external rays landing on it. For each z_i, denote this set of angles by A_i. We then call the collection $\{A_1, \ldots, A_n\}$ the orbit portrait $\mathcal{P} = \mathcal{P}(\mathcal{O})$ of the orbit $\mathcal{O}$. Call the number of elements in each A_i the valence v of the portrait. In other words, the valence is the number of rays landing at each point on the orbit $\mathcal{O}$. If none of the z_i are critical points, then the same number of rays land at each z_i and so the valence is well defined.

If $v \geq 2$ then the v rays landing at an orbit point z_i must split the plane up into v disjoint open regions, which we will call sectors. The angular width of a sector bounded by $R^{f_c}_{\theta_1}$ and $R^{f_c}_{\theta_2}$ (with $\theta_2 > \theta_1$) will be defined as $\theta_2 - \theta_1$. The width of a sector in the parameter plane is defined similarly, by using the distance between the angles of the two parameter rays bounding it.

We state an important fact about parameter rays which land at a common point in $\mathcal{M}$. Informally, it says that if two rays $R^{\mathcal{M}}_{\theta_1}$ and $R^{\mathcal{M}}_{\theta_2}$ land together at a point in $\mathcal{M}$, then the external rays $R^{f_c}_{\theta_1}$ and $R^{f_c}_{\theta_2}$ land at a common point in $J(f_c)$ if and only if the rays $R^{\mathcal{M}}_{\theta_1}$ and $R^{\mathcal{M}}_{\theta_2}$ separate c from the origin (note we have no assumption that $J(f_c)$ be connected here, although in practice it will be). First we need a preliminary result to define the critical value sector.

Theorem 1.4.5 ([Mil00b], Theorem 1.1)**.** *Let $\mathcal{O}$ be an orbit of period $p \geq 1$ for f. If there are $v \geq 2$ external rays landing at each point of $\mathcal{O}$, then there is one and only one sector based at some point $z_1 \in \mathcal{O}$ which contains the critical value $c = f(0)$, and whose closure contains no point other than z_1 of the orbit $\mathcal{O}$. This critical value sector can be characterised, among all of the pv sectors based at the points of $\mathcal{O}$, as the unique sector of smallest angular width.*

Given $c_0 \in \mathbb{C}$, let f_{c_0} be a polynomial which has an orbit $\mathcal{O}$ with portrait $\mathcal{P}(\mathcal{O})$ having valence $v \geq 2$. Let $0 < \theta_- < \theta_+ < 1$ be the angles of the two dynamic rays $R^K_{\theta_\pm}$ which bound the critical value sector S_1 for f_{c_0}.

Theorem 1.4.6 (Theorem 1.2, [Mil00b]). *The two corresponding parameter rays $R^M_{\theta_\pm}$ land at a single point $r_\mathcal{P}$ in the parameter plane. These rays, together with their landing point $r_\mathcal{P}$, cut the plane into two open subsets $W_\mathcal{P}$ and $\mathbb{C} \setminus W_\mathcal{P}$ with the following property: a quadratic map f_c has a repelling orbit with portrait $\mathcal{P}$ if and only if $c \in W_\mathcal{P}$, and has a parabolic orbit with portrait $\mathcal{P}$ if and only if $c = r_\mathcal{P}$.*

Notice that each wake $W_\mathcal{P}$ has two associated angles θ_- and θ_+ which are the angles used to define it. We can thus change notation slightly and focus on the angles rather than the portrait by writing $W_\mathcal{P}$ as $W_{(\theta_-,\theta_+)}$ and calling it the (θ_-, θ_+)-wake (see Figure 1.6). $r_\mathcal{P} = r_{(\theta_-,\theta_+)}$ will be called the root point of the wake. If $r_{(\theta_-,\theta_+)}$ is on the boundary of a hyperbolic component $\mathcal{H}$ and $R^\mathcal{M}_{\theta_-}$ and $R^\mathcal{M}_{\theta_+}$ separate this component from the origin, we say that $r_{(\theta_-,\theta_+)}$ is the root point of $\mathcal{H}$. Hence we see that, for example in this notation, the two rays of angle $1/3$ and $2/3$ land at the same repelling (necessarily fixed) point in $J(f_c)$ if and only if $c \in W_{(1/3,2/3)}$.

Theorem 1.4.6 is a very useful result, since it gives an easy way of checking if two dynamical rays land together on the Julia set of a map. In the sequel, we will usually be considering the parameters c which lie in $\mathcal{M}$ (in other words, parameters c for which $J(f_c)$ is connected), and so it makes sense to define the limbs of $\mathcal{M}$ as follows.

Definition 1.4.7. The set $W_{(\theta_-,\theta_+)} \cap \mathcal{M}$ is called the (θ_-, θ_+)-limb of $\mathcal{M}$, and we denote it by $\mathcal{M}_{(\theta_-,\theta_+)}$.

The limbs of the Mandelbrot set play an important part in the discussion of mating later. As well as this, it is a relatively simple way of describing where one is in the Mandelbrot set, since the landing points of parameter ways are natural choices of "landmarks" in the Mandelbrot set, especially in the case where they are the root points of hyperbolic components. We will take advantage of this fact when discussing internal addresses in Section 1.7.

1.5 Local connectivity of the boundary of Fatou components

In this section, we state some results concerning the local connectivity of certain sets arising from complex dynamics, and what conditions are required in order for us to be sure that local connectivity holds. Firstly, we state a result from [Mil06]. It will be extremely important in the context of this thesis, since we will be dealing with hyperbolic maps with connected Julia set.

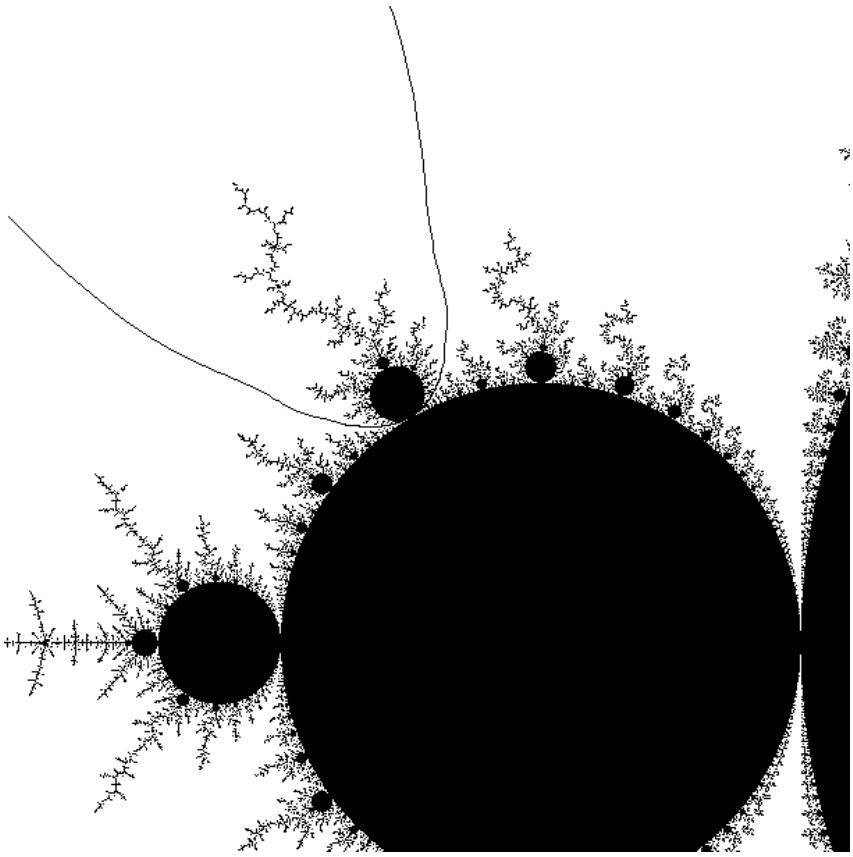

Figure 1.6: An example of parameter rays in $\mathcal{M}$. The region bounded by the rays is the $(22/63, 25/63)$-*wake*.

Theorem 1.5.1. *The Julia set of a hyperbolic map is locally connected if and only if it is connected.*

Since we will be focussing on bicritical rational maps, we also take advantage of the following result, which tells us the nature of the boundaries of Fatou components in the rational maps we are studying.

Theorem 1.5.2 (Pilgrim [Pil96])**.** *Let f be a critically finite rational map with exactly two critical points, not counted with multiplicity. Then exactly one of the following possibilities holds:*

- *f is conjugate to $z \mapsto z^d$ and the Julia set of f is a Jordan curve, or*
- *f is conjugate to a polynomial of the form $z^d + c$, $c \neq 0$, and the Fatou component corresponding to the basin of attraction for infinity under the conjugacy is the unique Fatou component which is not a Jordan domain, or*

- *f is not conjugate to a polynomial, and every Fatou component is a Jordan domain.*

The above results are reassuring, as it means that in all the cases we consider in this thesis - except for the basin of infinity in the case we are talking about polynomials - the Fatou components of the map will be Jordan domains. However, even in this exceptional case, the previous theorem shows us that the boundary of this basin, which is the Julia set, is still locally connected. This means we will not have any issues with local connectivity of the boundary of these components.

1.6 Filled Julia sets

In this section, we briefly describe some terminology which allows us to discuss the structure of Julia sets. Some of this will be a preliminary to the study of Hubbard trees in Section 1.7.

1.6.1 Internal rays

In this section we describe how to construct an analogue to external rays that exist inside the Fatou components of a rational map. We assume f is a rational map with (pre)periodic critical points.

Let

$$\phi_a(z) = \frac{z-a}{1-\bar{a}z} \quad (|a|<1).$$

We remark that ϕ_a will map the unit disk onto itself. We say that a map of the form

$$f(z) = e^{2\pi i t}\phi_{a_1}(z)\phi_{a_2}(z)\cdots\phi_{a_d}(z) \quad (t\in[0,1)) \tag{1.2}$$

is a *Blaschke product* of degree d. We then have the following ([Mil06], page 162).

Lemma 1.6.1. *A rational map of degree d carries the unit disk onto itself if and only if it is a Blaschke product.*

We use this result to construct internal rays inside the Fatou components of a degree d bicritical rational map F with disjoint periodic superattracting cycles. The construction can be carried out in more general cases but we restrict ourself only to the result required in this thesis. Given a periodic Fatou component U, the first return map $F^{\circ n}$ to the component is a degree d covering with precisely one critical point c_U. There exists a Riemann map $\Phi\colon \mathbb{D}\to U$ such that $\Phi(0)=c_U$.

Then we have a commutative diagram

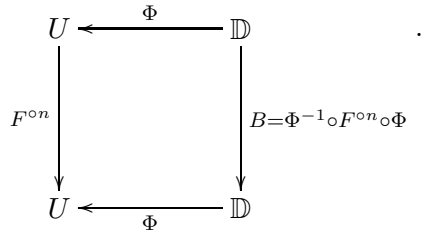

The map B is a rational map which will map the unit disk onto itself by a degree d covering, and so by Lemma 1.6.1 it is a Blaschke product, and so has the form (1.2). Furthermore, the only fixed point is 0, so $\phi_{a_j} = z$ for $j = 1, \ldots, d$ and so $B(z) = e^{2\pi i t} z^d$ for some $t \in [0, 1)$. We can normalise (by composition with a rotation) so that B is in fact equal to the map $z \mapsto z^d$ on the disk. Define the radial arcs

$$r_\theta = \{re^{2\pi i\theta} : \ 0 \leq r < 1\} \subset \mathbb{D}.$$

Then the internal ray of angle θ is the arc $\Phi^{-1}(r_\theta) \subset U$.

We make some observations about internal rays. Firstly, each internal ray has the centre as an endpoint, and the internal ray of angles $k/(d-1)$, $k = 0, 1, \ldots, d-2$ will be fixed under the first return map to the component, $F^{\circ n}$. Assuming the boundary of U is locally connected (which it will be in all cases we will consider), we can also discuss the landing of internal rays in the same way as with external rays. These landing points will belong to the Julia set of the map F.

Given a periodic cycle of superattracting basins, we can define the internal rays of each basin individually. However, we can construct the rays in such a way so that, if $F(U) = V$ in the cycle, then the internal ray of angle θ in U will map onto the internal ray of angle θ in V. This can be done by, if necessary, composing the Blaschke products with rotations so that this agreement is achieved. Furthermore, if U' is a pre-periodic Fatou component that maps onto a periodic superattracting basin, then there exists an integer k so that $F^{\circ k}(U')$ is a member U of the periodic superattracting cycle. The map $F^{\circ k}|_{U'}$ is a homeomorphism, and so we can define the internal ray of angle θ in U' to be the pre-image (under $F^{\circ k}$) of the internal ray of angle θ in U. Since all Fatou components are pre-periodic for hyperbolic rational maps, this defines the notion of internal rays for all Fatou components.

Now suppose that z is a periodic point in $J(F)$ of period p which lies on the boundary of the periodic Fatou components $U_1, U_2, \ldots, U_n$. Then z will be the landing point of precisely one internal ray from each U_i. The map $F^{\circ p}$ is a local homeomorphism and maps z to itself, and so Definition 1.4.3 means we can define

the combinatorial rotation number at z. Furthermore, if z is also the landing point of external rays, the combinatorial rotation number defined for internal rays is the same as that defined for external rays (Proposition 1.4.4).

1.6.2 Regulated arcs

Suppose f is a polynomial with locally connected (and hence path connected) Julia set. Sometimes we will want to construct paths in the filled Julia set $K(f)$. It will aid us if we have a canonical way of making these paths. If we have $J(f) = K(f)$, then the path between two points x, y in $J(f)$ is uniquely defined. However, if this is not the case, we need to decide how we will define the arc $[x, y]$. The problem occurs when we pass through the Fatou components, but fortunately the internal rays give us a way of passing through them in a way which can be consistently defined.

Definition 1.6.2. Let $x, y \in J(f)$. The arc $[x, y]$ will be called regulated if, for each Fatou component U, $U \cap [x, y]$ is contained in the union of (at most) two internal rays of U.

1.7 Symbolic Dynamics

In this section, we discuss how to encode complex dynamics in a symbolic form. This very powerful theory has come about from the work of Schleicher and Bruin [BS01], and more recently, Kaffl. The external rays from Section 1.3 play an important role here, since they are the device used to encode the dynamics.

One extremely surprising observation is that the objects defined in this section give us information in both the dynamical and parameter planes. For example, the internal address of a map f_c can be considered as being defined equivalently in a number of different ways; by looking at the internal address of the parameter c, or by looking at the positioning of periodic points in $J(f_c)$. Such a connection is just another example of the strong link between the dynamic and parameter planes, as already seen in Theorem 1.4.6. Furthermore, in a very simple sense, the symbolic dynamics allows us to focus almost entirely on the behaviour of the critical orbit of f_c, once again showing the important role played by the behaviour of critical points when studying dynamical systems.

The exposition of this section will be mainly concerned with the quadratic case. However, as shown in the work of Eike Lau and Dierk Schleicher (see for example [LS94],[Sch99]), many of the results will hold in the higher degree case. We start by giving the definition of itineraries and kneading sequences in the degree 2

case. It is possible to define this more generally for higher degrees, but we will not require the general case in this thesis.

Definition 1.7.1 (Itinerary and Kneading sequence)**.** Let θ be an external angle in the dynamical plane. We define the itinerary of ϕ with respect to the angle θ to be the sequence $\nu_\theta(\phi) = \nu_1\nu_2\nu_3\ldots$ where the ν_i satisfy the following:

$$\nu_i = \begin{cases} 0 & \text{if } \frac{\theta+1}{2} < 2^{i-1}\phi < \frac{\theta}{2}\ , \\ 1 & \text{if } \frac{\theta}{2} < 2^{i-1}\phi < \frac{\theta+1}{2}, \\ * & \text{if } 2^{i-1}\phi \in \{\frac{\theta}{2}, \frac{\theta+1}{2}\} \end{cases}$$

where the inequalities are with respect to the natural (cyclic) ordering on the unit circle. The most interesting type of itinerary is the case where $\theta = \phi$. Because of this, we give the itinerary $\nu_\theta(\theta)$ a special title; it is called the kneading sequence of the angle θ.

Here we include some examples to show the definition in action.

Example 1.7.2 ($\theta = 1/7$). Suppose that we take $\theta = 1/7$. On the Mandelbrot set, this angle (and its partner, $\tilde{\theta} = 2/7$) lands at the base point of the period 3 component which contains the parameter for *Douady's rabbit*. The interval $(\theta/2, (\theta+1)/2) = (1/14, 4/7)$ The orbit of θ is given by

$$\frac{1}{7} \to \frac{2}{7} \to \frac{4}{7} \to \frac{1}{7}.$$

Now, from the definition given above, we see that the kneading sequence $\nu_{\frac{1}{7}} = \overline{11*}$. This has period 3, which is also the period of the landing point of the 1/7-ray.

Let $\mathcal{H}$ be a hyperbolic component of the Mandelbrot set. Then it is well-known that there are precisely two parameter rays landing at the root point of this component (Theorem 1.4.6). The kneading sequence of the angles of these two parameter rays are equal (Theorem 12.2, [BS01]). Hence, even though kneading sequences are defined for angles, it is natural to associate these kneading sequences with the maps f that belong to $\mathcal{H}$, by saying that the kneading sequence of f is the kneading sequence of the two angles that land at the root point of $\mathcal{H}$. It is clear that this is well defined - all maps in the same hyperbolic component will have the same kneading sequence.

Definition 1.7.3 (ρ-function)**.** Given a kneading sequence, define the ρ-function

$(\rho_\nu : \mathbb{N} \to \mathbb{N} \cup \{\infty\})$ to be

$$\rho_\nu(n) = \inf\{k > n \,:\, \nu_k \neq \nu_{k-n}\}.$$

From this function, we construct the internal address.

Definition 1.7.4. The internal address of an angle θ is the orbit of $n = 1$ under the ρ-function.

$$\mathcal{I}_\theta = 1 \to \rho(1) \to \rho^{\circ 2}(1) \to \rho^{\circ 3}(1) \to \cdots .$$

Note that, if for some n, we have $\rho(n) = \infty$ in the internal address, then we cut the internal address so that it reads

$$\mathcal{I}_\theta = 1 \to \rho(1) \to \rho^{\circ 2}(1) \to \cdots \to \rho^{\circ n}(1).$$

We call this a *finite internal address*.

Similarly to the case with kneading sequences, we sometimes abuse notation and refer to the internal address of a function $f_c(z) = z^2 + c$. When we say this, we are referring to the internal address of the angles landing at the base of the hyperbolic component containing c.

It turns out there is a very nice interpretation of the internal address of an angle. Bearing in mind the abuse of notation outlined above, the internal address in some respects represents the periods of the hyperbolic components that one "passes through" when travelling to the parameter c from the main cardioid. We postpone a more formal treatment of characterisations of $\mathcal{I}$ until Section 1.7.2.

1.7.1 Hubbard Trees

The Hubbard tree can be constructed via an algorithm due to Schleicher and Bruin [BS01]. It is useful because it gives us a visual representation of the dynamics of a polynomial, without us having to calculate the Julia set. It also encodes, in a nice pictorial way, the critical orbit of a polynomial. The following definitions are those found in [BS01].

Definition 1.7.5. A tree T is a finite connected graph with no loops. Given a point $x \in T$, the (global) arms of x are the connected components of $T \setminus \{x\}$. A local arm at x is the intersection of a global arm with a sufficiently small neighbourhood of x in T. x will be called an endpoint of T if it has only one global arm, and a branch point if it has three or more arms.

Given two points x, y in a tree T, there exists a unique closed arc in T which connects x and y. We denote this arc by $[x, y]$ and its interior (x, y). Compare these arcs with the notion of regulated arcs found in [Zak00] and the previous section.

We will first give the definition of a Hubbard tree in a manner which does not require the tree to be associated with a particular polynomial.

Definition 1.7.6 (Hubbard Trees)**.** A (quadratic) Hubbard tree (T, f) is a tree T along with a map $f\colon T \to T$ and a marked point, the critical point x_0, which satisfies the following:

1. The map $f\colon T \to T$ is continuous and surjective (in particular, T is forward invariant under f).
2. Every point in T has at most two pre-images on T.
3. If x is not the critical point, f is a local homeomorphism at x.
4. All endpoints belong to the critical orbit $\{c_n = f^{\circ n}(x_0) : n \geq 0\}$.
5. The critical point is periodic or preperiodic, but not fixed (since this would give a trivial tree with no branches by the previous property).
6. The expansivity condition. If x and y are distinct branch points or points on the critical orbit, then there is an $n \geq 0$ such that $x_0 \in f^{\circ n}([x, y])$.

We sometimes refer to the Hubbard tree (T, f) by just T, to ease notation. In this thesis, all Hubbard trees will be considered to have periodic critical orbits.

We will say that a Hubbard tree is *admissible* if it is the Hubbard tree of some degree 2 polynomial $f_c(z) = z^2 + c$. In this case, it is well known that the Hubbard tree is made up of the convex hull of the critical orbit in the filled Julia set of the map, with the paths through the Fatou components being made up of internal rays. Most of the time we will only be considering Hubbard trees which are derived from polynomials, so this second definition will be the one used.

Given a Hubbard tree, there is a natural way of dividing the tree into two disjoint sets. Denote the critical point by c_0. Then the set $T \setminus \{c_0\}$ is made up of (at most) two connected components. The first contains the critical value and will be denoted T_1, the second (possibly empty) will be labelled T_0. Given a Hubbard tree (not necessarily that derived from a polynomial), it is then possible to define a

kneading sequence $\nu = \nu_1\nu_2\ldots$.

$$\nu_i = \begin{cases} 0 & \text{if } f^{\circ i}(c_0) \in T_0, \\ 1 & \text{if } f^{\circ i}(c_0) \in T_1, \\ * & \text{if } f^{\circ i}(c_0) = c_0. \end{cases}$$

Lemma 1.7.7. *Given a (quadratic) Hubbard tree (T, f) with period n critical orbit, there exists k such that the points $c_1, \ldots, c_{k-1}$ have only one local arm, and the points $c_k, \ldots, c_{n-1}$ have precisely two local arms, except for the case where all points on the critical orbit have precisely one local arm.*

Proof. The exceptional case is clear, since if all points have only one local arm, then $k = n$. So suppose c_k is a point on the critical orbit with two local arms. Then $f(c_k) = c_{k+1}$ must also have two local arms, by forward invariance and the fact that f is a local homeomorphism away from the critical point. Inductively, all the points $c_k, c_{k+1}, \ldots, c_n = c_0$ will have two local arms, again by forward invariance and f being a local homeomorphism. However, by definition, $c_1 = f(c_0)$ only has one local arm, and so there must exist some minimal integer k satisfying the lemma. □

1.7.2 Characterisation of the Internal Address

The internal address, defined as it is, does not appear (at first glance) to tell us anything about the dynamics of the map it represents. However, the following proposition shows that this is not the case, and the internal address reveals some useful data about the behaviour of periodic points. Most of what follows is from [BS01].

Informally, the internal address gives a list of components which tells how to find a hyperbolic component or Misiurewicz point in the Mandelbrot set (though to define a component uniquely we need to use the *angled internal address* which includes more information). However, the following theorem shows that the internal address can also tell us some facts about the dynamics of a map. First we need a definition.

Lemma 1.7.8 ([BS01], Lemma 4.1)**.** *Let (T, f) be the Hubbard tree with kneading sequence ν. Let $\mathcal{O} = \{z_1, z_2, \ldots, z_n = z_0\}$ be a periodic orbit which contains no endpoint of T.*

Then there are a unique point $z \in \mathcal{O}$ and two different components of $T \setminus \{z\}$ such that the critical value is contained in one component and 0 (the critical point) and all the other $z_k \in \mathcal{O}$ belong to the other component.

Definition 1.7.9 ([BS01], Definition 4.2)**.** The point z defined in the previous lemma is called the *characteristic (periodic) point* of $\mathcal{O}$.

We are now ready to discuss the different interpretations of the internal address, and how it reflects properties found both in the parameter plane and in the dynamic plane. The relevant characterisations are (cf. [BS01]):

1. The *internal address associated to the kneading sequence* ν using the ρ-map (see definition 1.7.4).

2. The *internal address of closest characteristic periodic points* is the sequence of exact periods S_k of characteristic periodic points p_k such that there is no periodic point of lower or equal period on $[p_k, c_1]$ (including periodic points with 2 local arms).

3. The *internal address in parameter space.* For a hyperbolic component or Misiurewicz point $\mathcal{A}$ consider all the hyperbolic components $\mathcal{B}$ on the interval $[0, \mathcal{A}]$ which have the property that no hyperbolic component on the interval $[\mathcal{B}, \mathcal{A}]$ has period less than or equal to the period of $\mathcal{B}$. With respect to the ordering of these components on the interval $[0, \mathcal{A}]$, their periods form an increasing sequence of integers starting with 1 (which represents the main cardioid).

Corollary 1.7.10. *If 2 appears in the internal address, there is a period 2 point on the arc between α and c_1. Conversely, if 2 does not appear in the internal address, then there cannot exist a period 2 point on $[\alpha, c_1]$.*

Proof. The first claim is an obvious restatement of the third interpretation of the internal address. To prove the second, suppose that there is a period 2 point w in $[\alpha, c_1]$ but 2 does not appear in the internal address. Then we must have a fixed point in the arc $(w, c_1) \subset (\alpha, c_1)$, by the second characterisation of the internal address. However, a quadratic rational map has only two fixed points, α, which is not equal to w by assumption, and β, which is an endpoint of the Julia set and so cannot be contained in any open arc $(z_1, z_2) \subset J$. □

It is immediately clear that the map from hyperbolic components to internal addresses is not injective (nor is it surjective, but that is another story, compare [BS01]). An easy way to see it is not injective is to note there are two period 3 components bifurcating from the main cardioid (the rabbit component and the anti-rabbit component), which must have internal address $1 \to 3$. However, there is a way to modify the internal address so it uniquely defines a component in $\mathcal{M}$.

Definition 1.7.11. We define the angled internal address as follows. Consider the third characterisation of the internal address (the internal address in the parameter plane). This gives a sequence

$$1 \to S_1 \to S_2 \to \cdots \to S_n,$$

where the S_i represent the periods of hyperbolic components. To each of these we add some additional information: the (internal) angle p_i/q_i at which one leaves the hyperbolic component of period S_i. This will provide a new sequence

$$1_{p_0/q_0} \to (S_1)_{p_1/q_1} \to \cdots \to S_n.$$

This new sequence is the angled internal address.

Again referring back to the characterisations of the internal address, this angled internal address has another interpretation. Recall that the entries in the internal address can also represent the positions of characteristic periodic points in the Hubbard tree. Then the subscripts from the angled internal address now tell us the combinatorial rotation number at these characteristic periodic points. Again, this observation can be found in [BS01], Definition 12.13.

We see that this new definition fixes the problem of injectivity of the internal address [BS01].

Proposition 1.7.12. *The angled internal address (if it is admissible) uniquely defines the hyperbolic component $\mathcal{H}$.*

It turns out that the denominators in the angled internal address are dependent only on the S_i.

Lemma 1.7.13. *In an angled internal address $(S_0)_{p_0/q_0} \to \cdots \to (S_k)_{p_k/q_k} \to (S_{k+1})_{p_{k+1}/q_{k+1}} \to \cdots$, the denominator q_k in the bifurcation angle is uniquely determined by the internal address $S_0 \to \cdots \to S_k \to S_{k+1} \to \cdots$ as follows: let ν be the kneading sequence associated to the internal address and let ρ be the function as defined in the definition of the internal address. Let $r \in \{1, 2, \ldots, S_k\}$ be congruent to S_{k+1} modulo S_k. Then*

$$q_k := \begin{cases} \frac{S_{k+1}-r}{S_k} + 1 & \text{if } S_k \in \mathrm{orb}_\rho(r), \\ \frac{S_{k+1}-r}{S_k} + 2 & \text{if } S_k \notin \mathrm{orb}_\rho(r). \end{cases}$$

Obviously, the numerators of the angles are not dependent on the S_i. Using

the same notation, Schleicher proved the following ([Sch08], Lemma 2.1). The proof holds for any degree.

Lemma 1.7.14. *If S_{k+1} is a multiple of S_k, then the component of period S_{k+1} is a bifurcation from that of period S_k.*

1.8 Rabbit components in $\mathcal{M}$

We now prove some results about angles (and components) in $\mathcal{M}$ which will be useful when considering cluster points in Chapters 3, 4 and 5. We first consider the rabbit components of $\mathcal{M}$; that is, maps belonging to the hyperbolic components which bifurcate directly off of the main cardioid.

Proposition 1.8.1. *A hyperbolic component has internal address $1 \to n$ if and only if it is a rabbit component.*

Proof. If $\mathcal{H}$ is a rabbit component of period n then it bifurcates from the main cardioid. Then there are no other hyperbolic components on the combinatorial arc between $\mathcal{H}$ and the main cardioid and so the internal address (using the third characterisation) is $1 \to n$.

Now suppose $\mathcal{H}$ has internal address $1 \to n$. Then by Lemma 1.7.14, since n is divisible by 1, $\mathcal{H}$ must be a bifurcation from a component of period 1, which is the main cardioid. □

Lemma 1.8.2 (See also [Wit88], Claim 10.1.1)**.** *Let f be an n-rabbit. Then $z \in J(f)$ is biaccessible iff it is a pre-image of the α-fixed point.*

Recall that the width of a sector is defined to be the difference between the angles of the two parameter rays bounding it. The following result is Proposition 2.4.3 of [Sch94]. The width of a hyperbolic component will be the width of the wake which is formed by the two parameter rays landing at its root point.

Proposition 1.8.3. *Given a hyperbolic component of period m and width δ, the width of its p/n-subwake is*

$$\frac{(2^m-1)^2}{2^{nm}-1}\delta. \tag{1.3}$$

Corollary 1.8.4. *The wakes of an n-rabbit component is narrow. That is, the width must be $1/(2^n-1)$.*

Proof. The rabbit component will bifurcate off of the main cardioid by Proposition 1.8.1, and lie in the p/n-subwake. Hence it has width

$$\frac{(2-1)^2}{2^n-1} = \frac{1}{2^n-1}.$$

□

The following corollary will be of use in Chapter 5, as it tells us which maps have a period two orbit with a given combinatorial rotation number.

Corollary 1.8.5. *Let $\mathcal{H}$ be a period $2n$ hyperbolic component which bifurcates off of the period 2 hyperbolic component of $\mathcal{M}$. Then there exists precisely one period $2n$ component $\mathcal{H}'$ in the wake of $\mathcal{H}$*

Proof. We first calculate the width $\delta_{\mathcal{H}}$ of the wake of the hyperbolic component $\mathcal{H}$. The width of the period 2 component is $1/3$, and so 1.3 gives us

$$\delta_{\mathcal{H}} = \frac{(2^2-1)^2}{2^{2n}-1} \cdot \frac{1}{3} = \frac{3}{2^{2n}-1}.$$

Therefore there are precisely two rays of angle with denominator $2^{2n}-1$ between the rays landing at the base of $\mathcal{H}$. Hence there must exists precisely one period $2n$ component $\mathcal{H}'$ in the wake of $\mathcal{H}$. □

By considering the limbs which bifurcate off of the period 2 component, we realise we have enough information to calculate the angled internal address of the second component $\mathcal{H}'$ that lies in the wake of the component of period $2n$ which bifurcates off of the period 2 component.

Proposition 1.8.6. *Let $\mathcal{H}$ be a period $2n$ hyperbolic component with angled internal address*

$$1_{1/2} \to 2_{p/n} \to 2n,$$

with p coprime to n. Then the other component $\mathcal{H}'$ of period $2n$ which is contained in the wake of $\mathcal{H}$ has angled internal address

$$1_{1/2} \to 2_{p/n} \to (2n-1)_{1/2} \to 2n.$$

Proof. Since $\mathcal{H}'$ is contained in the wake of $\mathcal{H}$, we know that the angled internal address begins

$$1_{1/2} \to 2_{p/n} \to (S_2)_{p_2/q_2} \to \cdots.$$

We will now show that $S_2 = 2n - 1$, which will prove the proposition. Note that if $S_2 = 2n$ then, by Lemma 1.7.14, $\mathcal{H}'$ bifurcates from the period 2 hyperbolic component, contradicting the assumption on $\mathcal{H}'$ being in the wake (and not equal to) the component $\mathcal{H}$ which bifurcates from the period 2 component. If $S_2 = 2m$ for some $m \neq n$, then this would represent a bifurcation of the period 2 component into the period $2m$ component (Lemma 1.7.14), which contradicts the assumption that $\mathcal{H}'$ is in the wake of the period $2n$ component. It follows that S_2 is odd.

Since S_2 is odd, it is congruent to 1 mod 2. Furthermore, we notice that $2 \in \text{orb}_\rho(1)$. Now using Lemma 1.7.13, we can substitute in what we already know to get

$$n = \frac{S_2 - 1}{2} + 1,$$

which when rearranged yields

$$S_2 = 2(n-1) + 1 = 2n - 1$$

as required. □

Lemma 1.8.7. *If (T, f) is the Hubbard tree of an n-rabbit f, then all the points in the critical orbit of f are endpoints of T.*

Proof. The proof is trivial. f has internal address $1_{p/n} \to n$, so the Hubbard tree contains a fixed point with n global arms. Each of these global arms has an endpoint, which must belong to the critical orbit. But there are only n elements in the critical orbit, so each one must be the endpoint of one of these global arms. □

1.8.1 Higher Degree Cases

In Chapter 4, it will be necessary to generalise the notion of a n-rabbit to higher degree cases. A lot of terminology from the symbolic dynamics of quadratic polynomials carries over the higher degree case, as was shown by Lau and Schleicher in [LS94]. In this section we will briefly state the results we need.

We first comment that a Multibrot set $\mathcal{M}_d$ will be the connectedness locus of polynomials of the form $z \mapsto z^d + c$, as an analogous definition to $\mathcal{M}$. That is

$$\mathcal{M}_d = \{c \in \mathbb{C} : \ z^d + c \text{ has connected Julia set}\}.$$

Figure 1.7 shows the degree 3 Multibrot set. We note that, in the non-quadratic case, the current characterisations of the (angled) internal address is not enough to uniquely define the hyperbolic components. For example, the degree 3 multibrot

set contains two degree 2 components, which each have angled internal address $1_{1/2} \to 2$. To fix this problem, we need to introduce the concept of "sectors" of hyperbolic components. Since we are not concerned with uniqueness in this thesis, we omit this discussion.

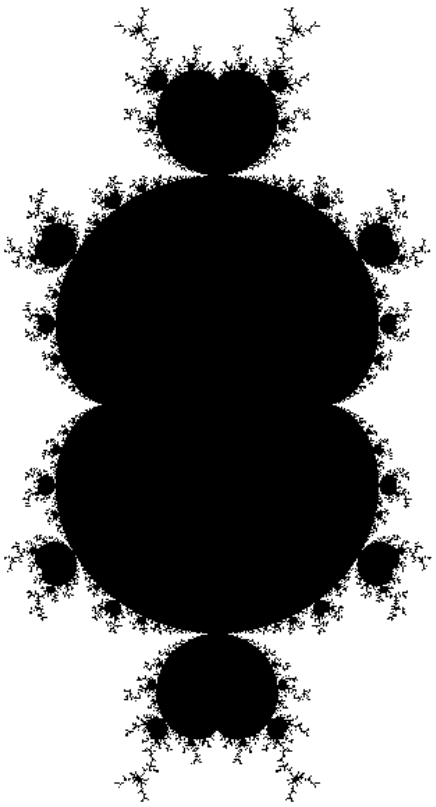

Figure 1.7: The degree 3 Multibrot set.

The hyperbolic components in $\mathcal{M}_d$ have $d-1$ root point. One of these is the landing point of precisely two parameter rays; this will be known as the *principal* root point. The other root points will be the landing point of one parameter ray, and will be called *non-principal* root points.

Recall that an n-rabbit was defined to be a map belonging to a hyperbolic component which bifurcates off of the cardioid in $\mathcal{M}$. We will similarly define an n-rabbit in degree d to be a map which belongs to a hyperbolic component which bifurcates off of the (unique) period 1 component of $\mathcal{M}_d$. By a similar proof to Proposition 1.8.1, such a map will have internal address $1 \to n$. Furthermore, it has angled internal address $1_{p/n} \to n$ and so, by the characterisation of internal

addresses, has a fixed point with combinatorial rotation number p/n.

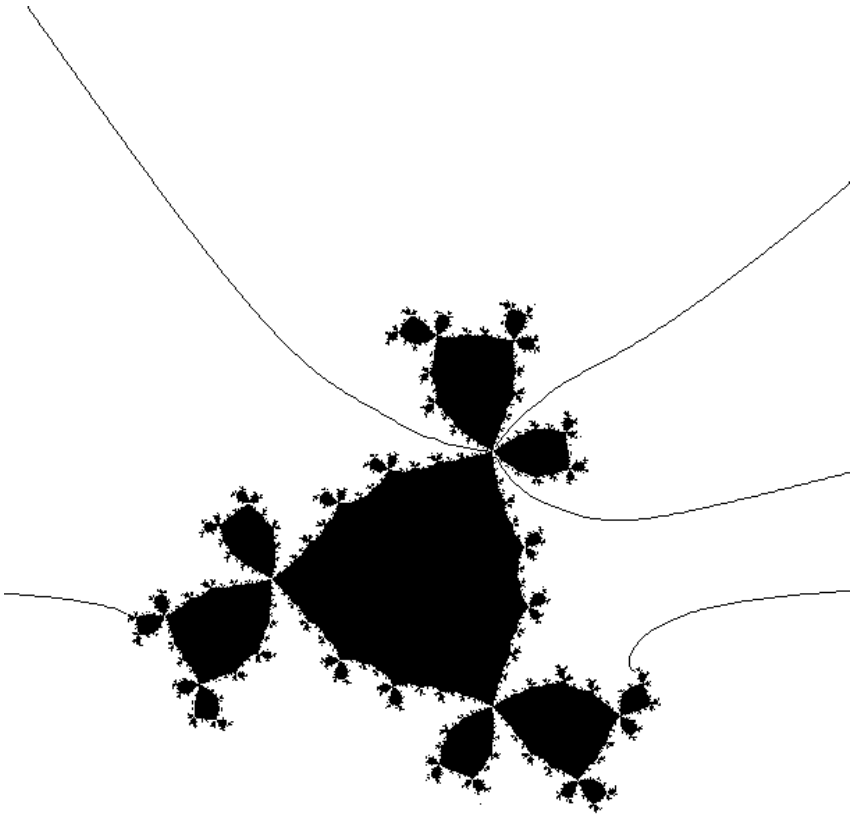

Figure 1.8: A degree 3 rabbit (corresponding to the parameter rays 1/26 and 3/26) and the external rays landing on the two β-fixed points and the α-fixed point.

Suppose f is a degree d n-rabbit. Then the landing point of the external rays of angles $k/(d-1)$ will be fixed points. There exists one more (finite) fixed point, which will be called the α-fixed point, in keeping with the terminology from the quadratic case. Figure 1.8 shows a degree 3 rabbit.

One final important point should be borne in mind. In the quadratic case, all root points of Fatou components are principal, meaning they are the landing point of two or more external rays. However, in the higher degree d case, we find that each Fatou component has $d-2$ non-principal root points. If the Fatou component U is periodic, there exists $d-1$ fixed points on the boundary of U. One of these is principal and the other $d-2$ are called non-principal and are the landing point of only one external ray. We will find that this extra complication makes the discussion slightly more difficult in Chapter 4 and also allows us to construct the example

constructed in Appendix E.

1.9 Some Useful Algorithms

There is an algorithm in [BS01] (Algorithm 11.2) which allows us to construct the Hubbard tree from the (angled) internal address. This will allow us to construct some Hubbard trees in chapter 3. We give the algorithm below, omitting the unnecessary steps required to deal with non-admissible Hubbard trees.

Algorithm 1.9.1. *Let ν be a $*$-periodic kneading sequence and $1 \to S_1 \to \ldots \to S_i$ be its internal address. Write $\nu = \overline{\nu_1\nu_2\ldots\nu_{S_i}*}$. We inductively define the Hubbard tree as follows.*

If the internal address is $1 \to S_1$, then the Hubbard tree is an S_1-star with a fixed central vertex (this is the α-fixed point) and all the S_1 arms at this point are permuted cyclically. The critical point is the endpoint of one of the arms and has period S_1.

For the inductive step, suppose we have constructed the Hubbard tree (T, f) for the internal address $1 \to \ldots \to S_k$. We now construct the Hubbard tree $(\tilde{T}, \tilde{f})$ with internal address $1 \to \ldots \to S_k \to S_{k+1}$.

Step 1. *Replace the critical point c_0 by a closed arc $[-p_0, p_0]$ where p_0 is adjacent to the ν_{S_k}-side of T. Rename the points $c_1, \ldots, c_{S_k-1}$ as $p_1, \ldots, p_{S_k-1}$. Let $f(p_{S_k-1}) = p_0$, $f(p_0) = f(-p_0) = p_1$ and leave the action on $p_1, \ldots, p_{S_k-2}$ as well as on the other points (the branch points) unchanged.*

This gives the point p_1 the itinerary $\overline{\nu_1\ldots\nu_{S_k}}$ (indeed, this point p_1 will be the characteristic periodic point of period S_k for the Hubbard tree we are constructing as defined in definition 1.7.2) and the action of f is defined on all the branch points and endpoints of $T \cup (p_0, -p_0)$ and their orbits. Extend f homeomorphically to the arcs connecting these points, except for $(-p_0, p_0)$.

Finally, define a new critical point $c_0 = c_{S_{k+1}}$ on the arc $(-p_0, p_0)$.

Step 2. *Write $S_{k+1} = aS_k + r$ $(1 \le r \le S_k)$ and let*

$$q = \begin{cases} a+1 & \text{if } S_k \in \mathrm{orb}_\rho(r), \\ a+2 & \text{if } S_k \notin \mathrm{orb}_\rho(r). \end{cases}$$

- *If $q > 2$ then set $d = (q-2)S_k$ and go to step 3.*
- *If $q = 2$ then set $d = 0$ and go to step 4.*

Step 3. *Attach $d = (q-2)$ closed arcs to each of the points $p_0, \ldots, p_{S_{k-1}}$. Map the*

interval $(-p_0, p_0)$ in a 2-to-1 fashion onto one of the arcs attached to p_1 so that its endpoint is $c_1 = f(c_0)$. Extend the function f as follows: let f map $[p_1, c_1]$ homeomorphically onto one of the new arcs at p_2, thus making $c_2 = f(c_1)$ the endpoint of this new arc. Continue in a similar vein by mapping $[p_2, c_2]$ homeomorphically onto one of the new arcs at p_3, so the new arc has endpoint $c_3 = f(c_2)$.

Continue this until we have defined the point $c_d = c_{(q-2)S_k}$ is defined, being the endpoint of the last remaining arc at p_0. This means f is defined on T with all its attached arcs, save for the arc $(p_0, c_d]$. Now go to step 4.

Step 4. *We now create the points c_i for $i \in \{S_{k+1} - 1, \ldots, d+1\}$. Find $y_{S_{k+1}-1}$ on the $\nu_{S_{k+1}-1}$ side of the tree created so far so that $f(y_{S_{k+1}-1})$ is closest to $c_0 = c_{S_{k+1}}$. In the case that $f(y_{S_{k+1}-1}) = c_0$ then we set $c_{S_{k+1}-1} = y_{S_{k+1}-1}$. Otherwise attach an arc $[y_{S_{k+1}-1}, c_{S_{k+1}-1}]$ to $y_{S_{k+1}-1}$ and let f map it homeomorphically onto $[f(y_{S_{k+1}-1}), c_0]$.*

Now continue in this way, replacing the $S_{k+1} - 1$ in the above with, consecutively, $S_{k+1} - 2$, $S_{k+1} - 3$ and so on, down to when y_{d+1} and c_{d+1} are defined.

Step 5. *There are two cases, depending on whether or not we skipped step 3.*

1. *If step 3 is skipped then $d = 0$. By construction we have $p_1 \in (c_1, c_0)$. So map $(-p_0, p_0)$ in a 2-to-1 fashion onto (p_1, c_1) so that $f(c_0) = c_1$.*

2. *If step 3 is carried out then we have $d = (q-2)S_k$. By construction we have $p_1 \in (c_{d+1}, c_0)$. Map (p_0, c_d) homeomorphically onto (p_1, c_{d+1}).*

The following algorithm will be very useful when answering the question of whether a map which can admit a clustered mating will indeed form a clustering. The algorithm is used to compute the external angle θ_1 of a map, given the configuration of the iterates $2^k\theta_1$ on the unit circle. We will use it in a more general sense in Chapter 3. It appears as Algorithm 13.9 in [BS01].

Algorithm 1.9.2. *Let $\theta_1 \in \mathbb{S}^1$ be a periodic angle of exact period $n \geq 2$, let $\theta_k := 2^{k-1}\theta_1$ for $k = 2, 3, \ldots$ (with $\theta_{n+1} = \theta_1$) and $\theta_0 := \theta_n + 1/2$ (the preperiodic preimage of θ_1). Knowing only the cyclic order of $\theta_0, \theta_1, \ldots, \theta_n$, the external angle θ_1 can be found as follows:*

1. *Among the two oriented intervals $[\theta_0, \theta_n]$ and $[\theta_n, \theta_0]$, let I_1 be the one containing θ_1 and I_0 be the other one. (This step splits the circle up in the same way as defined in the definition of the kneading sequence, see definition 1.7.1)*

2. *Find two consecutive points $\theta_i, \theta_j \in I_0$ such that $(\theta_{i+1}, \theta_{j+1}) \supset (\theta_i, \theta_j)$. Mark an arbitrary point $z \in (\theta_i, \theta_j)$ as a fixed point for angle doubling. The chosen point z will represent the angle $0 \in \mathbb{S}^1$, which has kneading sequence $\overline{0}$.*

3. *Find two consecutive points $\theta_{i'}, \theta_{j'} \in I_1$ such that $z \in (\theta_{i'+1}, \theta_{j'+1})$, and mark an arbitrary point $z' \in (\theta_{i'}, \theta_{j'})$. This point z' corresponds to the angle $1/2$, which is the preperiodic preimage of the angle 0, and has kneading sequence $1\overline{0}$.*

4. *Define two intervals $J_0 := (z, z')$ and $J_1 := (z', z)$ (with respect to the order inherited from $\mathbb{S}^1$). Define the numbers $x_1, x_2, \ldots, x_n \in \{0, 1\}$ such that $x_i = 0$ if $\theta_i \in J_0$ and $x_i = 1$ if $\theta_i \in J_1$. The splitting of the circle into J_0 and J_1 corresponds to splitting it into those angles less than 1/2 and greater than 1/2 respectively.*

5. *The binary representation of $\theta_1 \in (0, 1)$ is $0.\overline{x_1 x_2 \cdots x_n}$.*

It should be noted that this algorithm requires the cyclic ordering to be possible for an angle in $\mathbb{S}^1$. If the cyclic ordering is not admissible, it will not yield a solution. Not all cyclic ordering of kneading sequences are admissible.

The following lemma uses the position of the angles $\theta_0, \theta_1, \theta_2, \ldots, \theta_n$ on the circle as considered in step 1 of the previous algorithm.

Lemma 1.9.3. *If the two pre-images of θ_1, the angles θ_0 and θ_n, are adjacent in terms of the cyclic order on $\mathbb{S}^1$ then the map is an n-rabbit with internal address $1 \to n$.*

Conversely, if the map is an n-rabbit then the angles θ_n and θ_0 are adjacent in terms of the cyclic ordering.

Proof. If θ_0 and θ_n are adjacent in terms of the cyclic ordering, then there are no angles θ_k in the interior of the interval I_0. This means the kneading sequence of θ_1 will be $\overline{1 \cdots 1*}$ and so the internal address is $1 \to n$.

For the converse, suppose that the map is an n-rabbit. Then the kneading sequence of the angle is $\overline{1 \cdots 1*}$ and so there is no θ_i in the interior of I_0. This means θ_n and θ_0 are adjacent. □

Now suppose that we fix the cyclic ordering of $\theta_1, \ldots, \theta_n$ (the forward iterates of θ_1 on $\mathbb{S}^1$). Then we have a choice of n intervals (θ_i, θ_j) in which θ_0 could lie. By Algorithm 1.9.2, all of these choices (assuming they are admissible) correspond to an angle $\theta_1 \in \mathbb{S}^1$, and so the configuration corresponds to a quadratic polynomial. Furthermore, it is clear that two different configurations (in other words, a different choice of interval into which to place θ_0) must give rise to different angles in the algorithm. We can in fact say slightly more.

Proposition 1.9.4. *Given an ordering of $\theta_1, \ldots, \theta_n$ on $\mathbb{S}^1$, the choice of interval in which θ_0 lies uniquely defines the kneading sequence (and so the internal address) of the angle θ_1 calculated in Algorithm 1.9.2, except for the case that the map is an n-rabbit. In the exceptional case, there are two different choices of intervals which give the same n-rabbit.*

Proof. Choose a configuration for the angles (including θ_0) and label them in terms of anti-clockwise ordering on the circle:

$$\theta_1 := \theta_{i_1} < \theta_{i_2} < \cdots < \theta_{i_n} < \theta_{i_{n+1}} (< \theta_1). \tag{1.4}$$

In step 1 of the algorithm, θ_0 is one of the boundary points of the intervals $I_0, I_1 \subset \mathbb{S}^1$ and by definition $\theta_1 \in I_1$. Since I_1 is an interval, the set of angles lying in I_1 must be consecutive in terms of the ordering given in (1.4). Clearly, the angles in I_0 must also be consecutive as well. Let $I_0 = [\theta_{i_j}, \theta_{i_k}]$, (so $i_j, i_k \in \{0, n\}$) then the angles in I_0 are $\theta_{i_{j+1}}, \theta_{i_{j+2}}, \ldots, \theta_{i_{k-2}}, \theta_{i_{k-1}}$. Since $\theta_1 \notin I_0$ by definition, $k > j$.

We now notice that we can calculate the kneading sequence $\nu = \nu(\theta_1) = \overline{\nu_1 \nu_2 \ldots \nu_{n-1} *}$, using

$$\nu_j = \begin{cases} 0 & \text{for } \theta_j \in I_0\,, \\ 1 & \text{otherwise (i.e, when } \theta_j \in I_1)\,. \end{cases} \tag{1.5}$$

If θ_n and θ_0 are adjacent (it doesn't matter which comes first in the cyclic ordering), then by Lemma 1.9.3, the map is an n-rabbit. If they are not adjacent, then the choice of position of θ_0 uniquely defines the set of angles in I_0, and by (1.5) each of these sets give a different kneading sequence, and again by Lemma 1.9.3, the map cannot be an n-rabbit, since I_0 is non-empty. Since the kneading sequence uniquely defines the internal address (Definition 1.7.4), the proposition is proved. □

Notice that this result means that, given an ordering of $\theta_1, \ldots, \theta_n$ on $\mathbb{S}^1$, there are exactly $n - 2$ maps which are not n-rabbits that have this ordering on the iterates of θ_1. This fact will be useful when discussing the classifications of the maps which admit clustering in later chapters. A similar observation on sets which are preserved under angle-doubling can be found in [BS94].

We now introduce the notion of a triod, which will help us when discussing endpoints of Hubbard trees in Chapter 5.

Definition 1.9.5. A triod is a connected compact set homeomorphic to a subset of the letter Y. It is degenerate if it is homeomorphic to an arc or a point.

Triods are the natural way to talk about endpoints of Hubbard trees. We can take a triple of points in the critical orbit of h (or some extension of the critical orbit, perhaps including branch points in the Hubbard tree)) and check whether their convex hull forms a triod. Fortunately there is an algorithm in [BS01] that carries out this task for us. All we need to know is the kneading sequence for the associated angles of h.

First we recall that if the kneading sequence of a map is ν, then ν is the itinerary of the point c_1. Similarly, representing the shift map by σ (that is $\sigma(\nu_1\nu_2\ldots) = \nu_2\nu_3\ldots$) the itinerary of c_k in the Hubbard tree is given by $\sigma^{\circ(k-1)}(\nu)$. We denote an arbitrary itinerary using the notation $s = s_1s_2\ldots$ etc.

Algorithm 1.9.6. *Given a triple (s,t,u) of itineraries, define the map φ by*

$$\varphi(s,t,u) = \begin{cases} (\sigma(s),\sigma(t),\sigma(t)) & \text{if } s_1 = t_1 = u_1 \\ (\nu,\sigma(t),\sigma(u)) & \text{if } s_1 \neq t_1 = u_1 \\ (\sigma(s),\nu,\sigma(u)) & \text{if } s_1 = u_1 \neq t_1 \\ (\sigma(s),\sigma(t),\nu) & \text{if } s_1 = t_1 \neq u_1. \end{cases}$$

The triple $(\sigma^{\circ(j-1)}(\nu),\sigma^{\circ(k-1)}(\nu),\sigma^{\circ(\ell-1)}(\nu))$ represents the triod formed by (c_j,c_k,c_ℓ).

Iterate the map φ. We have three cases

1. *If the first entries of $(\sigma^{\circ(j-1)}(\nu),\sigma^{\circ(k-1)}(\nu)$ and $\sigma^{\circ(\ell-1)}(\nu))$ are the same, (with $*$ considered to be equal to 0 (respectively 1) if the other two entries are equal to 0 (respectively 1)) then the shifted triple represents the triod formed by $(c_{j+1},c_{k+1},c_{\ell+1})$.*

2. *If the first entries of $(\sigma^{\circ(j-1)}(\nu),\sigma^{\circ(k-1)}(\nu)$ and $\sigma^{\circ(\ell-1)}(\nu))$ are 0 (say twice) and 1 (say once) then we shift the sequences beginning with 0 and replace the sequence beginning with 1 by ν. This represents cutting off the triod at the critical point.*

3. *The first entries of $(\sigma^{\circ(j-1)}(\nu),\sigma^{\circ(k-1)}(\nu)$ and $\sigma^{\circ(\ell-1)}(\nu))$ are the set $\{0,1,*\}$. Then φ is not defined and the iteration stops. The triod is degenerate and the sequence with $*$ as its first point is an interior point of the triod.*

So beginning with some triple (s,t,u), we continue the iteration until we reach a loop or the iteration is stopped. If eventually each of the sequences is chopped off and replaced by ν, the triod is non-degenerate.

Chapter 2

Mating of Polynomials, Rational Maps and Branched Covers

The mating operation was first mentioned by Douady in [Dou83]. Informally, the construction allows us to take two complex polynomials f and g (along with their filled Julia sets $K(f)$ and $K(g)$) and paste them together to construct a rational map on the Riemann sphere. We will informally consider the mating operation to be a map from the ordered pairs (f, g) of polynomials to the space of branched covers of the sphere. For further reading on this subject, see (amongst others) [Tan92, Mil04, Wit88]. Here we will outline the general theory and emphasise the parts which we will want to use when dealing with clustering in the following chapters.

2.1 Definitions

We start out by outlining the theory of matings of polynomials, as well as giving some of the definitions from topological dynamics which are required to understand the phenomena.

We recall the following definitions from the introduction.

Definition 2.1.1. The *degree* of a rational map $R\colon \overline{\mathbb{C}} \to \overline{\mathbb{C}}$ is the number of pre-images (up to multiplicity) of each point in the image.

Definition 2.1.2. We denote the set of critical points of a rational map $f\colon \overline{\mathbb{C}} \to \overline{\mathbb{C}}$ by Ω_f. The postcritical set is given by

$$P_f := \bigcup_{n>0} f^{\circ n}(\Omega_f).$$

We say a polynomial is *postcritically finite* if $|P_f|$ is finite. Similarly, if $|P_f| = \infty$, then we say f is *postcritically infinite*.

Definition 2.1.3. A map $f\colon X \to Y$ will be called a branched covering if there exists a finite set $Z \subset Y$ such that the restricted map $f\colon X \setminus f^{-1}(Z) \to Y \setminus Z$ is a covering map.

Informally, a branched cover is a covering map away from a finite set of ramified points where the map is not locally a homeomorphism. Clearly, if the critical points are periodic, the function is postcritcally finite. We will mainly be concerned with postcritically finite maps in what follows. Indeed, the main focus will be on unicritical polynomials where the critical point 0 is periodic, and so is part of a superattracting orbit. There are in fact a few different notions of mating, and much work has been undertaken to check their equivalence. We consider a couple of examples of the mating construction.

2.1.1 Formal Mating

Perhaps the simplest method of mating is the formal mating. Let f and g be two monic degree d polynomials defined on the Riemann sphere. Open out the point at infinity to turn $\overline{\mathbb{C}}$ into $\widehat{\mathbb{C}}$ and extend f and g to $\hat{f}$ and $\hat{g}$ by $\hat{f}(\infty \cdot e^{2\pi i\theta}) = ((\infty \cdot e^{2\pi id\theta})$ and $\hat{g}(\infty \cdot e^{2\pi i\theta}) = ((\infty \cdot e^{2\pi id\theta})$. We label these two spaces $\widehat{\mathbb{C}}_f$ and $\widehat{\mathbb{C}}_g$ respectively. The extension defined above is continuous, but not analytic.

Recalling that $\uplus$ represents a disjoint union, now identify the two circles at infinity by defining $S^2_{f,g} = \widehat{\mathbb{C}}_f \uplus \widehat{\mathbb{C}}_g / (\infty \cdot e^{2\pi i\theta}, f) \sim (\infty \cdot e^{-2\pi i\theta}, g)$. $S^2_{f,g}$ is a topological sphere (notice that $S^2_{f,g}$ is not dependent on the maps f and g, the notation is used purely to serve as a reminder that the polynomials are f and g) and the formal mating is then defined to be the branched covering $f \uplus g\colon S^2_{f,g} \to S^2_{f,g}$ such that

$$\begin{aligned} f \uplus g|_{\widehat{\mathbb{C}}_f} &= f \quad \text{and} \\ f \uplus g|_{\widehat{\mathbb{C}}_g} &= g. \end{aligned}$$

In other words, the behaviour of $f \uplus g$ is equal to f on one hemisphere of $S^2_{f,g}$ and g on the other. The map $f \uplus g$ is an orientation preserving branched self-covering of a topological sphere. Trivially, this means it is not a rational map (which require there to be some analytic structure on the sphere), but in this chapter, with the aid of Thurston's theorem (and the notion of Thurston equivalence), we will show that $f \uplus g$ can be thought of as equivalent to a rational map in some sense.

The formal mating is the simplest notion of mating, but in order to discuss clustering in the later chapters we require a slightly different construction. It is actually possible to, in some cases, see mating as sticking the filled Julia sets of f and g together in such a way that the new space created is topologically a sphere. We discuss this below.

2.1.2 Topological mating

Recalling the definition of external rays, Definition 1.3.3, we construct the *topological mating* of two polynomials f_1 and f_2 as follows. Let $f\colon \mathbb{C} \to \mathbb{C}$ be a polynomial of degree $n > 1$. From Chapter 1 we know that the Julia set, $J(f)$, is the boundary of the filled Julia set, $K(f)$. Furthermore, if K is connected, then, since we have a superattracting fixed point at infinity, we can use Böttcher's theorem (Theorem 1.3.2); the complement of K is conformally isomorphic to the complement of the closed unit disk. Moreover, we can choose this isomorphism ϕ so that it conjugates f with the nth power map on $\mathbb{C} \setminus \mathbb{D}$; in other words

$$\phi(z^n) = f(\phi(z)).$$

Let f_1 and f_2 be monic polynomials - in terms of this thesis, it is enough to assume that they both are of the form $z \mapsto z^d + c$ for some $d > 1$. Assume the Julia sets $J(f_1)$ and $J(f_2)$ (equivalently, by Proposition 1.3.7, the filled Julia sets $K(f_1)$ and $K(f_2)$) are locally connected. The topological mating (denoted by $f_1 \perp\!\!\!\perp f_2\colon K(f_1) \perp\!\!\!\perp K(f_2) \to K(f_1) \perp\!\!\!\perp K(f_2)$, we define the space $K(f_1) \perp\!\!\!\perp K(f_2)$ below) is an onto, continuous map.

We now define the ray-equivalence relation $\sim$ on $S^2_{f,g}$. The equivalence relation $\sim_f$ on $\widehat{\mathbb{C}}_f$ is generated by $x \sim_f y$ if and only if $x, y \in \overline{R}^f_t$ for some t. Notice that the closure of the external ray contains both the landing point and the point on the circle at infinity. Define a similar equivalence relation on $\widehat{\mathbb{C}}_g$. Then the equivalence relation $\sim$ will be generated $\sim_f$ on $\widehat{\mathbb{C}}_f$ and $\sim_g$ on $\widehat{\mathbb{C}}_g$. We denote the equivalence class of x under this relation by $[x]$.

Denote the Carathéodory semiconjugacy derived from f_j by γ_j, so that $\gamma_j\colon \mathbb{R}/\mathbb{Z} \to \partial K(f_j)$. We see that the ray equivalence relation restricts to an equivalence relation $\sim'$ on the disjoint union of $K(f_1)$ and $K(f_2)$ by

$$\gamma_1(t) \sim' \gamma_2(-t) \quad \text{for each} \quad t \in \mathbb{R}/\mathbb{Z}.$$

We define $K(f_1) \perp\!\!\!\perp K(f_2)$ to be the quotient topological space $S^2_{f,g}/\sim$, where

every equivalence class is identified to a point. Making use of the fact that $\gamma_j(2t) = f_j(\gamma(t))$, we can piece together $f_1|_{K(f_1)}$ and $f_2|_{K(f_2)}$ to form a continuous map which we call $f_1 \amalg f_2$, which is the onto, continuous map we require. This is the topological mating.

The important cases will be when this quotient $K_1 \amalg K_2$ is homeomorphic to a sphere. When the quotient is not a sphere, we have no hope of the map being equivalent in any sense to a rational map on the Riemann sphere. It is clear, then, that it will be necessary to find out the nature of the quotient formed above. We can make use of the following classical result ([Moo25]).

Theorem 2.1.4. *Let $\sim$ be an equivalence relation on the sphere S^2 which is topologically closed. Furthermore, suppose that each equivalence class is connected but not the whole of S^2. Then the quotient space $S^2/\sim$ is itself homeomorphic to S^2 if and only if no equivalence class separates the sphere into two or more connected components.*

In the above, *topologically closed* means that all pairs (x, y) such that $x \sim y$ forms a closed subset of $S^2 \times S^2$. We will improve upon this result later by invoking results of Mary Rees and Tan Lei. A reasonable way of thinking of the topological mating is to consider it as the formal mating with the rays "drawn tight" and the "empty space" containing the external rays between the two filled Julia sets is collapsed.

2.1.3 Geometric mating

Suppose we have constructed the topological mating $f_1 \amalg f_2$. We say that a rational map F is the geometric mating of the two monic polynomials f_1 and f_2 if there exists a topological conjugacy h which is orientation preserving and holomorphic on $\overset{\circ}{K}_1$ and $\overset{\circ}{K}_2$ satisfying

$$h \circ (f_1 \amalg f_2) = F \circ h.$$

In this case, we will write $F \cong f_1 \amalg f_2$.

Of course, it is entirely possible that the map F could be equivalent to the mating of more than one pair of polynomials.

Definition 2.1.5. We say a mating is *shared* if the resulting rational map comes about from two different constructions. That is to say

$$f_1 \amalg f_2 \cong F \cong g_1 \amalg g_2$$

for different choices of the pairs (f_1, f_2) and (g_1, g_2).

2.2 Thurston's Theorem

When we carry out the (formal or topological) mating of two polynomials, we want to know if the branched self-cover we have created is in some sense equivalent to a rational map, without having to search for a conjugacy to show it is a geometric mating. Fortunately, there is a nice criterion which tells us when a branched covering is not equivalent to a rational map. In what follows we take F to be a post-critically finite branched covering of degree $d \geq 2$.

Definition 2.2.1. A simple closed curve $\gamma \subset S^2$ is said to be *non-peripheral* if it satisfies the following.

- $\gamma \cap P_F = \varnothing$.
- Each connected component of $S^2 \setminus \gamma$ contains at least two points of P_F.

Definition 2.2.2. Let $\Gamma = \{\gamma_1, \gamma_2, \ldots, \gamma_n\}$ be a collection of curves in S^2. If the $\gamma_i \in \Gamma$ are simple, closed, non-peripheral, disjoint and non-homotopic relative to P_F then we say Γ is a *multicurve*. We say the multicurve is *F-stable* if for any $\gamma_i \in \Gamma$, all the non-peripheral components of $F^{-1}(\gamma_i)$ are homotopic rel $S^2 \setminus P_F$ to elements of Γ.

Given an F-stable multicurve, we can define a non-negative matrix $F_\Gamma = (f_{ij})_{n\times n}$ in the following natural way. For each i, j, let $\gamma_{i,j,\alpha}$ be the components (these are all simple, closed curves) of $F^{-1}(\gamma_j)$ which are homotopic to γ_i in $S^2 \setminus P_F$. Now define

$$F_\Gamma(\gamma_j) = \sum_{i,\alpha} \frac{1}{\deg F|_{\gamma_{i,j,\alpha}} : \gamma_{i,j,\alpha} \to \gamma_j} \gamma_i$$

where deg denotes the degree of the map.

It is a standard result from Perron-Frobenius theory (see, for example [Sen81]) that a non-negative matrix has a leading eigenvalue λ - a non-negative real eigenvalue such that all other eigenvalues have absolute value less than or equal to λ.

Definition 2.2.3. Let $\lambda(\Gamma)$ be the leading eigenvalue of the matrix F_Γ. Then the multicurve Γ is called a Thurston obstruction if $\lambda(\Gamma) \geq 1$.

We are almost ready to state Thurston's theorem. However, before we do this, we need to state the definition of an orbifold. Since we will be focussing only on the case where our Riemann surface is the Riemann sphere, we can restrict our definition to this case only. For a more general definition of orbifold see e.g [DH93] or [Mil06], Appendix E.

Definition 2.2.4 ([DH93])**.** Let f be a holomorphic branched self-covering of $\overline{\mathbb{C}}$. Then we define the ramification function $\nu\colon \overline{\mathbb{C}} \to \mathbb{N} \cup \{\infty\}$ to be the smallest function satisfying

- $\nu(z) \neq 1$ if $z \in P_F$, and
- $\nu(z)$ is a multiple of $\nu(w) \cdot \deg_w(F)$ for each $w \in F^{-1}(z)$.

Definition 2.2.5. An orbifold will be a pair (S^2, ν). In other words, the sphere paired with a ramification function.

Definition 2.2.6. The Euler characteristic of an orbifold will be given by

$$\chi(\nu) = 2 - \sum \left(\frac{1}{\nu(z_i) - 1)} \right)$$

where the sum is over all ramified points (and so is in reality a finite sum by the definition of an orbifold.) The orbifold will be called hyperbolic if $\chi(\nu) < 0$.

We note that, if an orbifold is non-hyperbolic, then the size of the postcritical set is at most 4. In all cases we will consider in this thesis, the postcritical set will be larger than 4, and so the orbifolds will be hyperbolic.

Before we state Thurston's theorem, which tells us precisely when a branched covering is equivalent to a rational map, we need to state exactly what we mean by equivalent. The notation (f, P_f) for a branched covering means that the branched covering is f and its post-critical set is P_f. Note that in applications we can replace the set P_f by some set $A_f \supset P_f$. In this case we can refer to the set A_f as the extended or generalised post-critical set.

Definition 2.2.7 (Thurston Equivalence)**.** Two postcritically finite orientation-preserving branched self-coverings with labelled critical points (F, P_F) and (G, P_G) of S^2 are said to be *Thurston equivalent* (alternatively, *combinatorially equivalent* or just *equivalent*) if there exists orientation preserving homeomorphisms $\phi_1, \phi_2\colon S^2 \to S^2$ such that

- $\phi_1|_{P_F} = \phi_2|_{P_F}$

- The following diagram commutes.

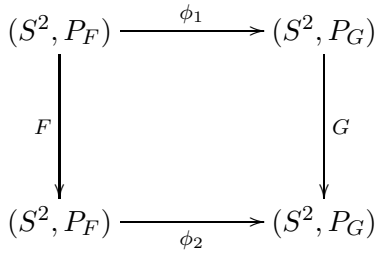

- ϕ_1 and ϕ_2 are isotopic via homeomorphisms ϕ_t, $t \in [0,1]$ satisfying $\phi_0|_{P_F} = \phi_t|_{P_F} = \phi_1|_{P_F}$ for each $t \in [0,1]$.

The final condition is often said as "ϕ_1 and ϕ_2 are isotopic rel(ative to) P_F. When two branched coverings are equivalent in this way, we write $F \cong G$.

We are now ready to state:

Theorem 2.2.8 (Thurston's Criterion)**.** *A post-critically finite branched covering $F\colon S^2 \to S^2$ of degree $d \geq 2$ with hyperbolic orbifold is equivalent to a rational map R on the Riemann sphere if and only if for any F-stable multicurve Γ we have $\lambda(\Gamma, F) < 1$. In that case the rational function R is unique up to conjugation by an automorphism of the Riemann sphere $\overline{\mathbb{C}}$ (i.e a Möbius transformation).*

Before continuing, the following theorem of Rees [Ree92] draws together the notion of formal and geometric matings.

Theorem 2.2.9. *Assume f_1 and f_2 are two postcritically finite hyperbolic polynomials. Then the formal mating $f_1 \uplus f_2$ is Thurston equivalent to a rational map $F\colon \overline{\mathbb{C}} \to \overline{\mathbb{C}}$ if and only if F is a geometric mating of f_1 and f_2.*

Although it in some sense gives a complete classification of which branched covers of S^2 are equivalent to rational maps, Thurston's theorem has a couple of problems in applications. Firstly, the proof is non-constructive, and it is not known in general how to find the rational map in the theorem. It follows that it is not always clear when two branched coverings are equivalent in the sense of Thurston. Moreover, it is not always clear whether we have a Thurston obstruction for our branched cover, since we would *a priori* have to check every single multicurve. Even though there are only finitely many homotopy classes of these curves (since the maps are post-critically finite), it would still take a large amount of time to check these curves when the size of P_F is large. Indeed, Thurston's theorem is more regularly used when trying to show that a branched cover is not equivalent to a

rational map, even though it still takes some effort to find a Thurston obstruction in many cases. However, in the degree 2 case (and also the bicritical case), we have a simpler criterion which we can use.

Definition 2.2.10. A multicurve $\Gamma = \{\gamma_1, \gamma_2, \ldots, \gamma_n\}$ is a *Levy cycle* if for each $i = 1, \ldots, n$, the curve γ_{i-1} (or γ_n if $i = 1$) is homotopic to some component γ_i' of $F^{-1}(\gamma_i)$ (rel P_F) and the map $F\colon \gamma_i' \to \gamma_i$ is a homeomorphism.

The full theory requires one to differentiate between the notion of "good", "degenerate" and "removable" Levy cycles. However, this problem only arises if they ray classes contain a point in the post-critical set, or the map is not bicritical. Since our polynomials will have super attracting orbits and our curves can be chosen to follow external rays, this terminology will not affect us - all our Levy cycles will be good Levy cycles. The notion of a Levy cycle allows us to state the following result, which is the culmination of work by Rees, Shishikura and Tan Lei, which greatly simplifies the search for Thurston obstructions [Tan92].

Lemma 2.2.11. *In the bicritical case, F has a Levy cycle if and only if it has a Thurston obstruction.*

We need to know what conditions are needed for us to be able to carry out mating and get a rational map. Once again assuming that we are dealing with polynomials with periodic critical orbits, we have following theorem, due to Mary Rees and Tan Lei. First of all we state another theorem derived from [Tan92], Theorem 4.1, which is used to prove Theorem 2.2.13. The original statement in the reference just states the equivalence of statements 1 and 4, but we will want to make use of more than this.

Theorem 2.2.12. *Let $F = f_1 \amalg f_2$ with α-fixed points labelled as α_1 and α_2 respectively. Then the following are equivalent.*

1. *F has a good Levy cycle $\Gamma = \{\gamma_1, \ldots, \gamma_n\}$.*
2. *F has a ray-equivalence class τ containing closed loops and two distinct fixed points.*
3. *$[\alpha_1] = [\alpha_2]$*
4. *In the quadratic case, f_1 and f_2 are in conjugate limbs of $\mathcal{M}$.*

The upshot of this result (in the case where the degree is 2) is the following.

Theorem 2.2.13. *The mating $f_1 \amalg f_2$ (or $f \uplus g$) is Thurston equivalent to a rational map F if and only if the parameters c_1 and c_2 do not belong to complex conjugate limbs of $\mathcal{M}$.*

In further work, Tan Lei and Shishikura [ST00] were able to say more. They proved the following generalisation of the above result.

Lemma 2.2.14. *Let F be a mating. Let $[x]$ be a periodic ray class such that $[x]$ contains a closed loop. Then each boundary curve of a tubular neighbourhood of $[x]$ generates a Levy cycle.*

This eases our task even further, since we now do not even have to check if a multicurve is a Levy cycle by the usual means, but instead can just check if a periodic equivalence class $[x]$ contains a loop. The latter is a far easier condition to check.

2.3 Properties of matings

We now discuss some of the properties of maps that come about as the result of matings. As this thesis will be focussing in the main on the mating of hyperbolic polynomials whose filled Julia set is full, we will assume that this is the case in this section. In other words, the critical points of the polynomials will be contained inside the Fatou set, and no external ray will ever meet a critical point or a pre-critical point. We will use the notation $[x]$ to denote the equivalence class of the point $[x]$ under the ray equivalence relation. We note that in general, the periodicity of a point may not be the same as the period of its class $[x]$. However, a slightly weaker result does hold.

Lemma 2.3.1. *Suppose z is a period n periodic point of f_1. Then the period of $[z]$ under the mating $f_1 \amalg f_2 = F$ is m, for some m dividing n.*

Proof. Here we use the fact that the dynamics is (topologically) preserved under the mating operation. Furthermore, we see that since $f_1^{\circ n}(z) = z$, by passing to the equivalence classes induced by mating, we have $F^{\circ n}([z]) = [z]$. Hence the period of $[z]$ divides n. □

We now study the periodic ray classes of the formal matings (in other words, we consider the branched cover created by the formal mating before all the ray classes are identified to a point). We say a mating is obstructed if the branched covering constructed in the mating has a Thurston obstruction.

Lemma 2.3.2. *Let $F = f_1 \uplus f_2$ be the formal mating of two hyperbolic polynomials which has no Thurston obstruction. Let $z_0, F(z_0) = z_1, \ldots, F^{\circ(n-1)} = z_{n-1}$ be a period n orbit of f_1 which is contained in $J(f_1)$ and has combinatorial rotation number different from 0. Then the periodic ray classes $[z_0], [z_1], \ldots, [z_{n-1}]$ are pairwise disjoint.*

Proof. Suppose there exists k with $[z_0] = [z_k]$. Then there exists a path through external rays γ from z_0 to z_k. The map $F^{\circ n}$ will take z_0 to z_0 and z_k to z_k and takes the path γ to some path γ', which is a path from z_0 to z_k. But γ' is not equal to γ, since the first return map to z_0 and z_k will permute the external rays landing there. Hence the union $\gamma \cup \gamma'$ contains a loop; and so the mating will be obstructed. This contradiction completes the proof. □

Lemma 2.3.3. *If the mating of two hyperbolic polynomials is not obstructed, each periodic ray class contains at most one periodic branch point with non-zero combinatorial rotation number.*

Proof. Let w_0 and z_0 be two periodic branch points with non-zero combinatorial rotation number, such that $[w_0] = [z_0]$. We will show that the periods of z_0 and w_0 are equal. Let the period of z_0 be n. Then the map $F^{\circ n}$ maps z_0 to itself, the periodic ray class $[z_0]$ to itself and w_0 to $w_n = F^{\circ n}(w_0)$. Then we must have $[w_0] = [z_0] = [w_n]$ and so $w_0 = w_n$ by Lemma 2.3.2. Hence the period of w_0 is divisible by n. An analogous argument shows the period of w_0 divides the period of z_0, and so the periods are the same. Denote this common period by n.

Now let γ be a path through external rays from w_0 to z_0. Since none of the rays meet a pre-critical point (since the maps f_1 and f_2 are hyperbolic), the nth iterate of γ, which we call γ', will also be a path from w_0 to z_0. Since the external rays at w_0 and z_0 are permuted under the first return map, $\gamma \neq \gamma'$, and so the curve $\gamma \cup \gamma'$ contains a loop, and so the mating is obstructed. □

2.3.1 A Combinatorial View of Periodic Ray Classes

In a combinatorial sense, we can consider a (periodic) ray class as a finite, connected (possibly labelled) graph, where the vertex set $V \subset J(f_1) \cup J(f_2)$ is the landing points of the external rays in the class and the edges E are the external rays themselves (in fact, they are the union of the external ray R^1_θ and $R^2_{-\theta}$). It is clear that each edge must connect a vertex in $J(f_1)$ to a point in $J(f_2)$. Furthermore, Lemma 2.2.14 tells us that as long as the matings are not obstructed, these graphs are acyclic; in other words they are trees. Such a visualisation allows us to talk about *endpoints*

of periodic ray classes; that is, vertices which are the end of only one edge (in the literature, these are sometimes called the leaves of the tree). Indeed, such points can be thought of as endpoints of the Julia set, since they are not cut points of the Julia set. We will sometimes use this notion when discussing ray classes, particularly when dealing with the ray classes containing cluster points in Chapters 3, 4 and 5. Essentially, this is an observation for the formal mating, before the external rays are "pulled together" and identified to a point in the topological mating. Since formal matings and topological matings of the same maps are Thurston equivalent to one another, this viewpoint is valid. We will also attempt to maintain the notion of cyclic ordering when talking about the graphs, the cyclic ordering being induced by those of the external rays with common landing points.

For example, suppose we are carrying out the mating of Douady's rabbit f_1 with the airplane f_2 and denote the α-fixed point of f_1 by α_1. The graph of $[\alpha_1]$ is topologically equivalent to the graph in Figure 2.1. This can be seen from the schematic diagram Figure 2.2.

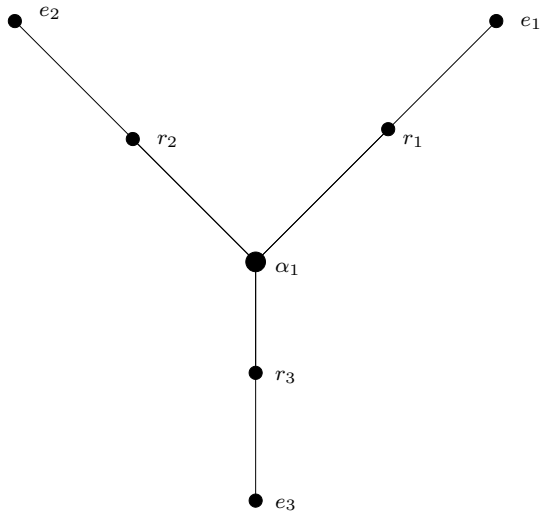

Figure 2.1: The graph which is topologically equivalent to $[\alpha_1]$.

The labellings e_i stand for endpoints (which belong to the Julia set of the rabbit) and r_i stand for rootpoints (which are the root points of critical orbit Fatou components of the airplane). As mentioned above, the endpoints are not just endpoints of the graph, but also, in some sense, endpoints of the Julia set, since the fact they are endpoints mean they cannot be biaccessible. The rootpoints are so called because they are the rootpoints of some critical orbit Fatou component. In Figure 2.2, we have labelled the external rays with their angles. It should be noted

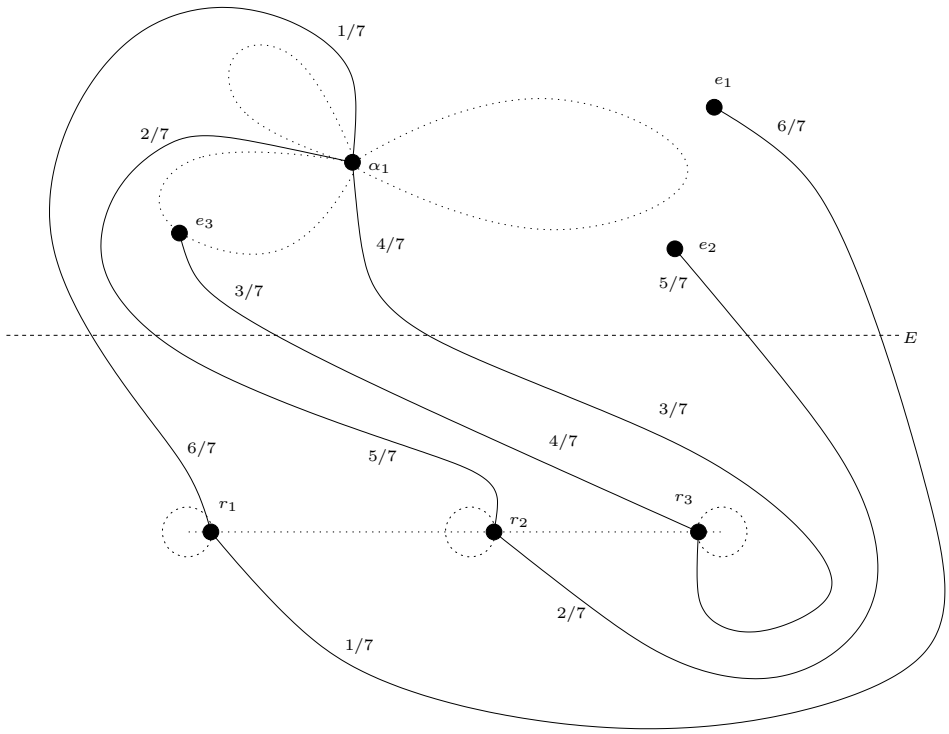

Figure 2.2: A schematic diagram showing the ray class $[\alpha_1]$. E is the equator.

that the "star" shape seen in Figure 2.1 occurs in general for the ray class of $[\alpha_1]$, the fixed point of the n-rabbit. We prove and make use of this fact in Section 4.4.

Given a vertex v in the graph Γ, we call the connected components of $\Gamma \setminus \{v\}$ the global arms at v. Note that this is entirely analogous with the definition given for Hubbard trees, and that this definition makes sense because, by Lemma 2.2.14, Γ is a tree.

As noted above, the graph has a form of rotational symmetry. This is because each global arm at α is mapped homeomorphically onto another, and so each global arm is topologically the same. We will refer to the point α as a *central vertex* of the graph (and generalise this terminology to ray classes of higher period). This terminology is not standard at all, but we use it to represent the fact that α will be fixed by the first return map to this ray class, and all the global arms are permuted around it by this first return map - in other words, α (or the point in the graph corresponding to it) is the centre of rotational symmetry.

This description of a periodic ray class is useful because it allows us to view each ray class independently. Furthermore, it means we can just focus on the topological features of ray classes, without having to worry about which external rays

actually are contained in this equivalence class. Since various properties of the ray classes persist when considering matings with cluster points, this language will allow us to make a more general statement in later chapters. Another usage of this is to help us construct curves which separate the sphere in the formal mating of two polynomials. Often we will find that the union of a ray class $[x]$ (or some subgraph of the ray class), along with some regulated arcs in the Julia sets of the two polynomials, will separate the sphere. Since rays cannot cross, this will show that certain rays cannot be in the same ray class as others.

Using this terminology, we have the following simple result. We write $F = f_1 \uplus f_2$.

Lemma 2.3.4. *Suppose a periodic ray class contains a point p which has combinatorial rotation number different from 0. Then $[p]$ does not contain any strictly pre-periodic points.*

Proof. By passing to an iterate of F if necessary, it suffices to consider the case where p is fixed. We begin with an observation. If $z \neq p$ is a periodic point, then z belongs to some global arm at p, ℓ. This arm will be periodic, say $F^{\circ k}(\ell) = \ell$. Then the period of z must be divisible by k.

Clearly p is not strictly pre-periodic, so if there exists a strictly pre-periodic point w then it must belong to one of the global arms at p. Denote this arm by ℓ and its period by k. Then since w is pre-periodic, there is some integer r so that $F^{\circ rk}(w)$ is equal to some periodic point z'. By the observation in the previous paragraph, the period of z' is mk for some m. There exists some integer s so that $ms > r$. Then $F^{\circ msk}(w) = z$ will be periodic and belongs to ℓ, and since it is in the same orbit as z', it will have period mk. Hence $F^{\circ msk}(z) = z = F^{\circ msk}(w) = z$. But this is a contradiction, since the point z has at least two pre-images in ℓ under the map $F^{\circ msk}$, but $F^{\circ msk}$ is a homeomorphism on the graph of the periodic ray class. Hence no pre-periodic point w can belong to any of the global arms at p. □

Essentially the above is just using the fact that a periodic ray shares an endpoint with another ray, then the two rays are periodic with the same period. Similarly, if a pre-periodic ray sharing an endpoint with another ray then they will have the same pre-period and period. We now have the following.

Lemma 2.3.5. *Suppose a periodic ray class contains a point p which has combinatorial rotation number different from 0. Then given any periodic orbit $\mathcal{O} = \mathcal{O}(z_0) = \{z_0, z_1, \ldots, z_{n-1}\}$, the intersection between any global arm at p and $\mathcal{O}$ contains at most one point.*

Proof. Clearly if $[p] \neq [z_i]$ for any i then the intersection of $\mathcal{O}(z)$ with any global arm will be empty. So assume without loss of generality that $[p] \cap [z_0] \neq \varnothing$. Let ℓ be a global arm at p in the periodic ray class. There exists some k so that $F^{\circ k}(\ell) = \ell$. If $\ell \cap \mathcal{O}$ is empty, then ℓ also contains no pre-images of points in $\mathcal{O}$, since otherwise some forward image of ℓ will contain a point in $\mathcal{O}$, and so $\ell \cap \mathcal{O}$ would be non-empty, a contradiction. Since ℓ contains no pre-images of points in $\mathcal{O}$, no forward iterate of ℓ can contain points of $\mathcal{O}$. Since global arms are mapped homeomorphically onto global arms, this means all the global arms have empty intersection with the orbit $\mathcal{O}$. Hence every global arm at p must contain at least one point of $\mathcal{O}$.

Suppose the global arm ℓ contains $r > 1$ elements of $\mathcal{O}$, $z_0, \ldots, z_{r-1}$. Under the first return map to ℓ, these elements must be permuted, since the orbit is periodic. Without loss of generality, we can assume the first element of $\ell \cap \mathcal{O}$ on the global arm (in terms of distance from p) is z_0. Then the second point (again, in terms of distance in the tree from p) in $\ell \cap \mathcal{O}$ is $F^{\circ k}(z_0) = z_k$ for some k. Let γ be the sub-arm from p to z_0. Then $\gamma' = F^{\circ k}(\gamma)$ is contained in ℓ and will be a path from p to z_k, since the global arm ℓ maps homeomorphically onto itself under the return maps (since the map F is a homeomorphism on the graphs of the ray equivalence classes). In particular, $z_0 \in \gamma'$. However, this means that there has to be a pre-image of z_0 in the path γ. However, by construction, there are no points in the orbit of z_0 in the interior of γ and by Lemma 2.3.4, there also does not exist any preperiodic points in γ. This contradiction means that the global arm ℓ must contain at most one point in $\mathcal{O}$. □

Remark 2.3.6. Essentially, this proof is using the fact that a homeomorphism of an interval onto itself (which fixes endpoints) cannot have any strictly pre-periodic points.

2.3.2 A Mating Criterion

It should be noted that the requirement that the rational map F is of type D (that is, the critical points belong to the basins of two distinct (super)attracting cycles) is not sufficient for F to be a mating. For example, there exists a type D degree 2 rational map with critical orbits of periods 3 and 4 which has been shown to not be equivalent to a mating (this example was found by Ben Wittner). However, there is a necessary and sufficient condition for a rational function to be equivalent to a mating. When considering the formal mating, it is clear that there is a curve which separates the critical orbits: the equator of the sphere, which corresponds to the circle where the two circles at infinity are glued together. This observation

motivates the following theorem from [ST00], where it was attributed to Thurston [Thu83], Levy [Lev85] and Wittner [Wit88].

Theorem 2.3.7. *Let F be a postcritically finite branched covering of degree d. Assume that F has no degenerate Levy cycle. Then F is equivalent to the mating of two polynomials f, g if and only if there is a closed curve $\gamma \subset S^2 \setminus P_F$ such that $F^{-1}(\gamma) = \gamma'$ is again a single closed curve and γ' is isotopic to γ rel P_F with the same orientation. Moreover, given the curve γ, the two polynomials f, g are uniquely determined.*

The curve γ in the above theorem will be called an *equator* for the mating $f \amalg g$. It follows that if a mating is shared then there is more than one equator for a rational map F. In Chapters 4 and 5, we will find the equators on rational maps which have clusters.

2.4 The Mapping Class Group

Given a surface S, it is possible to associate to S a group which can be thought of as the equivalence classes of isotopies on the surface. This will be important in Chapters 4 and 5, where we will require knowledge of the mapping class groups of the disk and annulus respectively. We include this section here since we will use the results when trying to show Thurston equivalence of two rational maps.

Let S be a surface with boundary ∂S. Denote by $\mathrm{Homeo}^+(S)$ the group of orientation-preserving homeomorphisms of the surface which fix ∂S pointwise, and define $\mathrm{Homeo}_0^+(S)$ to be those elements of $\mathrm{Homeo}^+(S)$ which are isotopic to the identity. $\mathrm{Homeo}_0^+(S)$ is a normal subgroup of $\mathrm{Homeo}^+(S)$, and so we get the following.

Definition 2.4.1. The Mapping Class Group of a surface S, denoted $\mathrm{MCG}(S)$ is the quotient

$$\mathrm{MCG}(S) = \mathrm{Homeo}^+(S)/\mathrm{Homeo}_0^+(S).$$

The mapping class group allows us to discuss isotopy classes of homeomorphisms on a surface. We state the following well known results without proof.

Proposition 2.4.2. *Let $\overline{\mathbb{D}}$ be the closed disk and $\overline{\mathbb{A}}$ be a closed annulus. Then*

1. $\mathrm{MCG}(\overline{\mathbb{D}}) = 0$,
2. $\mathrm{MCG}(\overline{\mathbb{A}}) \cong \mathbb{Z}$.

Furthermore, the mapping class group of an annulus is generated by the Dehn twist around the core curve in the annulus.

Chapter 3

Clustering in the Mating Operation

We now discuss what it means for a rational map to have a cluster point, or a cluster cycle. The original motivation for this work was to look at how the period two cluster case behaves compared to the period one cluster case. In fact, since there are some marked differences between the two, in some cases it is necessary to alter a definition depending on whether or not we are dealing with the period 1 or period 2 cluster case. In this chapter we will discuss the properties of clustering that holds in maps with cluster cycles of arbitrary period. However, it is perhaps evidence of the complexity of the problem increasing with the period that this chapter is so short. Calculations suggest that one needs to introduce different definitions depending on the period. We will focus on these differing definitions in the following chapters. For now, we concern ourselves with saying as much as we can for clusters of arbitrary period.

We remark that a bicritical map will only have one cluster cycle. This is because each attracting cycle must attract at least one critical point. Since the maps will have exactly two critical points, there will only be two attracting cycles.

3.1 Definitions

Definition 3.1.1. The following is the terminology we will use to describe certain Fatou components of a post-critically finite rational map F.

- A *critical (point) component* will be a Fatou component containing a critical point of F.

- A *critical value component* will be a Fatou component containing a critical value of F.
- A *critical orbit component* will be a Fatou component which contains an iterate of a critical point of F.

Note that critical components and critical value components are critical orbit components.

We will sometimes refer to a critical orbit component in a cluster as being provided by a critical point c_i. When we say this, we mean the component is a critical orbit component containing an iterate of the critical point c_i.

It is a well known fact (using the Riemann-Hurwitz formula) that a quadratic rational map on $\overline{\mathbb{C}}$ has precisely two critical points (for example, polynomials of the form $z \mapsto z^2 + c$ have critical points at 0 and ∞). We say that a rational map is of type D if the two critical points belong to the attracting basins of two disjoint periodic orbits. This terminology is due to Milnor, [Mil93], although it was Rees who originally classified the hyperbolic components of quadratic rational maps, and she referred to type D maps as type IV maps. We note that hyperbolic rational maps formed by mating are of type D. The same terminology can be applied to bicritical rational maps.

Definition 3.1.2. Let $F\colon \overline{\mathbb{C}} \to \overline{\mathbb{C}}$ be a bicritical rational map of type D with the property that the two critical orbits belong to superattracting orbits with the same period. Then a cluster point for F is a point in $J(F)$ which is the endpoint of the angle 0 internal rays of at least one critical orbit Fatou component from each of the two critical cycles.

We will define a cluster to be the union of the cluster point and the Fatou components meeting at it. The period of the cluster will be the period of the cluster point.

The star of a cluster will be the union of the cluster point and the associated 0 internal rays, including the points on the critical orbit.

Note that the star of a cluster is invariant under the first return map to the cluster. This allows us to define the notion of combinatorial rotation number of a cluster (see below). We will actually find it far easier to work with the star of a cluster than with the actual cluster itself. One quick observation is that the star of a cluster must map homeomorphically onto its image. This is because the 0-internal rays map homeomorphically onto their images (which are also 0-internal rays) under the rational map. It should also be noted that if we are not in the degree two case,

there is some sense of ambiguity as to what the 0-internal ray is. However, we comfort ourselves with the notion that if a rational map has the dynamics necessary to have clustering, it is possible to choose the internal rays of the critical orbit Fatou components in such a way so that the map does indeed have a periodic cluster cycle.

Example 3.1.3. Consider the mating of Douady's rabbit and the aeroplane polynomial (both polynomials have a superattracting orbit of period 3, and are post-critically finite). The result of this mating can be seen in Figure 3.1. This map has a fixed cluster point. In the figure, the basins of one of the critical points is white, the other basin is black. The cluster point is in the bottom right of the picture; its pre-image in the top left.

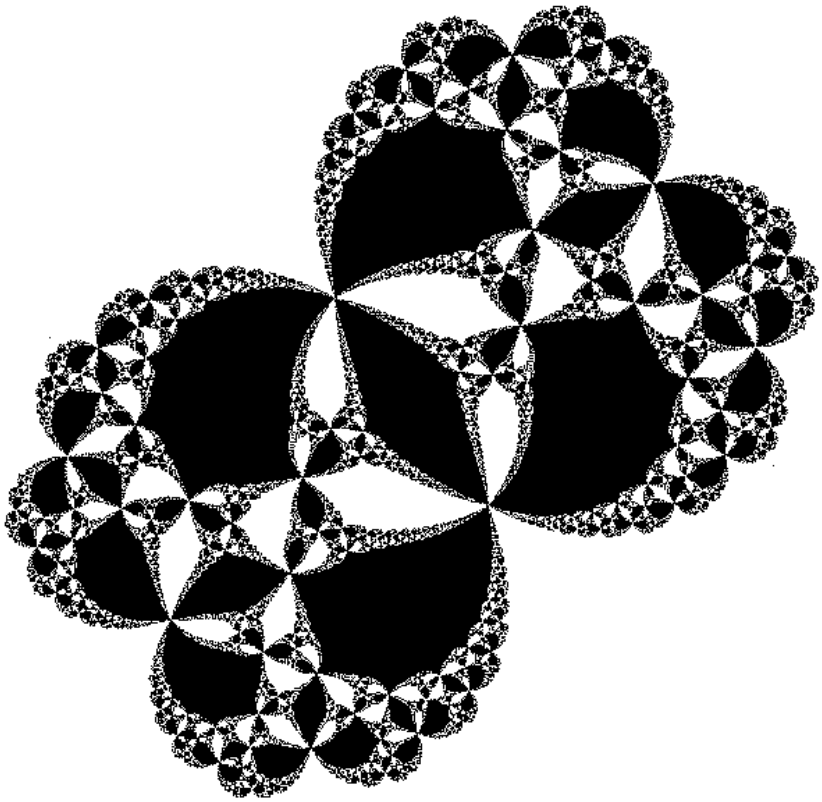

Figure 3.1: An example of a map with a cluster point.

There is an obvious way of creating a cluster through mating of polynomials. For example, in the period 2 case, take f_1 to be the "double" rabbit with internal address $1 \to 2 \to 2n$. Then there is a period 2 cycle around which the critical orbit components are already clustered (but note this is not strictly a cluster point).

Then there are n external rays landing at the "cluster point" where the critical point component clusters, see Figure 3.2. We then need to fill in these gaps at this period two cycle with critical orbit Fatou components from a second map, by carrying out a mating. In the one cluster case, we can do a similar construction with the n-rabbit (with angled internal address $1_{p/n} \to n$) (see Figure 3.3). Indeed, we will show in the one cluster case that every mating which admits a fixed cluster point is the mating of an n-rabbit with some other map with certain combinatorial characteristics. The situation is more complicated in the period 2 cluster case, as we will discuss in Chapter 5. As the period increases, we conjecture that it gets more and more complicated, see the discussion in Appendix F.

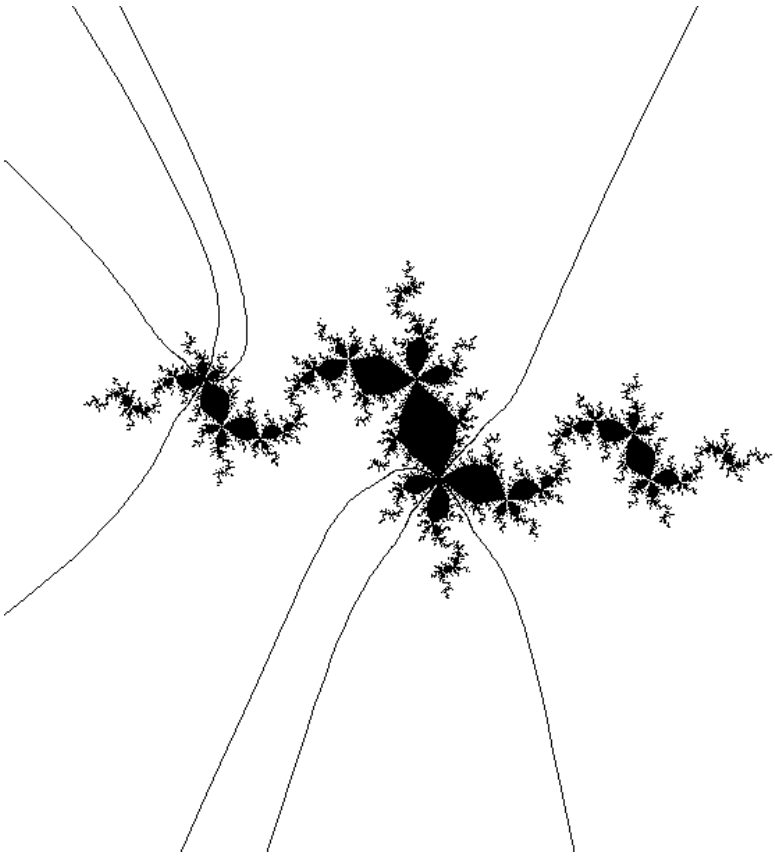

Figure 3.2: A "double rabbit" and some rays landing on the period 2 cycle.

The combinatorial rotation number is one of the two pieces of combinatorial data (the other is the critical displacement) we will use to classify our clustered matings. Unlike the critical displacement, the definition holds for cluster points of any period.

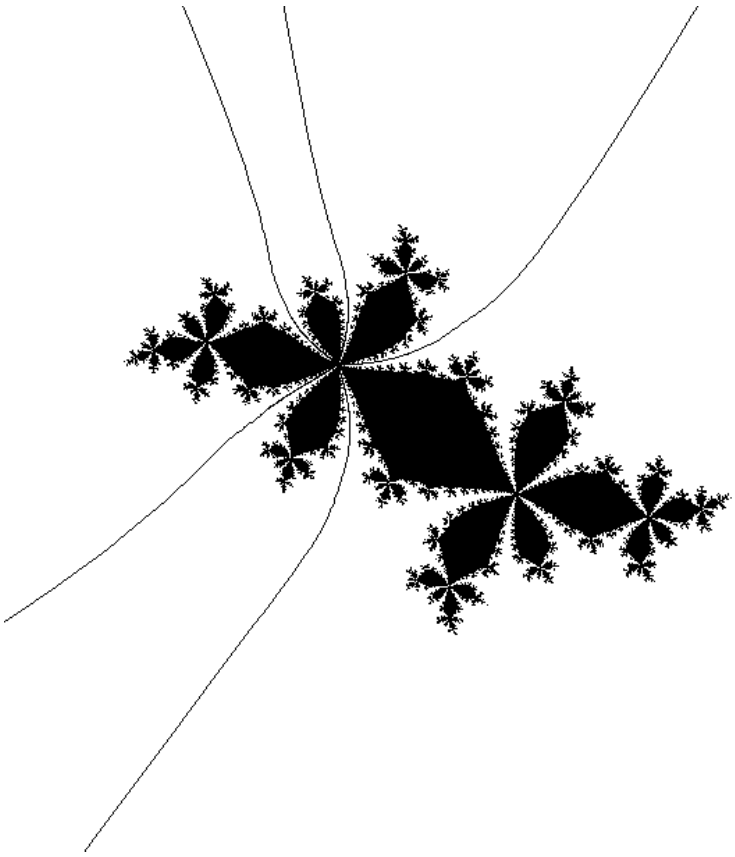

Figure 3.3: An n-rabbit and some rays landing on the α-fixed point.

If p is a period k cluster point of the bicritical rational map F, then by definition it is the landing point of a family of internal rays. The map $F^{\circ k}$ is a local homeomorphism which fixes the cluster point and the family of internal rays are invariant under this map. We then define the combinatorial rotation number of the cluster point by using Definition 1.4.3. Since the combinatorial rotation number is not dependent on the choice of point in the periodic cycle, we have defined the combinatorial rotation number of the cluster cycle.

Though we have not yet defined the critical displacement, we include the following definition here since the definition will hold in both the period one and period two cases. In higher period cases, it is likely that we would also have to include the data which says how many times we have to iterate forward from the cluster containing the critical point of f_1 until we reach the cluster containing the critical point of f_2(though this data can be perhaps included in the definition of the combinatorial displacement, see Appendix F. This is just one of the reasons as to

why there is increasing complexity when moving from the period 2 to the period three case. Informally, the critical displacement will represent the gap, in terms of combinatorial distance, between the critical points in the cluster cycle.

Definition 3.1.4. Let F be a bicritical rational map with a periodic cycle of clusters with combinatorial rotation number ρ and critical displacement δ (see Definition 4.1.1 in the one cluster case and Definition 5.1.4 in the two cluster case). Then the pair (ρ, δ) will be called the combinatorial data of the cluster cycle.

Since a map F has only one cluster cycle in the bicritical case, we will refer to the combinatorial data of F as the combinatorial data of the cluster cycle.

It is going to be useful to show that, in some sense, combinatorial rotation number is preserved under the mating operation. The most common definition of combinatorial rotation number for polynomials is derived from the cyclic permutation of external rays landing at periodic points [Mil00b]. However, our more general definition was made by noticing that external rays are an example of *invariant curves*, (families of) curves which are fixed under iteration. The issue with external rays is there is not an immediate analogue for non-polynomial rational maps, and we will want to use a definition which can be applied equally well in both polynomial and non-polynomial cases. In practice, we will be using a combination of the permutation of local arms in the Hubbard tree at a periodic point and the internal rays of angle 0 inside periodic Fatou components which have a periodic point on the boundary.

3.2 Structure of the clusters

The following section includes some simple facts about the clusters that allow us to see how the critical orbit components of the critical points c_1 and c_2 come together. There are two important points: firstly the two maps provide precisely the same number of components to each cluster; secondly, the components alternate between components from f_1 and components from f_2 as one checks cyclic ordering around the cluster point. Since the critical points belong to the Fatou set, both these facts are perhaps intuitively obvious if one recalls that the rational map F must map a neighbourhood of each cluster point homeomorphically onto the neighbourhood of its image.

Lemma 3.2.1. *Suppose a bicritical rational map has a period k cluster cycle. Then the period of the two critical orbits is nk for some $n \geq 1$ and each orbit has precisely n critical orbit Fatou components in each cluster.*

Proof. It is sufficient to show that each cluster in the periodic cycle contains the same number of Fatou components in it. However, we note that the star of each cluster maps homeomorphically onto its image star. Hence the number of Fatou components from the orbit of each critical point must be equal in each cluster. Since the critical points have the same period by assumption, the periods of the critical orbit Fatou components are also equal and so equal to nk for some $n \geq 1$. Furthermore, we see that each critical orbit must contain precisely n critical orbit Fatou components in each cluster. For if one cycle contained $m \neq n$ components then its image must also contain m components, once again because the stars map homeomorphically. □

Proposition 3.2.2. *The ordering of Fatou components in a cluster is alternating. That is, a Fatou component provided from the first critical point c_1 must be between two Fatou components provided by the orbit of the second critical point c_2.*

Proof. Suppose that two components from c_1, U_0 and U_1 appear next to each other in the cyclic ordering, with U anticlockwise from U_1 in the cyclic ordering around the period p cluster point c. The maps $F^{\circ pm}$ (for $m \in \mathbb{N}$) fix the cluster point c, and map U_0 and U_1 onto Fatou components provided by c_1. In particular, there exists a k such that $F^{\circ pk}(U_0) = U_1$. By the fact that cyclic ordering of components around the clusters is maintained under F and its iterates, $U_2 = F^{\circ pk}(U_1) = F^{\circ 2pk}(U_0)$ is the component immediately clockwise from $F^{\circ pk}(U_0) = U_1$. Since U_2 is the image of a Fatou component provided by c_1, it must itself be a component provided by c_1. Inductively, if $U_r = F^{\circ rpk}(U_0)$ is a component provided by c_1, then the component immediately clockwise of U_r in the cyclic ordering, $U_{r+1} = F^{\circ pk}(U_r) = F^{\circ (r+1)pk}(U_0)$ is a component provided by c_1. Hence all components in this cluster are provided by c_1, which is a contradiction to Lemma 3.2.1. □

In the following chapters, we will be paying close attention to rational maps with clustering that come about as the result of matings of polynomials. This description is purposefully ambiguous: we do not necessarily state which mating is being considered. This is because the rational map to which the mating is equivalent is not dependent on which mating is chosen (Theorem 2.2.9). However, it is clear that the definition of a cluster point requires us to consider the topological mating - the case where the two filled Julia sets are actually glued together. However, many of the results will make use of the structure of periodic ray equivalence classes and "ray-blocking" techniques, which by necessity force us to consider the formal mating, before the rays are drawn tight and the filled Julia sets glued together. With this in mind, we will often use the notation $F \cong f_1 \amalg f_2$ to discuss the mating of two

polynomials. This will mean that the rational map F is Thurston equivalent to the topological mating of f_1 and f_2.

Chapter 4

Fixed Cluster Points

In this chapter we will outline the behaviour of maps which have a fixed cluster point. In the first section, we define the critical displacement and show that the critical points cannot be adjacent to one another in the cluster. In the second section, we suppose that we have a rational map $F = f \perp\!\!\!\perp h$. We ask ourselves what properties can be stated for the two maps f and h. We find that one of the maps has to be an n-rabbit. The properties of the complementary map are not so exact, but we can still describe them using very simple combinatorial terminology.

Section 4.3 is concerned with the classification of rational maps with a fixed cluster point. We will show that the combinatorial data of the cluster completely defines a degree d bicritical rational map in the sense of Thurston. This result, coupled with the results from the previous section, will show us that degree 2 rational maps with fixed cluster points can be obtained from the mating of two monic polynomials. In fact, we have the following theorem.

Theorem 4.0.3. *Suppose that F is a bicritical rational map with a fixed cluster point and the combinatorial rotation number is p/n. Then F is the mating of an n-rabbit with angled internal address $1_{p/n} \to n$ and another map h. In the degree 2 case, h has an associated angle with angular rotation number $(n-p)/n$.*

The final section focuses on the notion of symbolic dynamics of quadratic polynomials. Here we show that there are, at least in the simple cases demonstrated here, patterns in the internal addresses of the non-rabbit maps in the matings which create rational maps with fixed cluster points. In higher degrees, it is interesting to note that the exact same patterns occur, at least in preliminary calculations.

4.1 Definitions

Recall that the star of a cluster is defined to be the union of the cluster point with the 0-internal rays of the periodic Fatou components meeting at the cluster point. There is a natural cyclic ordering of these internal rays around the cluster point. We call the internal rays the arms of the star at the cluster point c.

Definition 4.1.1. Let F be a rational map with a fixed cluster point. Label the endpoints of the star as follows. Let e_0 be the first critical point, and label the remaining arms in anticlockwise order by $e_1, e_2, \ldots, e_{2n-1}$. Then the second critical point is one of the e_j, and we call j the critical displacement of the cluster of F. We denote the critical displacement by δ.

Remark 4.1.2. We note that an equivalent definition is to measure the combinatorial distance between the critical values. Sometimes this will be a more useful definition, especially when considering rational maps constructed by mating.

Lemma 4.1.3. *The critical displacement is an odd number.*

Proof. This follows easily from Proposition 3.2.2. □

First, a comment on the critical displacement. Since the definition requires a choice to be made (in other words, since we are considering rational maps with labelled critical points), it seems that a rational map with a fixed cluster point and critical orbits of period n has two possible combinatorial data: (ρ, δ) could be thought of as having combinatorial data $(\rho, 2n - \delta)$ if a different choice was made. This will not concern us greatly, since our use of combinatorial data will be to prove combinatorial equivalence of rational maps with labelled critical points.

The following result (Proposition 4.1.5) shows that not all combinatorial data are obtained by rational maps. We first state a preliminary lemma from [Mil00a], where it appears as Lemma 3.4.

Lemma 4.1.4. *Let F be a bicritical rational map of degree d. Let $A \subset \overline{\mathbb{C}}$ be a region bounded by a simple closed curve which passes through neither critical value. Then the pre-image of A under F can be described as follows.*

1. *If A contains no critical value, $F^{-1}(A)$ consists of d disjoint simply-connected regions bounded by d disjoint simple closed curves.*
2. *If A contains just one critical value, $F^{-1}(A)$ is a single simply connected region bounded by a simple closed curve and maps onto A by a ramified d-fold covering.*

3. *If A contains both critical values, $F^{-1}(A)$ is a multiply connected region with d boundary curves, and maps onto A by a ramified d-fold covering.*

Proposition 4.1.5. *Suppose F is a bicritical rational map with a fixed cluster point, where both critical points have period n. Then the two critical point components cannot be adjacent. In other words, the critical displacement cannot be 1 or $2n-1$.*

Proof. We will assume, to obtain a contradiction, that U_0 is the adjacent component which is anticlockwise of V_0 in the cyclic ordering of components around the cluster point c, and that U_0 and V_0 are the components containing the critical points of F. We will use the notation that $U_k = F^{\circ k}(U_0)$ and $V_k = F^{\circ k}(V_k)$ to label the critical orbit components.

We begin with a description of the critical Fatou components of the map F. The cluster point c is fixed and belongs to $\partial U_1 \cap \partial V_1$. Since F is d-to-one on U_0 and V_0 and because they are Jordan domains (Theorem 1.5.2), there must exist pre-periodic pre-images ω_i, $i = 1, \ldots, d-1$ of c on $\partial U_0 \cap \partial V_0$. We label these points in order, so that travelling anticlockwise around ∂U_0 from c, the first point we meet is ω_1, then ω_2 and so on until we label the pre-image clockwise from c by ω_{d-1}. Another way of regarding the ω_j is that ω_j is the landing point of the internal ray of angle j/d. From this discussion, we see that $\partial U_0 \cap \partial V_0$ contains at least d points.

Denote the critical values of F by $v_1 \in U_1$ and $v_2 \in V_1$. First, consider the "V-shaped" curve Λ_1 formed by the following the 0-internal ray going from c towards v_1, forming a small anticlockwise loop around v_1 and then returning to c along the same 0-internal ray. It then follows the 0-internal ray from c towards v_2, forms a small anticlockwise loop around v_2 and then returns back to c. By construction, Λ_1 is contained entirely in $\overline{U_1} \cup \overline{V_1}$: see figure 4.1 for Λ_1 and its image $F(\Lambda_1) = \Lambda_2$ (dashed line).

We will use the curve Λ_1 to construct a Levy cycle. To do this, we modify Λ_1 by perturbing it away from c to form a simple closed curve γ_1 which separates the two critical values from the rest of the post-critical set and the cluster point c. Now, since F is one-to-one on the critical value Fatou components, it maps γ_1 homeomorphically to a curve γ_2. Similarly, F maps γ_2 homeomorphically to some curve γ_3 and so on inductively until we have constructed $\gamma_n = \gamma_0$, which separates the critical points c_1 and c_2 from the rest of the post-critical set. Indeed, notice that each γ_k separates the two points $F^{\circ k}(c_1)$ and $F^{\circ k}(c_2)$ from the rest of the post-critical set, and $\gamma_k \cap P_F = \varnothing$, hence each γ_k is a simple, non-peripheral, closed curve and they are pairwise disjoint (Figure 4.2). We add that, furthermore, the curves γ_i are constructed so that the intersection between γ_i and $U_j \cup V_j$ is empty unless $i = j$ (taken modulo n).

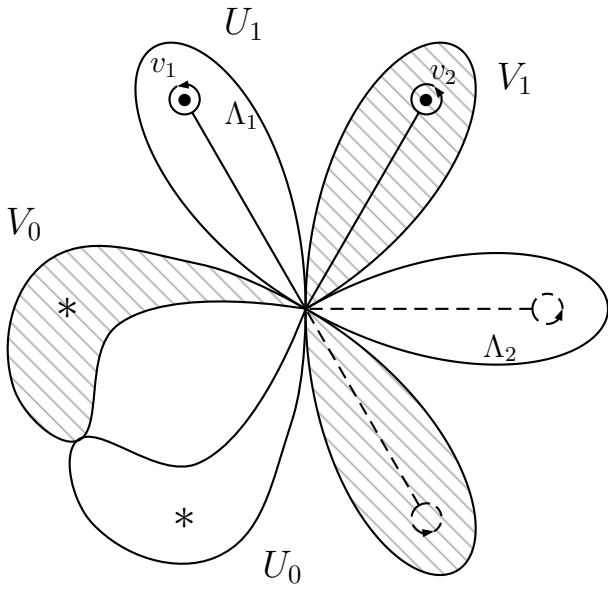

Figure 4.1: The "V-shaped" curve Λ_1.

We now will use the curve Λ and its iterates as this will help illuminate the behaviour of the pre-images of the γ_k. As long as $k \neq 1$, the pre-images of Λ_k are simple to visualise. One pre-image is contained in $\overline{U_{k-1}} \cup \overline{V_{k-1}}$, and is in fact equal to Λ_{k-1}. There are $d-1$ other pre-images (since the map is degree d) Λ_{k-1}^j, $j = 1, \ldots, d-1$, which are each contained in $\overline{U}_{k-1}^j \cup \overline{V}_{k-1}^j$, where the $\overline{U}_{k-1}^j$ and $\overline{V}_{k-1}^j$ are pre-periodic (but not periodic) Fatou components. Note that this is the only possible situation, as there is only one pre-image of c on the boundary of each component $U_{k-1}, U_{k-1}^j, V_{k-1}$ and V_{k-1}^j, and $c \in \partial U_{k-1} \cap V_{k-1}$.

The case $k = 1$ is slightly more complicated, since Λ_1 is contained in $\overline{U_1} \cup \overline{V_1}$. Since U_1 and V_1 are critical value components, they are mapped to in a d-to-one way by the critical point components U_0 and V_0. The pre-image $F^{-1}(\Lambda_1)$ consists of a small loop round the critical point c_1 which is connected to each ω_j by the internal ray of angle j/d in U_0, and a small loop around c_2 which is connected to the ω_j by the internal rays of angle $j/(d-1)$ in V_0.

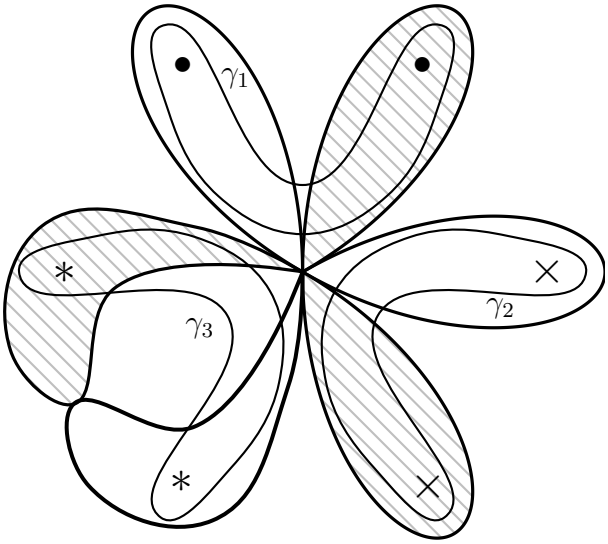

Figure 4.2: The multicurve Γ.

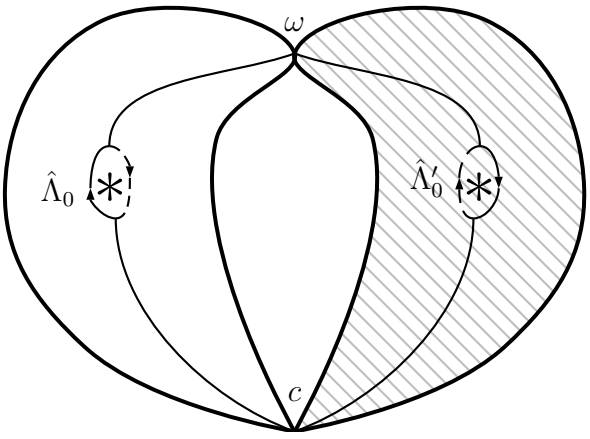

Figure 4.3: The curves $\hat{\Lambda}_0$ (continuous line) and $\hat{\Lambda}_0$ (dashed line).

Now we can show that $\Gamma = \{\gamma_1, \gamma_2, \ldots, \gamma_n\}$ is a Levy cycle. Note that the main difference between the Λ_k and the γ_k is that the γ_k are constructed so that they are simple closed curves, and the γ_k do not pass through the cluster point c so that we can get the pairwise disjointness required for a Levy cycle. We need to consider the pre-images of each γ_k ($k \neq 1$). One pre-image will be γ_{k-1}, by construction. The other pre-images are pairwise disjoint (and disjoint from γ_{k-1}) by Lemma 4.1.4 and, being small perturbations of the Λ_{k-1}^j (which did not separate the post-critical set), will be peripheral.

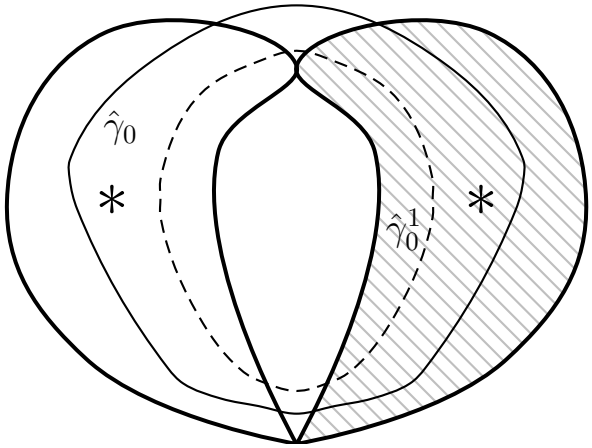

Figure 4.4: The curves $\hat{\gamma_0}$ and $\hat{\gamma}_0^1$ (dashed line) in the case $d = 2$.

So it just remains to consider the pre-image of γ_1. All pre-images are disjoint from all critical orbit Fatou components except for U_0 and V_0. We will show that one pre-image of γ_1 is homotopic to γ_0 and the other $d-1$ pre-images are all peripheral. Let A be the component of $\overline{\mathbb{C}}\backslash\gamma_1$ which contains v_1 and v_2. By Lemma 4.1.4, $F^{-1}(A)$ has d boundary curves, and these boundary curves are the components of $F^{-1}(\gamma_1)$. The region $F^{-1}(A)$ must contain the critical points. Hence one of the boundary curves, $\hat{\gamma}_0$, will separate the critical points from the rest of the post-critical set and the other $d-1$ boundary curves, $\hat{\gamma}_0^j$, $j = 1, \ldots, d-1$, (labelled so that $\hat{\gamma}_0^j$ is the curve which separates the critical points from ω_j) will be peripheral, see Figure 4.4.

To show Γ is a Levy cycle, it only remains to show that $\hat{\gamma}_0$ is homotopic to $\gamma_0 = \gamma_n = F^{\circ(n-1)}(\gamma_1)$. Both γ_0 and $\hat{\gamma}_0$ separate the critical points c_1 and c_2 from the connected set

$$X = \bigcup_{i=1}^{n-1} (\overline{U}_i \cup \overline{V}_i).$$

Notice that $P_F \setminus \{c_1, c_2\} \subset X$ and that $\overline{\mathbb{C}}\setminus X$ is simply connected. So the two curves γ_0 and $\hat{\gamma}_0$ are both homotopic to the boundary of a neighbourhood of X rel P_F. Hence they are homotopic to each other and so Γ is a Levy cycle. Hence F is not equivalent to a rational map. □

4.2 Properties of f and h

The aim of this section is to prove the following.

Theorem 4.2.1. *Suppose $F = f \perp\!\!\!\perp h$ is a rational map with a fixed cluster point*

with combinatorial rotation number p/n. Then precisely one of f and h is an n-rabbit, with angled internal address $1_{p/n} \to n$. In the degree 2 case, the other map has an associated angle with angular rotation number $(n-p)/n$

Moreover, in the degree 2 case, if h is not an n-rabbit and is a map with an associated angle that has angular rotation number $(n-p)/n$, then if f is the n-rabbit with internal address $1_{p/n} \to n$, the mating $f \perp\!\!\!\perp h$ will have a fixed cluster point.

We will also show that all combinatorial data, save for the case where the critical displacement is 1 or $2n-1$, can be obtained from matings.

4.2.1 The classification of f

We now start to discuss which pairs of maps (f_1, f_2) can be mated to create a rational map with a fixed cluster point. In fact, in this case, there is a very simple criterion for one of the maps; it must be an n-rabbit.

Proposition 4.2.2. *Let f_1 and f_2 be monic unicritical polynomials with a period n superattracting orbit. Suppose $F \cong f_1 \perp\!\!\!\perp f_2$ is a rational map that has a fixed cluster point. Then one of f_1 or f_2 (by convention, we will pick this to be f_1) is an n-rabbit; that is, it has internal address $1 \to n$.*

Proof. First, we remark that a quadratic rational map has three fixed points, counting multiplicities. We know that the β-fixed points of f_1 and f_2 are identified under mating (and are not identified with any other points). Furthermore, α_1 and α_2, the α-fixed points of f_1 and f_2 respectively must correspond to a fixed point of F. Since the cluster point is, by hypothesis, a fixed point, we have one of two cases: either (i) the two α-fixed points are identified under mating (and the cluster point is made by identifying non-fixed points) or (ii) one of the α-fixed points becomes the cluster point.

If we have case (i), we see that this is in fact statement 3 of Theorem 2.2.12. This means that the mating has a Levy cycle and so the mating is obstructed. So we are left to consider case (ii). Let the cluster point be $[\alpha_1]$. α_1 is the landing point for k external rays of angles $\theta_1, \ldots, \theta_k$ which are permuted under f_1; in other words, α_1 has a non-zero combinatorial rotation number. We remark briefly that k is at most n, since otherwise the map f_1 would have an α-fixed point with rotation number r/k for some r, and so the angled internal address would begin $1_{r/k} \to k$, but this is a contradiction since $k > n$ and the internal address is a strictly increasing sequence whose final entry is n. So $k \leq n$. The graph for the ray equivalence class $[\alpha_1]$ is a tree (or else the mating would be obstructed, and F would not be equivalent to a

rational map). There are k local arms at α_1 in this graph, corresponding to each of the external rays which land there. Furthermore, the map F (considered as the formal mating) permutes these arms at α_1, and each arm will map homeomorphically since no arm contains a critical point, as the polynomials f_1 and f_2 are hyperbolic.

Each arm must therefore contain the root points of n/k critical orbit Fatou components of f_1 and f_2. By Lemma 2.3.5, $n/k = 1$ and so $k = n$. Hence the map f_1 has α_1 with combinatorial rotation number of the form p/n and so the internal address is $1 \to n$. By Proposition 1.8.1, f_1 is an n-rabbit. □

Proposition 4.2.3. *Using the notation from the previous proposition, the combinatorial rotation number of the cluster point is the same as the combinatorial rotation number of the α-fixed point of the n-rabbit. In other words, if the cluster point has rotation number p/n, the angled internal address of f_1 is $1_{p/n} \to n$.*

Proof. By Proposition 4.2.2, the map f_1 is an n-rabbit and so has angled internal address

$$1_{\frac{p}{n}} \to n$$

for some p coprime to n. This means the arms of the star which belong to the critical orbit of the first critical point (that coming from the rabbit f_1) permute the arms with rotation number p/n. In order to maintain the cyclic order, all arms of the star must be permuted cyclically with rotation number p/n, which proves the proposition. □

So it turns out from the previous two results that in the fixed cluster point case the map f_1 is completely defined by the period and rotation number of the cluster. Informally, this is because the n-rabbit with internal address $1_{p/n} \to n$ has both the correct period of the critical cycle and also has a fixed point with the correct rotation number. Furthermore, it is the only map that has these two properties. Clearly, the choice of the second map, h, if it admits a clustered mating with f, will determine the critical displacement of the resultant rational map. We will investigate the properties of this map h in Section 4.2.2. As stated above, by convention we will write the first map in the mating to be the n-rabbit found in this section. In other words, when we write $F \cong f \perp\!\!\!\perp h$ and F has a fixed cluster point, we will assume that f is an n-rabbit. This again follows from the fact that we are discussing rational maps with labelled critical points, so by convention, we can label the critical points so that the critical point corresponding to the n-rabbit polynomial is the first critical point.

4.2.2 The classification of h

A sensible question to ask is: given the map f, with internal address $1_{p/n} \to n$, and the condition that $F = f \amalg h$ has a fixed cluster cycle, what properties are satisfied by the map h? Furthermore, if a map has these given properties, will it necessarily admit a clustered mating with f? It turns out we can give a simple combinatorial property for the map h which gives a necessary and sufficient condition for it to create a clustered mating with f. See Section 4.4 for more on the combinatorics of the map h. In this section we will be focussing on the degree 2 case, but it is believed that the generalisation to the degree d case should be fairly simple.

Definition 4.2.4. Let $\theta \in \mathbb{S}^1$ be periodic of period n, so that $\theta = a/(2^n - 1)$ for some a. Label the angles $2^j\theta$, $j = 0, \ldots, n-1$ cyclically by $\theta_1, \theta_2, \ldots, \theta_n$ with $\theta_1 = \theta$. Then we say that the angle θ has angular rotation number p/n if

$$2\theta_k = \theta_{k+p \mod n}$$

for each k.

Remark 4.2.5. Not every angle has an angular rotation number. We give a couple of examples of angles that do admit an angular rotation number and one that does not. Furthermore, in light of the discussion in the next chapter, this definition could be called the 1-angular rotation number, but we suppress this notation for now.

The author has recently discovered that the notion of angular rotation number was discussed in [BS94], in a slightly different context. In the aforementioned article, it was shown for any p/q, that there is a unique orbit of angles which have angular rotation number p/q under angle doubling, and these angles correspond to the angles of the rays landing at the α-fixed point of an n-rabbit. It is clear that this uniqueness property is no longer true under the map $t \mapsto dt$ on the circle. However, if we add the condition that the orbit must be contained in some arc $(k/(d-1), (k+1)/d-1)$ on the circle, then we get uniqueness again, and the angles in the orbit will once again correspond to the angles of rays landing at the α-fixed point of an n-rabbit.

First we give a simple example.

Example 4.2.6. Let $\theta = 1/(2^n - 1)$. Then the ordering of the angles on $\mathbb{S}^1$ is

$$0 < \theta_1 < \theta_2 < \cdots < \theta_{n-1} < \theta_n < 1.$$

Then the angular rotation number of θ is $1/n$. Indeed, the map corresponding to this angle is an n-rabbit which has an α-fixed point with combinatorial rotation

number $1/n$. Since all the iterates of the external ray of angle θ land at this point, the combinatorial rotation number at α induces the angular rotation number of the corresponding map. This is in fact true in general: if the iterates of θ all land at the same (fixed) point then the angular rotation number of the angle is the same as the combinatorial rotation number of the fixed point (see Lemma 4.2.9).

A more complicated example is given next.

Example 4.2.7. Let $\theta = 55/127$. Then the iterates of θ (taken as multiples of $1/127$) are (subscripts denoting dynamical order):

$$\theta_1 = 55,\ \theta_2 = 110,\ \theta_3 = 93,\ \theta_4 = 59,\ \theta_5 = 118,\ \theta_6 = 109,\ \theta_7 = 91,$$

which, when written in cyclic ordering (starting with θ_1) is

$$\theta_1 < \theta_4 < \theta_7 < \theta_3 < \theta_6 < \theta_2 < \theta_5.$$

This means that θ has angular rotation number $5/7$.

Finally, we consider an angle which doesn't have an angular rotation number. We will see later on that these cases are precisely the maps which cannot create a rational map with a fixed cluster point under mating.

Example 4.2.8. Let $\theta = 15/63$. Then the iterates of θ (taken as multiples of $1/63$) are

$$\theta_1 = 15,\ \theta_2 = 30,\ \theta_3 = 60,\ \theta_4 = 57,\ \theta_5 = 51,\ \theta_6 = 39.$$

Starting with θ_1, we get the cyclic ordering on the circle of these angles is given by

$$\theta_1 < \theta_2 < \theta_6 < \theta_5 < \theta_4 < \theta_3.$$

We see then that $\theta = 15/63$ does not have an angular rotation number.

Lemma 4.2.9. *Let f be an n-rabbit with combinatorial rotation number at the α-fixed point p/n. Then the angular rotation number of θ_1 and θ_2, the angles landing at the root point of the hyperbolic component containing f, is p/n.*

Proof. All the iterates of θ_i have corresponding rays landing at the same point, α. Then the external rays at this point are permuted with combinatorial rotation number p/n, and thus the angular rotation number of θ_i will be p/n. □

The following result is true in degree 2. We state the conjecture that this is true in the more general degree d below it, and outline the reasons why the generalisation is not immediate.

Lemma 4.2.10. *Suppose $F \cong f_1 \amalg f_2$ has a fixed cluster point and where f_1 is an n-rabbit. Let α_1 be the α-fixed point of f_1. The graph of the periodic ray class $[\alpha_1]$ is a tree with a central vertex (corresponding to α_1) with n edges from it, each of which has a second endpoint labelled r_i. These r_i have a second edge leaving them, which have a second endpoint at e_i.*

Proof. Compare with the discussion in Section 2.3.1. We discuss this proof using the formal mating $f_1 \uplus f_2$ so we can discuss the periodic ray classes (before the ray classes are "collapsed" in the topological mating $f_1 \amalg f_2$ - the rational map the mating is equivalent to is the same by Theorem 2.2.9). Each global arm at α_1 must contain a rootpoint of a critical orbit component of f_2. Let ℓ be an edge which has α_1 as an endpoint. Then the angle of the external ray associated to ℓ has denominator $2^n - 1$. If the other endpoint r is not a rootpoint of a critical orbit component of f_2, then it must be a branch point in $J(f_2)$, since otherwise it would be an endpoint of $J(f_2)$, and of the graph, and this global arm would not contain a rootpoint. Since r is a branch point, and cannot have non-zero combinatorial rotation number (Lemma 2.3.3), there are exactly two rays landing at r, and they are in separate orbits. So the point r is the endpoint of precisely two edges, one of which is the edge ℓ, and the other is an edge ℓ' whose other endpoint e is in $J(f_1)$. But e must be an endpoint, since it cannot be equal to α_1 (otherwise we would have a loop in the ray equivalence class, and the mating would be obstructed) and the external ray landing at e has denominator $2^n - 1$. But by Lemma 1.8.2, the only biaccessible point which is the landing point of external rays with denominator $2^n - 1$ is α_1.

So the global arm is a graph with $V = \{\alpha_1, r, e\}$ and an edge set $E = \{\alpha_1 r, re\}$. Since this global arm must contain the rootpoint of a critical orbit Fatou component of f_2, and r is the only vertex in the arm that belongs to $J(f_2)$, it follows that r is the required rootpoint. Since this argument holds for any of the global arms, since they are mapped homeomorphically onto each other under iteration of $f_1 \uplus f_2$, we are done. □

The difficulty in the degree d case comes about due to the fact that, when the degree is higher than 2, the Fatou components have non-principal root points, root points which are the landing point of only one external ray. With this being the case, it is possible that the ray class is even simpler than that described in Lemma 4.2.10. We know that one of the maps, f, must be an n-rabbit. Suppose that the ray of angle θ lands at the α-fixed point of f. Then, since the only periodic biaccessible point on $J(f)$ is α_f (by Lemma 1.8.2), the ray of angle $-\theta$ must land

at the root point of a critical orbit Fatou component of the complementary map h. If this root point is a principal root point (the landing point of two external rays), then the periodic ray class is as described in Lemma 4.2.10. However, it is possible (though we conjecture that this case never occurs) that this root point is non-principal (the landing point of only one external ray). In this case, the periodic ray class consists of a central vertex, corresponding to α_f, which has n branches, each with an endpoint r_i which is the (non-principal) root point of a critical orbit Fatou component of h. Since there are no other rays landing at the r_i, the only vertices of the ray class are α_f and the r_i.

Conjecture 4.2.11. *Lemma 4.2.10 is true in degree d. In other words, the root points of the critical orbit Fatou components of h that belong to the ray class $[\alpha_f]$ are principal root points, and so are the landing points of precisely two external rays.*

We now return to the degree 2 discussion, since we wish to make use of our definition of the angular rotation number.

Proposition 4.2.12. *Let f be an n-rabbit where the α-fixed point has combinatorial rotation number p/n. Suppose that h mates with f so that $F \cong f \perp\!\!\!\perp h$ has a fixed cluster point. Then one of the angles landing at the root of the critical value component of h has angular rotation number $(n-p)/n$.*

Proof. The ray equivalence class of the cluster point is the ray equivalence class $[\alpha_f]$. By Lemma 2.3.3 and Lemma 4.2.10, there are two rays landing at the root of each critical orbit Fatou component of h, and they belong to different ray cycles. Furthermore, if the ray R^f_θ lands on α_f, then the ray $R^h_{-\theta}$ lands on a root of a critical orbit Fatou component of h. Since the angle θ has angular rotation number p/n by assumption, the angle $-\theta$ and its iterates (which land at the root points of the critical orbit Fatou components of h) under angle doubling will have angular rotation number $(n-p)/n$. □

Remark 4.2.13. It is not true in general that both angles landing at the base of the critical value component have angular rotation number $(n-p)/n$.

Proposition 4.2.14. *All combinatorial data can be realised for a rational map with a fixed cluster point, save for $\delta = 1$ and $\delta = 2n-1$.*

Proof. The exception is a result of Proposition 4.1.5. Suppose we want to construct a rational map F with combinatorial data (ρ, δ). We show that such a map can be created by mating two polynomials f and h. Since we want to have rotation number

$\rho = p/n$, we take f to be the n-rabbit with internal address

$$1_{p/n} \to n.$$

By Proposition 4.2.3, the resultant rational map will have combinatorial rotation number $\rho = p/n$ at its cluster point. We now need to make a judicious choice for our secondary map h. There are n external rays landing on α_f, whose angles we label in anticlockwise order by $\theta_1, \theta_2, \ldots \theta_n$, setting the angle immediately anticlockwise from the critical value component to be θ_1. Note that the denominator of the θ_j is $2^n - 1$. Recall that the critical displacement can be defined as the combinatorial distance between critical values. In order to get $\delta = 2k - 1$, we need the critical value component of h to be the landing point of $R^h_{-\theta_k}$. So we simply choose h to be the centre of the hyperbolic component of $\mathcal{M}$ whose root point is the landing point of the parameter ray $R^{\mathcal{M}}_{-\theta_k}$. Clearly h will have period n. Then it is well known that $R^h_{-\theta_k}$ lands at the root point of the critical value sector (see for example [DH84, DH85] or [Mil00b]). Hence the map h exists and the mating $F \cong f \amalg h$ has combinatorial data (ρ, δ). □

The following is a converse to Proposition 4.2.12. It is actually a classification of all angles (and therefore, maps) which can create a fixed cluster point under mating with n-rabbits. In an informal sense, it says that any map which can create a fixed cluster point will indeed create a fixed cluster point.

Proposition 4.2.15. *Suppose h is not an n-rabbit. If an angle associated to the map h has angular rotation number $(n-p)/n$, then h will mate with the map with angled internal address $1_{p/n} \to n$ to create a rational map with a fixed cluster point. Furthermore, this cluster point will have combinatorial rotation number p/n.*

Proof. By Proposition 1.9.4, there are (at most) $n - 2$ maps with angular rotation number $(n-p)/n$ which are not n-rabbits. Also, all combinatorial data (excluding the obstructed cases $\delta = 1$ and $\delta = 2n - 1$, which do not create rational maps) can be obtained by mating (Proposition 4.2.14). There are therefore precisely $n-2$ possible combinatorial displacements, namely $\delta = 3, 5, \ldots, 2n - 3$. It follows from a simple counting argument that each map h has angular rotation number $(n-p)/n$, and each of these must give a distinct value for δ. The final statement follows from Proposition 4.2.3. □

Note that it is *a priori* possible that the cyclic ordering of the kneading sequence is not admissible in the case above. However, if any of the orderings were not admissible, then we would not have enough maps to create all the combinatorial

data, contradicting Proposition 4.2.14. Indeed, this proves that all cyclic orderings with angular rotation number p/n are admissible. The author does not know how much is known about admissible cyclic orderings of kneading sequences, but it is suggested in the introduction to [BS01] that very little can be said, in general.

We now prove Theorem 4.2.1.

Proof. By proposition 4.2.2, one of the maps must be an n-rabbit, and by Proposition 4.2.3, the internal address of this n-rabbit will be $1_{p/n} \to n$. From Proposition 4.2.12, the other map has an associated angle with angular rotation number $(n-p)/n$.

Now suppose that h is not an n-rabbit and has an associated angle θ that has angular rotation number $(n-p)/n$. By Proposition 4.2.15, the map $f \perp\!\!\!\perp h$ has a fixed cluster point. □

4.3 Classifying the rational maps

This aim of this section is to show that the combinatorial data of a map with a fixed cluster point completely determines it up to Möbius transformation. In actual fact, we will be showing that the combinatorial data completely defines the Thurston class of the rational map, and since each Thurston class contains only one rational map, this means that the result of this section completely classifies rational maps with a fixed cluster point. Note that in particular, no assumption is made on these rational maps being matings here, though this result will follow.

The following is a well known result which is known in the literature as the *Alexander trick*, named after J.W. Alexander. It allows us to study the simpler case of maps with only one cluster of critical points. There is some ambiguity as to the correct definition of the trick, so I have stated and proved the two versions, as both will be required in this section. The motivation behind both proofs is very similar - we "comb" the boundary values to a map on the whole of the closed disk. In the simple case this takes the form of an extension of a homeomorphism on the circle, whereas in the second case, the combing takes the form of an isotopy.

Lemma 4.3.1 (Alexander Trick - simple version)**.** *Any homeomorphism $f\colon S^1 \to S^1$ can be extended to a homeomorphism $\tilde{f}\colon \overline{\mathbb{D}} \to \overline{\mathbb{D}}$.*

Proof. Define $\tilde{f}\colon \overline{\mathbb{D}} \to \overline{\mathbb{D}}$ by $\tilde{f}(z) = tf(z/t)$. Then $\tilde{f}$ is the composition of three homeomorphisms σ, f and τ and hence is a homeomorphism (check the following proof for more details on the three homeomorphisms). □

Proposition 4.3.2 (Alexander Trick - isotopy version)**.** *Let $f, g\colon \overline{\mathbb{D}} \to \overline{\mathbb{D}}$ be homeomorphisms of the closed disk to itself. If $f = g$ on $\partial\overline{\mathbb{D}}$ then f and g are isotopic.*

Proof. By considering $g^{-1} \circ f$, it suffices only to consider the case where one of the maps is the identity. So let f be a homeomorphism of $\overline{\mathbb{D}}$ which is the identity on the boundary. Define the map $\Phi\colon \overline{\mathbb{D}} \times [0,1]$ by

$$\Phi(z,t) = \phi_t(z) = \begin{cases} tf\left(\frac{z}{t}\right), & 0 \le |z| < t; \\ z, & t \le |z| \le 1. \end{cases} \tag{4.1}$$

It is clear that ϕ_0 is the identity, and that $\phi_1 = f$, so Φ is a homotopy from the identity to f. It remains to show that Φ is indeed an isotopy, meaning that all the ϕ_t are homeomorphisms of the closed disk.

We already know that ϕ_t is a homeomorphism for $t \in \{0,1\}$. So fix $t \in (0,1)$. Then for all z with $|z| \ge t$, we have $\phi_t(z) = z$. So ϕ_t is a homeomorphism from the set $\{z : t \le |z| \le 1\}$ to itself. On the other hand, we will show that the map $z \mapsto tf(z/t)$ is a homeomorphism from $\overline{\mathbb{D}}_t$ to itself. Indeed, it is the composition of the three homeomorphisms

$$\begin{aligned} &\sigma\colon \overline{\mathbb{D}}_t \to \overline{\mathbb{D}}, && \sigma(z) = \frac{z}{t}, \\ &f\colon \overline{\mathbb{D}} \to \overline{\mathbb{D}}, && \\ &\tau\colon \overline{\mathbb{D}} \to \overline{\mathbb{D}}_t && \tau(z) = tz. \end{aligned}$$

Since the composition of two homeomorphisms is a homeomorphism, this means ϕ_t is a homeomorphism. So it remains to show that ϕ_t is continuous on the circle of radius t. Since the identity map and $z \mapsto tf(z/t)$ agree on the circle of radius t, and are both continuous on the boundary, ϕ_t a homeomorphism, and so Φ is an isotopy. □

The above proof shows that $\mathrm{MCG}(\overline{\mathbb{D}}) = 0$, the trivial group with one element. It is this rigidity of (orientation-preserving) homeomorphisms of the disk that allows us to obtain Thurston equivalence in the next section.

We will make use of the following fact from topology (see for example [HY61], Lemma 3.19).

Lemma 4.3.3. *Any continuous map from a compact space into a Hausdorff space is closed.*

In particular, if the map is a bijection, we can say even more (see e.g [Sut81], Theorem 5.9.1).

Proposition 4.3.4. *Let f be a continuous bijection from a compact space to a Hausdorff space. Then f is a homeomorphism.*

4.3.1 Proof of Thurston Equivalence

Recall that after Theorem 2.2.8, (Thurston's theorem), we discussed some of the problems of its applications. We will now use Alexander's Trick to show that the configuration of a cluster (in terms of its combinatorial rotation number and critical displacement) uniquely defines the rational map in the sense of Thurston. For more on the use of algebraic properties in the study of Thurston's theorem, see [Pil03, Kam01]. We will be using standard results about ramified covering maps, see for example [For81].

Theorem 4.3.5. *Suppose that two rational maps F and G (with labelled critical points) have a fixed cluster with combinatorial rotation number p/n and critical displacement δ. Then F and G are equivalent in the sense of Thurston.*

The proof will proceed as follows. To prove Thurston equivalence, we need to find homeomorphisms $\Phi, \widehat{\Phi} \colon \overline{\mathbb{C}} \to \overline{\mathbb{C}}$ which satisfy

1. $\Phi \circ F = G \circ \widehat{\Phi}$.
2. $\Phi|_{P_F} = \widehat{\Phi}|_{P_F}$.
3. Φ and $\widehat{\Phi}$ are isotopic rel P_F.

We will first construct the homeomorphism Φ. We then try to construct the homeomorphism $\widehat{\Phi}$ so that it satisfies the conditions 1 to 3 above. The first two conditions will be satisfied by the construction given, whilst the third will follow from an application of Alexander's Trick. The whole proof will be broken down into a sequence of lemmas.

In what follows, we will denote the stars of F and G by X_F and X_G respectively. Recall that the star X_F of a rational map F is made up of the union of the internal rays inside the critical orbit Fatou components and the cluster point. By Böttcher's theorem, the dynamics of the first return map on each critical orbit Fatou component is then conjugate to the map $z \mapsto z^d$ on the disk, $\mathbb{D}$. We also can label the critical orbit points cyclically as follows. Let c_0 be the first critical point, in terms of the ordering induced by the critical displacement, so that the critical displacement is defined to be the combinatorial distance (anticlockwise) around the star from c_0 to the other critical point. We label, counting anticlockwise, the other critical orbit points by $c_1, c_2, \ldots, c_{2n-1}$, and denote the Fatou component containing

c_i by U_i. Note that at this point we are not worried about which critical orbit the c_i are in, since we are only concerned with the dynamics of the first return map on each component. Finally let the 0-internal ray in U_i be labelled J_i.

In the following lemma, the objects associated with the map G will be given a $'$ to differentiate them from the objects associated with F. For example, the first critical point of X_G will be labelled c'_0, and it will be in the Fatou component U'_0.

Lemma 4.3.6. *Suppose F and G have the same combinatorial data. Then there exists a conjugacy $\phi\colon X_F \to X_G$. That is, $\phi \circ F = G \circ \phi$ on X_F. Furthermore, the conjugacy can be constructed so as to preserve the cyclic ordering of the internal rays in the star.*

Proof. We will show that there is a conjugacy between the dynamics on J_i and J'_i for each choice of i. There is a map $h_{F,i}$ conjugating the dynamics on U_i with that of $z \mapsto z^d$ on $\mathbb{D}$, so that $h_{F,i}(J_i) = [0, 1)$. Similarly, there exists a conjugacy $h_{G,i}$ from U'_i to $z \mapsto z^d$ on $\mathbb{D}$, with $h_{G,i}(J_i) = [0, 1)$. So the map $\phi_i = h^{-1}_{G,i} \circ h_{F,i}$ conjugates the dynamics on U_i with that on U'_i, and in particular takes J_i to J'_i. So the restriction of ϕ_i to J_i is the required conjugacy on J_i.

The required conjugacy ϕ is then defined by mapping the cluster point $c \in X_F$ to the cluster point $c' \in X_G$, (i.e, $\phi(c) = c'$) and then picking $\phi|_{J_i} = \phi_i$. □

Lemma 4.3.7. *The star X of a cluster point is locally connected.*

Proof. Let the star X have $2n$ branches. Denote the interval $[0, \exp(2\pi ik)/n)]$ by I_k. We will call the set

$$\mathcal{S}_{2n} = \bigcup_{k=0}^{2n-1} I_k$$

the $2n$-canonical star. It is clearly locally connected. This is because the local neighbourhoods of a point z look like a half-open interval, an open interval or a star depending on whether $|z| = 1$, $0 < |z| < 1$ or $z = 0$ respectively. Now let ϕ be a map taking $\mathcal{S}_{2n}$ homeomorphically onto X, so that 0 maps to the cluster point and the intervals I_k each map to a unique branch of the star X. Then X is the homeomorphic image of a locally connected space and so is locally connected. □

Lemma 4.3.8. *Let ϕ be a homeomorphism from a star X_F of a rational map F to a star X_G of a rational map G which preserves the cyclic ordering of the branches of the stars. Then there exists continuous maps $\tilde{\eta}_F$ and $\tilde{\eta}_G$ and a homeomorphism*

ψ such that the following diagram commutes.

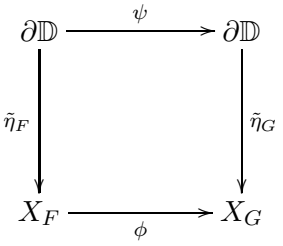

Proof. By using a Möbius transformation if necessary, we set the cluster points of X_F and X_G to be at $0 \in \overline{\mathbb{C}}$.

We remark that $\overline{\mathbb{C}} \setminus X_F$ is simply connected, since X_F is a connected set (see, for example [Con78], Chapter VIII, Theorem 2.2). Hence, by the Riemann Mapping Theorem, there exists a Riemann map $\eta_F \colon \overline{\mathbb{C}} \setminus \overline{\mathbb{D}} \to \overline{\mathbb{C}} \setminus X_F$. Similarly, there exists a Riemann map $\eta_G \colon \overline{\mathbb{C}} \setminus \overline{\mathbb{D}} \to \overline{\mathbb{C}} \setminus X_G$.

By Lemma 4.3.7, the set X_F is locally connected, and so by Carathéodory's Theorem (Theorem 1.3.6), we can extend the maps η_F and η_G to $\overline{\mathbb{C}} \setminus \mathbb{D}$ in a continuous way. We label these extensions $\tilde{\eta}_F$ and $\tilde{\eta}_G$.

Since ϕ is a homeomorphism, it maps arms of the star X_F to arms of X_G. Without loss of generality, we assume ϕ is such that $\phi([c, c_i]) = [c', c_i']$. In particular we have $\phi(c_i) = c_i'$. The general choice of ϕ will have $\phi([c, c_i]) = [c', c_{i+k}']$ for some k.

We now define the map ψ. Clearly, we would like to define $\psi = \tilde{\eta}_G^{-1} \circ \phi \circ \tilde{\eta}_F$. However, since most points in X_G (indeed, all points not in P_G) have more than one pre-image under the mapping $\tilde{\eta}_G$, this function is not well-defined. However, it is possible to use this motivating idea to construct ψ, by choosing the "correct" pre-image when necessary.

Note that each point in the postcritical set of F has precisely one pre-image under $\tilde{\eta}_F$, and the cyclic ordering of the $\tilde{\eta}_F^{-1}(c_i)$ is the same as the cyclic ordering of the c_i. Since the same is true for $\tilde{\eta}_G$ (that is, points on the postcritical set have only one pre-image), we can define $\psi = \tilde{\eta}_G^{-1} \circ \phi \circ \tilde{\eta}_F$ on the postcritical set. Since ϕ will rotate the arms of the star by k places anticlockwise, ψ will do the same. For ease of notation we will write $p_i = \tilde{\eta}_F^{-1}(c_i)$ and $p_i' = \tilde{\eta}_F^{-1}(c_i')$. With this new notation, therefore, we have $\psi(p_i) = p_i'$.

The cluster point c in X_F has $2n$ preimages under $\tilde{\eta}_F$, and each pre-image lies in one of the arcs (p_i, p_{i+1}) for $i = 0, \ldots, 2n-1$ (otherwise cyclic ordering would not be maintained). Label the pre-image in (p_i, p_{i+1}) by ξ_i. Similarly, the cluster point c' in X_G has $2n$ preimages under $\tilde{\eta}_G$, and each pre-image lies in one of the

arcs (c'_i, c'_{i+1}) for $i = 0, \ldots, 2n-1$. So we denote the pre-image in (c'_i, c'_{i+1}) by ξ'_i. We then define $\psi(\xi_i) = \xi'_i$, and note that this satisfies $\tilde{\eta}_G \circ \psi = \phi \circ \tilde{\eta}_F$, since $\phi(c) = c'$. Furthermore, this agrees with the cyclic ordering induced on the circle by the rotation of arms in the map ϕ. See Figure 4.5 for the construction so far in the case where the critical orbits have period 4.

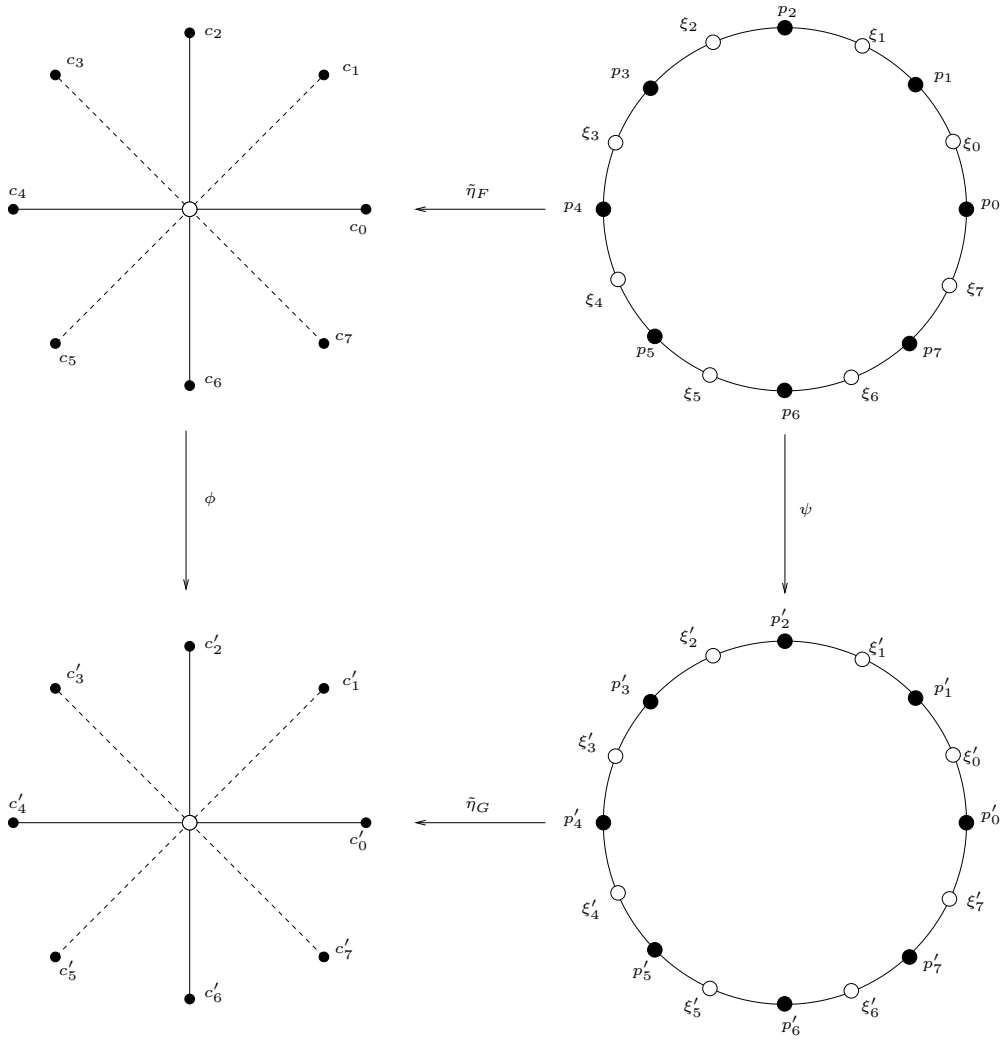

Figure 4.5: Construction of the map ψ in Lemma 4.3.8.

Now let $z \in X_F$ where z is not in the postcritical set or equal to the cluster point. Then z has precisely two pre-images under $\tilde{\eta}_F^{-1}$ and the point $z' = \phi(z) \in X_G$ has two pre-images under $\tilde{\eta}_G^{-1}$. For the diagram in the statement of the lemma to commute, we need to have $\psi(\tilde{\eta}_F^{-1}(z)) \in \tilde{\eta}_G^{-1}(z')$. It is clear that z must belong to the interior of some internal ray of the form $[0, c_i] \subset X_F$, hence z' belongs to the

internal ray $[0, c_i'] \subset X_G$. This means that there is a point w_1 of $\tilde{\eta}_F^{-1}(z)$ in the arc (ξ_{i-1}, p_i) and the other point w_2 must be in the arc (p_i, ξ_i). Furthermore, the two pre-images of z' (under the map $\tilde{\eta}_G$) are $w_1' \in (\xi_{i-1}', p_i')$ and $w_2' \in (p_i', \xi_i)$. We now define $\psi(w_1) = w_1'$ and $\psi(w_2) = w_2'$. This definition satisfies $\phi \circ \tilde{\eta}_F = \tilde{\eta}_G \circ \psi$. Notice further that this construction will preserve the cyclic ordering of the points on the circle.

We now show that ψ is a homeomorphism. The construction of ψ shows it is clearly bijective, so we only need to show ψ is continuous. Then, since ψ will be a continuous bijection from a compact space to a Hausdorff space, it will be a homeomorphism by Proposition 4.3.4. Indeed, since $\tilde{\eta}_F$ and ϕ are continuous maps, it is sufficient to check the choices we made for $\tilde{\eta}_G^{-1}$ are done in a continuous way. We have three cases.

Case 1: $z \notin \{p_0, \ldots, p_{2n-1}, \xi_0, \ldots, \xi_{2n-1}\}$. Suppose z lies in some arc (p_i, ξ_i). Then any sequence $v_n \to z$ will belong to (p_i, ξ_i) if n is large enough. Then by construction we will have $\psi(v_n) \in (p_i', \xi_i')$. Now we notice that $\tilde{\eta}_G$ is a homeomorphism on (p_i', ξ_i') and so we must have ψ is continuous at z as it is (locally) the composition of continuous maps. A similar argument holds when z belongs to some arc (ξ_i, p_{i+1}).

Case 2: $z = p_i$. Let $x_n \to z$. Then $\phi(\tilde{\eta}_F(x_n)) \in (0, c_i']$ for n sufficiently large and by continuity of $\tilde{\eta}_F$ and ϕ, $\phi(\tilde{\eta}_F(x_n)) \to c_i'$. Now the map $\tilde{\eta}_G$ is a branched covering when restricted to (ξ_{i-1}', ξ_i'), with image $(0, c_i']$. The unique branch point is p_i' which has its image at c_i'. So as we have $\phi(\tilde{\eta}_F(x_n)) \to c_i'$, we must have $\tilde{\eta}_G^{-1}(\phi(\tilde{\eta}_F(x_n))) \to \tilde{\eta}_G^{-1}(c_i') = p_i'$.

Case 3: $z = \xi_i$. Let $y_n \to z$. Then for n sufficiently large, $y_n \in (p_i, p_{i+1})$, $\phi(\tilde{\eta}_F(y_n)) \in [c', c_i') \cup [c', c_{i+1}))$ and $\phi(\tilde{\eta}_F(x_n)) \to c'$. So $\tilde{\eta}_G^{-1}(\phi(\tilde{\eta}_F(y_n))) \in (p_i', p_{i+1}')$, by the construction of ψ (the other pre-images of $\phi(\tilde{\eta}_F(y_n))$ cannot be the images of ψ, since as $y_n \in (p_i, p_{i+1})$, we must have $\psi(y_n) \in (p_i', p_{i+1}')$). We then use the fact that $\tilde{\eta}_G$ restricted to (p_i', p_{i+1}') is a homeomorphism, which once again means ψ is continuous at z.

Hence we have shown ψ is a homeomorphism. □

Remark 4.3.9. Given ϕ, the homeomorphism ψ is actually unique, which can be proved by considering the facts that we have the identity $\tilde{\eta}_F \circ \phi = \psi \circ \tilde{\eta}_G$ and there is a cyclic order induced by ϕ, $\tilde{\eta}_F$ and $\tilde{\eta}_G$.

We briefly comment on the properties of the Riemann maps $\tilde{\eta}_F$ and $\tilde{\eta}_G$. As discussed above, they are homeomorphisms on $\overline{\mathbb{C}} \setminus \overline{\mathbb{D}}$ and, by the local connectivity of the stars, they extend to continuous maps maps on $\overline{\mathbb{C}} \setminus \mathbb{D}$. This extension maintains the cyclic ordering of points, in a way similar to the way that external rays (and

their landing points) maintain the cyclic ordering of points when mapping from $\partial\mathbb{D}$ to $J(f)$. One way of seeing this is by thinking of the images of the radial lines

$$\{re^{2\pi i\theta} \mid r \in [1,\infty)\} \subset \overline{\mathbb{C}} \setminus \mathbb{D},$$

under $\tilde{\eta}_F$ and $\tilde{\eta}_G$, as an analogy to the external rays. This cyclic ordering will be an important detail that will need to be considered when using the extended Riemann maps to construct homeomorphisms later in this section.

Corollary 4.3.10. *Let ϕ be the map from Lemma 4.3.6. Then there exists (the extension of) Riemann maps $\tilde{\eta}_F$ and $\tilde{\eta}_G$ and a homeomorphism ψ such that*

$$\begin{array}{ccc} \partial\mathbb{D} & \xrightarrow{\psi} & \partial\mathbb{D} \\ \downarrow{\scriptstyle \tilde{\eta}_F} & & \downarrow{\scriptstyle \tilde{\eta}_G} \\ X_F & \xrightarrow[\phi]{} & X_G \end{array}$$

commutes.

Proof. Trivial, since by setting ϕ from Lemma 4.3.6 to be the ϕ in Lemma 4.3.8 we are done. □

Proposition 4.3.11. *The map ψ of Corollary 4.3.10 can be extended to a homeomorphism $\Psi\colon \overline{\mathbb{C}} \setminus \mathbb{D} \to \overline{\mathbb{C}} \setminus \mathbb{D}$. This map Ψ induces a homeomorphism $\Phi\colon \overline{\mathbb{C}} \to \overline{\mathbb{C}}$, such that $\Phi|_{X_F} = \phi$ (i.e, Φ is an extension of ϕ to the sphere) and*

$$\begin{array}{ccc} \overline{\mathbb{C}} \setminus \mathbb{D} & \xrightarrow{\Psi} & \overline{\mathbb{C}} \setminus \mathbb{D} \\ \downarrow{\scriptstyle \tilde{\eta}_F} & & \downarrow{\scriptstyle \tilde{\eta}_G} \\ \overline{\mathbb{C}} & \xrightarrow[\Phi]{} & \overline{\mathbb{C}} \end{array}$$

commutes.

Proof. The extension of ψ to Ψ is an application of the simple form of Alexander's Trick.

We want Φ to be an extension of ϕ, and hence it is necessary that we have $\Phi(z) = \phi(z)$ on X_F. Note that, considering $\tilde{\eta}_F^{-1}(z)$ as a set, the commutative

diagram for ψ in Corollary 4.3.10 suggests we can write $\phi(z) = (\tilde{\eta}_G \circ \psi)(\tilde{\eta}_F^{-1}(z))$ for $z \in X_F$. Bearing this in mind, define

$$\Phi(z) = \begin{cases} \eta_G \circ \Psi \circ \eta_F^{-1}(z), & z \in \overline{\mathbb{C}} \setminus X_F; \\ \phi(z), & z \in X_F. \end{cases}$$

The discussion above suggests that if $V \subset \overline{\mathbb{C}}$ then $\Phi^{-1}(V) = (\tilde{\eta}_G \circ \Psi \circ \tilde{\eta}_F^{-1})^{-1}(V) = \tilde{\eta}_F(\Psi^{-1}(\tilde{\eta}_G^{-1}(V)))$.

We will now show Φ is a homeomorphism. Let $V \subset \overline{\mathbb{C}}$ be closed. Then since $\tilde{\eta}_G$ and Ψ are continuous, the set $\Psi^{-1}(\tilde{\eta}_G^{-1}(V))$ is closed in $\overline{\mathbb{C}} \setminus \mathbb{D}$. Now we note that since $\tilde{\eta}_F$ is a continuous function from the compact space $\overline{\mathbb{C}} \setminus \mathbb{D}$ to the Hausdorff space $\overline{\mathbb{C}}$, by Lemma 4.3.3 it is a closed function. This means the set $\tilde{\eta}_F(\Psi^{-1}(\tilde{\eta}_G^{-1}(V)))$ is closed in $\overline{\mathbb{C}}$. Hence we have shown that if V is closed in $\overline{\mathbb{C}}$ then the set $\Phi^{-1}(V) = \tilde{\eta}_F(\Psi^{-1}(\tilde{\eta}_G^{-1}(V)))$ is closed in $\overline{\mathbb{C}}$, and so Φ is continuous. Now we see that Φ is a bijective continuous map from the compact space $\overline{\mathbb{C}}$ to the Hausdorff space $\overline{\mathbb{C}}$, and hence it is a homeomorphism by Proposition 4.3.4. □

Remark 4.3.12. The proof that Φ is a homeomorphism is essentially just using the fact that $\tilde{\eta}_F$ and $\tilde{\eta}_G$ are quotient maps. This means that $\tilde{\eta_G} \circ \Psi$ is a quotient map, and so an application of Corollary 22.3 in [Mun00] yields the necessary result.

We note that, so far in this section, we have not needed any requirement about the combinatorial data being equal, so these results hold in full generality. However, the next result is the point where the equality of combinatorial data is needed.

Before we prove the next proposition, we briefly discuss the space $\overline{\mathbb{C}} \setminus X_F$ and its pre-image $\overline{\mathbb{C}} \setminus F^{-1}(X_F)$. Informally, first note that the star X_F has d pre-images in $\overline{\mathbb{C}}$, and each pre-image is disjoint, save for the fact that they all contain the critical points of F. More exactly, we notice that the set $X_F \setminus \{\text{critical values}\}$ has d disjoint pre-images under F, and the union of one of these pre-images with the two critical points will map homeomorphically onto X_F. We call each of these pre-images, with its union with the critical points, a pre-image star of X_F. Note that there is a cyclic order of these pre-image stars at c_0 (the first marked critical point), so that we can label them as follows. Label X_F by X_1. Counting anticlockwise from this pre-image, label the remaining stars $X_2, X_3, \ldots X_d$.

Furthermore, we notice that $\overline{\mathbb{C}} \setminus F^{-1}(X_F) = \overline{\mathbb{C}} \setminus \bigcup_{j=1}^{d} X_j$ contains d connected components. Label these components in anticlockwise order, starting with $\mathcal{A}_1$ as the component anticlockwise from $X_F = X_1$ with respect to the cyclic ordering at c_0, and the others in order as $\mathcal{A}_2, \ldots, \mathcal{A}_d$. We remark that in this notation, the boundary

of $\mathcal{A}_j$ is contained in $X_j \cup X_{j+1}$. With this notation, the map $F|_{\mathcal{A}_j} \colon \mathcal{A}_j \to \overline{\mathbb{C}} \setminus X_F$ is a homeomorphism, and the map $F|_{\overline{\mathbb{C}} \setminus F^{-1}(X_F)} \colon \overline{\mathbb{C}} \setminus F^{-1}(X_F) \to \overline{\mathbb{C}} \setminus X_F$ is a degree d covering map. For ease of notation we write $F_j = F|_{\mathcal{A}_j}$. See Figure 4.6. We

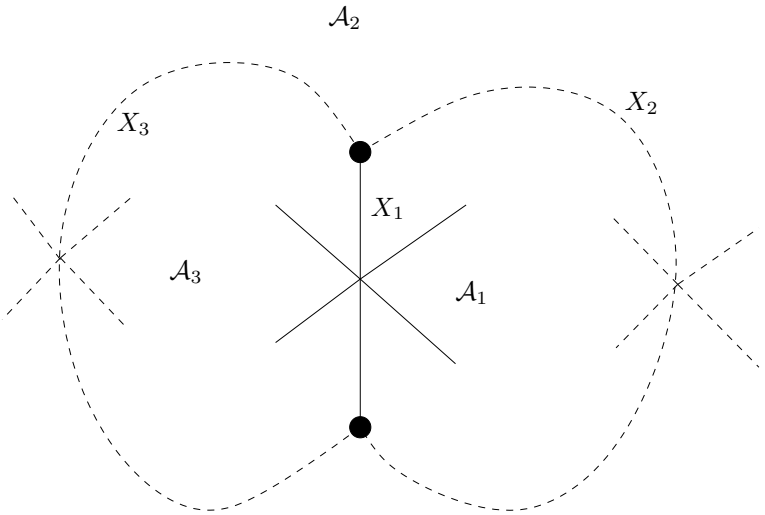

Figure 4.6: The star (bold line) and pre-image stars (dashed line) and how they separate the sphere. The black dots represent the critical points, where the star and pre-stars meet.

can carry out a similar construction with G. Using the same construction as above, the pre-image stars of X_G are $X_1', X_2', \ldots, X_d'$ and the connected components of $\overline{\mathbb{C}} \setminus G^{-1}(X_G)$ are $\mathcal{A}_1', \mathcal{A}_2', \ldots, \mathcal{A}_d'$. G_j will denote the map $G|_{\mathcal{A}_j'}$.

Proposition 4.3.13. *There exists a homeomorphism $\widehat{\Phi} \colon \overline{\mathbb{C}} \to \overline{\mathbb{C}}$ so that*

$$\begin{array}{ccc} \overline{\mathbb{C}} & \xrightarrow{\widehat{\Phi}} & \overline{\mathbb{C}} \\ {\scriptstyle F}\downarrow & & \downarrow{\scriptstyle G} \\ \overline{\mathbb{C}} & \xrightarrow[\Phi]{} & \overline{\mathbb{C}} \end{array}$$

commutes.

Proof. As with Lemma 4.3.8, this proof is constructive. First note that if $z \in X_F$, then we define $\widehat{\Phi}(z) = \phi(z) \in X_G$, taking advantage of the fact that ϕ is a conjugacy between the dynamics on X_F and X_G (Lemma 4.3.6).

Now suppose z is in $F^{-1}(X_F)$. The case where $z \in X_F$ is dealt with above, so we may assume $z \in X_j$ for some $j \in \{2, \ldots, d\}$. Then for the diagram to commute

we require $\widehat{\Phi}(z) \in G^{-1} \circ \Phi \circ F(z) = G^{-1} \circ \phi \circ F(z)$. The set $G^{-1} \circ \Phi \circ F(z)$ contains d elements, one each in $X'_1, \ldots, X'_d$. Since $z \in X_j$, we choose $\widehat{\Phi}(z) \in X'_j$.

Finally, suppose $z \in \overline{\mathbb{C}} \setminus F^{-1}(X_F)$. Then $z \in \mathcal{A}_j$ for some $j \in \{1, \ldots, d\}$. With a similar argument to that in the previous paragraph, the set $G^{-1} \circ \Phi \circ F(z)$ contains d elements, one in each of the $\mathcal{A}_j$. So as we have, $z \in \mathcal{A}_j$, we define $\widehat{\Phi}(z)$ to be the element of $G^{-1} \circ \Phi \circ F(z)$ in $\mathcal{A}'_j$.

We now show $\widehat{\Phi}$ is a homeomorphism. Let U be an open disc in $\overline{\mathbb{C}}$, which is disjoint from the critical points. We will show $\widehat{\Phi}^{-1}(U)$ is open. By commutativity, $\widehat{\Phi}^{-1}(U)$ is contained in $F^{-1}(\Phi^{-1}(G(U)))$. Since G is a rational map, $G(U)$ is an open set, and by continuity of Φ, $\Phi^{-1}(G(U))$ is also open. Furthermore, $\Phi^{-1}(G(U))$ is disjoint from the two critical values, and so $F^{-1}(\Phi^{-1}(G(U)))$ is made up of d disjoint open sets. By the construction of $\widehat{\Phi}$ given above, we see that precisely one of these is the set $\widehat{\Phi}^{-1}(U)$, which is therefore open. This proves continuity for the non-critical points.

If U is a disc which contains one critical point, then a similar argument shows that $F^{-1}(\Phi^{-1}(G(U)))$ is a single simply connected open set, and so $\widehat{\Phi}$ is continuous at the critical points. By Proposition 4.3.4, $\widehat{\Phi}$ is a homeomorphism. □

Lemma 4.3.14. *There exists a homeomorphism $\widehat{\Psi}\colon \overline{\mathbb{C}} \setminus \mathbb{D} \to \overline{\mathbb{C}} \setminus \mathbb{D}$ so that*

$$\begin{array}{ccc} \overline{\mathbb{C}} \setminus \mathbb{D} & \xrightarrow{\widehat{\Psi}} & \overline{\mathbb{C}} \setminus \mathbb{D} \\ \Big\downarrow{\scriptstyle \tilde{\eta}_F} & & \Big\downarrow{\scriptstyle \tilde{\eta}_G} \\ \overline{\mathbb{C}} & \xrightarrow[\widehat{\Phi}]{} & \overline{\mathbb{C}} \end{array}$$

commutes.

Proof. This is analogous to the proof of Proposition 4.3.11. We define

$$\widehat{\Psi}(z) = \begin{cases} \eta_G^{-1} \circ \widehat{\Phi} \circ \eta_F(z), & z \in \overline{\mathbb{C}} \setminus \overline{\mathbb{D}}; \\ \psi(z), & z \in \partial\mathbb{D}. \end{cases}$$

Again, continuity on $\overline{\mathbb{C}} \setminus \overline{\mathbb{D}}$ is assured by the fact that Ψ is defined as a composition of homeomorphisms there. So we only need to check continuity on the boundary, $\partial\mathbb{D}$.

The cyclic ordering induced by the Riemann maps and $\widehat{\Phi}$ is induced by the cyclic ordering from ϕ and ψ. Notice, if $x_n \to x \in X_F$, $\lim_{n\to\infty}(\widehat{\Phi}(x_n)) = \phi(x)$. Also

$\psi = \widehat{\Psi}|_{\partial\mathbb{D}}$ is chosen as the homeomorphism of the circle which satisfies $\phi \circ \tilde{\eta}_F(z) = \tilde{\eta}_G \circ \psi(z)$ for all z. This means that $\psi(z)$ is the element of $\tilde{\eta}_G(\tilde{\eta}_G^{-1} \circ \widehat{\Phi} \circ \tilde{\eta}_F(z))$ which maintains the cyclic ordering of the points. Hence any sequence converging to z must converge to $\psi(z)$ under $\widehat{\Psi}$ (else we would lose the ordering), and so the given boundary values for $\widehat{\Psi}$ gives continuity.

We now invoke Proposition 4.3.4 to show $\widehat{\Psi}$ is a homeomorphism. □

We are now ready to prove Theorem 4.3.5.

Proof of Theorem 4.3.5. We claim that we have the following commutative diagram.

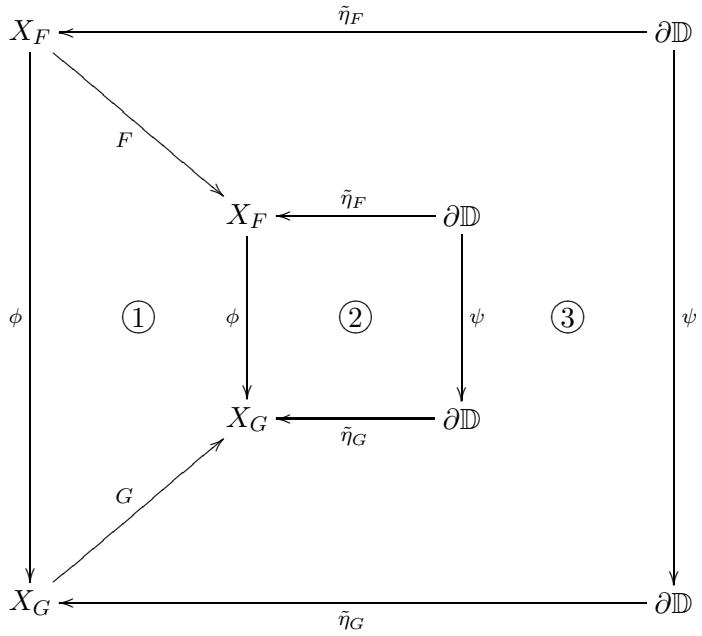

Each part of this diagram is justified as follows.

1. ϕ is a conjugacy so $\phi \circ F = G \circ \phi$. The existence of ϕ is given by Lemma 4.3.6.
2. Lemma 4.3.8
3. Lemma 4.3.8.

This diagram extends to give a commutative diagram:

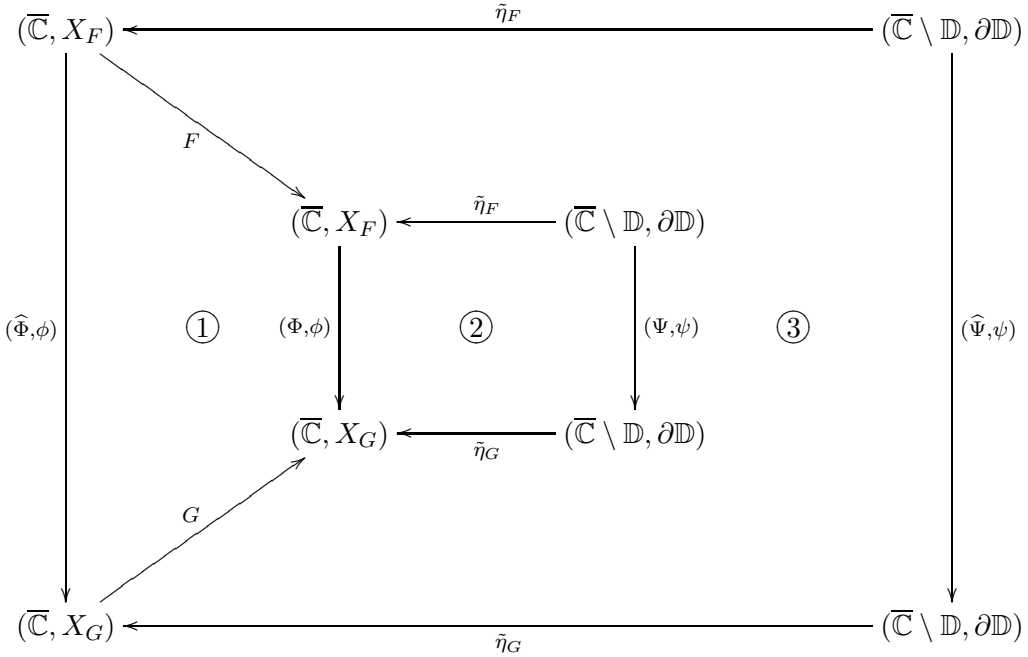

where the notation $(\Phi, \phi)\colon (\overline{\mathbb{C}}, X_F) \to (\overline{\mathbb{C}}, X_G)$ means the map is defined as Φ on $\overline{\mathbb{C}}$, and its restriction to X_F is ϕ. The other maps are defined analogously. This diagram is justified by

1. Proposition 4.3.13.
2. Proposition 4.3.11
3. Lemma 4.3.14

We now remark that the maps Φ and $\widehat{\Phi}$ agree on X_F, and so agree on the set $P_F \subset X_F$. Furthermore, Ψ is isotopic to $\widehat{\Psi}$, by Alexander's Trick (Proposition 4.3.2), and so we see that the commutative diagram above (and the fact that $\tilde{\eta}_F$ and $\tilde{\eta}_G$ are homeomorphisms on $\overline{\mathbb{C}} \setminus \overline{\mathbb{D}}$) gives us that Φ and $\widehat{\Phi}$ are isotopic rel X_F and so isotopic rel P_F. Hence F and G are Thurston equivalent. □

We now prove Theorem 4.0.3.

Proof. By Proposition 4.2.14, all admissible combinatorial data can be obtained by matings, and by Theorem 4.3.5 the combinatorial data fixes the rational map in the sense of Thurston. By Theorem 4.2.1, if the combinatorial rotation number of F is p/n, then one of the maps is an n-rabbit with angled internal address $1_{p/n} \to n$ and the other map has an associated angle with angular rotation number $(n-p)/n$. □

4.4 Combinatorial Progressions

It follows from the preceding work that every map with a one cluster can be thought of as a mating, as Theorem 4.3.5 shows that combinatorial data completely describes a rational map, and Proposition 4.2.14 shows that all (permitted) combinatorial data can be realised by the mating construction. Furthermore, Proposition 4.2.2 says that precisely one of the maps in the mating is an n-rabbit.Recall from Chapter 2 that a necessary and sufficient condition for F to be a mating is that there exists an equator.

Before starting the next proposition, we introduce some terminology. Recall that the star of F is the union of the cluster point c and the 0-internal rays of the critical orbit Fatou components. By Proposition 3.2.2, the components alternate cyclically between components of the first critical point c_1 and components of the second critical point c_2. Consider the subset of the star made up of union of the cluster point with the 0-internal rays of the critical orbit components of the critical point c_i. Denote this set by X_F^i and call it the ith substar of X_F. We remark that $X_F^1 \cap X_F^2 = \{c\}$. We drop the subscript F when the map F is clear in the context.

Proposition 4.4.1. *Let F be a rational map with a fixed cluster point, and let X be the star of F. Then there are precisely two equators. Each equator is (isotopic to) the boundary of a tubular neighbourhood of one of the substars X^i (see Figure 4.7).*

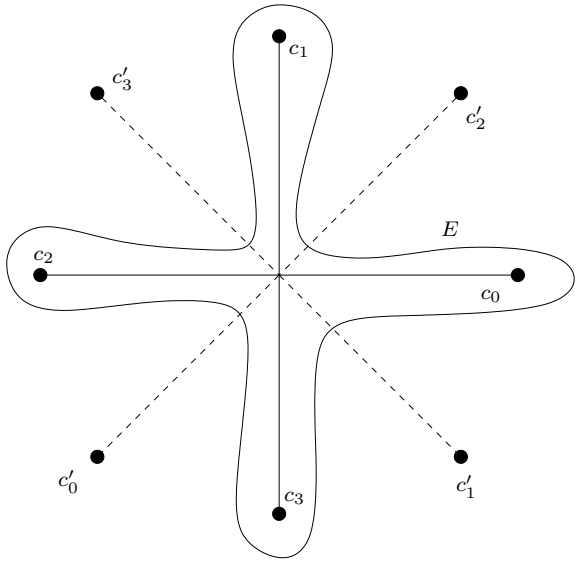

Figure 4.7: The (isotopy class of the) equator in the fixed cluster point case.

Proof. We first show that a tubular neighbourhood E of the substar is an equator. The pre-image $F^{-1}(E)$ of this tubular neighbourhood of the substar is a tubular neighbourhood of the substar and its pre-images. Since the preimage of the substar will not contain any points in the postcritical set of F, this pre-image will be isotopic to the tubular neighbourhood of the star rel P_F (see Figure 4.8). Hence E is an equator.

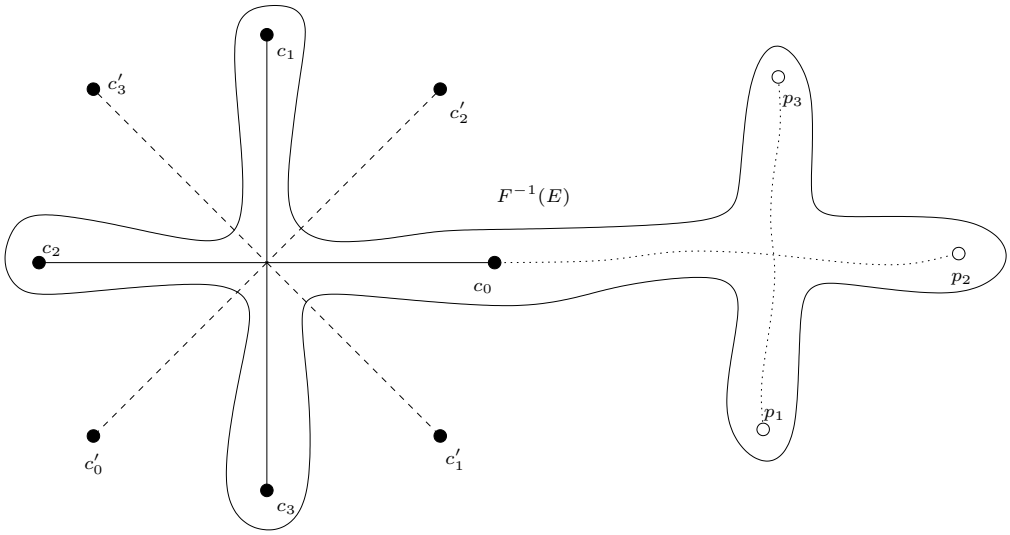

Figure 4.8: The pre-image of the equator from Figure 4.7.

We note that these are the only two equators by Proposition 4.2.2. Since one of the maps must be an n-rabbit, there are only two matings which yield this rational map. Hence there can only be two equators. □

The above result comes about from the observation that, at least in this case, the equators can be seen as tubular neighbourhoods of the Hubbard tree. Indeed, the Hubbard tree of an n-rabbit is already in the form of a substar. It is also possible to consider that the equator can also be thought of (isotopically) as a tubular neighbourhood of the second map, an observation which leads to the following proposition.

To set our ideas, we will from now on suppose that the first map is the n-rabbit when considering the critical displacement. We now study some of the behaviour one finds for the non-rabbit map for given combinatorial data. In particular, we will be focussing on describing these maps using the language of Section 1.7.

We begin with an algorithm.

Algorithm 4.4.2. *Suppose F has a fixed cluster cycle with star X and with combinatorial data (ρ, δ). Then the following steps yields the kneading sequence (and hence, the internal address) of the secondary map h.*

1. *Let the period of the critical orbits be n. We number the endpoints of the star as follows. Setting c_1, the first critical point, to be at e_0, label the other endpoints in anticlockwise order by $1, 2, \ldots, 2n-1$. Notice that c_2 will be at position $e_\delta = e_{2k+1}$, by definition of the critical displacement.*

2. *These endpoints (excluding $c_2 = e_{2k+1}$) that belong to the orbit of c_2 can be divided into two sets. One is the set of endpoints $\{e_1, e_3, \ldots, e_{2k-1}\}$ and the other is the set of endpoints $\{e_{2k+3}, e_{2k+5}, \ldots, e_{2n-1}\}$. Denote the set containing $F(c_2)$ by Y_1 and the other set by Y_0.*

3. *Denote the critical orbit of c_2 by $F(c_2) = z_1, F^{\circ 2}(c_2) = z_2, \ldots F^{\circ(n-1)}(c_2) = z_{n-1}$ and $F^{\circ n}(c_2) = c_2 = z_n$. Note that in this notation we have $z_1 \in Y_1$.*

4. *Compute the kneading sequence as follows. Set $\nu_n = *$. If $z_i \in Y_j$, then write $\nu_i = j$.*

5. *The kneading sequence of h is $\nu = \nu_1\nu_2 \cdots \nu_n$.*

Proof. We first make an observation about the ray equivalence class of the cluster point, which by the preceding work is precisely the ray equivalence class of α_1. By Lemma 4.2.10, this class is star shaped. Let γ be the global arm of the star which contains the rootpoint of the critical point component of f_2. Then this arm separates the set $\overline{\mathbb{C}} \setminus (K(f_1) \cup K(f_2))$ into two halves. In particular, this arm cuts the f_2 plane into two connected components A_1, which contains the critical value of f_2, and A_0. However, we note that these components correspond precisely to the division of the plane induced by the kneading sequence definition. Hence the kneading sequence $\nu = \nu_1\nu_2, \ldots$ for the map f_2 has $\nu_j = 1$ if and only if $f_2(0) \in A_1$. But, using the notation of the statement of the algorithm, we have $P_{f_2} \cap A_1 = Y_1$ and $P_{f_2} \cap A_0 = Y_0$.

Hence the algorithm gives the correct kneading sequence for f_2. □

4.4.1 Rotation number $\rho = 1/n$

Before making full use of Algorithm 4.4.2, we tackle the simple case where the rotation number is $1/n$.

Proposition 4.4.3. *Suppose F has a fixed cluster point with rotation number $\rho = 1/n$. Then the internal addresses of the secondary maps f_2 are given in Table 4.1.*

Critical displacement	Internal address of f_2
1	$1 \to n$ (Obstructed)
3	$1 \to n-1 \to n$
5	$1 \to n-2 \to n-1 \to n$
7	$1 \to n-3 \to n-2 \to n-1 \to n$
$\cdots$	$\cdots \quad \cdots \quad \cdots$
$2n-5$	$1 \to 3 \to 4 \to 5 \to \cdots \to n-1 \to n$
$2n-3$	$1 \to 2 \to 3 \to 4 \to \cdots \to n-1 \to n$
$2n-1$	$1 \to n$ (Obstructed)

Table 4.1: Internal addresses in the rotation number $1/n$ case.

Proof. Denote $f_2^{\circ j}(0) = c_j$ for each j. Then if the critical displacement is $2k+1$, then the set Y_0 contains k elements: $Y_0 = \{c_{n-k}, c_{n-(k-1)}, \ldots, c_{n-2}, c_{n-1}\}$. Hence $Y_1 = \{c_1, c_2, \ldots, c_{n-k-1}\}$ and so the kneading sequence for f_2 is made up of a string of $(n-k-1)$ 1s, followed by a string of k 0s and then a $*$. In other words $\nu = 1^{n-k-1}0^k*$.

A simple calculation then yields the internal address $1 \to n-k \to n-(k-1) \to \cdots \to n-1 \to n$. □

Proposition 4.4.4. *Suppose we fix the critical displacement $\delta = 2k+1$ and have rotation number $\rho = 1/n$. Letting n go to infinity, the sequence of maps giving δ as the critical displacement is as in Table 4.2.*

Denominator of ρ	Internal address of f_2
$k+1$	$1 \to n$ (Obstructed)
$k+2$	$1 \to 2 \to 3 \to \cdots \to k+2$
$k+3$	$1 \to 3 \to 4 \to \cdots \to k+3$
$\cdots$	$\cdots \quad \cdots \quad \cdots$
$k+\ell$	$1 \to \ell \to \ell+1 \to \cdots \to k+\ell$
$\cdots$	$\cdots \quad \cdots \quad \cdots$

Table 4.2: Internal addresses for $\delta = 2k+1$ for ρ of the form $1/n$.

Proof. Label the points on the star which belong to the critical orbit of the second critical point by taking e_0 to be the critical point, and $e_1, e_2, \ldots, e_{n-1}$ to be the other points in anticlockwise order. Clearly for a fixed cluster point with two period n orbits, the largest the critical displacement can be is $2n-1$. Hence the lowest period yielding a critical displacement of $2k+1$ is period $k+1$. In this case we have the critical points being adjacent, and so the mating is obstructed. Furthermore,

the set $Y_1 = \{e_1, e_2, \ldots, e_n\}$, hence the kneading sequence is $1 \cdots 1*$ and the internal address is $1 \to n$.

Now suppose we have the rotation number is $1/(k+j)$. Then if the critical displacement is $2k+1$ then the set $Y_0 = \{e_j, e_{j+1}, \ldots, e_{k+j-2}, e_{k+j-1}\}$. This gives a kneading sequence of $1^{j-1}0^k*$, and hence an internal address $1 \to j \to j+1 \to \cdots \to k+j$. □

4.4.2 Rotation number $\rho = 2/n$

Proposition 4.4.5. *Suppose F has a fixed cluster point with rotation number $\rho = 2/n$. Then the internal addresses of the secondary maps f_2 are given as in Table 4.3.*

δ	Internal address of f_2
1	$1 \to n$ (Obstructed)
3	$1 \to \frac{n-1}{2} \to n-1 \to n$
5	$1 \to \frac{n-1}{2} \to n$
7	$1 \to \frac{n-3}{2} \to \frac{n-1}{2} \to n-2 \to n-1 \to n$
9	$1 \to \frac{n-3}{2} \to \frac{n-1}{2} \to n$
$\cdots$	$\cdots \quad \cdots \quad \cdots$
$4k-1$	$1 \to \frac{n-(2k-1)}{2} \to \frac{n-(2(k-1)-1)}{2} \to \cdots \to \frac{n-1}{2}$ $\to n-k \to n-(k-1) \to \cdots \to n$
$4k+1$	$1 \to \frac{n-(2k-1)}{2} \to \frac{n-(2(k-1)-1)}{2} \to \cdots \frac{n-1}{2} \to n$
$\cdots$	$\cdots \quad \cdots \quad \cdots$
$2n-5$	$1 \to 3 \to 4 \to 5 \to \cdots \to n-1 \to n$
$2n-3$	$1 \to \frac{n+1}{2} \to n$
$2n-1$	$1 \to n$ (Obstructed)

Table 4.3: Internal addresses in the rotation number $2/n$ case.

Proof. If the rotation number is $2/n$, then n is an odd integer. Using the same notation as in the proof of the previous proposition, we remark that it is a simple calculation that

$$
\begin{aligned}
e_1 &= c_{\frac{n+1}{2}}, \\
e_2 &= c_1 \\
e_3 &= c_{\frac{n+3}{2}} \\
e_4 &= c_2 \\
\cdots &\quad \cdots \\
e_{2j-1} &= c_{\frac{n+(2j-1)}{2}} \\
e_{2j} &= c_j \\
\cdots &\quad \cdots \\
e_{n-3} &= c_{\frac{n-3}{2}} \\
e_{n-2} &= c_{n-1} \\
e_{n-1} &= c_{\frac{n-1}{2}}.
\end{aligned}
$$

This follows from observing the orbit of the generator 2 in the group $(\mathbb{Z}_n, +)$.

If $\delta = 1$ or $2n-1$, then in both cases we have $Y_0 = \varnothing$ and so the internal address is $1 \to n$. If $\delta = 2n-3$ then $Y_0 = e_1 = c_{\frac{n+1}{2}}$ and so the internal address is $1 \to \frac{n+1}{2} \to n$. We now consider all the other critical displacements.

If $\delta = 4k-1$ then the first critical point must be between $e_{n-(2k-1)}$ and e_{n-2k} in the cyclic ordering. Hence

$$
\begin{aligned}
Y_0 &= \{e_{n-1}, e_{n-2}, e_{n-3}, \ldots, e_{n-(2k-1)}\} \\
&= \{c_{\frac{n-1}{2}}, c_{n-1}, c_{\frac{n-3}{2}}, c_{n-2}, \ldots, c_{\frac{n-(2(k-1)-1)}{2}}, c_{n-(k-1)}, c_{\frac{n-(2k-1)}{2}}\} \\
&= \{c_{\frac{n-(2k-1)}{2}}, c_{\frac{n-(2(k-1)-1)}{2}}, \ldots, c_{\frac{n-1}{2}}, c_{n-(k-1)}, c_{n-(k-2)}, \cdots, c_{n-1}\}
\end{aligned}
$$

This gives a kneading sequence that looks like

$$
\underbrace{1\cdots1}^{\frac{n-2k-1}{2}}\underbrace{0\cdots0}^{k}\underbrace{1\cdots1}^{\frac{n-(2k-1)}{2}}\underbrace{0\cdots0}^{k-1}*,
$$

and a (somewhat laborious!) calculation yields the correct internal address $1 \to \frac{n-(2k-1)}{2} \to \frac{n-(2(k-1)-1)}{2} \to \cdots \frac{n-1}{2} \to n-k \to n-(k-1) \to \cdots \to n$.

If $\delta = 4k+1$ then the first critical point will be in between e_{n-2k} and e_{n-2k+1} in the cyclic ordering. Comparing to the example with $\delta = 4k-1$, we see that this means that Y_0 is almost the same in this case, save for the addition of the element

c_{n-k}. In other words

$$Y_0 = \{c_{\frac{n-(2k-1)}{2}}, c_{\frac{n-(2(k-1)-1)}{2}}, \ldots, c_{\frac{n-1}{2}}, c_{n-k}, c_{n-(k-1)}, c_{n-(k-2)}, \cdots, c_{n-1}\}$$

which gives the kneading sequence

$$\overbrace{1\cdots1}^{\frac{n-2k-1}{2}}\overbrace{0\cdots0}^{k}\overbrace{1\cdots1}^{\frac{n-2k-1}{2}}\overbrace{0\cdots0}^{k}*,$$

and this again yields the correct internal address $1 \to \frac{n-(2k-1)}{2} \to \frac{n-(2(k-1)-1)}{2} \to \cdots \frac{n-1}{2} \to n$. □

An interesting question is to see if it makes any sense to take limits of combinatorial data. In other words, given some combinatorial data (ρ, δ) with perhaps ρ irrational, can we find a sequence of combinatorial data (which each correspond to a unique rational map F_n up to Möbius transformation) converging to (ρ, δ) and then see if these rational maps F_n converge in some sense. Also, would this limit be independent of the sequence? Initial attempts have been made to answer this question.

We can also do this in the language of matings. We take the pairs of maps (f_n, g_n) which give the combinatorial data (ρ_n, δ_n) converging to (ρ, δ). We then see if the maps f_n and g_n converge (perhaps in the sense of their parameters) and take the mating of these limits.

Chapter 5

Period 2 Cluster Points

We now move on to the study of maps which have a period two cluster cycle. Though there are some marked similarities with the one cluster case, numerous calculations revealed that this case actually has an increased level of complexity. Conjecturally, this complexity will increase even further as the period is made larger. This chapter will focus solely on the degree 2 case: the far more more complicated consideration of the higher degree case will hopefully be the focus of further work, see the appendices for some preliminary results. The earlier sections in this chapter will follow the same course, as far as possible, as the previous chapter. We will remark upon the differences as they occur.

5.1 Combinatorial invariants

In this section we discuss how to define the combinatorial data of a cluster with a period 2 cluster cycle. Before moving on, we discuss the potential differences with the fixed point case. The combinatorial rotation number was defined in Chapter 3, and when we defined it we took into account that the period of the cluster could be arbitrarily large.

The second piece of combinatorial data for the fixed cluster case was the combinatorial displacement, δ. As shown in Section 4.3.1, in the fixed cluster case, the pair (ρ, δ) of combinatorial data is enough classify the degree d rational map in the sense of Thurston. If we want to make a similar statement in the two cluster case then, we need to define the combinatorial data in this case.

Clearly, the definition in the previous chapter profitted from the fact that there was only one cluster, and so the critical points (and critical values) of a map were forced to be in the same cluster. However, *a priori*, we see there are a couple

of issues with trying to extend the fixed cluster definition to the period 2 case. Firstly, we don't know if the two critical points are in the same cluster. If they are not, then attempting to measure the combinatorial displacement as the cyclic distance between the two critical point components is clearly impossible, and so a new definition is required.

The next few results will show us that, in actual fact, the critical points cannot appear in the same cluster. Following these results, we see it is necessary to modify our definition of critical displacement from the fixed cluster case to take into account this new fact. This leads to the new statement, Definition 5.1.4.

Theorem 5.1.1. *Let $F \cong f_1 \amalg f_2$ be a degree 2 rational map with a period 2 cycle of cluster points. Then precisely one of the maps f_1 or f_2 belongs to the $(1/3, 2/3)$-limb of $\mathcal{M}$.*

Proof. It is clear that both f_1 and f_2 cannot belong to the $(1/3, 2/3)$-limb, since then the mating would be obstructed by Tan Lei's Theorem (Theorem 2.2.13). So it only remains to show that both of f_1 and f_2 cannot lie outside $\mathcal{M}_{(1/3,2/3)}$.

So assume f_1 and f_2 lie outside $\mathcal{M}_{(1/3,2/3)}$. By Theorem 1.4.6, if f_i is not in $\mathcal{M}_{(1/3,2/3)}$, the external rays of angles $1/3$ and $2/3$ must land at distinct points. Since these angles have period 2 under angle doubling, they must land at points with period dividing 2. As $R_{1/3}$ and $R_{2/3}$ land at different points, these landing points must be a period 2 cycle.

Now notice that, under mating, we have the identifications

$$\gamma_{f_1}\left(\frac{1}{3}\right) \sim \gamma_{f_2}\left(\frac{2}{3}\right) \quad \text{and} \quad \gamma_{f_2}\left(\frac{1}{3}\right) \sim \gamma_{f_1}\left(\frac{2}{3}\right)$$

and these points are not identified with each other, or any other points. In particular, these points cannot be cluster points. Since $f_i(\gamma_{f_i}(1/3)) = \gamma_{f_i}(2/3)$ and $f_i(\gamma_{f_i}(2/3)) = \gamma_{f_i}(1/3)$, these pairs form a period 2 cycle for the map $F \cong f_1 \amalg f_2$. However, since F already has a period 2 cycle (the cluster point cycle) by assumption, we see that this second period 2 cycle cannot exist, since a degree 2 rational map can only have one period 2 cycle. Hence both of the maps cannot lie outside $\mathcal{M}_{(1/3,2/3)}$, and so precisely one of them lies in $\mathcal{M}_{(1/3,2/3)}$. □

We can restate this in terms of internal addresses.

Corollary 5.1.2. *Let $F \cong f_1 \amalg f_2$ be a degree 2 rational map with a period 2 cycle of cluster points. Then precisely one of the maps f_1 or f_2 has internal address beginning $1 \to 2 \to \cdots$.*

Proof. This follows directly from the definition of the internal address. If f lies in $\mathcal{M}_{(1/3,2/3)}$ then we must pass through the period 2 component to get to it from the main cardioid. This means 2 appears in the internal address. □

Recall from Section 1.7 that the internal address can be considered as the sequence of closest characteristic periodic points in the Hubbard tree. Thus the 2 in the internal address represents a period 2 point on the arc $[c_0, c_1]$. In fact, as we will show later, this period 2 point becomes one of the cluster points; its image (which is also contained in the Hubbard tree, by forward invariance) becomes the other cluster point.

The author is grateful to Mary Rees for suggesting the proof of the following result.

Proposition 5.1.3. *There does not exist a rational map R with a period 2 cluster cycle such that the critical points are in the same cluster.*

Proof. We begin with some notation. We suppose that R is a branched cover and the critical points are in the same cluster. Denote the critical points by c_0 and $\tilde{c}_0$, and denote $c_i = R^{\circ i}(c_0)$ and $\tilde{c}_j = R^{\circ j}(\tilde{c}_0)$. We will set both critical points to have period $2n$, and so $P_R = \{c_0, \ldots, c_{2n-1}, \tilde{c}_0, \ldots, \tilde{c}_{2n-1}\}$. Since the critical points are in the same cluster and the clusters are period 2, the set of post-critical points in the first cluster $\mathcal{C}_0$ are those of the form c_{2i} and $\tilde{c}_{2j}$ (i.e those points with even index), whilst the remaining post-critical points lie in the second cluster $\mathcal{C}_1$. Denote the star of $\mathcal{C}_0$ by X_0 and the star of $\mathcal{C}_1$ by X_1.

Now consider the curve γ, the boundary of a tubular neighbourhood U of X_0. Then γ separates the two clusters and in particular is non-peripheral. By Lemma 3.4 in [Mil00a], $R^{-1}(\gamma)$ is made up of d disjoint curves, each of which is the boundary of a tubular neighbourhood of a pre-image star of X_0. If the pre-image star is not X_1, then the curve in $R^{-1}(\gamma)$ bounding its tubular neighbourhood must be peripheral. The boundary of the tubular neighbourhood of X_1, $\gamma' \in R^{-1}(\gamma)$ separates the two clusters, and so is isotopic to γ. $R : \gamma' \to \gamma$ is a homeomorphism, hence $\Gamma = \{\gamma\}$ is a Levy cycle and hence such a branched cover cannot be equivalent to a rational map. □

It is now clear from the above that we will need to define critical displacement in the 2 cluster case using a different definition from the one cluster case. There are other ways in which one could define it, but this appears to be the most natural and leads to neater statements in later sections.

Definition 5.1.4 (Critical displacement)**.** Let F be a rational map with a period two cluster cycle. Choose one of the critical points to be c_1, and label the cluster containing it to be $\mathcal{C}_1$. Then (by Proposition 5.1.3) the other critical point c_2 is in the second cluster $\mathcal{C}_2$. We define the critical displacement δ as follows. Label the arms in the star of $\mathcal{C}_1$, starting with the arm with endpoint c_1, in anticlockwise order $\ell_0, \ell_1, \ldots, \ell_{2n-1}$. Then $F(c_2)$ is the endpoint of one of the ℓ_k. This integer k is the critical displacement (see Figure 5.1).

Remark 5.1.5. Again, this definition depends on the choice of which critical point is c_1. Again, since we are dealing with rational maps with labelled critical points, this issue will not cause us problems. Also, with a similar argument as with the one cluster case, we see that the critical displacement must be an odd integer.

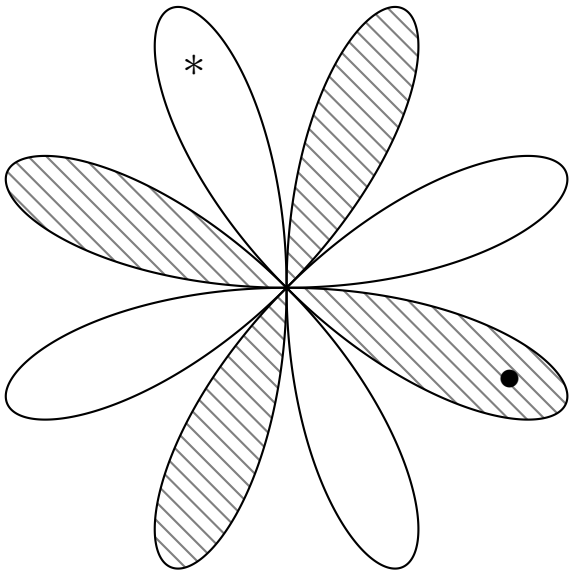

Figure 5.1: A cluster with critical displacement 5. We use $*$ to represent the critical point c_1 and the dot to represent the critical value which is the image of the second critical point c_2. The shading is used to differentiate between components for the orbit of c_1 and c_2.

5.2 Properties of maps in the mating operation

Suppose we have a mating $F \cong f_1 \amalg f_2$ with a period 2 cluster cycle. From Section 3.2, we already know how the critical orbit components from the two polynomials piece together to create the clusters. However, a natural question to ask is

what we can say about the two maps f_1 and f_2, given that they produce a 2 cluster under mating.

5.2.1 Properties of the map in $\mathcal{M}_{(1/3,2/3)}$

Recall that in Chapter 4, Proposition 4.2.2, we showed that a mating producing a fixed cluster point must have one of the maps being an n-rabbit. There is a similar result for period 2 cluster orbits. However, it is not so simple as the previous case, as there are in fact two maps that could play the role of the "rabbit-like map".

Proposition 5.2.1. *Let f_1 and f_2 be quadratic polynomials with period $2n$ superattracting orbits. Suppose $F \cong f_1 \amalg f_2$ is a rational map that has a period 2 cluster cycle. Then one of f_1 or f_2 has internal address*

1. $1 \to 2_{r/n} \to 2n$, *or*
2. $1 \to 2_{r/n} \to 2n-1 \to 2n$.

That is, a map which is either the tuning of the basilica by an n-rabbit (a "double rabbit"), or the (unique) other period $2n$ component lying in the wake of this double rabbit.

Figure 5.2 shows the position of these two maps in the period 8, rotation number 1/4 case.

Proof. First we note that if we have an angled internal address starting

$$1_{\frac{1}{2}} \to 2_{\frac{r}{n}}$$

then the corresponding map will have a period 2 orbit with combinatorial rotation number r/n, by the dynamic characterisation of internal addresses. The content of this proof will be to show that no other maps can have such a period 2 orbit, and that such an orbit is required if the mating is going to create a period 2 cluster cycle. Indeed, the period two orbit will become the cluster points for the period 2 cluster cycle.

By Corollary 5.1.2, we know that one of the maps (without loss of generality, f_1) must have internal address starting $1 \to 2$. By Corollary 1.7.10, this means exists a period 2 point p_1 on the arc $[\alpha, c_1]$. Since the 2 appears in the internal address, the dynamical characterisation of the internal address means this period two point will have non-zero combinatorial rotation number. We will show that this point will become one of the cluster points, and along with its image $p_2 = f(p_1)$

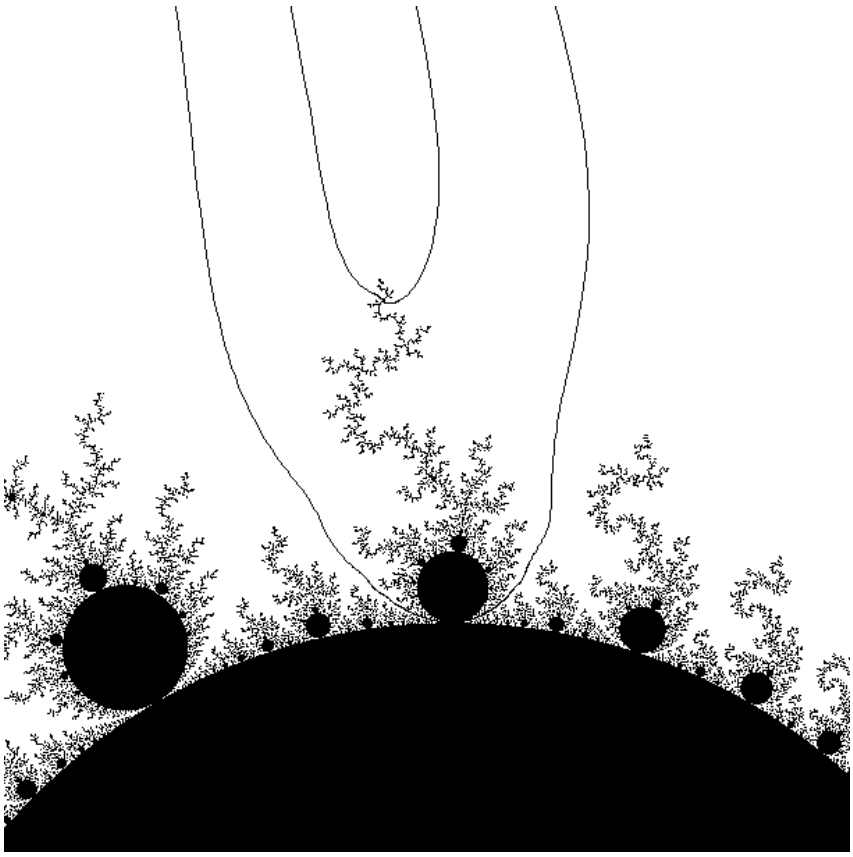

Figure 5.2: The double rabbit component and secondary map component of period 8, rotation number 1/4 case.

(which also lies on the Hubbard tree, by forward invariance), will form the period 2 cycle of cluster points. By Lemma 2.3.1, the period of $[p_1]$ under mating will be either 1 or 2.

We will show that the period of $[p_1]$ cannot be 1. If this were to be the case, then we must have $[p_1] = [p_2]$. Then p_1 and p_2 belong to the same ray class and both have non-zero combinatorial rotation number. This contradicts Lemma 2.3.3. If the period of $[p_1]$ is 2, then it must become a cluster point. For if not, the cluster cycle will be a period 2 cycle for the rational map F which is distinct from the period two orbit $[p_1]$ and $[p_2]$. Since a degree 2 rational map must have precisely one period 2 orbit, this is a contradiction.

We now show that the combinatorial rotation number of p_1 must be r/n for some r. Suppose the denominator of the combinatorial rotation number is k. Then there are k external rays landing at p_1. Each of these corresponds to a global arm at

p_1 in the graph of the ray class $[p_1]$. By Lemma 2.3.5, each arm can contain at most one point of the periodic cycle of root points of the critical orbit components of f_2. Since global arms map homeomorphically onto their images, if one arm contains a root point, then all arms contain a root point. So there are k root points of critical orbit components of f_2 in this ray class, and since the ray class is period two, there are $2k$ root points in the union. Since we need all root points to belong to the union of these ray classes, this gives us $k = n$.

So we now know the internal address must start $1 \to 2_{r/n} \to \cdots$. By Corollary 1.8.5 there are exactly two maps of period $2n$ satisfying this internal address, and the internal addresses are given by the discussion following Corollary 1.8.5 and Proposition 1.8.6. These are precisely the internal addresses given in the statement of this result. □

Corollary 5.2.2. *Let $F \cong f_1 \amalg f_2$ be a rational map with a period two cluster cycle and let f_1 be the map with internal address starting $1 \to 2_{p/n} \to \cdots$. Then the combinatorial rotation number of F will be p/n.*

Proof. From the previous result, the cluster cycle is made up of the periodic ray classes $[p_1]$ and $[p_2]$. Each global arm at p_1 in $[p_1]$ contains precisely one root point from the periodic cycle of root points of the critical orbit components of f_2. By assumption, the external rays, and therefore the global arms, are permuted with rotation number p/n. Hence the critical orbit components of f_2 are also permuted with rotation number p/n, and so the combinatorial rotation number of F is p/n. □

Essentially, the previous two results say that, to create a map with a period two cluster cycle with combinatorial rotation number ρ, it is necessary that one of the maps in the mating has a period two orbit with combinatorial rotation number (as defined for polynomials) ρ. Similarly, we found in the fixed cluster point case that we had a similar result: one of the maps had to be an n-rabbit, with an α-fixed point having the same combinatorial rotation number as that of the resultant rational map. It seems likely that similar proofs extend this observation to higher periods. Underlying this is the realisation that rotation numbers are preserved under mating, and so we cannot create a point with non-zero rotation number if one did not exist before the mating took place. Indeed, this follows from the discussion of periodic ray classes in Chapter 2.

We include pictures of the two possible maps to help fix our ideas, see Figures 5.3 and 5.4. These pictures show not only the filled Julia sets of the maps, but also the external rays landing on the α-fixed point and the period 2 points in the

Julia set. In addition, the picture of the second map shows the rays landing on the root points of the critical orbit components.

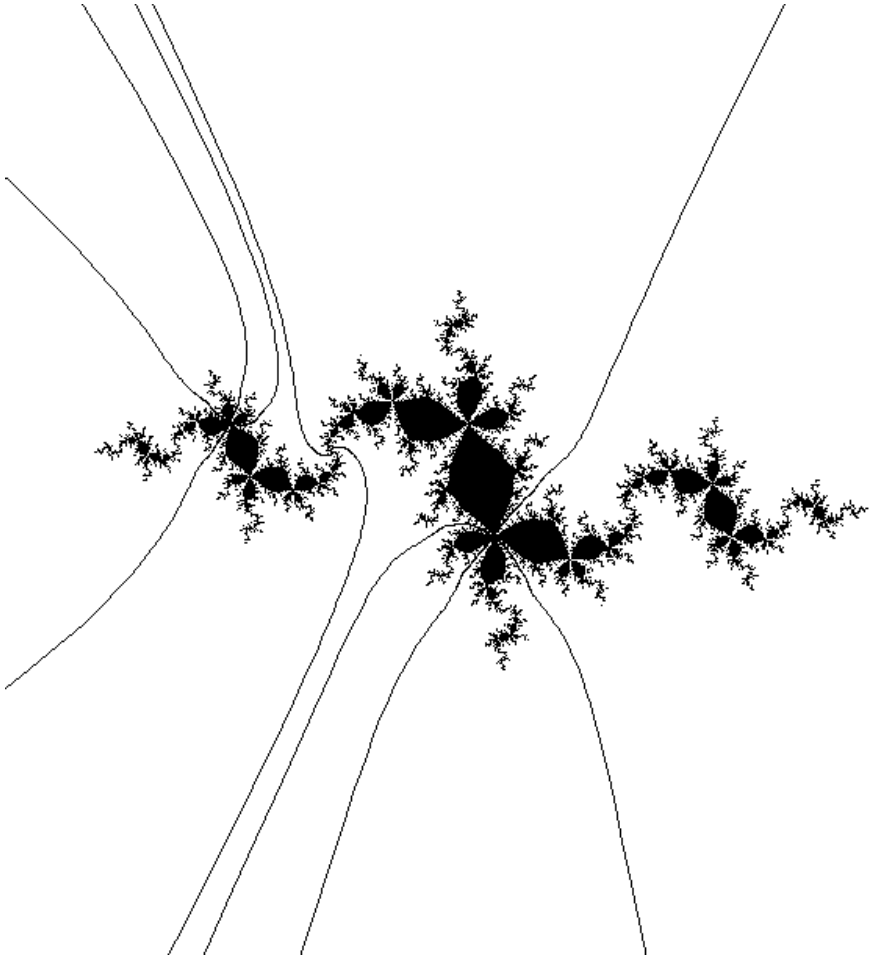

Figure 5.3: The double rabbit, corresponding to the parameter rays in Figure 5.2 with the external rays landing on the period 2 orbit and on the α-fixed point.

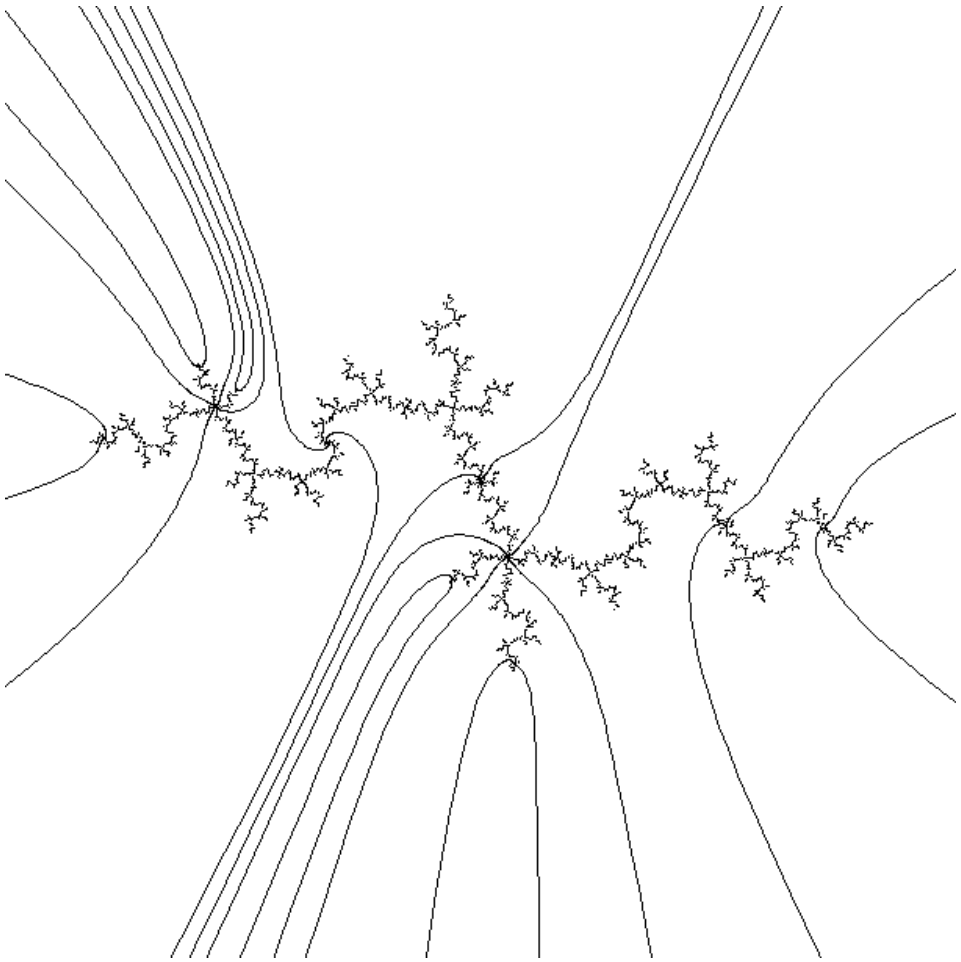

Figure 5.4: The secondary map that belongs to the wake of the limb containing the double rabbit in Figure 5.3, with the external rays landing on the period 2 orbit and the α-fixed point. Also included are the rays landing at the root points of the critical orbit Fatou components.

We now make a quick observation about the angles landing on the period two orbits for the maps found in Proposition 5.2.1.

Lemma 5.2.3. *Let $f \in \mathcal{M}_{(1/3,2/3)}$ but is not in the period two hyperbolic component. Let $\{p_1, p_2\}$ be the period two orbit of f, where p_1 is the point which lies on the regulated arc $[\alpha, f(0)]$. Then the angles of the rays landing at p_1 are all in $(1/3, 2/3)$, and the angle of the rays landing at p_2 are in $(2/3, 1/3)$.*

Proof. $f \in \mathcal{M}_{(1/3,2/3)}$ so the external rays of angle $1/3$ and $2/3$ land on the α-fixed point of f. Since f is not in the period two component, the period two orbit will be repelling, and so each point is the landing point of some rays of rational angle. Since

$p_1 \in [\alpha, f(0)]$, the rays landing on p_1 must all be in $(1/3, 2/3)$, since otherwise the rays would cross. Since $f(p_1) = p_2$ and the image of $(1/3, 2/3)$ under angle doubling is $(2/3, 1/3)$, the angles of the rays landing on p_2 must all lie in $(2/3, 1/3)$. □

5.2.2 Properties of h

The previous section gave us a classification of the maps in $\mathcal{M}_{(1/3,2/3)}$, and the results were perhaps not that surprising, considering the results that were found in the study of the fixed cluster case in Chapter 4. Perhaps of more interest is the question as to what we can say about the map that does not belong to $\mathcal{M}_{(1/3,2/3)}$. Are there any properties that this map is required to have? As in the previous chapter, we see that it is actually possible to say a lot about these "complementary" maps in the matings which yield period two cluster cycles.

Notation 5.2.4. In what follows, f will, in general, be a map with internal address $1 \to 2 \to 2n$ - we will call maps of this form "double rabbits". The map g will be the second map in the wake of f, with internal address $1 \to 2 \to 2n-1 \to 2n$. This will be called the "secondary map". The map h will be the complementary map in the mating. We will use the notation $f_{r/n}$ to denote the map with angled internal address $1 \to 2_{r/n} \to 2n$ and $g_{r/n}$ for the map with angled internal address $1 \to 2_{r/n} \to 2n-1 \to 2n$.

For the moment, we will be looking at the matings of the form $F = f_{r/n} \amalg h$ which have a period two cluster cycle. In the next section, we will focus on the case where the mating is $g_{r/n} \amalg h$. We first discuss the periodic ray classes that become the cluster points in the matings of the form $f \amalg h$.

The following result is an analogue to Lemma 1.8.2 in the period two case.

Lemma 5.2.5. *Suppose that z is a biaccessible periodic point in $J(f_{r/n})$. Then z is either the α-fixed point or belongs to the period 2 orbit $\{p_1, p_2\}$.*

Proof. The map $f_{r/n}$ belongs to only two wakes: the wake $W_{(1/3,2/3)}$ and the wake $W_{(\theta_-,\theta_+)}$, where $\theta_- < \theta_+$ are the angles of the parameter rays landing at the root point of the hyperbolic component containing $f_{r/n}$. So by Theorem 1.4.6, there are only two periodic repelling orbits with valence greater than 1. The first of these is the α-fixed point, which has portrait $\{\{1/3, 2/3\}\}$ and the other is the portrait corresponding to the pair θ_- and θ_+. Since we know $f_{r/n}$ has a period 2 repelling orbit $\{p_1, p_2\}$ the portrait corresponding to these angles must correspond to the period 2 orbit. Every other orbit portrait has valence 1, and so all other periodic repelling points are the landing point of exactly one external ray. Hence the only

biaccessible periodic points in $J(f_{r/n})$ are the period two orbit and the α-fixed point. □

Lemma 5.2.6. *If $F \cong f_{r/n} \perp\!\!\!\perp h$ has a period two cluster cycle, then each ray class $[p_i]$ corresponding to a cluster point, has a central vertex p_i (corresponding to one of the period two points of f, p_i) which has n edges leaving it. Each of these edges has a second endpoint r_i, which corresponds to a root point of a critical orbit component of h. There is a second edge at each r_i, which has a second endpoint e_i, which corresponds to a point on the Julia set of $f_{r/n}$ which is the landing point of only one external ray.*

Compare this case with that of the period one case in Lemma 4.2.10; each of the two graphs is homeomorphic to that case.

Proof. We note that each global arm at p_i contains at most two other periodic points in $J(f) \cup J(h)$. This is because any member of $J(f)$ that appears in one of the global arms cannot be biaccessible, by Lemma 5.2.5. Hence the global arm will contain a periodic point of $J(h)$ and a periodic point of $J(f)$. In order for $[p_i]$ to be a cluster point, the periodic point of $J(h)$ in the arm must be the root point r_i of a critical orbit component of h. There will be only two edges leaving r_i, since otherwise it would have non-zero combinatorial rotation number, contradicting Lemma 2.3.3. The end point of this second edge must be an endpoint of the graph of the ray class, by the reasoning of the opening two sentences.

Since the ray classes are homeomorphic, and since the global arms map homeomorphically onto their images, every global arm satisfies the description above. □

First of all, we can place a restriction on the angles associated with the map h.

Proposition 5.2.7. *Suppose $F = f_{r/n} \perp\!\!\!\perp h$ has a period two cluster cycle. Then the angles landing at the critical value component of h lie in $(1/6, 1/3) \cup (2/3, 5/6)$.*

Proof. We observe that the both the angles $\theta_- < \theta_+$ landing at the root point of the critical value component of h are in $(2/3, 1/3)$, since h cannot belong to $\mathcal{M}_{(1/3,2/3)}$. By Lemma 5.2.6 and Lemma 5.2.3, the rays $R^f_{-\theta_-}$ and $R^f_{-\theta_+}$ land on the point $p_2 \in J(f_{r/n})$. Hence the rays $R^f_{-2\theta_-}$ and $R^f_{-2\theta_+}$ land on the point p_1. Hence $-2\theta_-, -2\theta_+ \in (1/3, 2/3)$ by Lemma 5.2.3 and so $2\theta_-, 2\theta_+ \in (1/3, 2/3)$. The pre-image of $(1/3, 2/3)$ under angle doubling is the set $(1/6, 1/3) \cup (2/3, 5/6)$. Hence $\theta_-, \theta_+ \in (1/6, 1/3) \cup (2/3, 5/6)$. □

We now describe a feature of these maps that is analogous with that of angular rotation number in the previous chapter. We will make a simple observation about the ordering of external angles of maps which mate with the double rabbit with internal address $1 \to 2_{p/n} \to 2n$. Before this, we need to state a definition, which is the period 2 analogue of the angular rotation number defined in the previous chapter.

Definition 5.2.8. Let $\theta \in S^1$ have the property that $2^{2n}\theta = \theta \mod 1$. Consider the disjoint sets $A_0 = A_0(\theta) = \left\{\theta, 2^2\theta, 2^4\theta, \ldots, 2^{2k}\theta, \ldots, 2^{2(n-1)}\theta\right\}$ and $A_1 = A_1(\theta) = \left\{2\theta, 2^3\theta, \ldots, 2^{2k+1}\theta, \ldots, 2^{2n-1}\theta\right\}$. We say θ has 2-angular rotation number p/n if the following conditions are satisfied.

- The sets A_0 and A_1 are contained in disjoint arcs on the circle.
- The sets A_0 and A_1 have 1-angular rotation number p/n under the map $\theta \mapsto 4\theta$.

It is of course possible to generalise this definition in the two obvious ways. Firstly, if one were to consider degree d polynomials, one could ask for the angular rotation number to exist for the mapping $\theta \mapsto d\theta$. Secondly, if one wanted to tackle period k cluster cycles, one can define the k-rotation number for any k by considering sets $A_0, A_1, \ldots, A_{k-1}$ and checking they each have the same 1-angular rotation number. This discussion is a generalisation of the results as found in [BS94]. A similar consideration has appeared in [BMM$^+$06].

We briefly discuss what each of the conditions in Definition 5.2.8 represent. The first condition is introduced since we know that A_1 should be contained in the arc $(1/3, 2/3) \subset \mathbb{S}^1$ and A_0 in the arc $(2/3, 1/3)$. The second condition just makes sure the angles are permuted cyclically with rotation number p/n under the first return map. We remark that the map $t \mapsto 2t$ from A_0 to A_1 or from A_1 to A_0 will preserve cyclic ordering, depending on the location of the non-periodic pre-image of the angle θ.

As was the case in the previous chapter, we need to consider the properties of the graphs of the ray equivalence classes to discuss some of the combinatorics of the maps involved in matings that produce a period two cluster cycle. We currently do not have enough information to discuss the graphs when the map in $\mathcal{M}_{(1/3,2/3)}$ is g, so we postpone that until Section 5.2.3. However, we can discuss the ray graph when the map in $\mathcal{M}_{(1/3,2/3)}$ is a tuned rabbit f.

We state without proof that a double rabbit of internal address $1 \to 2_{p/n} \to 2n$ has 2-angular rotation number p/n - the proof is similar to that of Lemma 4.2.9.

Proposition 5.2.9. *Suppose $F \cong f_{p/n} \amalg h$ is a rational map with a period 2 cluster cycle. Then one of the angles associated to h has 2-angular rotation number $(n-p)/n$.*

Proof. Denote one of the angles associated to $f_{p/n}$ by θ. The map $f_{p/n}$ is a double rabbit and so both its associated angles have 2-angular rotation number p/n, hence $-\theta$ has 2-angular rotation number $(n-p)/n$. By Lemma 5.2.6, we see that the rays $R^h_{-2^k\theta}$ land at the root points of critical orbit components of h. Hence one of the angles associated with h will have 2-angular rotation number $(n-p)/n$. □

We can then combine Propositions 5.2.7 and 5.2.9 to say even more.

Corollary 5.2.10. *Let h be a map such that $f_{p/n} \amalg h$ has a period 2 cluster cycle. Then there is an angle θ associated to h that has 2-angular rotation number $(n-p)/n$ and has $A_1(\theta) \subset (1/6, 1/3) \cup (2/3, 5/6)$.*

Proof. The existence of the angle θ is given by Proposition 5.2.9. In order to create a cluster, all the rays in A_0 must belong to $(1/3, 2/3)$. Hence the pre-images of these rays must lie in $A_1 \subset (1/6, 1/3) \cup (2/3, 5/6)$. A_1 is contained in the pre-images of the angles in A_0, so we are done. □

We now focus a bit more on the set A_1. Suppose $\theta \in (1/6, 1/3)$. The pre-image of this interval is $(1/12, 1/6) \cup (7/12, 2/3)$. Since the periodic pre-image of θ must lie in $A_0 \subset (1/3, 2/3)$, we see that the periodic pre-image (the one corresponding to the angle of the ray landing at the root point of the critical point Fatou component) is in $(7/12, 2/3)$ and the pre-periodic pre-image is in $(1/12, 1/6)$. Similar considerations show that if $\theta \in (2/3, 5/6)$ then the periodic pre-image of θ is in $(1/3, 5/12)$ and the pre-periodic pre-image is in $(5/6, 11/12)$.

The knowledge of where the pre-periodic pre-image of θ is will help us in two ways. Firstly, we will use it to help classify the properties of maps h that mate with $f_{p/n}$ to form a rational map with a period 2 cluster cycle. The second use will be in its role of calculating the kneading sequences of the h in Section 5.5.2.

In fact, in both cases, we are more concerned with where this pre-image θ_0 lies in relation to the orbit of θ, and in particular the points of A_1. The angle θ_0 will separate the set A_1 into two disjoint sets: those contained in the interval $(\theta_0, 1/3)$ and those contained in $(2/3, \theta_0)$. We can in fact simplify this.

Lemma 5.2.11. $A_1 \cap (\theta_0, 1/3) = A_1 \cap (0, 1/3)$.

Proof. The set $A_1 \cap (0, \theta_0)$ is empty, since if there exists $\phi \in A_1 \cap (0, \theta_0)$ then $\phi \in (5/6, 0)$ or $(0, 1/6)$. But this is a contradiction of Corollary 5.2.10. □

So the above separation of the set A_1 can done by considering the complementary intervals to the angle 0 in A_1.

Lemma 5.2.12. *Let p_2 be the periodic point of period 2 that lies on the boundary of the critical point component of $f_{p/n}$. Denote by $R_{\phi_1}^{f_{p/n}}$ and $R_{\phi_2}^{f_{p/n}}$ the rays landing at p_2 that separate the Fatou component containing $f_{p/n}^{\circ(2n-2)}(0)$ from the rest of the critical orbit. Then the cyclic ordering satisfies*

$$\phi_1 < 0 < \phi_2.$$

Proof. The images of $R_{\phi_1}^{f_{p/n}}$ and $R_{\phi_2}^{f_{p/n}}$, which are respectively $R_{2\phi_1}^{f_{p/n}}$ and $R_{2\phi_2}^{f_{p/n}}$ land on $f_{p/n}(p_2) = p_1$, and these rays separate the component containing $f_{p/n}^{\circ(2n-1)}(0)$ from the critical orbit Fatou components containing odd iterates of the critical point 0. This means that $(\phi_1, \phi_2) \subset (2\phi_1, 2\phi_2)$ (considered as arcs on the circle) and so (ϕ_1, ϕ_2) contains a fixed point of the map $t \mapsto 2t$. But the only fixed point of angle doubling is 0 and so the result is proved. □

The above lemma gives us a very simple way of calculating the number of rays that land on p_2 that land anti-clockwise of the ray of angle 0 for $f_{p/n}$. The combinatorial rotation number of the orbit of rays at p_2 is p/n. The rays separating the component containing $f_{p/n}^{\circ(2n-2)}(0)$ from the other critical orbit components map onto the rays bounding the critical point component of $f_{p/n}$. Since the rotation number is p/n, there are p angles in A_1 that are anticlockwise from 0 in A_1.

The angle 0 will separate the set of angles of rays landing at p_2 in $f_{p/n}$, and this separation must be compatible with the separation of A_1 by the angle 0. This follows from the fact that the β-fixed points are identified under mating, and since the rays landing at p_2 will be the those of angle ϕ satisfying $-\phi \in A_1(\theta)$, where θ is the angle corresponding to the map h which has 2-angular rotation number $(n-p)/n$. We then get the following.

Proposition 5.2.13. *Suppose $F \cong f_{p/n} \perp\!\!\!\perp h$. Then h has an associated angle with 2-angular rotation number $(n-p)/n$ and the set $A_1 \cap (2/3, 0) = A_1 \cap (2/3, \theta_0)$ for this angle contains precisely p elements.*

We note here that in the previous chapter, we stated a result which showed that having the correct angular rotation number was a necessary and sufficient condition to form clustering with a rabbit. In fact, it is not true that if h has 2-angular rotation number $(n-p)/n$ then it will mate with $f_{p/n}$ to create a rational map with a period 2 cluster cycle.

Example 5.2.14. Consider the angle $\theta = 26/63$, which has internal address $1 \to 2 \to 4 \to 6$. A simple calculation shows that θ has 2-angular rotation number $2/3$. However, if h is the associated map to θ, we see that $f_{1/3} \amalg h$ cannot be a rational map, since both f and h belong to $\mathcal{M}_{(1/3,2/3)}$.

It should be noted, however, that in the formal mating of f and h, we notice that the graphs of the ray equivalence classes for the points belonging to the period two cycle of $f_{p/n}$ look precisely like the ray equivalence classes formed when the mating actually creates a rational map with a period 2 cluster cycle.

Since we know that h has associated angles in $(1/6, 1/3) \cup (2/3, 5/6)$, we ask if this, paired with the requirement to have 2-angular rotation number $(n-p)/n$, is sufficient for a map to create a two cluster when mated with $f_{p/n}$. To do this, we show there are only n maps satisfying these two conditions, and a pigeonhole principle argument, as in the last chapter, will give the result.

Proposition 5.2.15. *There are precisely n angles that have 2-angular rotation number $(n-p)/n$ and have $A_0 \subset (1/3, 2/3)$ such that $A_1 \cap (2/3, 0)$ contains exactly p elements .*

Proof. We will show that the map $t \mapsto 2t$ from A_0 to A_1 maintains the cyclic ordering. This is easy because $A_0 \subset (1/3, 2/3)$ which maps homeomorphically onto $(2/3, 1/3)$. Hence the ordering maintains the cyclic order on the circle.

This means that picking the position of one angle θ in A_0 fixes the ordering of all the other angles in the orbit of θ: those in A_0 are fixed by the 2-angular rotation number and the ordering in A_1 fixed by the fact the angle doubling map on $(1/3, 2/3)$ is a homeomorphism.

Recall Algorithm 1.9.2. Then if we know the position of the non-periodic pre-image of θ, we get a unique angle from the algorithm. But Proposition 5.2.13 tells us that the position of the non-periodic pre-image is determined by the 2-angular rotation number and the assumption on A_1. Hence picking the position of the first angle in the cyclic ordering of A_0 uniquely defines the angle.

Since there are n angles in A_0 and any of these can be the first angle, we see that there are precisely n angles satisfying the given properties. □

Corollary 5.2.16. *The map $F \cong f_{p/n} \amalg h$ has a period two cluster cycle if and only if h has an associated angle satisfying the properties in Proposition 5.2.15.*

Proof. There are n possible choices for the critical displacement and all are realisable by matings. Hence each map having the given properties will create a period two cluster cycle when mated with $f_{p/n}$. □

It is highly likely that this statement is true under the weaker assumption that $h \notin \mathcal{M}_{(1/3,2/3)}$.

The next result is perhaps more suited to the section on combinatorial results. However, since it essentially only requires the definition of 2-angular rotation number, we include it here. It offers a restriction on which limbs of the Mandelbrot set the map h can lie in.

Proposition 5.2.17. *Let $F \cong f \amalg h$ be the mating of two quadratic polynomials, such that the map F has a period 2 cluster cycle. Then the internal address of h starts $1 \to 2m+1 \to \cdots$ for some $m \geq 1$.*

Proof. Suppose that the the internal address of h starts $1 \to 2m \to \cdots$ for some $m \geq 1$. If $m = 1$ then the mating will be obstructed and F could not be a rational map so we assume $m > 1$.

The combinatorial rotation number of α_h will be $p/2m$, where p is odd. The case where $p = 1$ or $p = 2m-1$ is easy, since if R^h_θ lands at the root point of the Fatou component containing c_1, then the angle θ is separated on S^1 from $2^2\theta$ by 2θ and $2^3\theta$. This means θ cannot have a well defined 2-angular rotation number.

So suppose $p \neq 1, 2m-1$. The map h has an associated angle θ with 2-angular rotation number $(n-p)/n$ by Proposition 5.2.9. Label the local branches at α_h by anticlockwise cyclic ordering, starting with ℓ_0 being the branch containing the critical point c_0. This means c_1 is the endpoint of the branch ℓ_p. Denote the endpoint of ℓ_{p-1} by c_j and the endpoint of ℓ_{p+1} by c_k. Then necessarily $j, k \leq 2m$ and both are even. The former is a standard result about Hubbard trees and the latter follows from the fact that p is odd, see Figure 5.5.

This means that the angles $\theta, 2^2\theta, \ldots$ belong to a different interval in the circle to the angles $2\theta, 2^3\theta, \ldots$. But this means that $2^2\theta$ must be in the same complementary interval of $S^1 \setminus \{2^{j-1}\theta, 2^{k-1}\theta\}$ as θ. This forces c_3 to not be an endpoint of the Hubbard tree. But since at least one of j or k is greater than 3 and c_j and c_k are endpoints, this is a contradiction of the Hubbard tree being forward invariant under h. Hence our assumption that the internal address of h starts $1 \to 2m \to \ldots$ is false. □

5.2.3 Mating with the Secondary Map

Here we make some observations about what properties we can expect to find for maps h which create a period 2 cluster cycle with the secondary map with internal address $1 \to 2 \to 2n-1 \to 2n$. That is, the maps h so that $F \cong g \amalg h$ has a period two cluster cycle. We note that this section has no analogue with the previous

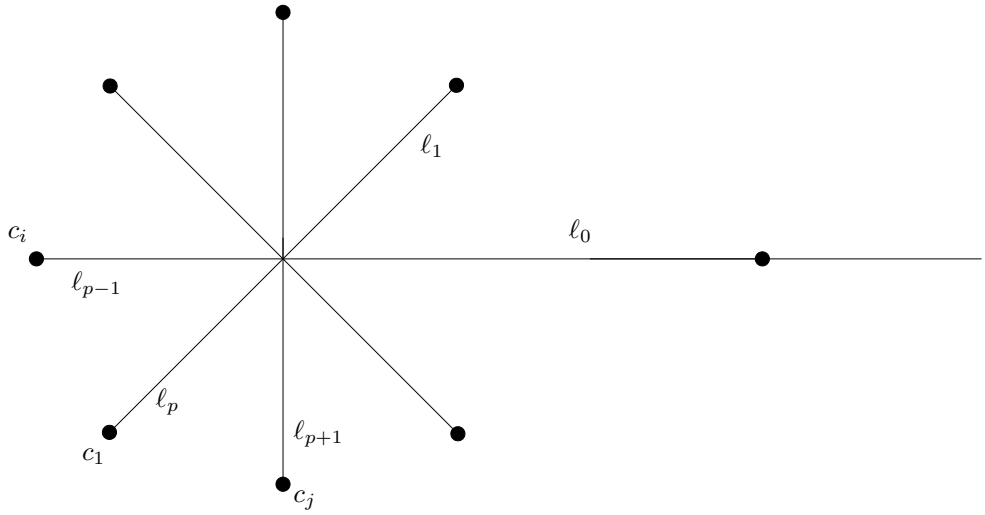

Figure 5.5: Diagram for proof of proposition 5.2.17.

chapter, since the existence of this secondary map is a new phenomenon which does not occur in the fixed cluster case.

We also need to make an observation about the ordering of the angles associated to the critical orbit of the secondary map, that with internal address $1 \to 2 \to 2n-1 \to 2n$. The Hubbard trees for low period examples are given in Appendix D. We describe the general structure of these Hubbard trees.

Proposition 5.2.18. *The Hubbard tree of a map with internal address $1 \to 2 \to 2n-1 \to 2n$ can be described as follows. There are two period 2 points p_1 and p_2 with n arms. One of the global arms at p_1 contains the critical point c_0 and the other global arms at p_1 have endpoints $c_1, c_3, \ldots, c_{2n-3}$. The point p_2 has one global arm which contains the critical point c_0, and the endpoints of the other global arms are $c_2, c_4, \ldots, c_{2n-2}$. The point c_{2n-1} is on the arc (p_2, c_{2n-1}). Finally, there are no branch points on the arc (p_1, p_2), and c_0 lies on (p_1, p_2).*

Proof. Using Algorithm 1.9.1 yields the tree with the above features. See Figure 5.6 for an example of such a tree. □

Lemma 5.2.19. *Suppose $F \cong g \perp\!\!\!\perp h$ is a rational map. Then the critical displacement of F will be 1 or $2n-1$.*

Proof. The branch at the period two point p_1 in the Hubbard tree containing the critical value of g is separated from the other branches at the period two point by two rays, of angle θ and $\theta + 3$ (we suppress the denominator $2^{2n}-1$). The rays of

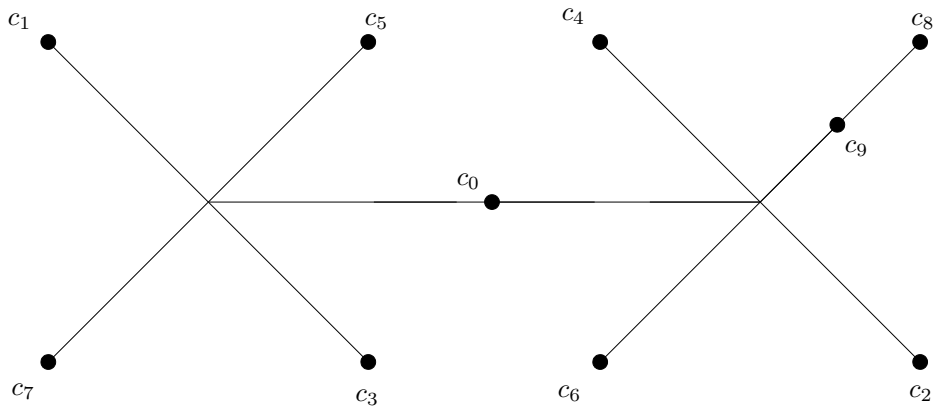

Figure 5.6: Hubbard tree for $1 \to 2_{2/5} \to 9 \to 10$.

angles $\theta + 1$ and $\theta + 2$ land at the root point of the critical value component of g, see Figure 5.7.

We claim that the ray graph containing the point p_1 (as in the picture) must have (precisely) one of the following two properties. The branch of the graph of the ray equivalence class containing the root point r of the critical value component U_1 of g (in other words, the landing point of the rays of angle $\theta + 1$ and $\theta + 2$) must contain either the ray of angle θ or the ray of angle $\theta + 3$. We will show that every other possibility is impossible.

It is clear that each branch of the graph must contain exactly one of the rays landing at the point p_1. If it contained more than one then they would form a loop and thus would generate a Levy cycle. Suppose the branch containing r contains a ray of angle $\phi \notin \{\theta, \theta + 3\}$, and R^g_ϕ lands at p_1. Let γ denote the (unique) path through external rays from r to p_1. Since the only possible biaccessible points in $J(g)$ on this path are r and p_1, we see that (using $[p, r]$ as the notation for the regulated arc from p to r):

$$\Gamma = \gamma \cup [p_1, r]$$

separates the sphere into two pieces. In particular, it separates the root point r' on the branch anticlockwise in the cyclic order from r from the ray of angle ϕ' which is the first angle anticlockwise round from ϕ in the cyclic ordering of rays at p. But since F has to maintain this cyclic ordering, the branch containing r' has to contain the ray of angle ϕ', and since rays cannot cross this is a contradiction, see Figure 5.8.

So we now know that the branch of the graph of the ray equivalence class containing r must contain the ray R^g_θ or $R^g_{\theta+3}$. We now study this branch in more detail. Suppose that the ray $R^h_{-(\theta+1)}$ lands at the same point as $R^h_{-\theta}$. This common

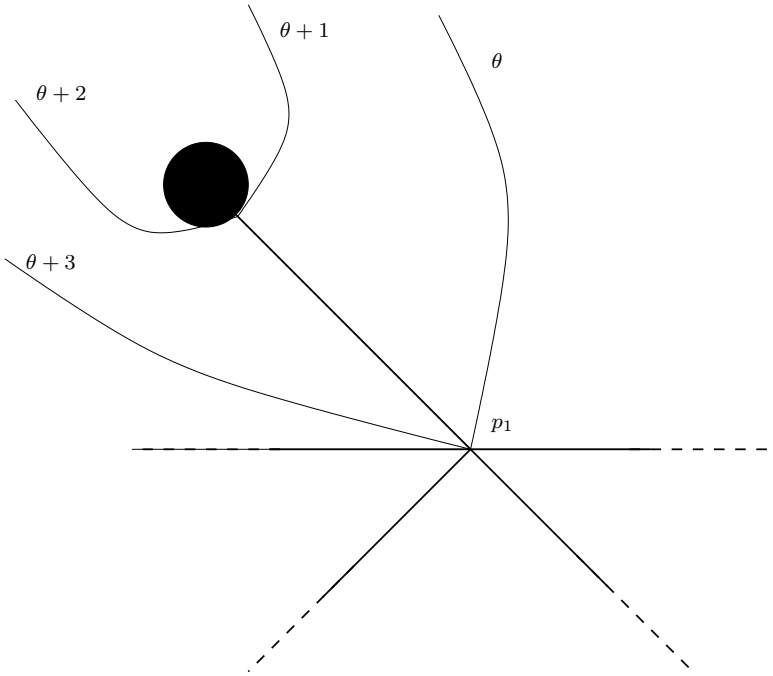

Figure 5.7: The rays landing at the period two point and critical value component of the map g.

landing point ζ cannot be the root point of a critical orbit component, since the size of the sector would mean this would have to be a critical value component, and so the critical values would be in the same cluster, a contradiction of Proposition 5.1.3. However, the angular width of the sector bounded by ζ and the external rays $R^h_{-(\theta+1)}$ and $R^h_{-\theta}$ is the smallest it can possibly be, and so by Theorem 1.4.5 it must contain the root point of the Fatou component which contains critical point of h. But this is another contradiction since the root point of the critical value component needs to be in the ray equivalence class of $f(p_1)$ and it is separated from this point. The proof of when $R^h_{-(\theta+2)}$ lands at the same point as $R^h_{-(\theta+3)}$ is analogous to the above.

The only remaining possibility is that the rays $R^h_{-(\theta+2)}$ and $R^h_{-\theta}$ land at the same point or the rays $R^h_{-(\theta+1)}$ and $R^h_{-(\theta+3)}$ land at the same point. Since both situations are essentially the same will we discuss only the first one. The common landing point ξ of the two rays must be the root point of a critical orbit component. For if not, we notice that

$$R^g_{\theta+2} \cup R^h_{-(\theta+2)} \cup R^h_{-\theta} \cup R^g_{\theta}$$

separates the ray $R^h_{-(\theta+1)}$ from all other rays with the necessary denominator. Since

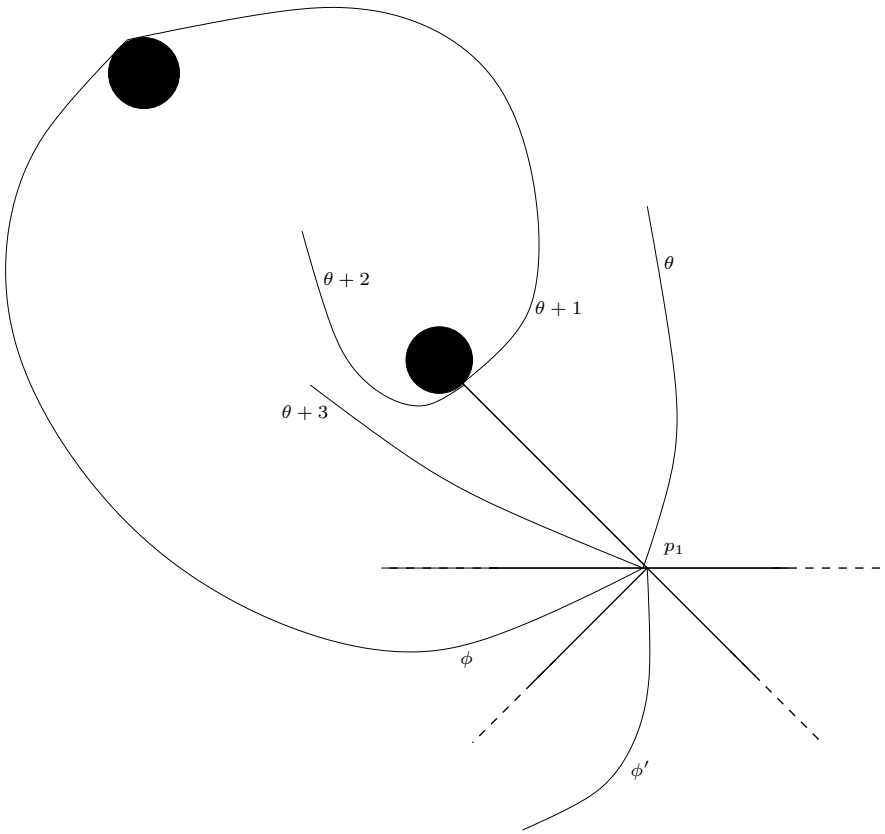

Figure 5.8: The case where the branch containing r contains the ray of angle ϕ.

the root point of a critical orbit component must have at least two rays landing on it, this means that this branch of the graph of the ray equivalence class cannot contain a root point of a critical orbit component. But then none of the branches can, as each one maps homeomorphically onto its image and they are periodic.

Hence the rays $R^h_{-(\theta+2)}$ and $R^h_{-\theta}$ land at the root point $\hat{r}$ of a critical orbit component. The angular width of the sector containing this component is 2, and so the angular width of its pre-image is 1. This means that the pre-image sector contains the critical value, and so in particular the pre-image of $\hat{r}$ is the root point of the critical value component. Hence $\hat{r}$ is the root point of the component V_2 containing the second iterate of the critical point of h. Since V_2 is adjacent to U_1, it follows their pre-images are adjacent, and so the critical point component of g will be adjacent to the critical value component of h. This means that the critical displacement of the resultant rational map will have to be ± 1, or equivalently, equal to 1 or $2n - 1$.

We remark finally that which value δ takes is dependent on which pair of

rays land together. We give more details in Corollary 5.2.27. □

Figure 5.9 shows how the rays piece together.

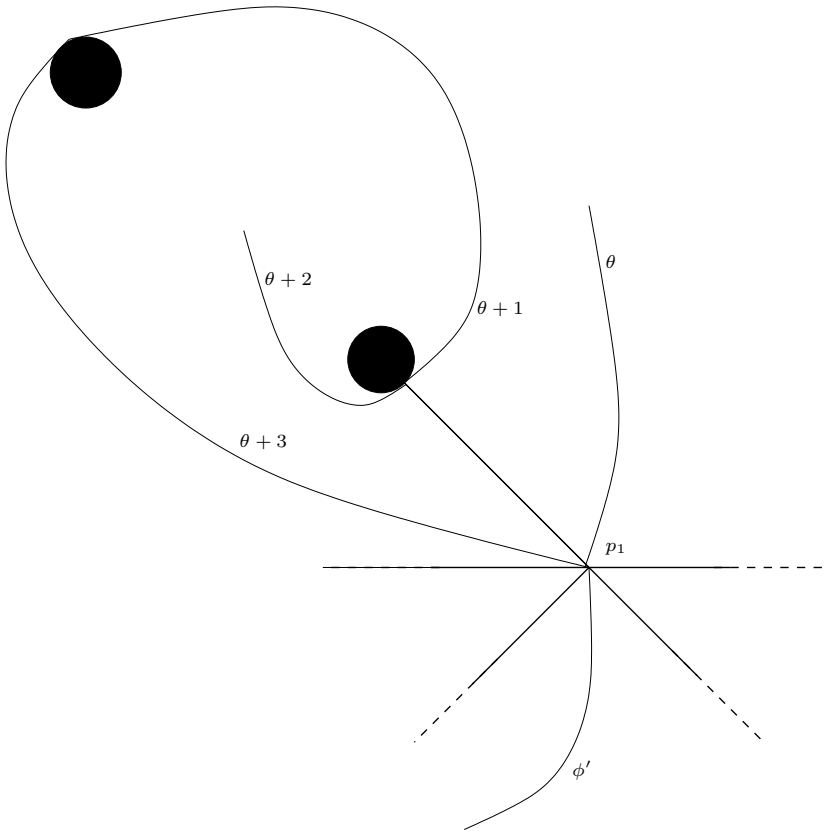

Figure 5.9: How the ray class is formed near the critical value component of g. $R^h_{-(\theta+2)}$ must be an endpoint.

Corollary 5.2.20. *The hyperbolic component containing h is narrow. That is, it has width $1/(2^{2n}-1)$.*

Proof. The rays landing at the root point of the critical orbit component containing the second iterate of the critical point differ by $2/(2^{2n}-1)$ by the previous result. Hence the rays landing at the root point of the critical value component differ by $1/(2^{2n}-1)$. Therefore the rays landing at the root point of the hyperbolic component containing h differ by $1/(2^{2n}-1)$ and so the component is narrow. □

Corollary 5.2.21. *One of the rays $R^h_{-(\theta+1)}$ or $R^h_{-(\theta+2)}$ lands at an endpoint of $J(h)$.*

Proof. If $R^h_{-\theta}$ and $R^h_{-(\theta+2)}$ land at the same (root) point in $J(h)$, then there are no possible partner rays for $R^h_{-(\theta+1)}$. Hence the point is not biaccessible, and so it must be an endpoint of $J(h)$. A similar argument holds if $R^h_{-(\theta+1)}$ and $R^h_{-(\theta+3)}$ land at the same point in $J(h)$; this causes $R^h_{-(\theta+2)}$ to land at an endpoint. □

Corollary 5.2.22. *Each branch of the ray equivalence class corresponding to the cluster points in $g \perp\!\!\!\perp h$ can be described as follows. Starting at p, there is an edge to the rootpoint of a critical orbit component of h. From this there is another edge to the root point of a critical orbit component of g. Finally, from this point there is an edge going to a point of $J(h)$ which is the landing point of only one ray.*

Proof. The branch containing the root point of the critical value component of g starts with the period two point p_1. One of the rays $R^g_\theta \cup R^h_{-\theta}$ or $R^g_{\theta+3} \cup R^h_{-(\theta+3)}$ lands at the root point of a critical orbit component of h. Suppose it is $R^g_\theta \cup R^h_{-\theta}$ (the other case is identical). As shown in the proof of Lemma 5.2.19, $R^h_{-\theta}$ lands at the same point as $R^h_{-(\theta+2)}$, and this is a root point of a critical orbit component of h. The next edge is then the ray $R^h_{-(\theta+2)} \cup R^g_{\theta+2}$, which lands at the root point of the critical value component of g. The partner ray to $R^g_{\theta+2}$ is $R^g_{\theta+1}$, and the ray $R^g_{\theta+1} \cup R^h_{-(\theta+1)}$ must land at an endpoint of $J(h)$, by Corollary 5.2.21.

The fact that this structure holds for all branches of the ray equivalence classes holds because each branch maps homeomorphically onto its image and the branches are periodic. □

We now describe the ray equivalence class of the cluster points in the case that the map in $\mathcal{M}_{(1/3,2/3)}$ is g. This result, along with Lemma 5.2.6 gives the only two possibilities for the ray classes of a period two cluster point.

Lemma 5.2.23. *If $F \cong g \perp\!\!\!\perp h$ then each graph has a central vertex p, which has n edges leaving it. The second endpoints of these edges are labelled r_i, which correspond to root points of critical orbit components of h. Each of these r_i has another edge starting at them, whose second endpoint are q_i, which correspond to root points of critical orbit components of g. Finally, each q_i has a second edge leaving it, whose endpoint is e_i and corresponds to a point on the Julia set of h which is the landing point of only one external ray.*

Proof. From Proposition 5.2.1, the period 2 orbit $\{p_1, p_2\}$ of g becomes the cluster cycle, and so the ray classes that become the cluster point are the ray classes $[p_1]$ and $[p_2]$. Since the class maps homeomorphically onto itself under $F^{\circ 2}$, and p_i is fixed under this iterate, the branches at p_i are homeomorphic. The structure of

these branches is as in Corollary 5.2.22, and this structure is as in the statement of the lemma. □

We now return to the case where the mating is of the form $f \amalg h$. This case is similar to the period one case, and so allows us to make similar observations to those found in the previous chapter.

Lemma 5.2.24. *Suppose $F \cong f \amalg h$ is a mating with a period 2 cluster cycle, where f is the tuned rabbit with internal address $1 \to 2_{p/n} \to 2n$. Then one of the angles landing at the root point of the critical value component of h has 2-angular rotation number $(n-p)/n$.*

Proof. The graph of the ray equivalence classes of the two cluster points looks identical to that of the ray equivalence class of the cluster point in the fixed cluster point case, (the only difference being the periodicity of the graph as a whole). Hence each graph is invariant under the second iterate of F, and this has the action of sending the ray of angle θ to the ray of angle 4θ. Furthermore, if θ is the angle of an external ray landing at one of the period 2 points of f, this angle will have angular rotation number p/n under $t \mapsto 4t$ by the observation preceding this lemma (compare Lemma 4.2.9). Hence the angle $-\theta$ will have 2-angular rotation number $(n-p)/n$. □

We can actually refine this result. It is in fact true that the set of maps that mate with g to make a rational map with a period 2 cluster cycle is a subcollection of the maps that mate with f to make a rational map with a period two cluster cycle.

Proposition 5.2.25. *Suppose $F \cong g \amalg h$ is a rational map with a period 2 cluster cycle and g is the secondary map with internal address $1 \to 2_{p/n} \to 2n-1 \to 2n$. Then h mates with the map f with internal address $1 \to 2_{p/n} \to 2n$ to create a map with a period two cluster cycle.*

Proof. Recall that there are precisely two rays landing at the root points of the critical orbit components of h, and these ray orbits are disjoint. If h mates with g to create a map with a period 2 cluster cycle, then one of these ray orbits are made up of rays of angles $-\theta_i$ such that the rays of angles θ_i land on the period two orbit in the Julia set of g. But these are precisely the angles landing at the period two orbit in $J(f)$, and so the rays $R^f_{\theta_i}$ and $R^h_{-\theta_i}$ form two periodic ray classes which become a period two cluster cycle. □

Recall that the critical displacement of $g \perp\!\!\!\perp h$, if it has a period 2 cluster cycle, is 1 or $2n-1$. Since we now know that $f \perp\!\!\!\perp h$ also has a period two cluster cycle, we can ask what the critical displacement of $f \perp\!\!\!\perp h$ will be.

Lemma 5.2.26. *Suppose $F \cong g \perp\!\!\!\perp h$ is a rational map with period 2 cluster cycle. Then $F' \cong f \perp\!\!\!\perp h$ is a rational map with a period 2 cluster cycle and has critical displacement 1 or $2n-1$.*

Proof. The fact that F' is a rational map with a period 2 cluster is the content of Proposition 5.2.25. Recall from the proof of Lemma 5.2.19 that (using the same notation) the rays landing at the root point of the critical orbit component containing $h^{\circ 2}(0)$ are

$$R^h_{-\theta} \text{ and } R^h_{-(\theta+2)} \quad \text{or} \quad R^h_{-(\theta+1)} \text{ and } R^h_{-(\theta+3)}.$$

The rays bounding the critical value component of f are R^f_θ and $R^f_{\theta+3}$, and so we see that the critical value component of f is adjacent to the Fatou component of h containing $h^{\circ 2}(0)$. Then the critical point component of f is adjacent to the critical value component of h in the cyclic ordering and so the critical displacement is 1 or $2n-1$. □

Corollary 5.2.27.

1. *If $g \perp\!\!\!\perp h$ has critical displacement 1 then $f \perp\!\!\!\perp h$ has critical displacement $2n-1$.*
2. *If $g \perp\!\!\!\perp h$ has critical displacement $2n-1$ then $f \perp\!\!\!\perp h$ has critical displacement 1.*

Proof. This result comes from the following observation. We know that the critical orbit component U containing $h^{\circ 2}(0)$ has precisely two rays landing at its root point. These pairs are either $R^h_{-\theta}$ and $R^h_{-(\theta+2)}$ or $R^h_{-(\theta+1)}$ and $R^h_{-(\theta+3)}$. Suppose it is the former (the second case is entirely analogous). Then we see that the ray $R^h_{-(\theta+2)} \cup R^g_{\theta+2}$ goes from the root point of U to the root point of the critical value component of g. However, when we carry out the mating $f \uplus h$ (again, we want to discuss the mating before collapsing of ray classes takes place in the topological mating), we see that now it is the rays $R^h_{-\theta} \cup R^f_\theta$ that go from the root point of U to the root point of the critical value component of f. This means that the cyclic ordering of the components have changed, and since there are only two choices for what the critical displacement can be, we are done. □

Before finishing this section, we need to discuss the ordering of the angles landing on the root points of the critical orbit Fatou components of $g_{p/n}$. We already know that the angles landing at the period two orbit have 2-angular rotation number

p/n. However, the behaviour of the angles landing at the root points is just as important when we are considering a mating with g. A look at the Hubbard tree of $g_{p/n}$ yields the following observation: save for the angles of the rays landing at the root point of the critical orbit component U containing $\tilde{c}_{2n-1}$, the angles associated to the map $g_{p/n}$ satisfy the two conditions in the definition of 2-angular rotation number being p/n, as can be seen by observing the ordering of the endpoints of the local arms of the members of the period two orbit in the Hubbard tree.

Also, by the construction in Lemma 5.2.19, the branch of the ray equivalence class (of the formal mating) containing the root point of the critical value component of g also contains the root point of the critical orbit component containing $h^{\circ 2}(0)$. Iterating forwards, we see that the branch of the ray equivalence class containing the root point of the component containing $g_1^{\circ k}(0)$ contains the root point of the component containing $h^{\circ(k+1)}(0)$.

We briefly discuss how the position of critical orbit points in the Hubbard tree affects the cyclic ordering of the rays landing at the root points of the Fatou components containing them. Suppose that the root points are the landing points of two separate orbits of rays, as is the case for the map h. If c_j and c_k are endpoints of the Hubbard tree, then the sectors created by the rays landing at the root points of the Fatou components containing them are disjoint. This means that the cyclic ordering of the rays is the same for both orbits of rays. On the other hand, if c_j is not an endpoint and c_k is an endpoint of a global arm at c_j, the cyclic ordering of the rays landing at the root points of the respective Fatou components is different for each orbit, see Figures 5.10 and 5.11 for the two different cases.

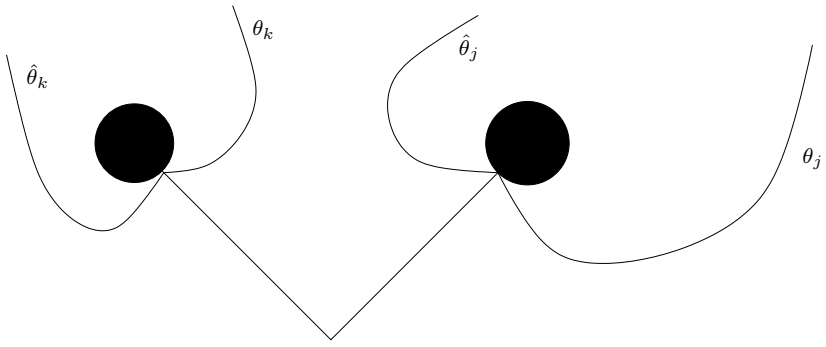

Figure 5.10: When c_j and c_k are endpoints of the Hubbard tree, the cyclic ordering of the rays is maintained.

Proposition 5.2.28. *Suppose $F \cong g \perp\!\!\!\perp h$ is a rational map with a period 2 cluster cycle. Then the elements of the forward orbit of the critical point of h, $\{h^{\circ k}(0) : k =$*

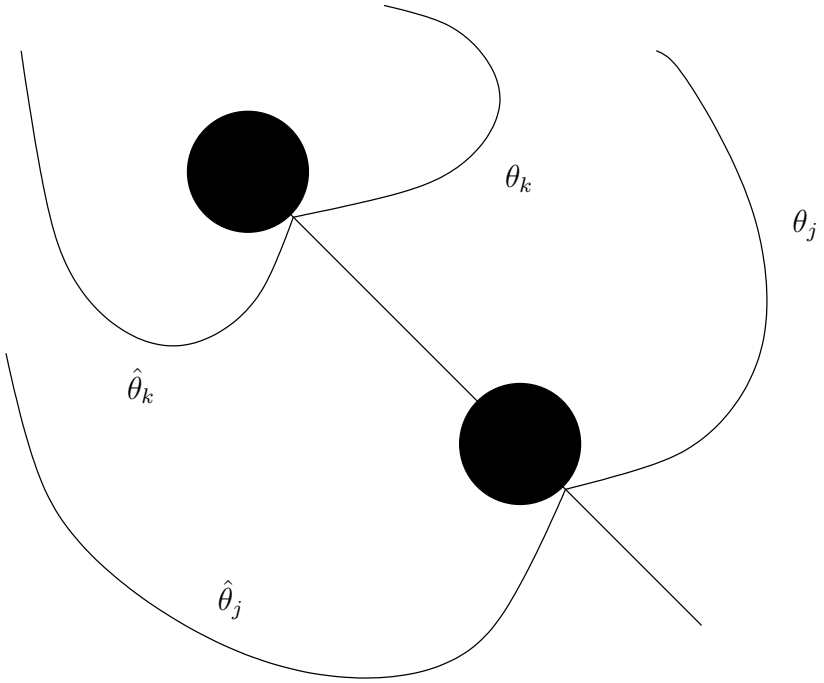

Figure 5.11: If c_j is not an endpoint, then the cyclic ordering of the two ray orbits is changed.

$1, \ldots, 2n-1\}$*, are all endpoints on the Hubbard tree of* h*. In other words, the only point in the post-critical set of* h *which is a branch point of the Hubbard tree of* h *is the critical point* 0*.*

Proof. We first note that 0 will be a branch point in the Hubbard tree, since if this were not the case, h would be an n-rabbit. If h mates with g to create a rational map with a period two cluster cycle, then by Proposition 5.2.25 it also mates with the map with internal address $1 \to 2_{p/n} \to 2n$ to create a period two cluster cycle, and so by Lemma 5.2.24 one of its associated angles θ_1 will have 2-angular rotation number $(n-p)/n$.

The ordering of the angles landing on the root points of the critical orbit components of g is discussed above - all save for the rays landing at the root point of the component containing the point $g^{\circ(2n-1)}(0)$ have ordering with 2-angular rotation number p/n. This means the rays partnering them must have 2-angular rotation number $(n-p)/n$. The only ray to which this doesn't apply is the one which pairs with the ray R which lands at the root point of the critical orbit component containing $g^{\circ(2n-1)}(0)$. But this ray is precisely the one which lands at the root point of the critical point component of h. Since all the other rays maintain cyclic

ordering, their associated critical orbit points must be endpoints of the Hubbard tree. □

Recall the definition of a triod from Section 1.9.

Proposition 5.2.29. *Suppose $F \cong g \perp\!\!\!\perp h$ is a rational map with a period 2 cluster cycle and g has internal address $1 \to 2 \to 2n-1 \to 2n$. Then the entry ν_{2n-1} in the kneading sequence of h is equal to 0.*

Proof. Suppose that $\nu_{2n-1} = 1$. We will show that c_{2n-1} is not an endpoint of the Hubbard tree, contradicting Proposition 5.2.28. The first entry in the internal address of ν is odd, so the kneading sequence begins $11\ldots$. The internal address is not $1 \to 2n$, and so there exists at least one 0 in the kneading sequence, and so there exists a critical orbit point c_k with itinerary beginning $10\ldots$. Finally, the itinerary of the point c_{2n-1} begins $1*$ by assumption.

So now apply Algorithm 1.9.6 to the triod formed by c_1, c_k and c_{2n-1}. They all agree in the first position, so we shift each sequence. But then we realise that the second entries are 1, 0 and $*$ respectively, meaning that the original triod was degenerate and the interior point is c_{2n-1}. □

Looking at Appendix B, we see that another result suggests itself.

Conjecture 5.2.30. *If h maps with g to create a rational map with a period two cluster cycle then the internal address of h contains $2n-1$.*

5.3 Classifying the rational maps

In this section, we will show - at least for the quadratic case - that the combinatorial data is enough combinatorial information to uniquely define the rational map in the sense of Thurston. This section is very similar to Section 4.3. As well as proving the main result (Theorem 5.3.2), we will also try to show in the exposition why the result seems likely to be false in the higher degree case.

There are now two stars. Denote the star containing the first critical point of F by X_F^1 and the one containing the second critical point X_F^2. We similarly define the stars X_G^1 and X_G^2. $\overline{\mathbb{C}} \setminus (X_F^1 \cup X_F^2)$ is doubly connected and so in what follows we will need to consider the conformal equivalence of doubly connected regions. A region is said to be n-connected if it comprises of a disk with n disks removed from its interior. The following result is derived from [Con95], Chapter 15 Theorem 2.1.

Theorem 5.3.1. *If G is a non-degenerate n-connected region, then G is conformally equivalent to an analytic n-Jordan region Ω. Moreover, Ω can be chosen so that its inner boundary is $\partial\mathbb{D}$ and $\infty \notin \Omega$.*

The following result is entirely analogous to Theorem 4.3.5. The added complexity comes about because we no longer have an analogue to the isotopy version of Alexander's Trick. Informally, this is because the space $\overline{\mathbb{C}} \setminus (X_1 \cup X_2)$ is no longer simply connected, and so is not conformally equivalent to a disk. Indeed, it is conformally equivalent to an annulus. The simplicity of Theorem 4.3.5 resulted from the mapping class group of the disk being trivial. For the annulus, the mapping class group is now $\mathbb{Z}$, and so we see that there is an extra difficulty when we consider the period two cluster case.

Theorem 5.3.2. *Suppose that two quadratic rational maps F and G have a period two cluster cycle with rotation number p/n and critical displacement δ. Then F and G are equivalent in the sense of Thurston.*

Again, as in the previous chapter, the proof of this theorem will require us to prove a sequence of results which will piece together to prove the theorem itself. Indeed, our general method will proceed as in the previous chapter: we will construct the homeomorphism Φ, and then try to use this map to construct the homeomorphism $\widehat{\Phi}$ so that the pair $(\Phi, \widehat{\Phi})$ satisfy the conditions required of the homeomorphisms for Thurston equivalence. A number of the results are identical to that used in Section 4.3.1, and as such will be stated here without a detailed proof. One of the difficulties in the exposition is differentiating between the two stars of each map. This fact is important, because we need a labelling of the stars in order to define the critical displacement of the map.

We also emphasise that, unlike in the previous chapter, we only prove the result in the case that the rational maps F and G have degree 2. There is strong evidence to suggest that, in fact, the theorem is not true in the higher degree case. With this in mind, we will follow the method of proof through as if we are dealing with the degree d case, and highlight the point at which the degree being equal to 2 is necessary. This will allow us to discuss the possible modifications that would be required to complete a proof in the general degree d case - or indeed, what further data would be required. We begin with an analogue to Lemma 4.3.6.

Lemma 5.3.3. *There exists a conjugacy $\phi\colon (X_F^1 \cup X_F^2) \to (X_G^1 \cup X_G^2)$ so that $\phi \circ F = G \circ \phi$.*

Proof. The proof of this lemma is essentially the same as that for Lemma 4.3.6. Notice in particular that we require the stars to be marked, so that we know which

one contains the first critical point in the definition of combinatorial displacement. □

The next result is the first point where we notice a difference with the previous chapter. By the Riemann mapping theorem for simply connected regions (not equal to the whole of $\mathbb{C}$), we saw that the complement to the star in the sphere will be conformally isomorphic to the unit disk. However, in this case, in light of Theorem 5.3.1, we see that the complement to the stars will be conformally equivalent to some annulus A. However, two annuli A_1 and A_2 are conformally equivalent to each other if and only if the ratio of the radii of their boundary circles are the same. In other words, if we normalise so that the radius of the inner boundary circle is 1, we see that two annuli are conformally equivalent if and only if their outer boundary circles have the same radii.

Proposition 5.3.4. *Let F be a rational map with a period two cluster cycle. Then there exists a conformal map $\eta_F\colon A_F \to \overline{\mathbb{C}} \setminus (X_F^1 \cup X_F^2)$, where A_F is an annulus. Furthermore, this conformal equivalence can be extended to a continuous function $\tilde{\eta}_F\colon \overline{A}_F \to \overline{\mathbb{C}}$.*

Proof. The existence of the conformal equivalence is given by Theorem 5.3.1, and the continuous extension follows from the fact that the stars are locally connected (in a proof analogous to Lemma 4.3.7). □

We now set our notation so that $A_F = \{z : 1 < |z| < e^{R_F}\}$, $A_G = \{z : 1 < |z| < e^{R_G}\}$ and $\eta_F\colon A_F \to \overline{\mathbb{C}} \setminus (X_F^1 \cup X_F^2)$ and $\eta_G\colon A_G \to \overline{\mathbb{C}} \setminus (X_G^1 \cup X_G^2)$ are conformal equivalences. We will also take advantage of the fact that the annuli A_F and A_G are respectively covered by the strips $\Sigma_F = \{a + bi : a \in [0, R_F]\}$ and $\Sigma_G = \{a + bi : a \in [0, R_G]\}$ by the map $z \mapsto \exp z$.

Proposition 5.3.5. *Let ψ be a homeomorphism defined on the boundary of the annulus A_F mapping to the boundary of the other annulus A_G, which preserves the orientation on each boundary circle. Then ψ can be extended to a homeomorphism $\Psi\colon A_F \to A_G$.*

Proof. The map ψ induces a map $\overline{\psi}\colon \partial\Sigma_F \to \partial\Sigma_G$, by defining $\overline{\psi} = \log \circ \psi \circ \exp$ and taking the branch of the logarithm to be such that $\mathrm{Im}(\overline{\psi}(0)) \in [0, 2\pi)$. We remark that $\overline{\psi}$ is $2\pi i$-periodic. To define the map $\overline{\Psi}$, consider the straight line $\ell_b = \{a + bi : 1 \leq a \leq R_F\}$. Map this to the straight line between $\overline{\psi}(0 + bi)$ and $\overline{\psi}(R_F + bi)$, by setting

$$\overline{\Psi}(a + bi) = \frac{R_G}{R_F} a + \left(\frac{\mathrm{Im}(\overline{\psi}(R_F + bi)) - \mathrm{Im}(\overline{\psi}(bi))}{R_F} a + \mathrm{Im}(\overline{\psi}(bi)) \right) i. \tag{5.1}$$

We will show that this construction yields a homeomorphism between the strips, which then induces a homeomorphism between the annuli.

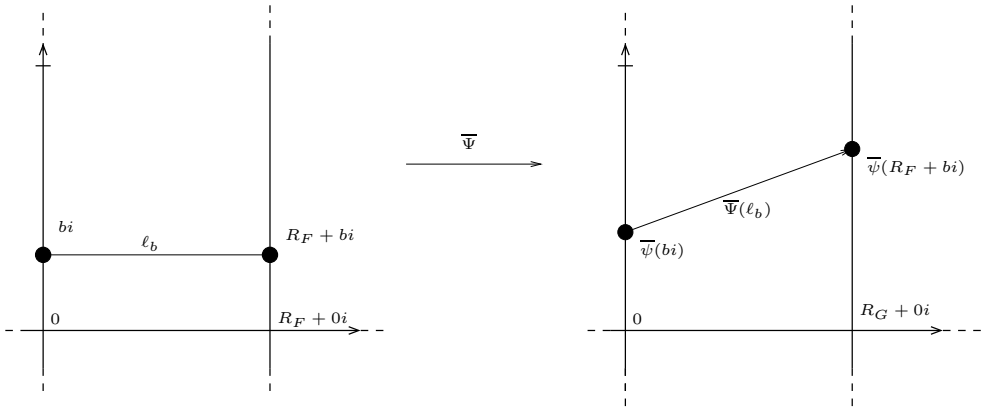

Figure 5.12: The map $\overline{\Psi}$.

First we show that $\overline{\psi}$ is a bijection.

- *Injectivity.* Suppose $\overline{\psi}(a+bi) = \overline{\psi}(c+di)$. Then by (5.1) we must have $a = c$. Suppose without loss of generality that $b < d$, then since $\overline{\psi}$ is increasing on each boundary component, we must have $\overline{\psi}(bi) < \overline{\psi}(di)$ and $\overline{\psi}(R_F + bi) < \overline{\psi}(R_F + di)$. For $\overline{\psi}(a+bi) = \overline{\psi}(c+di)$ we would need the images of ℓ_b and ℓ_d to cross. In particular this means $\overline{\psi}(bi) > \overline{\psi}(di)$ or $\overline{\psi}(R_F + bi) > \overline{\psi}(R_F + di)$, which is a contradiction. So $\overline{\Psi}$ is injective.

- *Surjectivity.* Consider the vertical line

$$\tilde{\ell}_a = \left\{ z \in \Sigma_G : \operatorname{Re}(z) = \frac{R_G}{R_F} a \right\}.$$

Then this line is mapped onto by the vertical line $\{z \in \Sigma_F : \operatorname{Re}(z) = a\}$. Since each $z \in A_G$ belongs to exactly one of these lines $\tilde{\ell}_a$, surjectivity is proved.

We now prove continuity of $\overline{\Psi}$. Notice that for fixed b, if $a \neq a'$, since $\overline{\Psi}$ is $2\pi i$-periodic we have

$$\left|\overline{\Psi}(a+bi) - \overline{\Psi}(a'+bi)\right| \leq \frac{2\pi C}{R_G} \left|a - a'\right|. \tag{5.2}$$

for some constant C. Furthermore, if $b \neq b'$ and then for fixed a we have

$$\left|\overline{\Psi}(a+bi) - \overline{\Psi}(a+b'i)\right| \leq \max\left\{ \left|\overline{\psi}(bi) - \overline{\psi}(b'i)\right|, \left|\overline{\psi}(R_F+bi) - \overline{\psi}(R_F+b'i)\right| \right\}. \tag{5.3}$$

Also, since $\overline{\psi}$ is a homeomorphism, we have $\overline{\psi}(b'i) \to \overline{\psi}(bi)$ and $\overline{\psi}(R_F + b'i) \to \overline{\psi}(R_F + bi)$ as $b' \to b$. Hence

$$\begin{aligned}
\left|\overline{\Psi}(a+bi) - \overline{\Psi}(a'+b'i)\right| &= \left|\overline{\Psi}(a+bi) - \overline{\Psi}(a'+bi) + \overline{\Psi}(a'+bi) - \overline{\Psi}(a'+b'i)\right| \\
&\leq \left|\overline{\Psi}(a+bi) - \overline{\Psi}(a'+bi)\right| + \left|\overline{\Psi}(a'+bi) - \overline{\Psi}(a'+b'i)\right| \\
&\leq \frac{2\pi C}{R_G}\left|a - a'\right| \\
&\quad + \max\left\{\left|\overline{\psi}(bi) - \overline{\psi}(b'i)\right|, \left|\overline{\psi}(R_F+bi) - \overline{\psi}(R_F+b'i)\right|\right\} \\
&\to 0
\end{aligned}$$

as $a' \to a$ and $b' \to b$ by (5.2) and (5.3). Hence $\overline{\Psi}$ is continuous and by considering its restriction to compact subsets, we see that by Proposition 4.3.4 it is a homeomorphism. This homeomorphism $\overline{\Psi}$ then induces a homeomorphism $\Psi\colon A_F \to A_G$. □

To read more about the extensions of homeomorphisms defined on the boundaries of 2-manifolds, the reader is referred to [You48] (indeed, this reference guarantees the existence of the extension in the above proposition). We will not be using any specific properties of the homeomorphism constructed in Proposition 5.3.5. This is because we do not know enough, in general, about the maps η_F and η_G.

Lemma 5.3.6. *The homeomorphism Ψ induces a homeomorphism $\Phi\colon \overline{\mathbb{C}} \to \overline{\mathbb{C}}$. Moreover, $\Phi|_{X_F^1 \cup X_F^2} = \phi$.*

Proof. We define

$$\Phi(z) = \begin{cases} \eta_G \circ \Psi \circ \eta_F^{-1}(z), & z \in \overline{\mathbb{C}} \setminus (X_F^1 \cup X_F^2); \\ \phi(z), & z \in X_F^1 \cup X_F^2. \end{cases}$$

Clearly Φ is a bijection, and it is a homeomorphism with a similar argument as in Proposition 4.3.11. □

We now define the homeomorphism $\widehat{\Phi}$ to be the lifting of Φ under F and G; that is $\widehat{\Phi} = G^{-1} \circ \Phi \circ F$. At the moment we assume that F and G are of degree d (our restriction to degree 2 will take place later), so we realise that there are in fact d choices for the map $\widehat{\Phi}$, since G is a d-fold ramified covering and each choice corresponds to which cover is chosen. In the previous chapter, we constructed the map $\widehat{\Phi}$ in Proposition 4.3.13, starting off with the observation that ϕ was a conjugacy on the stars X_F and X_G, and so we could set $\widehat{\Phi}$ to equal ϕ on X_F. It was then a fortunate consequence of the fixed cluster case that this restriction still allowed us to construct the homeomorphism $\widehat{\Phi}$ which satisfied all the required properties.

We are not so fortunate in the case where there is more than one cluster. In this case, it may be that, *a priori*, the map $\widehat{\Phi}$ we construct that satisfies $\widehat{\Phi} = G^{-1} \circ \Phi \circ F$ may not satisfy $\widehat{\Phi}|_{(X_F^1 \cup X_F^2)} = \phi$. However, we notice that it is at least possible to set $\widehat{\Phi}|_{X_F^1} = \Phi|_{X_F^1}$, since

$$\begin{aligned} z \in X_F^1 &\implies F(z) \in X_F^2 \\ &\implies \Phi(F(z)) = \phi(F(z)) \in X_G^2 \\ &\implies G^{-1}(\phi(F(z)) \in G^{-1}\left(X_G^2\right). \end{aligned}$$

The set $G^{-1}(X_G^2)$ contains the star X_G^1 and all the non-periodic pre-image stars of X_G^2. Of course, we are at liberty to pick the lift (the branch of G^{-1}) that gives us $\widehat{\Phi}(X_F^1) = X_G^1$. This choice will uniquely define our choice of G^{-1} and so our map Φ. However, this choice may not give us $\widehat{\Phi}(X_F^2) = X_G^2$, but instead will map it to some pre-image star (or pre-star, for short), and so our choice of pair $(\Phi, \widehat{\Phi})$ may not satisfy the requirements for the homeomorphisms in Thurston's theorem. However, we will show that in the degree 2 case we can carry out some suitable modifications to get two homeomorphisms which do satisfy the requirements. In higher degree cases, we can modify so that the maps Φ and $\widehat{\Phi}$ agree on the stars, but in this case it may not be true that they are isotopic relative to the postcritical set of F.

The reader may be suspicious about the above claim that the conditions $\widehat{\Phi} = G^{-1} \circ \Phi \circ F$ and $\widehat{\Phi}(X_F^1) = X_G^1$ are enough to uniquely define the homeomorphism. We briefly explain why this is the case below.

Let the critical points of F be $c_1 \in X_F^1$ and $c_2 \in X_F^2$. Let γ be a path between $v_1 = F(c_1)$, the critical value in X_F^2 and v_2, the critical value in X_F^1 and with $\gamma \cap (X_F^1 \cup X_F^2) = \varnothing$. Then $F^{-1}(\gamma)$ is made up of d curves from c_1 to c_2, and these split the sphere into d regions, which we label anticlockwise around the critical point c_1 by $\mathcal{A}_1, \ldots, \mathcal{A}_d$, chosen so that $X_F^1 \subset \mathcal{A}_1$. The map $F_i \colon \mathcal{A}_i \to \overline{\mathbb{C}} \setminus \gamma$, the restriction of F to $\mathcal{A}_i$, is a homeomorphism for each i. This can be extended continuously to the boundary.

With a similar argument we see that $\Phi(\gamma) =: \gamma'$ is a path between the critical points v_1' and v_2'. Hence $G^{-1}(\gamma')$ splits the sphere into d regions, which we similarly label anticlockwise by $\mathcal{A}_1', \ldots \mathcal{A}_d'$, starting with $\mathcal{A}_1'$ being the region component containing X_G^1. Again the restriction $G_i \colon \mathcal{A}_i' \to \overline{\mathbb{C}} \setminus \gamma'$ is a homeomorphism and it can be extended continuously to the boundary.

We now define $\widehat{\Phi}$ by mapping $\mathcal{A}_i$ onto $\mathcal{A}_i'$ so that $\widehat{\Phi} = G^{-1} \circ \Phi \circ F$.

Lemma 5.3.7. *$\widehat{\Phi}$ is a homeomorphism.*

Proof. The details of this proof are similar to Proposition 4.3.13. □

We would like to follow the method of the previous chapter by transferring the maps Φ and $\widehat{\Phi}$ to maps on the annulus and then comparing them there. However, as it stands this is not possible since we would require $\widehat{\Phi}|_{(X_F^1 \cup X_F^2)} = \Phi|_{(X_F^1 \cup X_F^2)}$. We now outline how we can fix this problem.

Let $\tau \subset \overline{\mathbb{C}}$ be a simple closed curve which is disjoint from the stars X_G^1 and X_G^2 and which intersects γ' in only one place and so that the winding number of τ about the first cluster point p_1' is 1. Denote by D_τ the Dehn twist about this curve τ in the anticlockwise direction. The plan is to modify Φ to a new function $\Phi_1 = D_\tau^{\circ j} \circ \Phi$ so that the pair Φ_1 and $\widehat{\Phi}_1 = G^{-1} \circ \Phi_1 \circ F$ equal ϕ on the stars.

By construction we map X_F^1 onto X_G^1 under $\widehat{\Phi}$. Suppose that we have $X_F^2 \subset \mathcal{A}_k$ and $X_G^2 \subset \mathcal{A}_\ell'$. If $k = \ell$ then $\widehat{\Phi}$ maps $\mathcal{A}_k$ onto A_k' and so $\widehat{\Phi}(X_F^2) = X_G^2$ and we are done. If $k \neq \ell$ then replace Φ with $\Phi_1 = D_\tau^{\circ(\ell-k)} \circ \Phi$. Φ_1 is a homeomorphism since it is the composition of two homeomorphisms. We get a new path $\gamma_1 = \Phi_1(\gamma)$ (γ defined as before) and hence we can define the regions $\mathcal{B}_1, \ldots, \mathcal{B}_d$ as the connected components of the complement of $G^{-1}(\gamma_1)$ in the sphere. As before we label anticlockwise round the first critical point and set $X_G^1 \subset \mathcal{B}_1$. Now define $\widehat{\Phi}_1 = G^{-1} \circ \Phi_1 \circ F$, mapping $\mathcal{A}_i$ onto $\mathcal{B}_i$ and forming the homeomorphism in the usual way.

Lemma 5.3.8. *$\widehat{\Phi}_1(X_F^1) = X_G^1$ and $\widehat{\Phi}_1(X_F^2) = X_G^2$.*

Proof. The first equality is clear since by construction we have $X_F^1 \subset \mathcal{A}_1$ and $X_G^1 \subset \mathcal{B}_1$. Also by assumption we have $X_F^2 \subset \mathcal{A}_k$. So all we need to show is that $X_G^2 \subset \mathcal{B}_k$.

Notice that since the regions $\mathcal{B}_i$ are ordered anticlockwise cyclically at the first critical point c_1', they are ordered clockwise cyclically at c_2'. We will compare the paths in $G^{-1}(\gamma')$ and those in $G^{-1}(\gamma_1)$. Loosely speaking, we will be using the fact that, when pulled back under the map G^{-1}, the Dehn twist $D_\tau^{\circ(\ell-k)}$ becomes a "partial twist" of $(\ell - k)/d$. This is because each region $\mathcal{B}_i$ maps onto $\overline{\mathbb{C}} \setminus \gamma_1$. Since the twist is the identity outside some small neighbourhood of τ, we see that γ_1 and γ will agree outside of this neighbourhood. However, the pre-image paths, when lifted, will look slightly different, since the twisting means the "heads" and "tails" of the pre-image curves will match up in a different way.

We describe the above more formally. Label the paths in $G^{-1}(\gamma')$ by $\sigma_1, \ldots, \sigma_d$, going anticlockwise starting with σ_1 being anticlockwise adjacent to X_G^1. The paths ζ_j in $G^{-1}(\gamma_1)$ can be thought of as being made up of three parts. The path ζ_j is equal to σ_j, starting at c_1', until it reaches some point a_j. Similarly, it will also be equal to another pre-image curve $\sigma_{j+(\ell-k)}$ of $G^{-1}(\gamma)$ from a point $b_{j+(\ell-k)}$ to the point c_2'.

We now discuss how ζ_j goes from a_j to $b_{j+(\ell-k)}$. The discrepancy is caused by the Dehn twist, lifted under the pre-image G^{-1}. Since D is defined to be an anticlockwise twist, the curve ζ_j will be twisted anticlockwise, and so will pass through the regions $\mathcal{A}_{j+1}, \ldots, \mathcal{A}_{j+(\ell-k)}$, meeting with the point $b_{j+(\ell-k)}$ when it meets the boundary of $\mathcal{A}_{j+(\ell-k)}$. See Figure 5.13 and Figure 5.14.

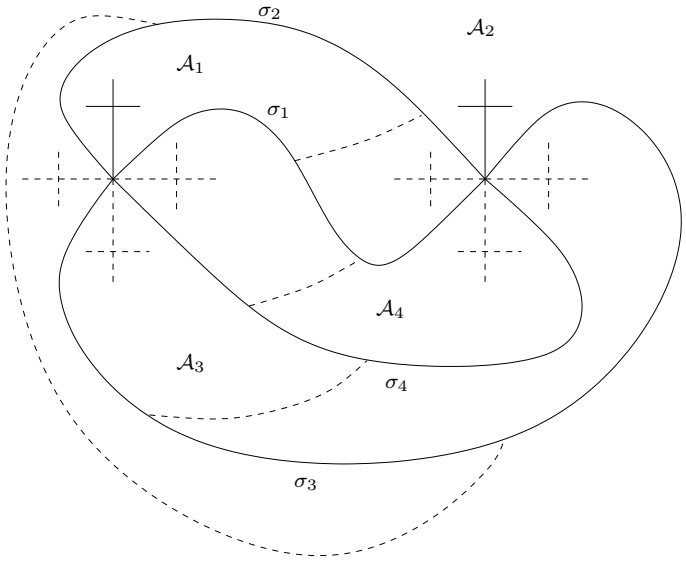

Figure 5.13: Diagram for the proof of Lemma 5.3.8. The dashed lines represent the modification that comes about if we add a Dehn twist in the range before pulling back under G. Compare with Figure 5.14.

Since $X_G^2 \subset \mathcal{A}'_\ell$, we see that the paths $\sigma_{\ell-1}$ and σ_ℓ are the paths coming into c'_2 adjacent to X_G^2. In other words the paths $\sigma_{\ell-1}$ and σ_ℓ bound the components $\mathcal{A}'_\ell$. From the discussion in the above paragraph, we see that the rays bounding $\mathcal{B}_k$ are described as follows. One starts at c'_1 and travels along σ_{k-1} until it reaches a_{k-1}. It then follows a path from a_{k-1} to $b_{k-1+(\ell-k)} = b_{\ell-1}$ and then follows $\sigma_{\ell-1}$ to c'_2. The other begins at c'_1 and follows σ_k to a_k. It then passes from a_k to b_ℓ and then follows σ_ℓ and finally to c'_2. Notice that in particular this means that we must have $X_G^2 \subset \mathcal{B}_k$ and so we are done. □

So we now have Φ_1 and $\widehat{\Phi}_1$ agree on the stars. So we now compare the induced maps Ψ_1 and $\widehat{\Psi}_1$ from A_F to A_G. Both these maps will equal ψ on ∂A_F and so $\widehat{\Psi}_1^{-1} \circ \Psi_1$ is a homeomorphism of A_F which fixes the boundary pointwise. By Proposition 2.4.2, this homeomorphism is isotopic to $D^{\circ k}$ for some $k \in \mathbb{Z}$, where D is the Dehn twist around the (anticlockwise) core curve of the annulus A_F. At this point we finally restrict ourselves to the degree 2 case; we can think of this core

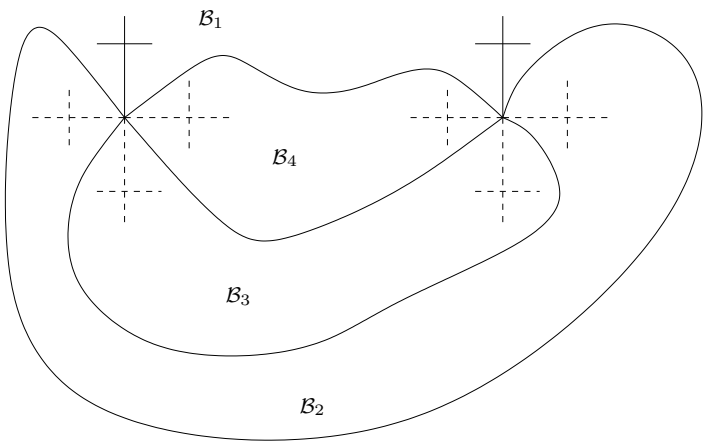

Figure 5.14: The "modified" diagram from Figure 5.14, with the new regions $\mathcal{B}_1, \ldots, \mathcal{B}_d$ labelled.

curve C as being the pre-image under η_F of some curve κ separating the stars in the F-sphere. Note that the curve $\kappa' = F^{-1}(\kappa)$ maps onto κ by a two to one covering. Also, the curve $C' = \eta_F^{-1}(\kappa')$ is homotopic to the curve C.

Proposition 5.3.9. *We can modify the homeomorphisms Φ_1 and $\widehat{\Phi}_1$ to homeomorphisms Φ_2 and $\widehat{\Phi}_2$ which satisfy the conditions of the homeomorphisms in Thurston's theorem.*

Proof. We begin by remarking that the homeomorphisms Φ_1 and $\widehat{\Phi}_1$ satisfy $G \circ \widehat{\Phi}_1 = \Phi_1 \circ F$ and agree on the $X_F^1 \cup X_F^2$. So all that remains is to modify them so that these two conditions are preserved and that furthermore they are isotopic to one another. This is equivalent to making sure some suitable modification of Ψ_1 and $\widehat{\Psi}_2$ are isotopic to one another. It should be borne in mind that the definitions of Φ_2 and $\widehat{\Phi}_2$ rely on each other, since we require $\Phi_i \circ F = G \circ \widehat{\Phi}_i$ for $i = 1, 2$. Hence modifying one will force the modification of the other.

A quick comment on the curves C and C'. Since κ' maps to κ in a two to one covering, a Dehn twist around C' will correspond to the second power of a Dehn twist around C, again in light of the fact that $\Phi_i \circ F = G \circ \widehat{\Phi}_i$ and because F and G are degree 2.

Working on the annulus A_F, we define $\widehat{\Psi}_2 = \widehat{\Psi}_1 \circ D_{C'}^{\circ(-k)}$ and $\Psi_2 = \Psi_1 \circ D_C^{\circ(-2k)}$. Since C and C' are homotopic, the Dehn twist around them has the same effect on the element of the mapping class group, hence we drop the subscript from

now on. So we calculate

$$\begin{aligned}\widehat{\Psi}_2^{-1} \circ \Psi_2 &= D^{\circ k} \circ \widehat{\Psi}_1^{-1} \circ \Psi_1 \circ D^{\circ(-2k)} \\ &\cong D^{\circ k} \circ D^{\circ k} \circ D^{\circ(-2k)} \\ &= \mathrm{Id}.\end{aligned}$$

Hence $\widehat{\Psi}_2$ and Ψ_2 are isotopic on the annulus and hence the maps $\widehat{\Phi}_2$ and Φ_2 which are obtained by passing forward onto the Riemann sphere (using the maps $\tilde{\eta}_F$ and $\tilde{\eta}_G$) satisfy the conditions for the homeomorphisms in Thurston's theorem. Hence F and G are Thurston equivalent. □

5.3.1 The Higher Degree Case

We now discuss the problems with generalising the above method to a higher degree case. Since we carried out the proof in the degree d case up until Proposition 5.3.9, it is the method of this proof that we need to focus on. Informally, we are using the fact that the difference in the homeomorphisms Φ_1 and $\widehat{\Phi}_1$ can be thought of as some power of a Dehn twist, $D^{\circ k}$.

Thinking of Φ as the homeomorphism on the range and $\widehat{\Phi}$ as the homeomorphism on the domain, we see that if we carry out one Dehn twist in the domain, then we will need to carry out the Dehn twist d times in the range. We require the use of Dehn twists to "undo" the difference between the two homeomorphisms.

To give an example, suppose we are in the degree 4 case and that we found $\widehat{\Psi}_1^{-1} \circ \Psi_1$ was isotopic to D. Then, if we carry out k twists in the domain we carry out $4k$ twists in the range, and we see that we can solve for the number of twists required to make $\widehat{\Psi}_1^{-1}$ and Ψ_1 isotopic by solving the equation $1 = 4k - k = 3k$. But this does not have an integer solution, and so we cannot carry out a (power of a) Dehn twist to correct the discrepancy. Hence the above technique would not supply a proof of equivalence in the higher degree case.

In fact, there are some preliminary calculations that suggest that the statement is no longer true in the higher degree case. It appears, then, that we would require an extra piece of combinatorial data to be sure of Thurston equivalence. A possible counterexample to the Thurston equivalence in degree 3 can be found in Appendix E.

Question 5.3.10. *How can we characterise this extra piece of data? Why does it not appear in the quadratic case?*

5.4 Equators

In contrast to the one cluster case, the question of what the equators look like in the period two case is a little more involved. There is the simple case, where the equator is a tubular neighbourhood of the Hubbard tree of a tuned rabbit. This equator will exist no matter what the combinatorial data are.

Construct a loop E as follows. Let X^1 and X^2 be the two substars belonging to the orbit of one of the critical points c_0, with $c_0 \in X^1$. Then denote by γ a path from c_0 to $F^{\circ(2n-1)}(c_0) = c_{2n-1}$, the periodic pre-image of c_0 and take a tubular neighbourhood of $X^1 \cup X^2 \cup \gamma$. Then the curve E is the boundary of this tubular neighbourhood (see Figure 5.15).

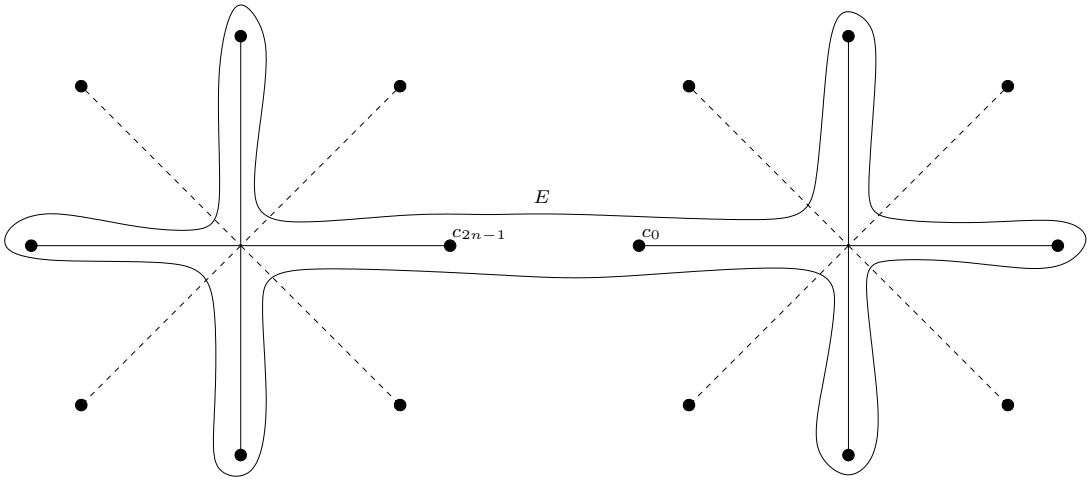

Figure 5.15: An equator in the period 2 case, corresponding to when one of the maps is a tuned rabbit.

Proposition 5.4.1. *Assume that a pre-image of γ is not a path from c_{2n-1} to c_{2n-2}. Then E is an equator for a rational map F.*

Proof. We need to show the pre-image $F^{-1}(E)$ is isotopic to E rel P_F. First note that the tubular neighbourhood of X^1 has d disjoint pre-images, one of which is a tubular neighbourhood of X^2 and the rest which are tubular neighbourhoods of pre-image stars. The tubular neighbourhood of X^2 is made up of a tubular neighbourhood of all its d pre-image substars (one of which is X^1), which all meet at c_0.

The path γ also has d pre-images, each of which goes from a pre-image of c_0 to a pre-image of c_{2n-1}. In particular one of the pre-images has endpoint c_{2n-1}, and

the path goes from c_{2n-1} to some $\tilde{c}_{2n-2}$, a pre-image of c_{2n-1} which belongs to some pre-image star of X^1 (in particular, this pre-image star is not X^2). Then there is a path $\tilde{\gamma}$ from c_{2n-1} to c_0 made up of this pre-image of γ and then the internal rays from $\tilde{c}_{2n-2}$ to c_0. We then see that $F^{-1}(E)$ is isotopic to a tubular neighbourhood of $X^1 \cup \tilde{\gamma} \cup X^2$ rel P_F, and this is isotopic to E. □

Figure 5.16 shows the pre-image of the equator described in the above proof.

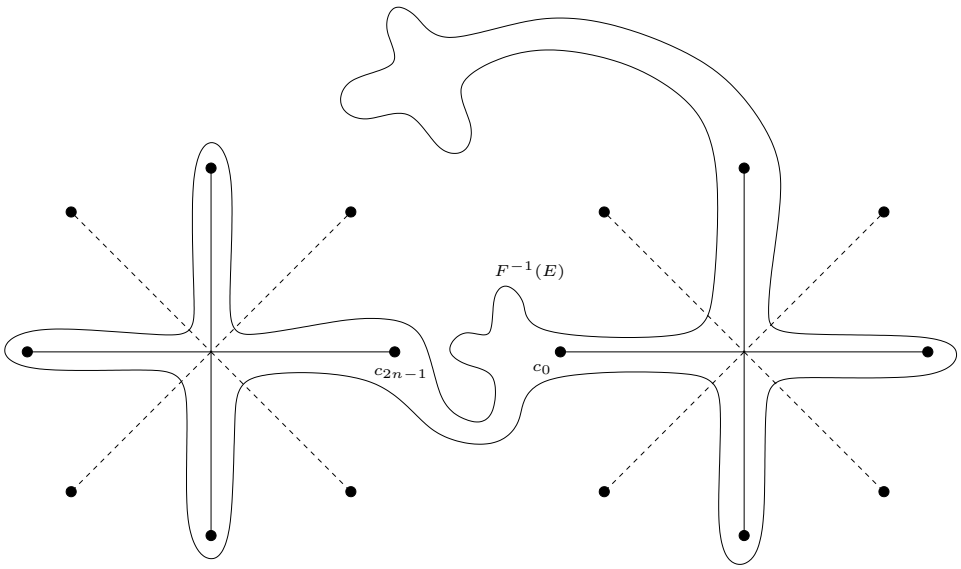

Figure 5.16: The pre-image of the equator E.

The considerations of Section 5.2 show that it is possible that a rational map with a period two cluster cycle can be formed in a different way. One obvious way is to change which map we consider to be the tuned rabbit, but this equator is formed in exactly the same way as in the above. However, if c_1 is adjacent to $F(c_2)$ in the cyclic ordering, it is possible that neither map is a tuned rabbit and so by Theorem 2.3.7 there must be a different equator.

Notice that in the one cluster case and the case where one of the maps is a tuned rabbit in the period 2 cluster case, the ray equivalence classes are very simple. In particular the ray equivalence classes contain only one point on the Hubbard tree of the rabbit or tuned rabbit, meaning the Hubbard tree does not twist much in the geometric mating and there are no identifications on the Hubbard tree. This means a tubular neighbourhood of the Hubbard tree should be a very good approximation (at least isotopically) to an equator.

We see that when it is no longer the case that one of the maps is a tuned rabbit

- in the language of Section 5.2, when the mating is $g \amalg h$ - there are identifications on the Hubbard trees of g and h under the equivalence relation induced by the ray equivalence classes. This is because each branch of the ray equivalence class contains not only the period two point that becomes the cluster point, but also the root point of a critical orbit component of the map g. For the identifications of h, all the root points landing at critical orbit components of the same parity are identified together at the cluster point. Hence in both cases the Hubbard tree "twists" during the mating and so a tubular neighbourhood of the Hubbard tree no longer is a suitable guess for the equator. At the moment it is not known how to describe the equator in general for this mating, except in the cases with low period.

Question 5.4.2. *Is there a general description of the equators corresponding to the mating $g \amalg h$?*

5.5 Combinatorial Phenomena

5.5.1 Combinatorial properties of the map h

We now discuss some properties of the map h, the complementary map to the maps f or g in the mating. We characterised the maps which mate with f to form a rational map with a period 2 cluster cycle earlier, with the aid of the notion of 2-angular rotation number. However, not every map which mates with f to create a period 2 cluster cycle will mate with g to create a period 2 cluster cycle, although the converse is true (Proposition 5.2.25). Here we will see what further conditions are required on the map h for it to mate with g to create clustering. We already know some non-combinatorial properties of h from Section 5.2.

In the previous chapter, we noticed that we were able to construct an algorithm which gave us the kneading sequence of the complementary map to f, the n-rabbit, in a mating which produces a rational map with a fixed cluster point. Here we will assume that one of the maps in the mating is f, since this case gives a simpler condition on the ordering of the associated angles of the map h. Furthermore, by Proposition 5.2.25, any map which mates with g to create a rational map with a period two cluster cycle will also mate with f to create a map with a period two cluster cycle.

We now state an algorithm. It uses ideas from Algorithm 1.9.2.

Algorithm 5.5.1. *The following algorithm computes the kneading sequence of the map h such that $F \cong f \amalg h$ has a period 2 cluster cycle with critical displacement $2k-1$ and combinatorial rotation number p/n.*

1. *Split S^1 into two complementary arcs and label them I_0 and I_1. Choose n points in each I_j and label the points in I_j in* clockwise order *by $(j,1),(j,2),\ldots,(j,n)$.*

2. *Put θ_1 at position $(1,k)$.*

3. *Label all the other positions so that the angle θ_1 will have 2-angular rotation number $(n-p)/n$, with the points in I_j being considered as the points in A_j. For example, this puts θ_{2n} at position $(0,k)$.*

4. *Add a new point θ_0 between positions $(1,p)$ and $(1,p+1)$. The points θ_0 and θ_{2n} divide the circle into 2 complementary intervals. Label the one containing θ_1 by J_1 and the other one by J_0.*

5. *The kneading sequence of θ_1 is $\nu = \nu_1 \ldots \nu_{2n-1}*$, where $\nu_k = j$ when $\theta_k \in J_j$. This kneading sequence is the kneading sequence of the map h.*

Proof. This is essentially a repeat of a number of results from Section 5.2. Clearly the two intervals I_0 and I_1 correspond to the two intervals containing A_0 and A_1. Then the positions $(1,m)$ represent the partner rays to the ones landing on the period 2 point in f which lies on the boundary of the critical point component. Clearly then putting θ_1 at $(1,k)$ will put the critical value component of h a total of $2k-1$ components round from the critical point component of f.

The cyclic ordering of the other angles θ_i follows from the fact that, for the map h, the cyclic ordering of the angles is maintained when one maps from A_0 to A_1. The position of θ_0 is given by Proposition 5.2.15 and the derivation of the kneading sequence from the intervals is just the standard definition of the kneading sequence. □

Note in particular we do not need to calculate the actual numerical value of any angles with this algorithm.

There is another way of calculating the kneading sequence of the map h, using a technique very similar to Algorithm 4.4.2. Recall the form of the equator as described in Proposition 5.4.1. The equator was chosen as a tubular neighbourhood of the Hubbard tree of some $f_{p/n}$ since, as discussed above, the Hubbard tree does not twist too much in the geometric mating. Of course, the Hubbard tree of h does not twist much in the geometric mating either. With this in mind, we notice that the curve in Figure 5.17 is isotopic to the equator in Figure 5.15, and this should be itself isotopic to some tubular neighbourhood of the Hubbard tree of h. The reason why we leave a gap at the point c_{2n-2} is because, as seen in Proposition 5.4.1, there

is a pre-image of γ running from this point to a pre-image of c_0. Hence the two choices of equators are entirely compatible.

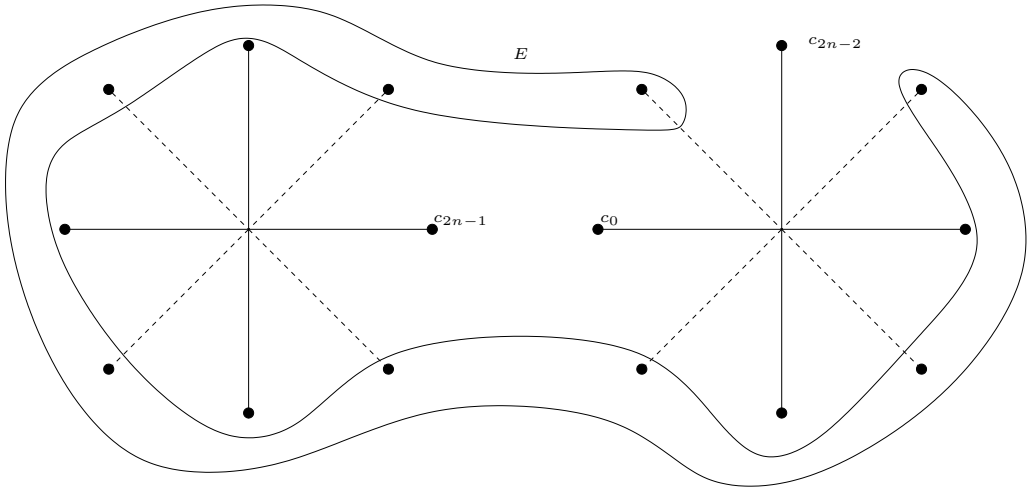

Figure 5.17: A curve isotopic to the equator E in Figure 5.15. This is isotopic rel P_F to a tubular neighbourhood of the Hubbard tree of h.

We notice that the equator in Figure 5.17 provides a form of cyclic ordering to the points in P_h. We describe this ordering more formally in the following algorithm.

Algorithm 5.5.2. *The following is an algorithm to compute the kneading sequence of the map h which creates a rational map with a period 2 cluster cycle and the mating $f_{p/n} \amalg h$ with combinatorial displacement δ. Start off by drawing the two stars of the cluster corresponding to the mating we require. The combinatorial data is enough to draw these (in other words place the critical value c_1' δ places anti-clockwise from the critical point c_0). Then follow the steps below.*

1. *Label the critical orbit of the second critical point ω_2 as follows. The points lying anti-clockwise in the star between c_{2n-2} and c_0, the first critical point are $c'_{i_1}, c'_{i_2}, \ldots, c'_{i_k}$. We then label the points in the other star, starting with the point adjacent and anti-clockwise from c_{2n-1}, by $c'_{i_{k+1}}, c'_{i_{k+2}} \ldots, c'_{i_{k+\ell}}$. Finally we return to the first star and label the remaining points, starting with the one adjacent and anticlockwise of c_0 by $c'_{i_{k+\ell+1}}, \ldots, c'_{i_{2n}}$.*

2. *Each c_{i_j} corresponds to some $c'_m = F^{\circ m}(c_0)'$, as derived from the cyclic ordering around the stars determined by the combinatorial data.There exists r so that $c_{i_r} = c'_0$, the second critical point. The set $\{c'_{i_j} : j = 1, 2, \ldots, 2n, j \neq r\}$*

is then split into two subsets

$$\{c'_{i_j} : j < r\} \quad \textit{and} \quad \{c'_{i_j} : j > r\}. \tag{5.4}$$

Denote the subset containing c'_1 by I_1 and the other one by I_0. The kneading sequence is $\nu = \nu_1\nu_2 \ldots \nu_{2n-1}*$ where $\nu_j = 1$ if $c'_j \in I_1$ and $\nu_j = 0$ if $c'_j \in I_0$.

Proof. We use a similar "separating" argument to that in Algorithm 4.4.2. Consider the branch of the graph of the ray equivalence class containing the root point of the Fatou component containing the critical point of h. The branch consists of the ray leaving the period two point p_1 which then lands at the root point of the critical point component of h, and then the second ray leaving the critical point component of h and landing at some endpoint in $J(f)$. In particular this ray class divides the h-plane into two regions in the same way as the construction of the kneading sequence.

The ordering from the listing in the algorithm means that the two regions split the points in the post-critical set of h in the manner described by (5.4).

Hence we can pick the region containing the critical value of h to be I_1 and the other region to be I_0 and then construct the kneading sequence as described above. □

We can then use either of the two algorithms to calculate progressions of internal addresses.

5.5.2 Progressions

We compute some simple examples of progressions of internal addresses.

Proposition 5.5.3. *Suppose $F \cong f_{1/n} \perp\!\!\!\perp h$ has a period two cluster cycle with combinatorial rotation number $\rho = 1/n$. Then the internal addresses of the secondary maps h are given as in Table 5.1.*

Proof. We use Algorithm 5.5.1. Note that there will only be one member anticlockwise between A_0 and θ_0, the non-periodic pre-image of θ_0. This will be $\theta_{2n-\delta}$, where $\delta = 2k-1$ is the critical displacement. Moreover, the points clockwise between θ_{2n} and A_1 are $\theta_{2n-2}, \theta_{2n-4}, \ldots, \theta_{2n-(2k-2)}$. If the critical displacement is not $2n-1$, the interval J_0 contains precisely the points mentioned above: that is it contains $\theta_{2n-(2k-1)}$, and $\theta_{2n-2}, \theta_{2n-4}, \ldots, \theta_{2n-(2k-2)}$. A simple calculation then gives kneading sequence and the internal address.

Critical displacement	Internal address of h
1	$1 \to 2n-1 \to 2n$
3	$1 \to 2n-3 \to 2n-2 \to 2n$
5	$1 \to 2n-5 \to 2n-4 \to 2n-2 \to 2n$
$\cdots$	$\cdots \quad \cdots \quad \cdots$
$2n-5$	$1 \to 5 \to 6 \to 8 \to \cdots \to 2n-2 \to 2n$
$2n-3$	$1 \to 3 \to 4 \to 6 \to \cdots \to 2n-2 \to 2n$
$2n-1$	$1 \to 3 \to 5 \to 7 \to \cdots \to 2n-3 \to 2n-1 \to 2n$

Table 5.1: Internal addresses in the rotation number $1/n$ case.

If the critical displacement is $2n-1$, then we see that the interval J_1 contains $\theta_1, \theta_2, \theta_4, \ldots, \theta_{2n-1}$. This then gives the internal address for critical displacement $2n-1$. □

We now consider the case where the rotation number is $\rho = 2/n$.

Proposition 5.5.4. *Suppose $F \cong f_{1/n} \perp\!\!\!\perp h$ has a period two cluster cycle with combinatorial rotation number $\rho = 2/n$. Then the internal addresses of the secondary maps h are given as in Table 5.2.*

δ	Internal address of h
1	$1 \to n \to 2n-1 \to 2n$
3	$1 \to n-2 \to n-1 \to 2n-3 \to 2n-1 \to 2n$
5	$1 \to n-2 \to n-1 \to 2n$
7	$1 \to n-4 \to n-3 \to n-1 \to 2n-5 \to 2n-3 \to 2n-2 \to 2n$
9	$1 \to n-4 \to n-3 \to n-1 \to 2n$
$\cdots$	$\cdots \quad \cdots \quad \cdots$
$4k-1$	$1 \to n-2k \to n-2k+1 \to n-k+3 \to \cdots \to n-1 \to 2n-2k-1$ $\to 2n-2k+1 \to 2n-2k+2 \to 2n-2k+4 \to \cdots \to 2n$
$4k+1$	$1 \to n-2k \to n-2k+1 \to n-2k+3 \to \cdots \to n-1 \to 2n$
$\cdots$	$\cdots \quad \cdots \quad \cdots$
$2n-5$	$1 \to 3 \to 4 \to 6 \to \cdots \to n-1 \to 2n$
$2n-3$	$1 \to 3 \to 5 \to \cdots \to n \to n+1 \to 2n$
$2n-1$	$1 \to 3 \to 5 \to \cdots n-2 \to n+1$ $\to n+2 \to n+4 \to \cdots \to 2n-1 \to 2n$

Table 5.2: Internal addresses in the rotation number $2/n$ case.

Proof. This time we use Algorithm 5.5.2. Notice that of course n is odd in this case. This time there are 2 elements of P_h anticlockwise between c_{2n-2} and c_0.

We first tackle the case where the critical displacement is 1. In this case the two points between c_{2n-2} and c_0 are c'_{2n-1} and c'_n. The first point in the ordering that we meet in the second star is c_0. Hence the kneading sequence will have $\nu_i = 0$ if and only if $i = n$ or $i = 2n-1$.

We now split into two cases: when the critical displacement is $4k-1$ and when it is $4k+1$.

Suppose $\delta = 4k-1$. Then $c'_{i_1} = c'_{n-2k}$ and $c'_{i_2} = c'_{2n-2k+1}$. Passing to the second star,

$$\begin{aligned}
c'_{i_3} &= c'_{n-2k+1} \\
c'_{i_4} &= c'_{2n-2(k-1)} \\
c'_{i_5} &= c'_{n-2(k-1)+1} \\
c'_{i_6} &= c'_{2n-2(k-2)} \\
&\cdots \\
c'_{i_{n+1}} &= c'_{n-2k-1} \\
c'_{i_{n+2}} &= c'_{2n-2k}.
\end{aligned}$$

The critical point is at $c_{i_{2(k+1)}}$. If $c'_1 \neq c'_{i_1}$ (which is equivalent to critical displacement $2n-3$) then the set I_0 is $\{c'_{i_j} : j < 2(k+1)\}$. Then $\nu_j = 0$ when $j = n-2k, n-2k+1, n-2(k-1)+1, \ldots, n-1$ and when $j = 2n-2k+1, 2n-2(k-1), 2n-2(k-2), \ldots, 2n-2$. This yields the kneading sequence and internal address as given.

When $\delta = 2n-3$ then $c'_1 = c'_{i_1}$ and $c'_{i_2} = c_{n+2}$. The other members of I_1 are those c'_j with even index, save for c'_{n+1} (and c'_0). Again a simple calculation is required to achieve the result.

Now suppose $\delta = 4k+1$. Then $c'_{i_1} = c'_{2n-2k-1}$ and $c'_{i_2} = c'_{n-2k}$. Passing to the second star,

$$\begin{aligned}
c'_{i_3} &= c'_{2n-2k} \\
c'_{i_4} &= c'_{n-2k+1} \\
c'_{i_5} &= c'_{2n-2(k-1)} \\
c'_{i_6} &= c'_{n-2(k-1)+1} \\
&\cdots \\
c'_{i_{n+1}} &= c'_{2n-2k-2} \\
c'_{i_{n+2}} &= c'_{n-2k-1}.
\end{aligned}$$

If $\delta = 2n-1$ then $c'_{i_2} = c'_1$ and $c'_{i_1} = c'_n$. Except for the critical point, c'_0, all c'_j with even index lie in I_1, so $I_1 = \{c'_1, c'_n\} \cup \{c_{2k} : k = 1, 2, \ldots, n-1\}$ and the kneading sequence and internal address follow.

Now suppose $\delta \neq 2n-1$. The critical point is at $c'_{i_{2(k+1)+1}}$. We see that $\nu_j = 0$ when $j = 2n-2k-1, 2n-2k, 2n-2(k-1), \ldots, 2n-2$ or $j = n-2k, n-2k+1, n-2(k-1)+1, \ldots, n-1$. Notice that if r appears in the first list, then $r-(n-1)$ appears in the second list and so we get the kneading and internal addresses as above. □

Clearly we can use these algorithms to compute internal addresses and kneading sequences for different rotation numbers, but the calculations get even more involved. In particular, the structure of the table for $\rho = k/n$ is dependent on all three of n, k and the value of $n \mod k$. One can see more examples of progressions in the appendices.

Appendix A

Data for the period 1 case

We give the raw data for the period 1 case. That is, the case where the mating admits a map with a single cluster of hyperbolic components. In this case, the critical displacement is given by the number of components one has to travel anti-clockwise round the cluster to go from the critical point of f_1 to the critical point of f_2. The map f_1 will be the n-rabbit of given rotation number r/n in each case, with internal address

$$1_{r/n} \to n.$$

A.1 Period 3 - denominator 7.

Rotation number 1/3.

Angles are (1/7,2/7).

Crit. disp.	**Angles for f_2**	**Internal address of f_2**
3	(3,4)	$1 \to 2 \to 3$

Rotation number 2/3.

Angles are (5/7,6/7).

Crit. disp.	**Angles for f_2**	**Internal address of f_2**
3	(3,4)	$1 \to 2 \to 3$

A.2 Period 4 - denominator 15.

Rotation number 1/4.

Angles are (1/15,2/15).

Crit. disp.	**Angles for f_2**	**Internal address of f_2**
3	(11,12)	$1 \to 3 \to 4$
5	(7,8)	$1 \to 2 \to 3 \to 4$

Rotation number 3/4.

Angles are (13/15,14/15).

Crit. disp.	**Angles for f_2**	**Internal address of f_2**
3	(7,8)	$1 \to 2 \to 3 \to 4$
5	(3,4)	$1 \to 3 \to 4$

A.3 Period 5 - denominator 31.

Rotation number 1/5.

Angles are (1/31,2/31).

Crit. disp.	**Angles for f_2**	**Internal address of f_2**
3	(27,28)	$1 \to 4 \to 5$
5	(23,24)	$1 \to 3 \to 4 \to 5$
7	(15,16)	$1 \to 2 \to 3 \to 4 \to 5$

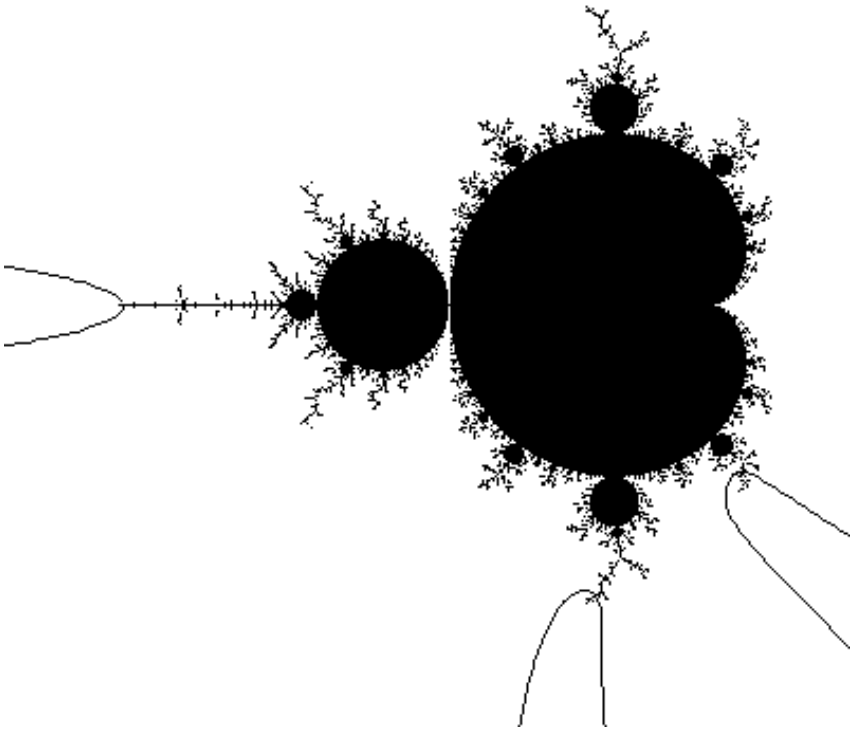

Figure A.1: Period 5, Rotation number 1/5

Rotation number 2/5.

Angles are (9/31,10/31).

Crit. disp.	**Angles for f_2**	**Internal address of f_2**
3	(13,18)	$1 \to 2 \to 4 \to 5$
5	(11,12)	$1 \to 2 \to 5$
7	(25,26)	$1 \to 3 \to 5$

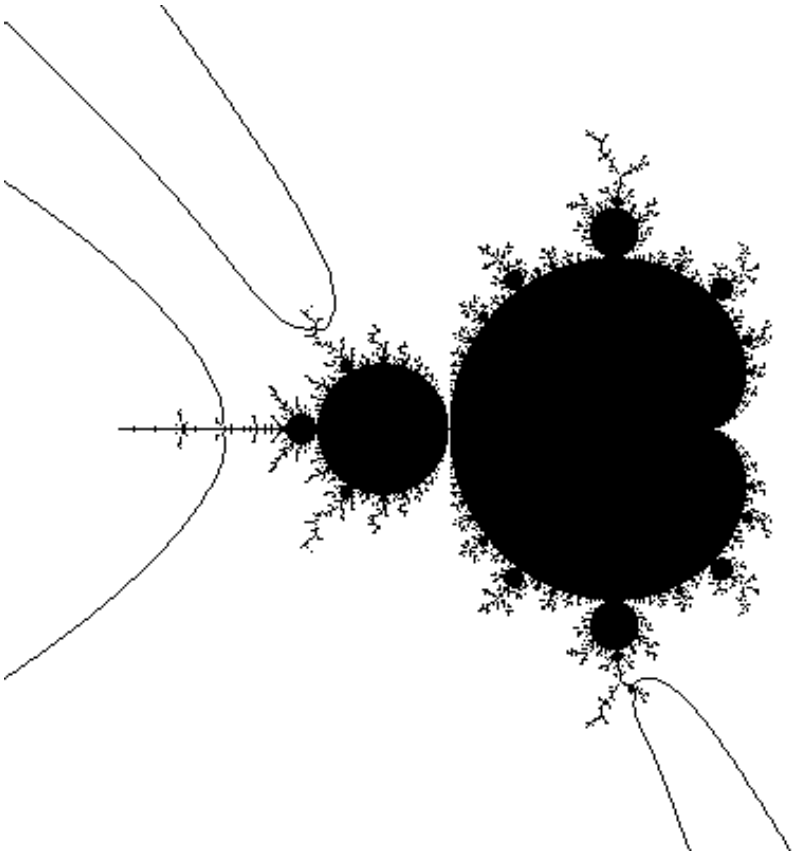

Figure A.2: Period 5, Rotation number 2/5

Rotation number 3/5.

Angles are (21/31,22/31).

Crit. disp.	**Angles for f_2**	**Internal address of f_2**
3	(5,6)	$1 \to 3 \to 5$
5	(19,20)	$1 \to 2 \to 5$
7	(13,18)	$1 \to 2 \to 4 \to 5$

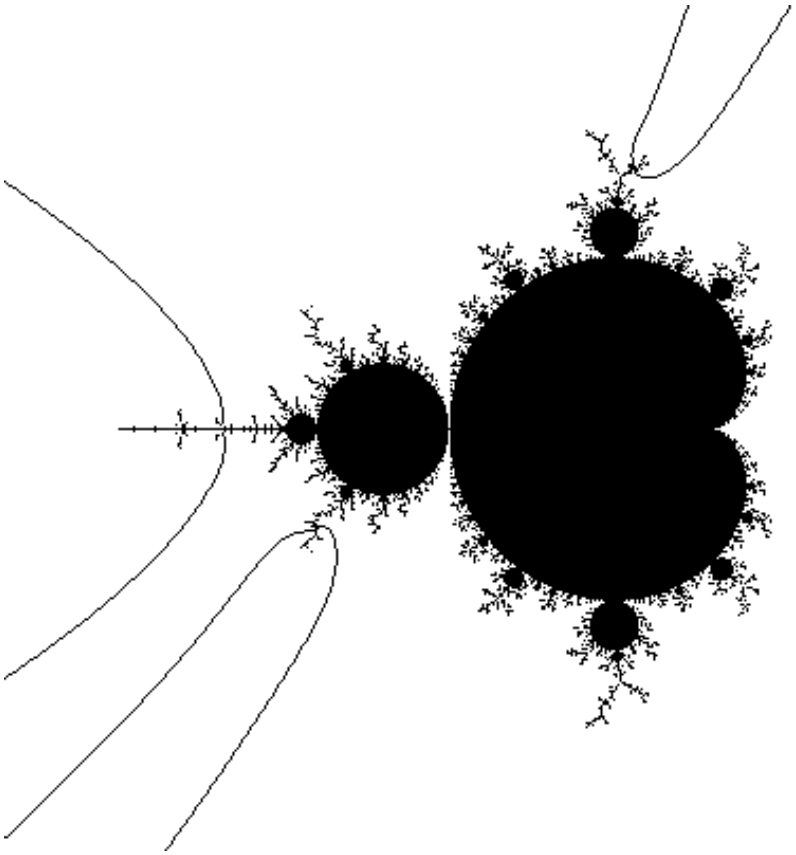

Figure A.3: Period 5, Rotation number 3/5

Rotation number 4/5.

Angles are (29/31,30/31).

Crit. disp.	**Angles for f_2**	**Internal address of f_2**
3	(15,16)	$1 \to 2 \to 3 \to 4 \to 5$
5	(7,8)	$1 \to 3 \to 4 \to 5$
7	(3,4)	$1 \to 4 \to 5$

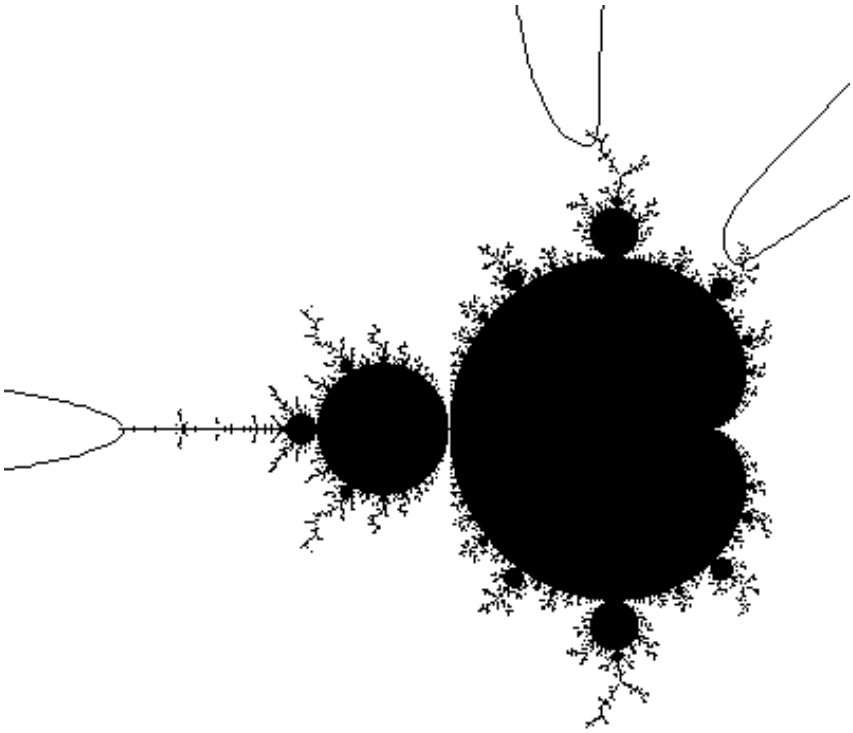

Figure A.4: Period 5, Rotation number 4/5

A.4 Period 6 - denominator 63.

Rotation number 1/6.

Angles are (1/63,2/63).

Crit. disp.	**Angles for f_2**	**Internal address of f_2**
3	(59,60)	$1 \to 5 \to 6$
5	(55,56)	$1 \to 4 \to 5 \to 6$
7	(47,48)	$1 \to 3 \to 4 \to 5 \to 6$
9	(31,32)	$1 \to 2 \to 3 \to 4 \to 5 \to 6$

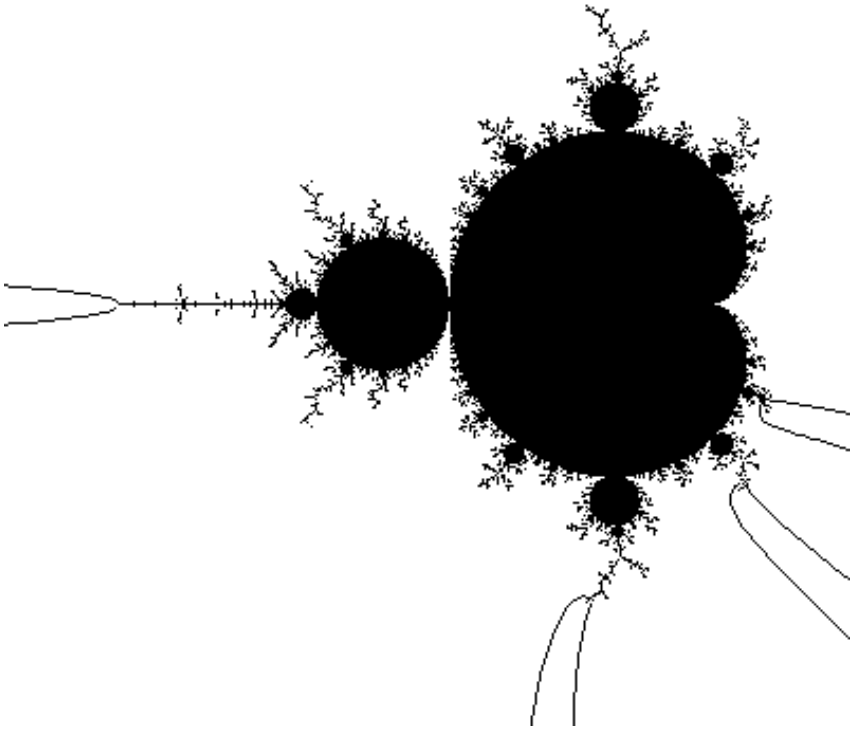

Figure A.5: Period 6, Rotation number 1/6

A.5 Period 7 - denominator 127.

Rotation number 1/7.

Angles are (1/127,2/127).

Crit. disp.	**Angles for f_2**	**Internal address of f_2**
3	(123,124)	$1 \to 6 \to 7$
5	(119,120)	$1 \to 5 \to 6 \to 7$
7	(111,112)	$1 \to 4 \to 5 \to 6 \to 7$
9	(95,96)	$1 \to 3 \to 4 \to 5 \to 6 \to 7$
11	(63,64)	$1 \to 2 \to 3 \to 4 \to 5 \to 6 \to 7$

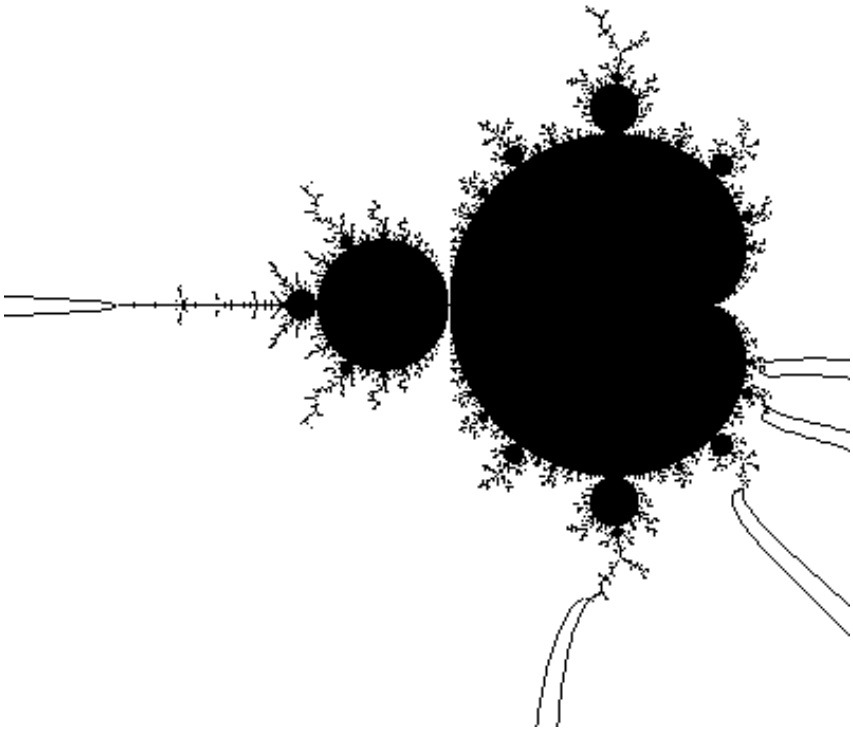

Figure A.6: Period 7, Rotation number 1/7

Rotation number 2/7.

Angles are (17/127,18/127).

Crit. disp.	**Angles for f_2**	**Internal address of f_2**
3	(93,102)	$1 \to 3 \to 6 \to 7$
5	(91,92)	$1 \to 3 \to 7$
7	(59,68)	$1 \to 2 \to 3 \to 5 \to 6 \to 7$
9	(55,56)	$1 \to 2 \to 3 \to 7$
11	(117,118)	$1 \to 4 \to 7$

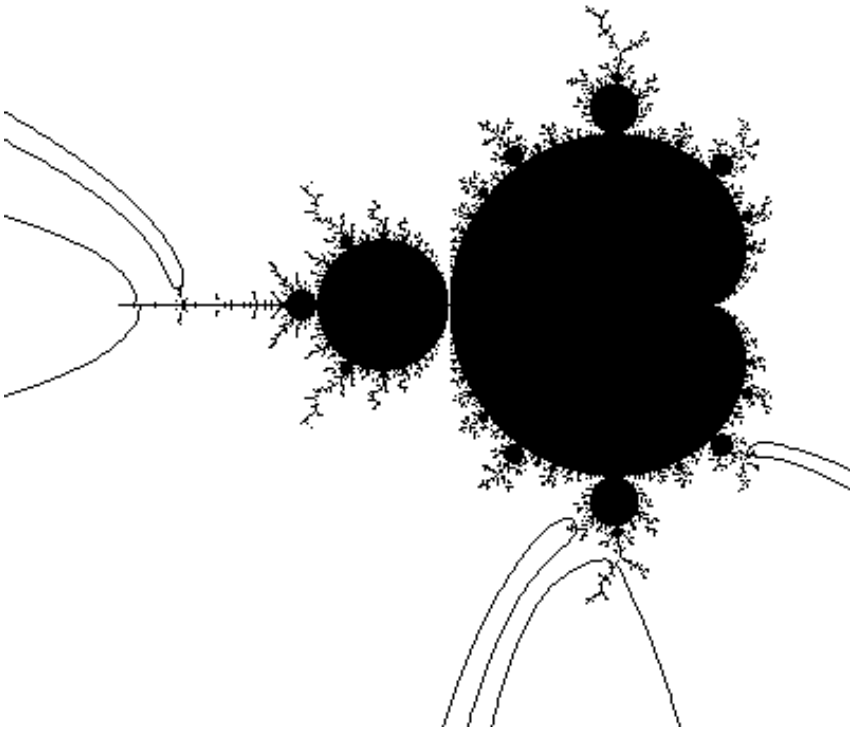

Figure A.7: Period 7, Rotation number 2/7

Rotation number 3/7.

Angles are (41/127,42/127).

Crit. disp.	**Angles for f_2**	**Internal address of f_2**
3	(53,74)	$1 \to 2 \to 4 \to 6 \to 7$
5	(45,50)	$1 \to 2 \to 6 \to 7$
7	(43,44)	$1 \to 2 \to 7$
9	(105,106)	$1 \to 3 \to 5 \to 7$
11	(89,90)	$1 \to 5 \to 7$

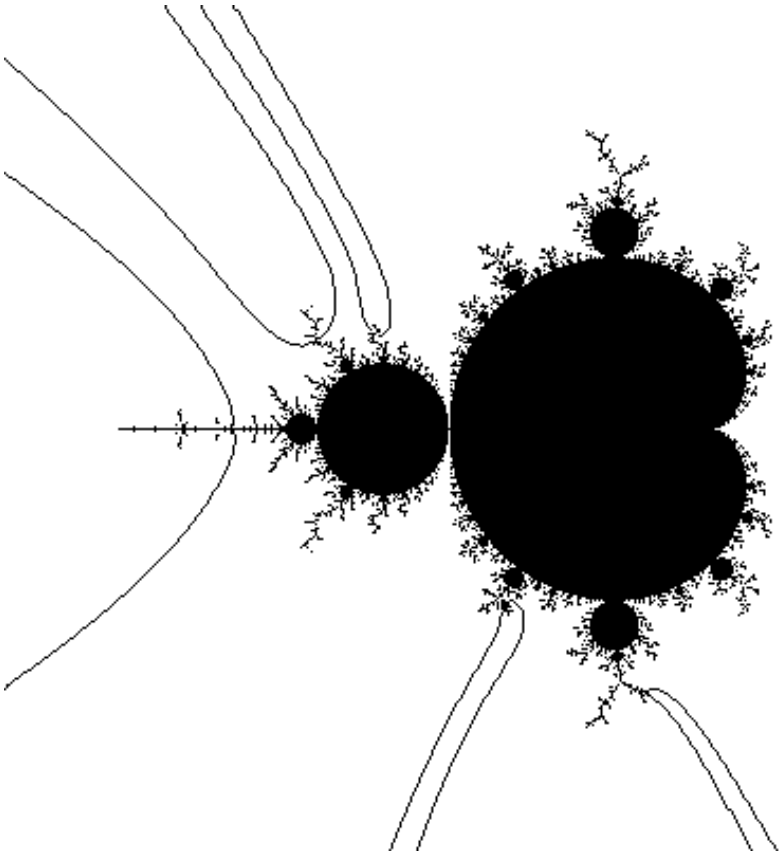

Figure A.8: Period 7, Rotation number 3/7

A.6 Period 8 - denominator 255.

Rotation number 1/8.

Angles are (1/255,2/255)

Crit. disp.	**Angles for f_2**	**Internal address of f_2**
3	(251,252)	$1 \to 7 \to 8$
5	(247,248)	$1 \to 6 \to 7 \to 8$
7	(239,240)	$1 \to 5 \to 6 \to 7 \to 8$
9	(223,224)	$1 \to 4 \to 5 \to 6 \to 7 \to 8$
11	(191,192)	$1 \to 3 \to 4 \to 5 \to 6 \to 7 \to 8$
13	(127,128)	$1 \to 2 \to 3 \to 4 \to 5 \to 6 \to 7 \to 8$

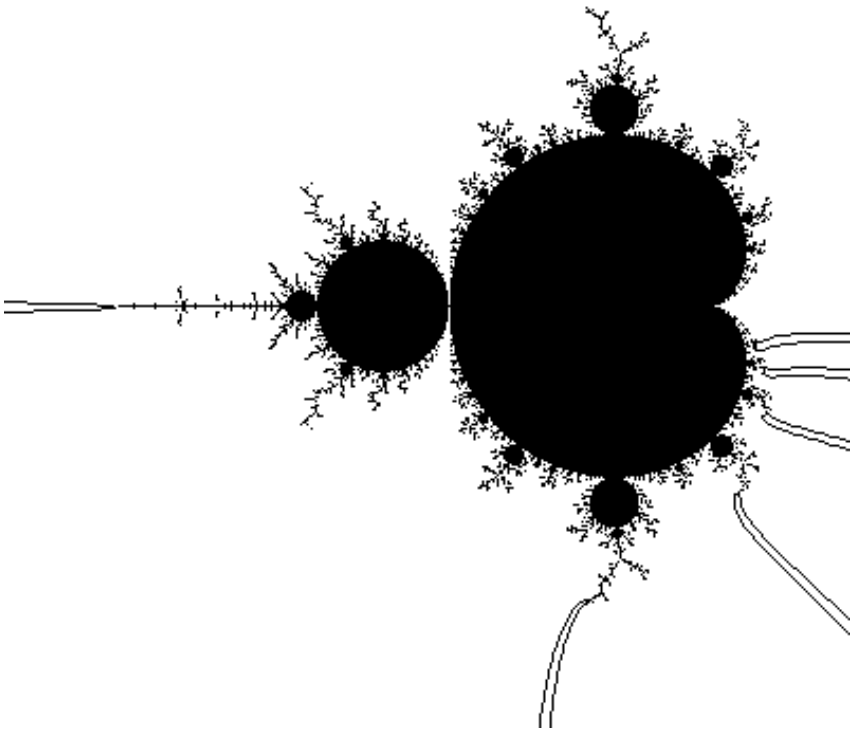

Figure A.9: Period 8, Rotation number 1/8

Rotation number 3/8.

Angles are (73/255,74/255).

Crit. disp.	**Angles for f_2**	**Internal address of f_2**
3	(173,174)	$1 \to 5 \to 8$
5	(109,146)	$1 \to 2 \to 4 \to 5 \to 7 \to 8$
7	(107,108)	$1 \to 2 \to 4 \to 5 \to 8$
9	(91,92)	$1 \to 2 \to 5 \to 8$
11	(217,218)	$1 \to 3 \to 8$
13	(205,214)	$1 \to 3 \to 6 \to 8$

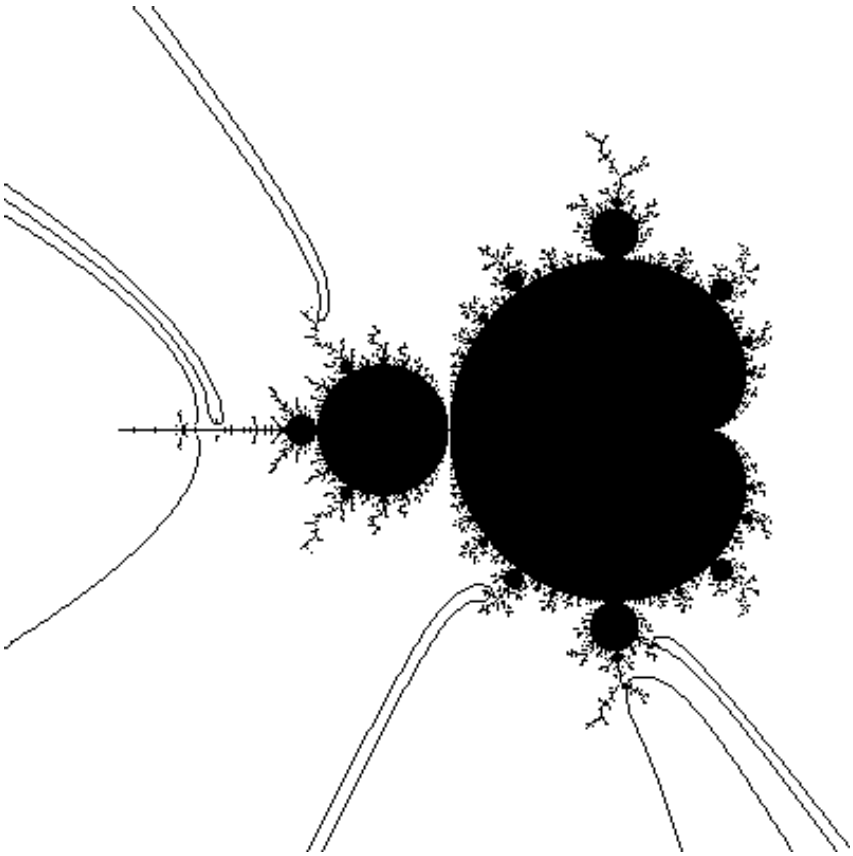

Figure A.10: Period 8, Rotation number 3/8

A.7 Period 9 - denominator 511.

Rotation number 1/9

Crit. disp.	**Angles for f_2**	**Internal address of f_2**
3	(507,508)	$1 \to 8 \to 9$
5	(503,504)	$1 \to 7 \to 8 \to 9$
7	(495,496)	$1 \to 6 \to 7 \to 8 \to 9$
9	(479,480)	$1 \to 5 \to 6 \to 7 \to 8 \to 9$
11	(447,448)	$1 \to 4 \to 5 \to 6 \to 7 \to 8 \to 9$
13	(383,384)	$1 \to 3 \to 4 \to 5 \to 6 \to 7 \to 8 \to 9$
15	(255,256)	$1 \to 2 \to 3 \to 4 \to 5 \to 6 \to 7 \to 8 \to 9$

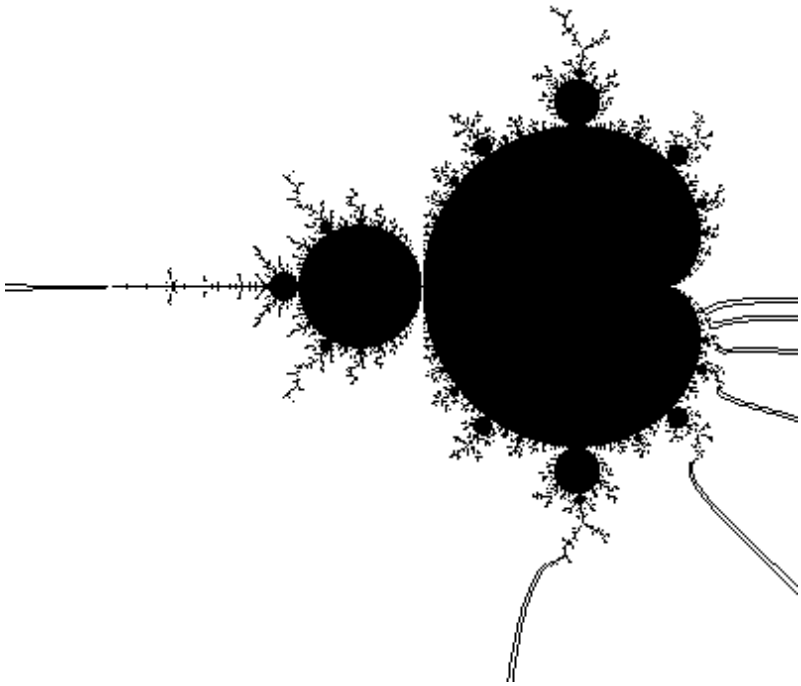

Figure A.11: Period 9, Rotation number 1/9

Rotation number 2/9.

Angles are (33/511,34/511).

Crit. disp.	**Angles for f_2**	**Internal address of f_2**
3	(445,462)	$1 \to 4 \to 8 \to 9$
5	(443,444)	$1 \to 4 \to 9$
7	(379,396)	$1 \to 3 \to 4 \to 7 \to 8 \to 9$
9	(375,376)	$1 \to 3 \to 4 \to 9$
11	(247,264)	$1 \to 2 \to 3 \to 4 \to 6 \to 7 \to 8 \to 9$
13	(239,240)	$1 \to 2 \to 3 \to 4 \to 9$
15	(493,494)	$1 \to 5 \to 9$

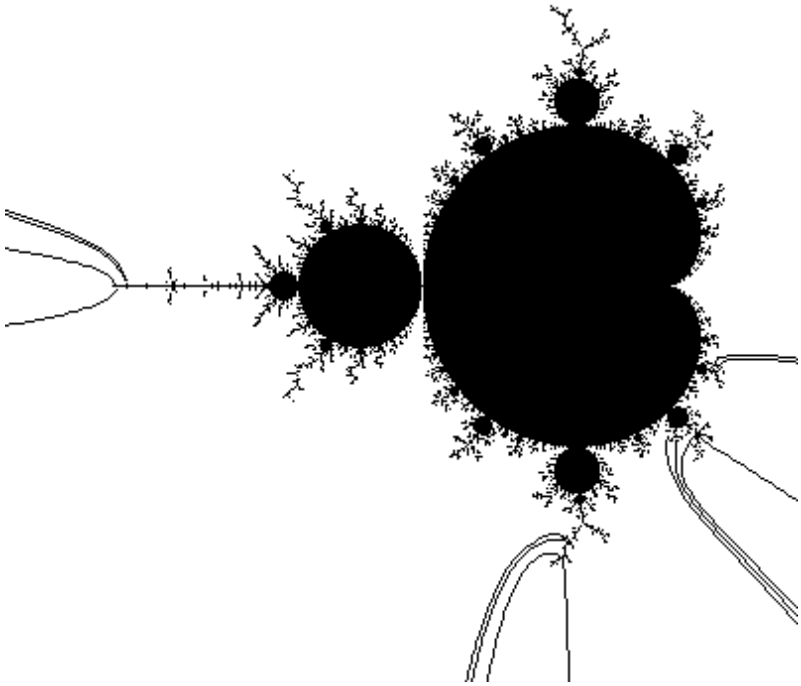

Figure A.12: Period 9, Rotation number 2/9

Rotation number 4/9.

Angles are (169/511,170/511).

Crit. disp.	**Angles for f_2**	**Internal address of f_2**
3	(213,298)	$1 \to 2 \to 4 \to 6 \to 8 \to 9$
5	(181,202)	$1 \to 2 \to 6 \to 8 \to 9$
7	(173,178)	$1 \to 2 \to 8 \to 9$
9	(171,172)	$1 \to 2 \to 9$
11	(425,426)	$1 \to 3 \to 5 \to 7 \to 9$
13	(361,362)	$1 \to 5 \to 7 \to 9$
15	(345,346)	$1 \to 7 \to 9$

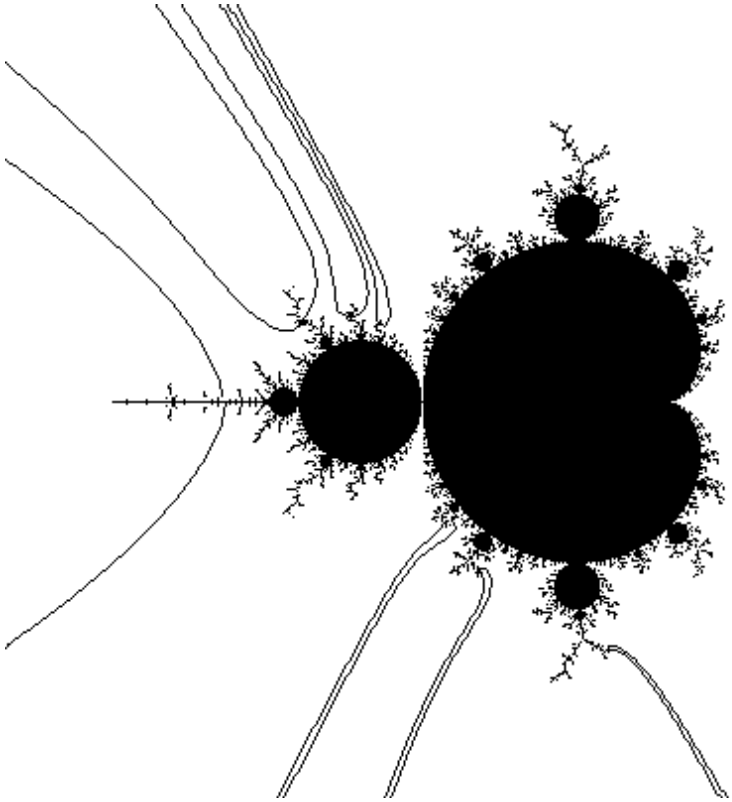

Figure A.13: Period 9, Rotation number 4/9

A.8 Period 10 - denominator 1023.

Rotation number 1/10.

Angles are (1/1023,2/1023).

Crit. disp.	**Angles for f_2**	**Internal address of f_2**
3	(1019,1020)	$1 \to 9 \to 10$
5	(1015,1016)	$1 \to 8 \to 9 \to 10$
7	(1007,1008)	$1 \to 7 \to 8 \to 9 \to 10$
9	(991,992)	$1 \to 6 \to 7 \to 8 \to 9 \to 10$
11	(959,960)	$1 \to 5 \to 6 \to 7 \to 8 \to 9 \to 10$
13	(895,896)	$1 \to 4 \to 5 \to 6 \to 7 \to 8 \to 9 \to 10$
15	(767,768)	$1 \to 3 \to 4 \to 5 \to 6 \to 7 \to 8 \to 9 \to 10$
17	(511,512)	$1 \to 2 \to 3 \to 4 \to 5 \to 6 \to 7 \to 8 \to 9 \to 10$

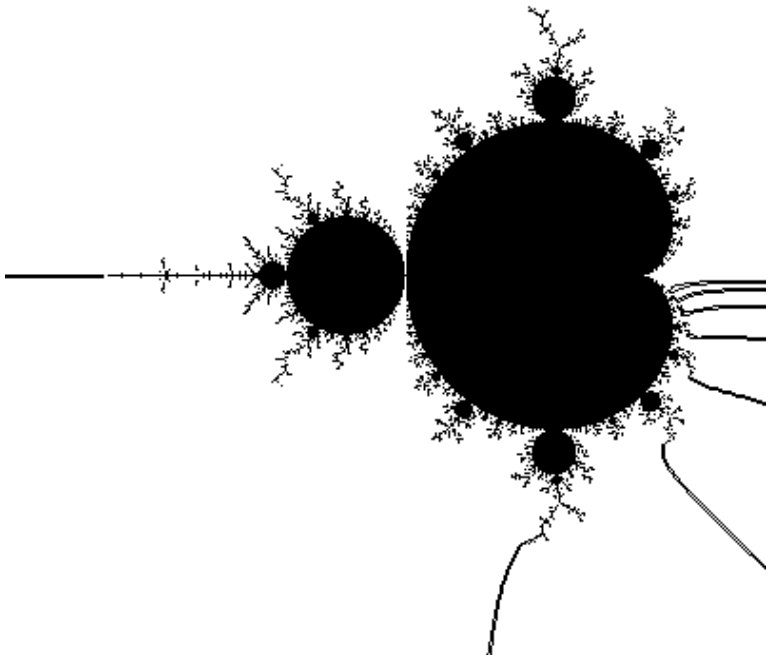

Figure A.14: Period 10, Rotation number 1/10

Rotation number 3/10.

Angles are (145/1023,146/1023).

Crit. disp.	**Angles for f_2**	**Internal address of f_2**
3	(749,822)	$1 \to 3 \to 6 \to 9 \to 10$
5	(733,742)	$1 \to 3 \to 9 \to 10$
7	(731,732)	$1 \to 3 \to 10$
9	(475,548)	$1 \to 2 \to 3 \to 5 \to 6 \to 8 \to 9 \to 10$
11	(443,452)	$1 \to 2 \to 3 \to 8 \to 9 \to 10$
13	(439,440)	$1 \to 2 \to 3 \to 10$
15	(949,950)	$1 \to 4 \to 7 \to 10$
17	(885,886)	$1 \to 7 \to 10$

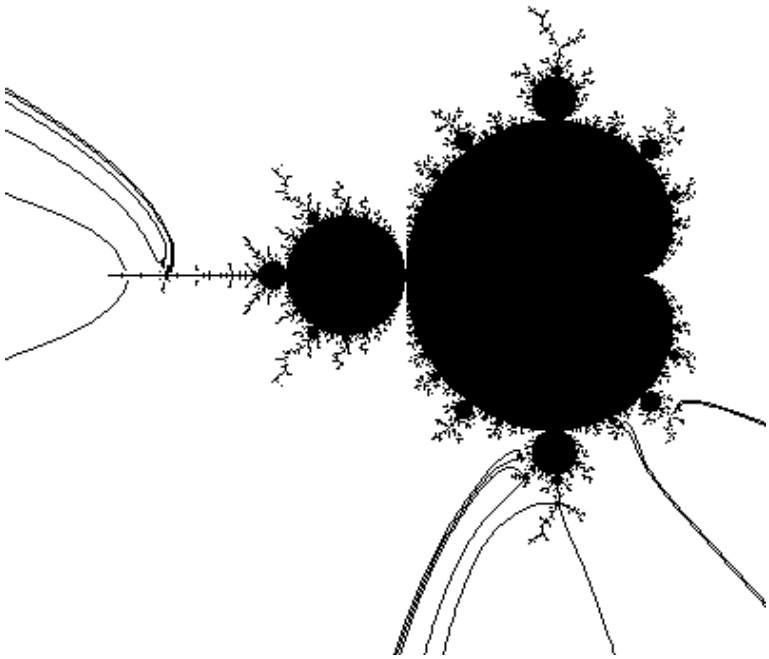

Figure A.15: Period 10, Rotation number 3/10

A.9 Period 11 - denominator 2047.

Rotation number 1/11.

Angles are (1/2047,2/2047).

C. disp.	f_2 **angles**	**Internal address of** f_2
3	(2043,2044)	$1 \to 10 \to 11$
5	(2039,2040)	$1 \to 9 \to 10 \to 11$
7	(2031,2032)	$1 \to 8 \to 9 \to 10 \to 11$
9	(2015,2016)	$1 \to 7 \to 8 \to 9 \to 10 \to 11$
11	(1983,1984)	$1 \to 6 \to 7 \to 8 \to 9 \to 10 \to 11$
13	(1919,1920)	$1 \to 5 \to 6 \to 7 \to 8 \to 9 \to 10 \to 11$
15	(1791,1792)	$1 \to 4 \to 5 \to 6 \to 7 \to 8 \to 9 \to 10 \to 11$
17	(1535,1536)	$1 \to 3 \to 4 \to 5 \to 6 \to 7 \to 8 \to 9 \to 10 \to 11$
19	(1023,1024)	$1 \to 2 \to 3 \to 4 \to 5 \to 6 \to 7 \to 8 \to 9 \to 10 \to 11$

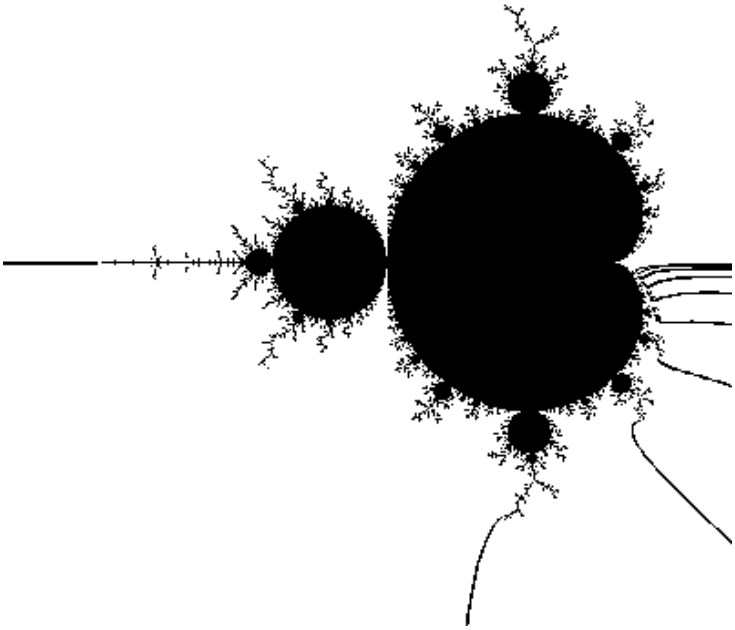

Figure A.16: Period 11, Rotation number 1/11

Rotation number 2/11.

Angles are (65/2047,66/2047).

Crit. disp.	**Angles for f_2**	**Internal address of f_2**
3	(1917,1950)	$1 \to 5 \to 10 \to 11$
5	(1915,1916)	$1 \to 5 \to 11$
7	(1787,1820)	$1 \to 4 \to 5 \to 9 \to 10 \to 11$
9	(1783,1784)	$1 \to 4 \to 5 \to 11$
11	(1527,1560)	$1 \to 3 \to 4 \to 5 \to 8 \to 9 \to 10 \to 11$
13	(1519,1520)	$1 \to 3 \to 4 \to 5 \to 11$
15	(1007,1040)	$1 \to 2 \to 3 \to 4 \to 5 \to 7 \to 8 \to 9 \to 10 \to 11$
17	(991,992)	$1 \to 2 \to 3 \to 4 \to 5 \to 11$
19	(2013,2014)	$1 \to 6 \to 11$

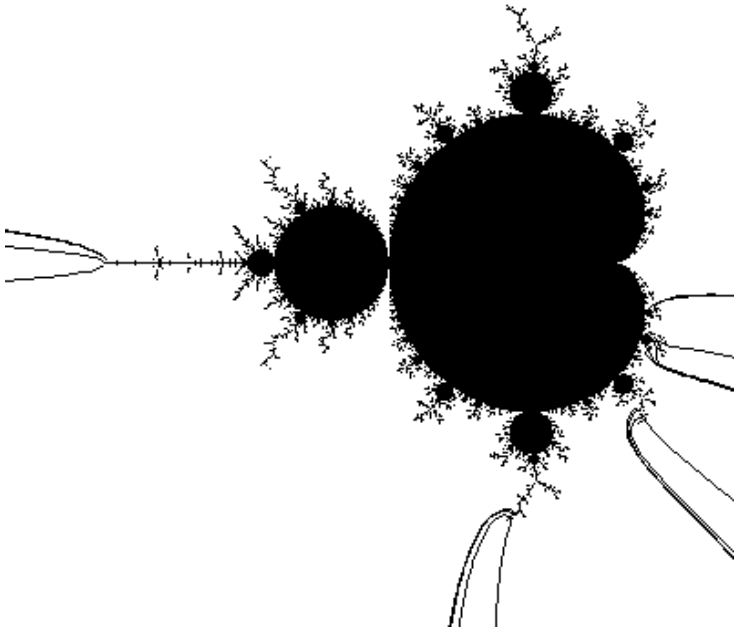

Figure A.17: Period 11, Rotation number 2/11

Rotation number 3/11.

Angles are (273/2047,274/2047).

Crit. disp.	**Angles for f_2**	**Internal address of f_2**
3	(1757,1758)	$1 \to 7 \to 11$
5	(1501,1638)	$1 \to 3 \to 6 \to 7 \to 10 \to 11$
7	(1499,1500)	$1 \to 3 \to 6 \to 7 \to 11$
9	(1467,1468)	$1 \to 3 \to 7 \to 11$
11	(955,1092)	$1 \to 2 \to 3 \to 5 \to 6 \to 7 \to 9 \to 10 \to 11$
13	(951,952)	$1 \to 2 \to 3 \to 5 \to 6 \to 7 \to 11$
15	(887,888)	$1 \to 2 \to 3 \to 7 \to 11$
17	(1909,1910)	$1 \to 4 \to 11$
19	(1885,1902)	$1 \to 4 \to 8 \to 11$

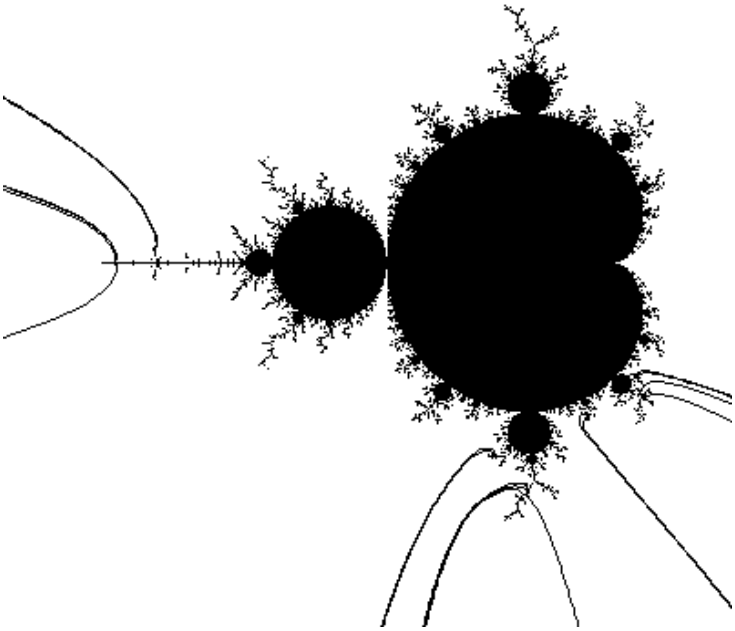

Figure A.18: Period 11, Rotation number 3/11

Rotation number 4/11.

Angles are (585/2047,586/2047).

Crit. disp.	**Angles for f_2**	**Internal address of f_2**
3	(1453,1454)	$1 \to 8 \to 11$
5	(1389,1390)	$1 \to 5 \to 8 \to 11$
7	(877,1170)	$1 \to 2 \to 4 \to 5 \to 7 \to 8 \to 10 \to 11$
9	(875,876)	$1 \to 2 \to 4 \to 5 \to 7 \to 8 \to 11$
11	(859,860)	$1 \to 2 \to 4 \to 5 \to 8 \to 11$
13	(731,732)	$1 \to 2 \to 5 \to 8 \to 11$
15	(1753,1754)	$1 \to 3 \to 11$
17	(1741,1750)	$1 \to 3 \to 9 \to 11$
19	(1645,1718)	$1 \to 3 \to 6 \to\to 9 \to 11$

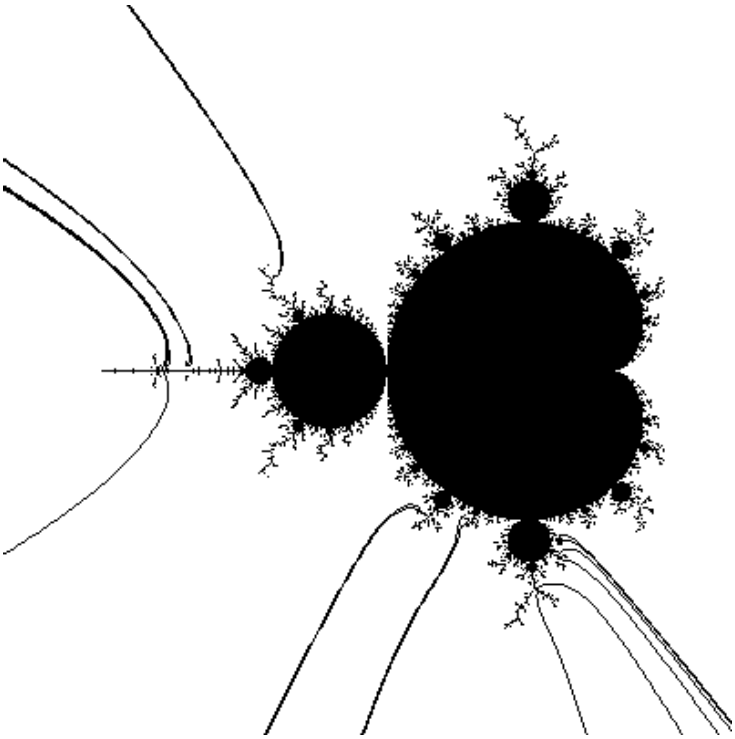

Figure A.19: Period 11, Rotation number 4/11

Rotation number 5/11.

Angles are (681/2047,682/2047).

Crit. disp.	**Angles for f_2**	**Internal address of f_2**
3	(853,1194)	$1 \to 2 \to 4 \to 6 \to 8 \to 10 \to 11$
5	(725,810)	$1 \to 2 \to 6 \to 8 \to 10 \to 11$
7	(693,714)	$1 \to 2 \to 8 \to 10 \to 11$
9	(685,690)	$1 \to 2 \to 10 \to 11$
11	(683,684)	$1 \to 2 \to 11$
13	(1705,1706)	$1 \to 3 \to 5 \to 7 \to 9 \to 11$
15	(1449,1450)	$1 \to 5 \to 7 \to 9 \to 11$
17	(1385,1386)	$1 \to 7 \to 9 \to 11$
19	(1369,1370)	$1 \to 9 \to 11$

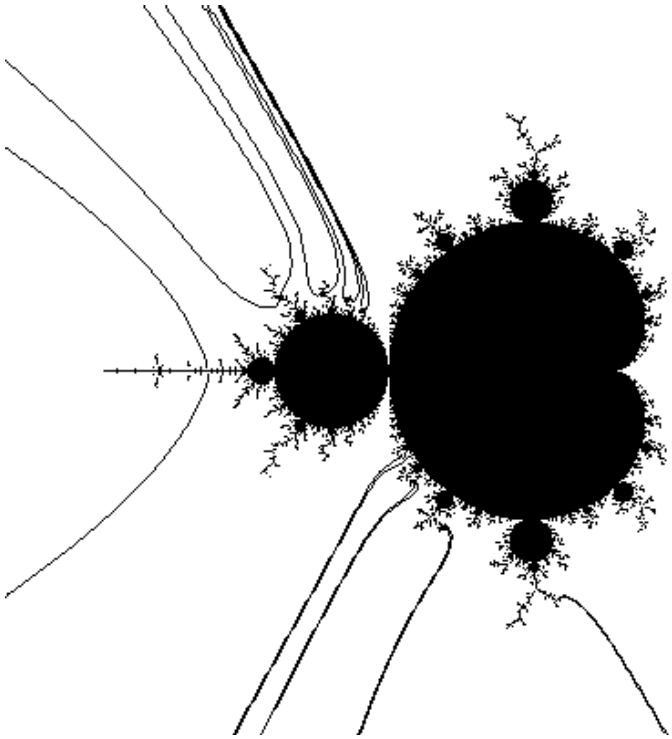

Figure A.20: Period 11, Rotation number 5/11

A.10 Period 12 - denominator 4095.

Rotation number 1/12.

Angles are (1/4095,2/4095).

C. d.	f_2 **angles**	**Internal address of** f_2
3	(4091,4092)	$1 \to 11 \to 12$
5	(4087,4088)	$1 \to 10 \to 11 \to 12$
7	(4079,4080)	$1 \to 9 \to 10 \to 11 \to 12$
9	(4063,4064)	$1 \to 8 \to 9 \to 10 \to 11 \to 12$
11	(4031,4032)	$1 \to 7 \to 8 \to 9 \to 10 \to 11 \to 12$
13	(3967,3968)	$1 \to 6 \to 7 \to 8 \to 9 \to 10 \to 11 \to 12$
15	(3839,3840)	$1 \to 5 \to 6 \to 7 \to 8 \to 9 \to 10 \to 11 \to 12$
17	(3583,3584)	$1 \to 4 \to 5 \to 6 \to 7 \to 8 \to 9 \to 10 \to 11 \to 12$
19	(3071,3072)	$1 \to 3 \to 4 \to 5 \to 6 \to 7 \to 8 \to 9 \to 10 \to 11 \to 12$
21	(2047,2048)	$1 \to 2 \to 3 \to 4 \to 5 \to 6 \to 7 \to 8 \to 9 \to 10 \to 11 \to 12$

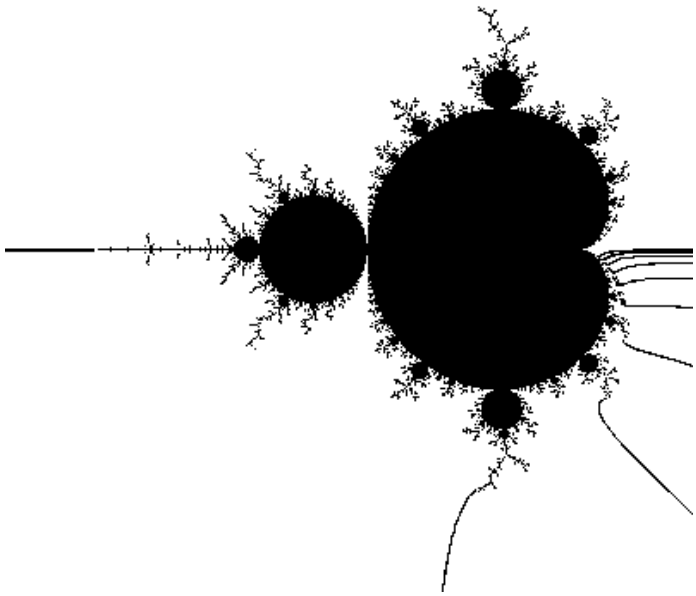

Figure A.21: Period 12, Rotation number 1/12

Rotation number 5/12.

Angles are (1321/4095,1322/4095).

Crit. disp.	**Angles for f_2**	**Internal address of f_2**
3	(2741,2742)	$1 \to 7 \to 12$
5	(1717,2378)	$1 \to 2 \to 4 \to 6 \to 7 \to 9 \to 11 \to 12$
7	(1709,1714)	$1 \to 2 \to 4 \to 6 \to 7 \to 12$
9	(1453,1586)	$1 \to 2 \to 6 \to 7 \to 11 \to 12$
11	(1451,1452)	$1 \to 2 \to 6 \to 7 \to 12$
13	(1387,1388)	$1 \to 2 \to 7 \to 12$
15	(3433,3434)	$1 \to 3 \to 5 \to 12$
17	(3385,3418)	$1 \to 3 \to 5 \to 8 \to 10 \to 12$
19	(2905,2906)	$1 \to 5 \to 12$
21	(2869,2902)	$1 \to 5 \to 10 \to 12$

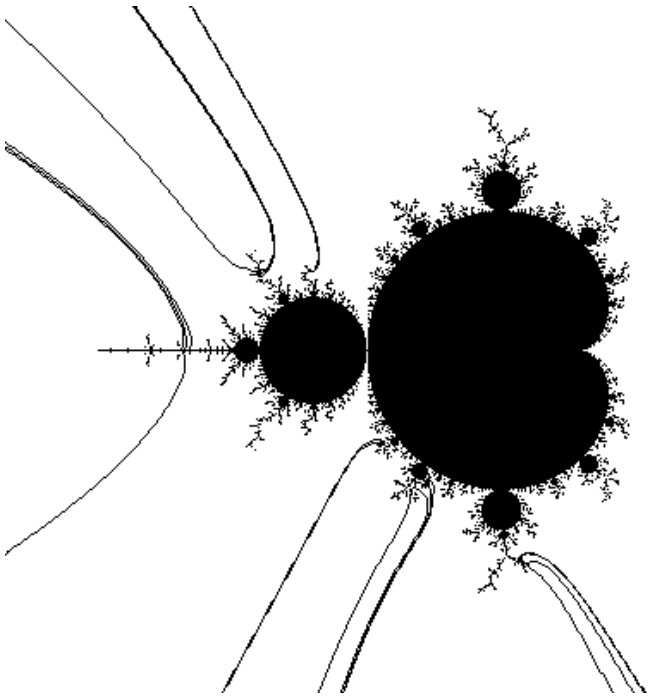

Figure A.22: Period 12, Rotation number 5/12

Appendix B

Data for the period 2 case

This is the data found when finding maps with a period 2 cycle of cluster points. In this case, the critical displacement is given as the gap (in terms of hyperbolic components) in an anticlockwise direction between the critical point component of f_1 and the critical value component of f_2. In what follows, f_1 will be the *tuned-n-rabbit* with internal address

$$1_{1/2} \to 2_{r/n} \to 2n,$$

and g_1 will be the secondary component which lies beyond the tuned-n-rabbit, with internal address

$$1_{1/2} \to 2_{r/n} \to (2n-1)_{1/2} \to 2n.$$

B.1 Period 4 - denominator 15.

Rotation number 1/2

f_1: $(6/15, 9/15)$
g_1: $(7/15, 8/15)$

Internal address	f_2 **angles**	**C. disp. with** f_1	**C. disp with** g_1
$1 \to 3 \to 4$	(3,4)	1	3
$1 \to 3 \to 4$	(11,12)	3	1

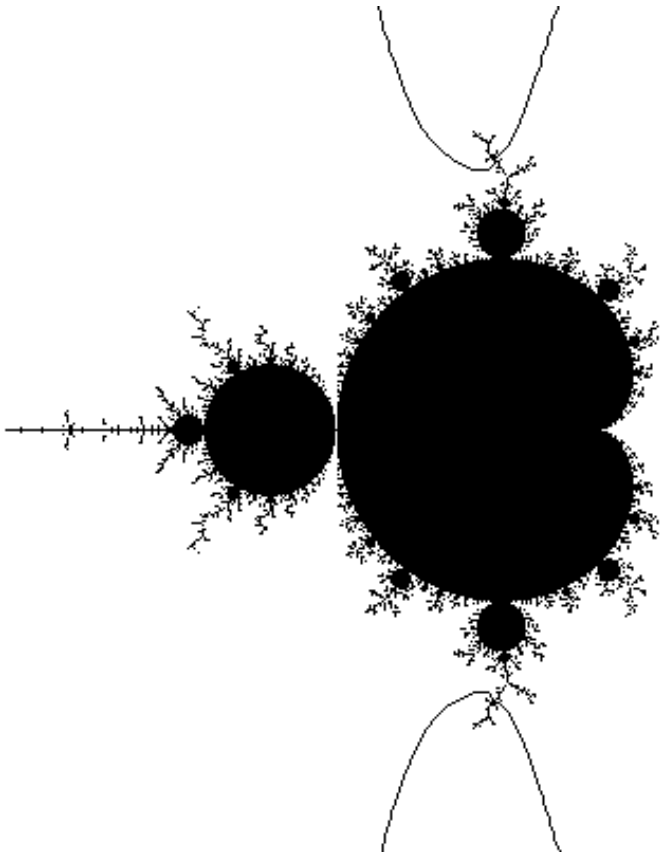

Figure B.1: Period 4, Rotation number 1/2

B.2 Period 6 - denominator 63.

Rotation number 1/3

f_1: $(22/63, 25/63)$

g_1: $(23/63, 24/63)$

Internal address	**Angles for f_2**	**C. disp. with f_1**	**C. disp with g_1**
$1 \to 5 \to 6$	(19,20)	1	5
$1 \to 3 \to 4 \to 6$	(13,14)	3	$\times$
$1 \to 3 \to 5 \to 6$	(51,52)	5	1

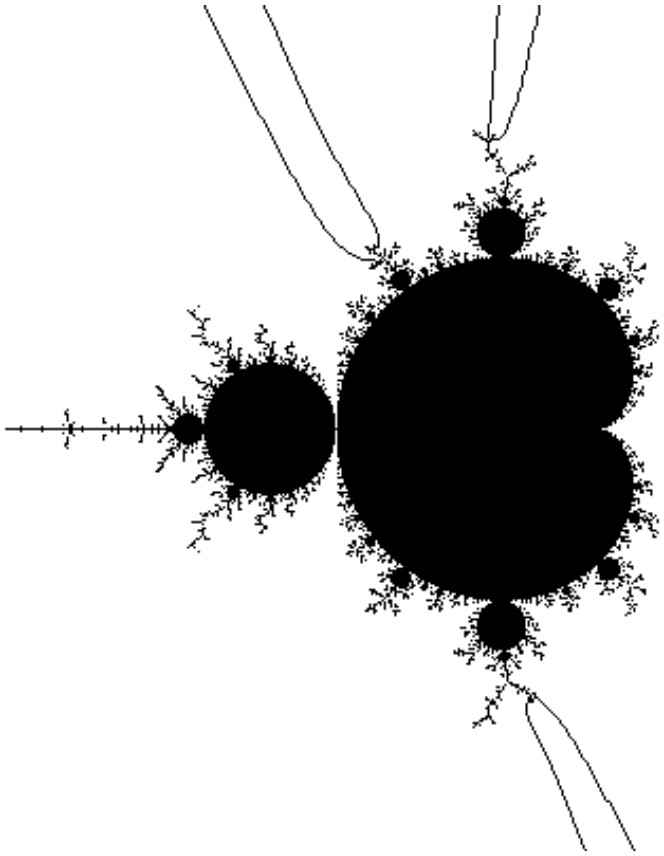

Figure B.2: Period 6, Rotation number 1/3

B.3 Period 8 - denominator 255.

Rotation number 1/4.

f_1: $(86/255, 89/255)$
g_1: $(87/255, 88/255)$

Internal address	**Angles for f_2**	**C. disp. with f_1**	**C. disp with g_1**
$1 \to 7 \to 8$	(83,84)	1	7
$1 \to 5 \to 6 \to 8$	(77,78)	3	$\times$
$1 \to 3 \to 4 \to 6 \to 8$	(53,54)	5	$\times$
$1 \to 3 \to 5 \to 7 \to 8$	(211,212)	7	1

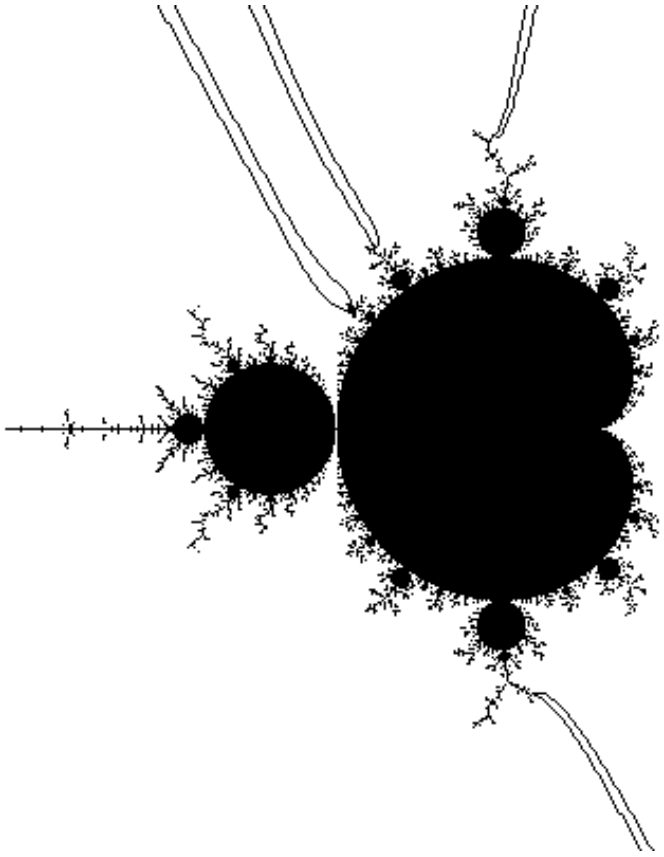

Figure B.3: Period 8, Rotation number 1/4

B.4 Perod 10 - denominator 1023.

Rotation number 1/5.

f_1: $(342/1023, 345/1023)$
g_1: $(343/1023, 344/1023)$

Internal address	**Angles for f_2**	**C. d. with f_1**	**C. d. with g_1**
$1 \to 9 \to 10$	(339,340)	1	9
$1 \to 7 \to 8 \to 10$	(333,334)	3	$\times$
$1 \to 5 \to 6 \to 8 \to 10$	(309,310)	5	$\times$
$1 \to 3 \to 4 \to 6 \to 8 \to 10$	(213,214)	7	$\times$
$1 \to 3 \to 5 \to 7 \to 9 \to 10$	(851,852)	9	1

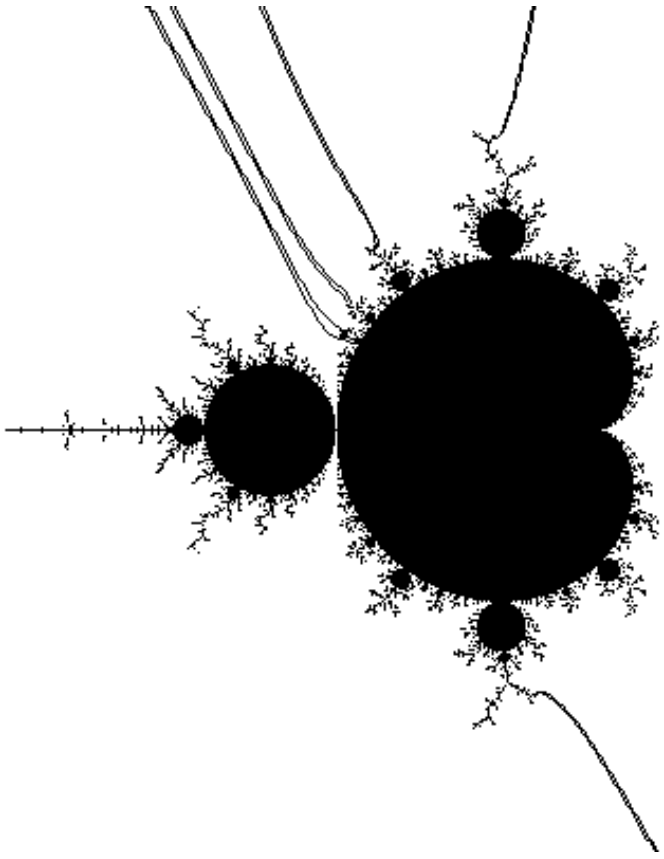

Figure B.4: Period 10, Rotation number 1/5

Rotation number 2/5.

f_1: $(406/1023, 409/1023)$

g_1: $(407/1023, 408/1023)$

Internal address	**Angles for f_2**	**C. d. with f_1**	**C. d. with g_1**
$1 \to 5 \to 9 \to 10$	(307,308)	1	9
$1 \to 3 \to 4 \to 7 \to 9 \to 10$	(211,228)	3	$\times$
$1 \to 3 \to 4 \to 10$	(205,206)	5	$\times$
$1 \to 3 \to 5 \to 6 \to 10$	(843,844)	7	$\times$
$1 \to 3 \to 6 \to 7 \to 9 \to 10$	(819,820)	9	1

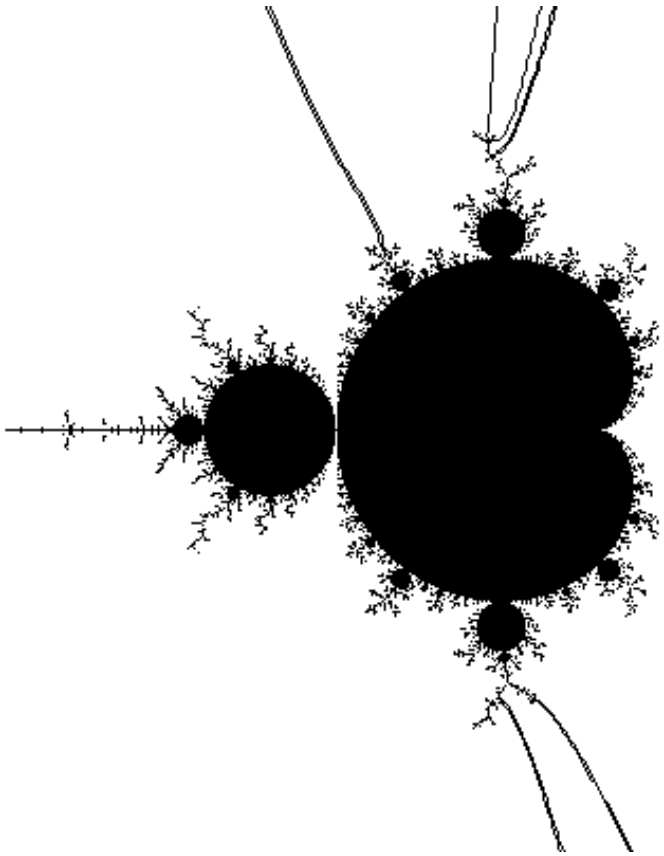

Figure B.5: Period 10, Rotation number 2/5

B.5 Period 12 - denominator 4095.

Rotation number 1/6.

f_1: $(1366/4095, 1369/4095)$

g_1: $(1367/4095, 1368/4095)$

Internal address	f_2 **angles**	**C.d. with** f_1	**C.d. with** g_1
$1 \to 11 \to 12$	(1363,1364)	1	11
$1 \to 9 \to 10 \to 12$	(1357,1358)	3	$\times$
$1 \to 7 \to 8 \to 10 \to 12$	(1333,1334)	5	$\times$
$1 \to 5 \to 6 \to 8 \to 10 \to 12$	(1237,1238)	7	$\times$
$1 \to 3 \to 4 \to 6 \to 8 \to 10 \to 12$	(853,854)	9	$\times$
$1 \to 3 \to 5 \to 7 \to 9 \to 11 \to 12$	(3411,3412)	11	1

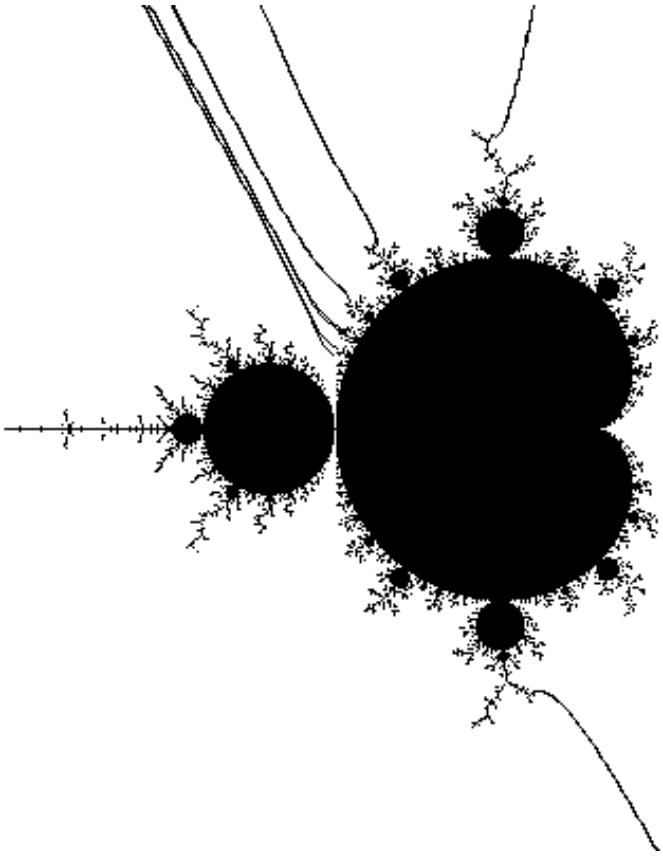

Figure B.6: Period 12, Rotation number 1/6

B.6 Period 14 - denominator 16383.

Rotation number 1/7.

f_1: $(5462/16383, 5465/16383)$

g_1: $(5463/16383, 5464/16383)$

Internal address	f_2 **angles**	**C.d. w/** f_1	**C.d. w/** g_1
$1 \to 13 \to 14$	(5459,5460)	1	13
$1 \to 11 \to 12 \to 14$	(5453,5454)	3	$\times$
$1 \to 9 \to 10 \to 12 \to 14$	(5429,5430)	5	$\times$
$1 \to 7 \to 8 \to 10 \to 12 \to 14$	(5333,5334)	7	$\times$
$1 \to 5 \to 6 \to 8 \to 10 \to 12 \to 14$	(4949,4950)	9	$\times$
$1 \to 3 \to 4 \to 6 \to 8$ $\to 10 \to 12 \to 14$	(3413,3414)	11	$\times$
$1 \to 3 \to 5 \to 7 \to 9$ $\to 11 \to 13 \to 14$	(13651,13652)	13	1

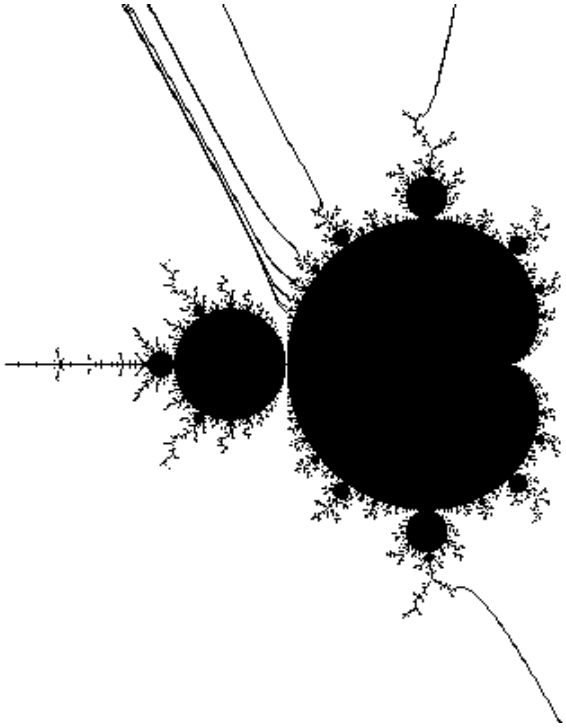

Figure B.7: Period 14, Rotation number 1/7

Rotation number 2/7.

f_1: $(5718/16383, 5721/16383)$

g_1: $(5719/16383, 5720/16383)$

Internal address	f_2 **angles**	**C.d.** f_1	**C.d.** g_1
$1 \to 7 \to 13 \to 14$	(5331,5332)	1	13
$1 \to 5 \to 6 \to 11 \to 13 \to 14$	(4947,5012)	3	$\times$
$1 \to 5 \to 6 \to 14$	(4941,4942)	5	$\times$
$1 \to 3 \to 4 \to 6 \to 9 \to 11 \to 12 \to 14$	(3405,3470)	7	$\times$
$1 \to 3 \to 4 \to 6 \to 14$	(3381,3382)	9	$\times$
$1 \to 3 \to 5 \to 7 \to 8 \to 14$	(13619,13620)	11	$\times$
$1 \to 3 \to 5 \to 8 \to 9 \to 11 \to 13 \to 14$	(13523,13524)	13	1

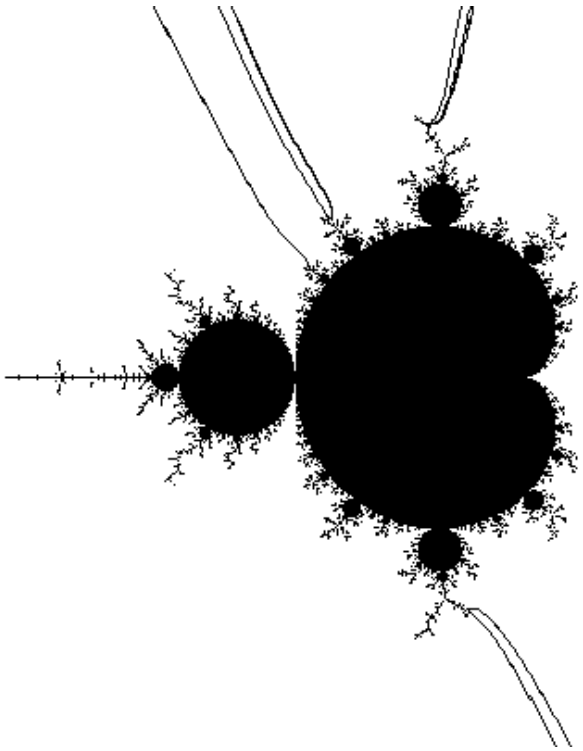

Figure B.8: Period 14, Rotation number 2/7

Rotation number 3/7.

f_1: $(6550/16383, 6553/16383)$

g_1: $(6551/16383, 65520/16383)$

Internal address	f_2 **angles**	**C.d.** f_1	**C.d.** g_1
$1 \to 5 \to 9 \to 13 \to 14$	(4915,4916)	1	13
$1 \to 3 \to 4 \to 7 \to 9 \to 12 \to 13 \to 14$	(3379,3652)	3	$\times$
$1 \to 3 \to 4 \to 11 \to 13 \to 14$	(3283,3300)	5	$\times$
$1 \to 3 \to 4 \to 14$	(3277,3278)	7	$\times$
$1 \to 3 \to 5 \to 6 \to 10 \to 14$	(13515,13516)	9	$\times$
$1 \to 3 \to 6 \to 7 \to 9 \to 10 \to 14$	(13131,13131)	11	$\times$
$1 \to 3 \to 6 \to 7 \to 10 \to 11 \to 13 \to 14$	(13107,13108)	13	1

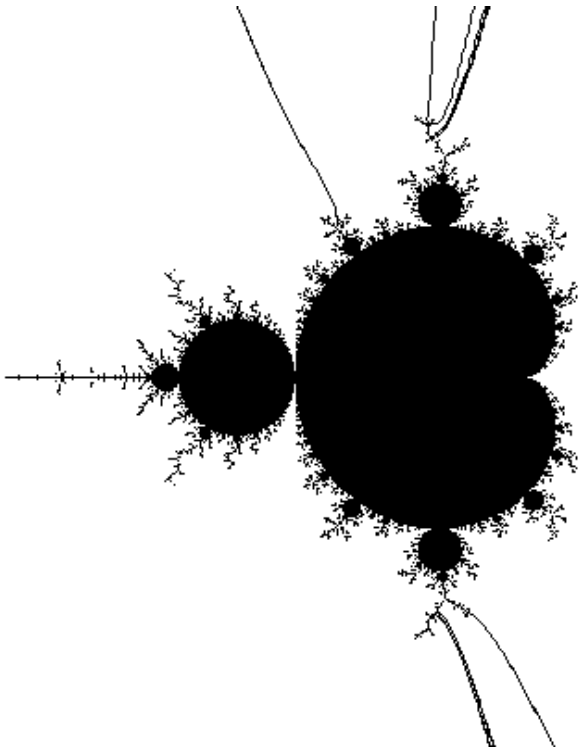

Figure B.9: Period 14, Rotation number 3/7

B.7 Period 16 - denominator 65535.

Rotation number 1/8.

f_1: $(21846/65535, 21849/65535)$

g_1: $(21847/65535, 21848/65535)$

Internal address	f_2 **angles**	**C.d.** f_1	**C.d.** g_1
$1 \to 15 \to 16$	(21843,21844)	1	15
$1 \to 13 \to 14 \to 16$	(21837,21838)	3	$\times$
$1 \to 11 \to 12 \to 14 \to 16$	(21813,21814)	5	$\times$
$1 \to 9 \to 10 \to 12 \to 14 \to 16$	(21717,21718)	7	$\times$
$1 \to 7 \to 8 \to 10 \to 12 \to 14 \to 16$	(21333,21334)	9	$\times$
$1 \to 5 \to 6 \to 8 \to 10 \to 12 \to 14 \to 16$	(19797,19798)	11	$\times$
$1 \to 3 \to 4 \to 6 \to 8$ $\to 10 \to 12 \to 14 \to 16$	(13653,13654)	13	$\times$
$1 \to 3 \to 5 \to 7 \to$ $9 \to 11 \to 13 \to 14 \to 16$	(54611,54612)	15	1

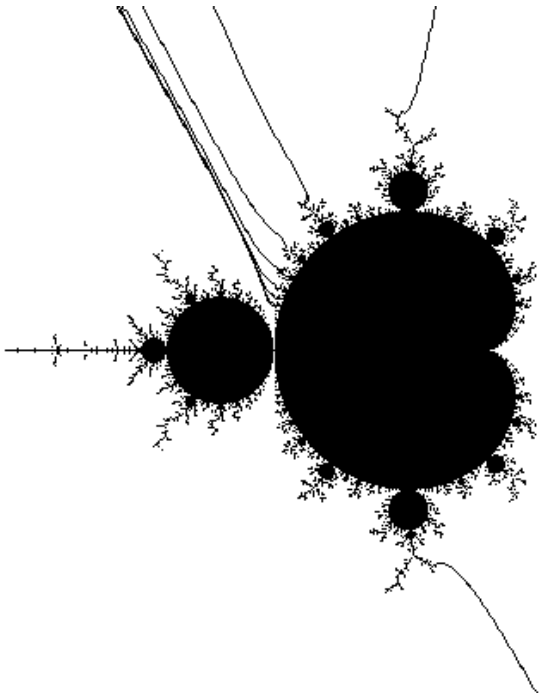

Figure B.10: Period 16, Rotation number 1/8

Rotation number 3/8.

f_1: $(26006/65535, 26009/65535)$

g_1: $(26007/65535, 26008/65535)$

Internal address	f_2 **ang.**	**C.d.** f_1	**C.d.** g_1
$1 \to 5 \to 10 \to 11 \to 15 \to 16$	(19763,19764)	1	15
$1 \to 5 \to 9 \to 10 \to 16$	(19667,19668)	3	×
$1 \to 3 \to 4 \to 7 \to 9 \to 12 \to 13 \to 15 \to 16$	(13523,14564)	5	×
$1 \to 3 \to 4 \to 7 \to 9 \to 10 \to 16$	(13517,13518)	7	×
$1 \to 3 \to 4 \to 10 \to 16$	(13133,13134)	9	×
$1 \to 3 \to 5 \to 6 \to 16$	(54091,54092)	11	×
$1 \to 3 \to 5 \to 6 \to 11 \to 13 \to 15 \to 16$	(54003,54068)	13	×
$1 \to 3 \to 6 \to 7 \to 9 \to 12 \to 13 \to 15 \to 16$	(52531,52532)	15	1

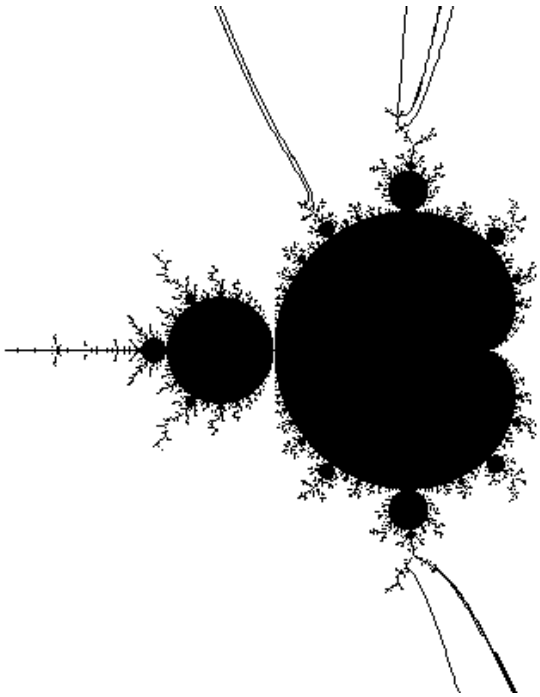

Figure B.11: Period 16, Rotation number 3/8

B.8 Period 18 - denominator 262143.

Rotation number 1/9.

f_1: $(87382/262143, 87385/262143)$

g_1: $(87383/262143, 87384/262143)$

Internal address	f_2 **angles**	**C.d.** f_1	**C.d.** g_1
$1 \to 17 \to 18$	(87379,87380)	1	17
$1 \to 15 \to 16 \to 18$	(87373,87374)	3	$\times$
$1 \to 13 \to 14 \to 16 \to 18$	(87349,87350)	5	$\times$
$1 \to 11 \to 12 \to 14 \to 16 \to 18$	(87253,87254)	7	$\times$
$1 \to 9 \to 10 \to 12 \to 14 \to 16 \to 18$	(86869,86870)	9	$\times$
$1 \to 7 \to 8 \to 10 \to 12 \to 14 \to 16 \to 18$	(85333,85334)	11	$\times$
$1 \to 5 \to 6 \to 8 \to 10$ $\to 12 \to 14 \to 16 \to 18$	(79189,79190)	13	$\times$
$1 \to 3 \to 4 \to 6 \to 8 \to$ $10 \to 12 \to 14 \to 16 \to 18$	(54613,54614)	15	$\times$
$1 \to 3 \to 5 \to 7 \to 9 \to 11$ $\to 13 \to 15 \to 17 \to 18$	(218451,218452)	17	1

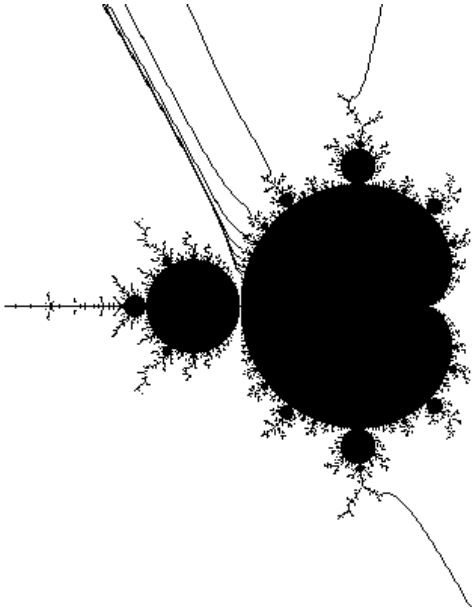

Figure B.12: Period 18, Rotation number 1/9

Rotation number 2/9.

f_1: $(88406/262143, 88409/262143)$

g_1: $(88407/262143, 88408/262143)$

Internal address	f_2 **angles**	**C.d.** f_1	**C.d.** g_1
$1 \to 9 \to 17 \to 18$	(86867,86868)	1	17
$1 \to 7 \to 8 \to 15 \to 17 \to 18$	(85331,85588)	3	$\times$
$1 \to 7 \to 8 \to 18$	(85325,85326)	5	$\times$
$1 \to 5 \to 6 \to 8 \to 13 \to 15 \to 16 \to 18$	(79181,79438)	7	$\times$
$1 \to 5 \to 6 \to 8 \to 18$	(79157,79158)	9	$\times$
$1 \to 3 \to 4 \to 6 \to 8 \to 11 \to 13$ $\to 14 \to 16 \to 18$	(54581,54838)	11	$\times$
$1 \to 3 \to 4 \to 6 \to 8 \to 18$	(54485,54486)	13	$\times$
$1 \to 3 \to 5 \to 7 \to 9 \to 10 \to 18$	(218323,218324)	15	$\times$
$1 \to 3 \to 5 \to 7 \to 10 \to 11 \to 13$ $\to 15 \to 17 \to 18$	(217940,217939)	17	1

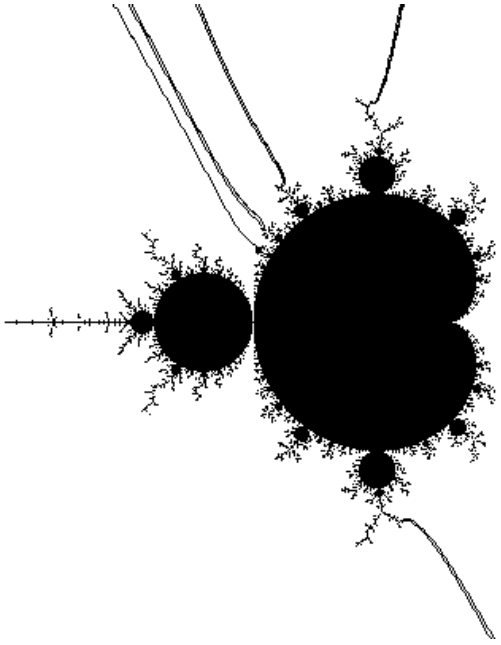

Figure B.13: Period 18, Rotation number 2/9

Rotation number 4/9.

f_1: $(104854/262143, 104857/262143)$

g_1: $(104855/262143, 104856/262143)$

Internal address	f_2 **angles**	**C.d.** f_1	**C.d.** g_1
$1 \to 5 \to 9 \to 13 \to 17 \to 18$	(78643,78644)	1	17
$1 \to 3 \to 4 \to 7 \to 9 \to 12$ $\to 13 \to 16 \to 17 \to 18$	(54067,58436)	3	$\times$
$1 \to 3 \to 4 \to 11 \to 13 \to 16 \to 17 \to 18$	(52531,52804)	5	$\times$
$1 \to 3 \to 4 \to 15 \to 17 \to 18$	(52435,52452)	7	$\times$
$1 \to 3 \to 4 \to 18$	(52429,52430)	9	$\times$
$1 \to 3 \to 5 \to 6 \to 10 \to 14 \to 18$	(216267,216268)	11	$\times$
$1 \to 3 \to 6 \to 7 \to 9 \to 10 \to 14 \to 18$	(210123,210124)	13	$\times$
$1 \to 3 \to 6 \to 7 \to 10 \to 11$ $\to 13 \to 14 \to 18$	(209739,209740)	15	$\times$
$1 \to 3 \to 6 \to 7 \to 10 \to 11 \to 14$ $\to 15 \to 17 \to 18$	(207915,207916)	17	1

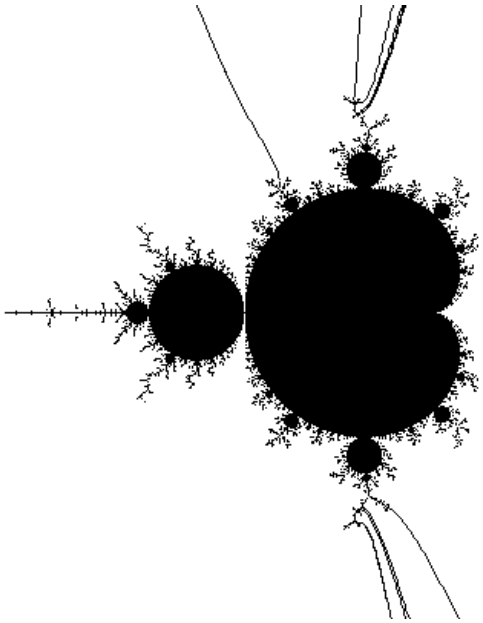

Figure B.14: Period 18, Rotation number 4/9

B.9 Period 20 - denominator 1048575.

Rotation number 1/10.

f_1: $(349526/1048575, 349529/1048575)$

g_1: $(349527/1048575, 349528/1048575)$

Internal address	f_2 **angles**	$\delta\ f_1$	$\delta\ g_1$
$1 \to 19 \to 20$	(349523,349524)	1	19
$1 \to 17 \to 18 \to 20$	(349517,349518)	3	$\times$
$1 \to 15 \to 16 \to 18 \to 20$	(349493,349494)	5	$\times$
$1 \to 13 \to 14 \to 16 \to 18 \to 20$	(349397,349398)	7	$\times$
$1 \to 11 \to 12 \to 14 \to 16 \to 18 \to 20$	(349013,349014)	9	$\times$
$1 \to 9 \to 10 \to 12 \to 14 \to 16 \to 18 \to 20$	(347477,347478)	11	$\times$
$1 \to 7 \to 8 \to 10 \to 12$ $\to 14 \to 16 \to 18 \to 20$	(341333,341334)	13	$\times$
$1 \to 5 \to 6 \to 8 \to 10 \to 12$ $\to 14 \to 16 \to 18 \to 20$	(316757,316758)	15	$\times$
$1 \to 3 \to 4 \to 6 \to 8 \to 10 \to 12$ $\to 14 \to 16 \to 18 \to 20$	(218453,218454)	17	$\times$
$1 \to 3 \to 5 \to 7 \to 9 \to 11 \to 13$ $\to 15 \to 17 \to 19 \to 20$	(873811,873812)	19	1

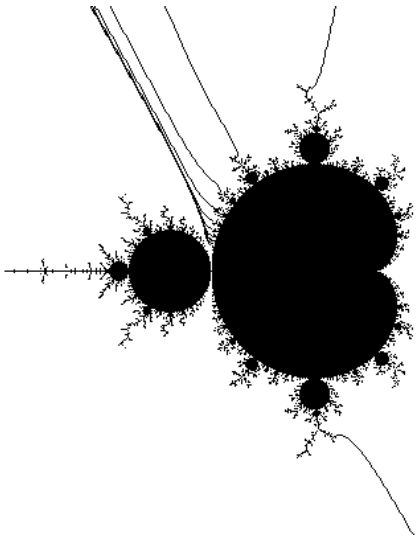

Figure B.15: Period 20, Rotation number 1/10

Rotation number 3/10.

f_1: $(366166/1048575, 366169/1048575)$

g_1: $(366167/1048575, 366168/1048575)$

Internal address	f_2 **angles**	**C.d.** f_1	**C.d.** g_1
$1 \to 7 \to 13 \to 19 \to 20$	(341203,341204)	1	19
$1 \to 5 \to 6 \to 11 \to 13 \to 18 \to 19 \to 20$	(316627,320788)	3	$\times$
$1 \to 5 \to 6 \to 17 \to 19 \to 20$	(316243,316308)	5	$\times$
$1 \to 5 \to 6 \to 20$	(316237,316238)	7	$\times$
$1 \to 3 \to 4 \to 6 \to 9 \to 11$ $\to 12 \to 15 \to 17 \to 18 \to 20$	(217933,222094)	9	$\times$
$1 \to 3 \to 4 \to 6 \to 15 \to 17 \to 18 \to 20$	(216397,216462)	11	$\times$
$1 \to 3 \to 4 \to 6 \to 20$	(216373,216374)	13	$\times$
$1 \to 3 \to 5 \to 7 \to 8 \to 14 \to 20$	(871731,871732)	15	$\times$
$1 \to 3 \to 5 \to 8 \to 9 \to 11$ $\to 13 \to 14 \to 20$	(865587,865588)	17	$\times$
$1 \to 3 \to 5 \to 8 \to 9 \to 11$ $\to 14 \to 15 \to 17 \to 19 \to 20$	(865491,865492)	19	1

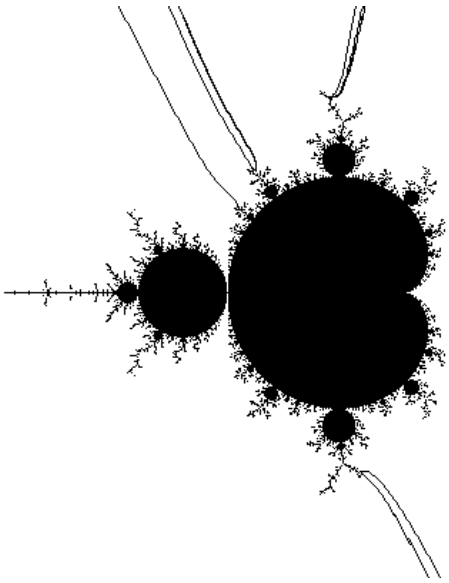

Figure B.16: Period 20, Rotation number 3/10

B.10 Period 22 - denominator 4194303.

Rotation number 1/11.

f_1: (1398102/4194303, 1398105/4194303)

g_1: (1398103/4194303, 1398103/4194303)

Internal address	f_2 **angles**	**C.d.** f_1	**C.d.** g_1
$1 \to 21 \to 22$	(1398099,1398100)	1	21
$1 \to 19 \to 20 \to 22$	(1398093,1398094)	3	×
$1 \to 17 \to 18 \to 20 \to 22$	(1398069,1398070)	5	×
$1 \to 15 \to 16 \to 18 \to 20 \to 22$	(1397973,1397974)	7	×
$1 \to 13 \to 14 \to 16 \to 18 \to 20 \to 22$	(1397589,1397590)	9	×
$1 \to 11 \to 12 \to 14 \to 16 \to 18$ $\to 20 \to 22$	(1396053,1396054)	11	×
$1 \to 9 \to 10 \to 12 \to 14 \to 16$ $\to 18 \to 20 \to 22$	(1389909,1389910)	13	×
$1 \to 7 \to 8 \to 10 \to 12 \to 14$ $\to 16 \to 18 \to 20 \to 22$	(1365333,1365334)	15	×
$1 \to 5 \to 6 \to 8 \to 10 \to 12$ $\to 14 \to 16 \to 18 \to 20 \to 22$	(1267029,1267030)	17	×
$1 \to 3 \to 4 \to 6 \to 8 \to 10$ $\to 12 \to 14 \to 16 \to 18 \to 20 \to 22$	(873813,873814)	19	×
$1 \to 3 \to 5 \to 7 \to 9 \to 11 \to$ $13 \to 15 \to 17 \to 19 \to 21 \to 22$	(3495251,3495252)	21	1

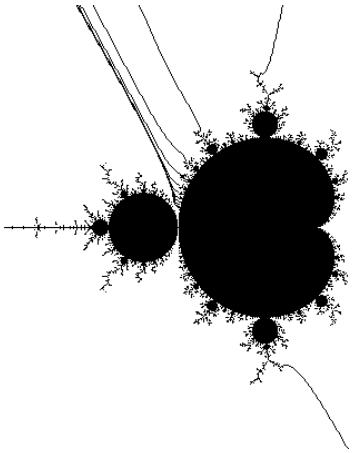

Figure B.17: Period 22, Rotation number 1/11

Rotation number 2/11.

f_1: $(1402198/4194303, 1402201/4194303)$

g_1: $(1402199/4194303, 1402200/4194303)$

Internal address	f_2 **angles**	**C.d.** f_1	**C.d.** g_1
$1 \to 11 \to 21 \to 22$	(1396051,1396052)	1	21
$1 \to 9 \to 10 \to 19 \to 21 \to 22$	(1389907,1390932)	3	$\times$
$1 \to 9 \to 10 \to 22$	(1389901,1389902)	5	$\times$
$1 \to 7 \to 8 \to 10 \to 17 \to 19$ $\to 20 \to 22$	(1365325,1366350)	7	$\times$
$1 \to 7 \to 8 \to 10 \to 22$	(1365301,1365302)	9	$\times$
$1 \to 5 \to 6 \to 8 \to 10 \to 15$ $\to 17 \to 18 \to 20 \to 22$	(1266997,1268022)	11	$\times$
$1 \to 5 \to 6 \to 8 \to 10 \to 22$	(1266901,1266902)	13	$\times$
$1 \to 3 \to 4 \to 6 \to 8 \to 10 \to 13$ $\to 15 \to 16 \to 18 \to 20 \to 22$	(873685,874710)	15	$\times$
$1 \to 3 \to 4 \to 6 \to 8 \to 10 \to 22$	(873301,873302)	17	$\times$
$1 \to 3 \to 5 \to 7 \to 9 \to 11 \to 12 \to 22$	(3494739,3494740)	19	$\times$
$1 \to 3 \to 5 \to 7 \to 9 \to 12$ $\to 13 \to 15 \to 17 \to 19 \to 21 \to 22$	(3493203,3493204)	21	1

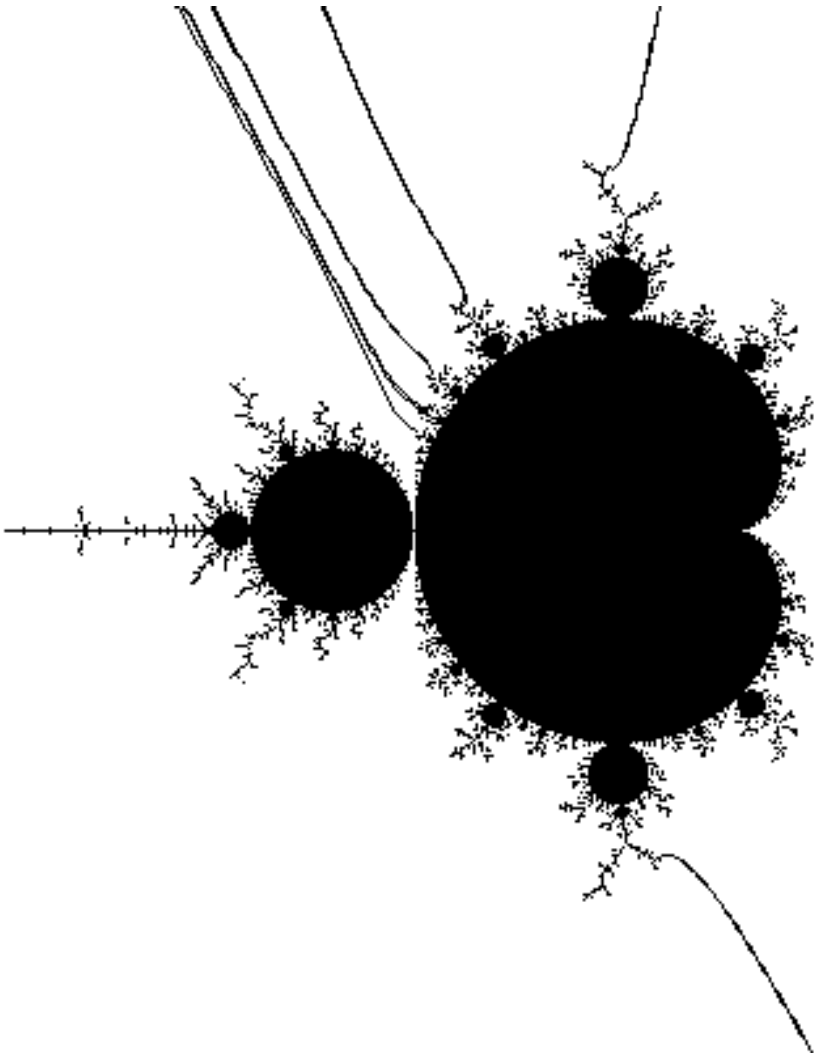

Figure B.18: Period 22, Rotation number 2/11

Rotation number 3/11.

f_1: (1463894/4194303, 1463897/4194303)

g_1: (1463895/4194303, 1463896/4194303)

Internal address	f_2 **angles**	**C.d.** f_1	**C.d.** g_1
$1 \to 7 \to 14 \to 15 \to 21 \to 22$	(1365203,1365204)	1	21
$1 \to 7 \to 13 \to 14 \to 22$	(1364819,1364820)	3	×
$1 \to 5 \to 6 \to 11 \to 13 \to 14$ $\to 19 \to 21 \to 22$	(1266515,1282964)	5	×
$1 \to 5 \to 6 \to 11 \to 13 \to 14 \to 22$	(1266509,1266510)	7	×
$1 \to 5 \to 6 \to 14 \to 22$	(1264973,1264974)	9	×
$1 \to 3 \to 4 \to 6 \to 9 \to 11 \to 12$ $\to 14 \to 17 \to 19 \to 20 \to 22$	(871757,888206)	11	×
$1 \to 3 \to 4 \to 6 \to 9 \to 11$ $\to 12 \to 14 \to 22$	(871733,871734)	13	×
$1 \to 3 \to 4 \to 6 \to 14 \to 22$	(865589,865590)	15	×
$1 \to 3 \to 5 \to 7 \to 8 \to 22$	(3487027,3487028)	17	×
$1 \to 3 \to 5 \to 7 \to 8 \to 15$ $\to 17 \to 19 \to 21 \to 22$	(3486675,3486932)	19	×
$1 \to 3 \to 5 \to 8 \to 9 \to 11$ $\to 13 \to 16 \to 17 \to 19 \to 21 \to 22$	(3462355,3462356)	21	1

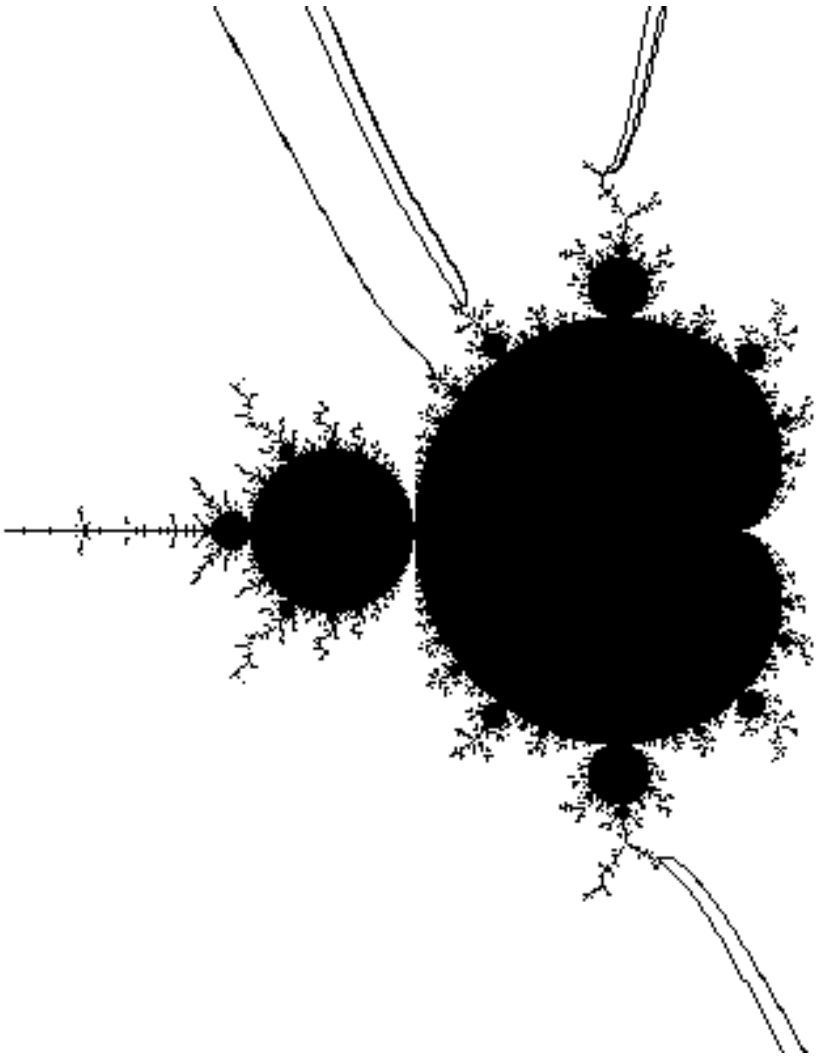

Figure B.19: Period 22, Rotation number 3/11

Rotation number 4/11.

f_1: $(1664406/4194303, 1664409/4194303)$

g_1: $(1664407/4194303, 1664408/4194303)$

Internal address	f_2 **angles**	$\delta(f_1)$	$\delta(g_1)$
$1 \to 5 \to 10 \to 11 \to 16 \to 17$ $\to 21 \to 22$	(1264947,1264948)	1	21
$1 \to 5 \to 10 \to 11 \to 15 \to 16 \to 22$	(1264851,1264852)	3	$\times$
$1 \to 5 \to 9 \to 10 \to 16 \to 22$	(1258707,1258708)	5	$\times$
$1 \to 3 \to 4 \to 7 \to 9 \to 10 \to 13$ $\to 15 \to 16 \to 19 \to 21 \to 22$	(865491,932068)	7	$\times$
$1 \to 3 \to 4 \to 7 \to 9 \to 10$ $\to 13 \to 15 \to 16 \to 22$	(865485,865486)	9	$\times$
$1 \to 3 \to 4 \to 7 \to 9 \to 10 \to 16 \to 22$	(865101,865102)	11	$\times$
$1 \to 3 \to 4 \to 10 \to 16 \to 22$	(840525,840526)	13	$\times$
$1 \to 3 \to 5 \to 6 \to 22$	(3461963,3461964)	15	$\times$
$1 \to 3 \to 5 \to 6 \to 17 \to 19 \to 21 \to 22$	(3461940,3461875)	17	$\times$
$1 \to 3 \to 5 \to 6 \to 11 \to 13 \to 15$ $\to 18 \to 19 \to 21 \to 22$	(3456243,3460404)	19	$\times$
$1 \to 3 \to 6 \to 7 \to 9 \to 12$ $\to 13 \to 15 \to 18 \to 19 \to 21 \to 22$	(3362099,3362100)	21	1

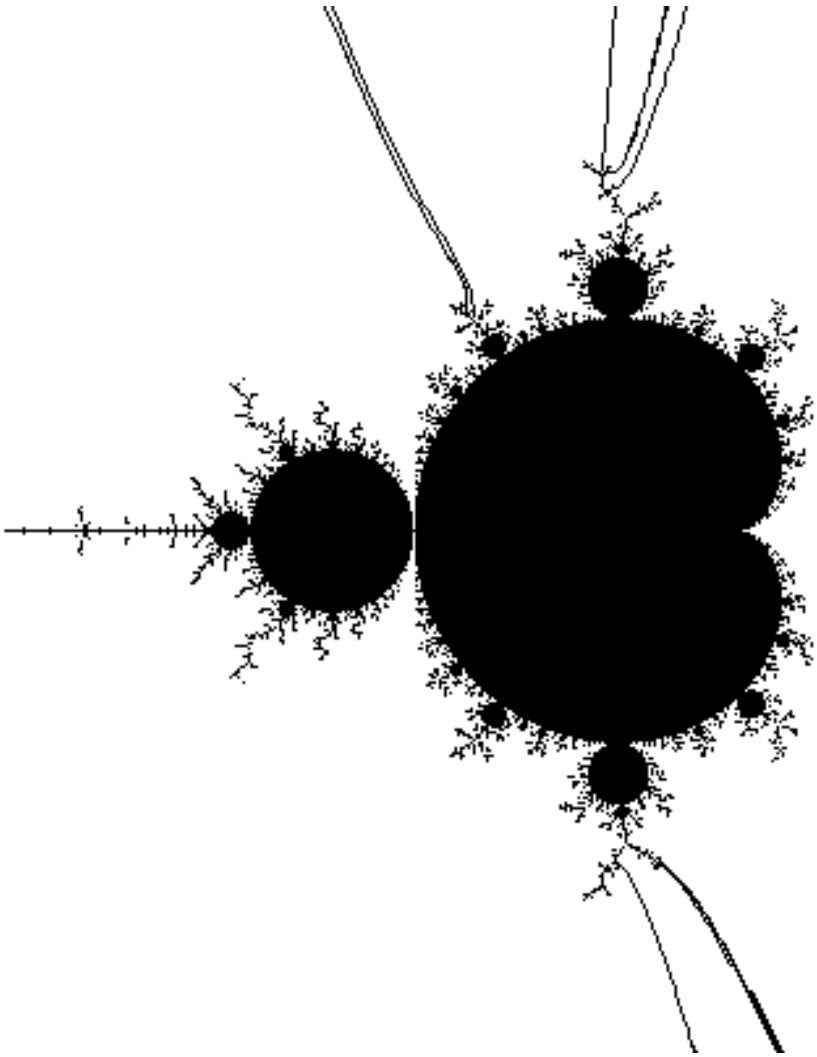

Figure B.20: Period 22, Rotation number 4/11

Rotation number 5/11.

f_1: $(1664406/4194303, 1664409/4194303)$

g_1: $(1664407/4194303, 1664408/4194303)$

Internal address	f_2 **angles**	$\delta(f_1)$	$\delta(g_1)$
$1 \to 5 \to 9 \to 13 \to 17 \to 21 \to 22$	(1258291,1258292)	1	21
$1 \to 3 \to 4 \to 7 \to 9 \to 12 \to 13$ $\to 16 \to 17 \to 20 \to 21 \to 22$	(865075,934980)	3	$\times$
$1 \to 3 \to 4 \to 11 \to 13 \to 16$ $\to 17 \to 20 \to 21 \to 22$	(840499,844868)	5	$\times$
$1 \to 3 \to 4 \to 15 \to 17 \to 20 \to 21 \to 22$	(838963,839236)	7	$\times$
$1 \to 3 \to 4 \to 19 \to 21 \to 22$	(838867,838884)	9	$\times$
$1 \to 3 \to 4 \to 22$	(838861,838862)	11	$\times$
$1 \to 3 \to 5 \to 6 \to 10 \to 14 \to 18 \to 22$	(3460299,3460300)	13	$\times$
$1 \to 3 \to 6 \to 7 \to 9 \to 10 \to 14 \to 18 \to 22$	(3361995,3361996)	15	$\times$
$1 \to 3 \to 6 \to 7 \to 10 \to 11 \to 13$ $\to 14 \to 18 \to 22$	(3355851,3355852)	17	$\times$
$1 \to 3 \to 6 \to 7 \to 10 \to 11$ $\to 14 \to 15 \to 17 \to 18 \to 22$	(3355467,3355468)	19	$\times$
$1 \to 3 \to 6 \to 7 \to 10 \to 11$ $\to 14 \to 15 \to 18 \to 19 \to 21 \to 22$	(3355443,3355444)	21	1

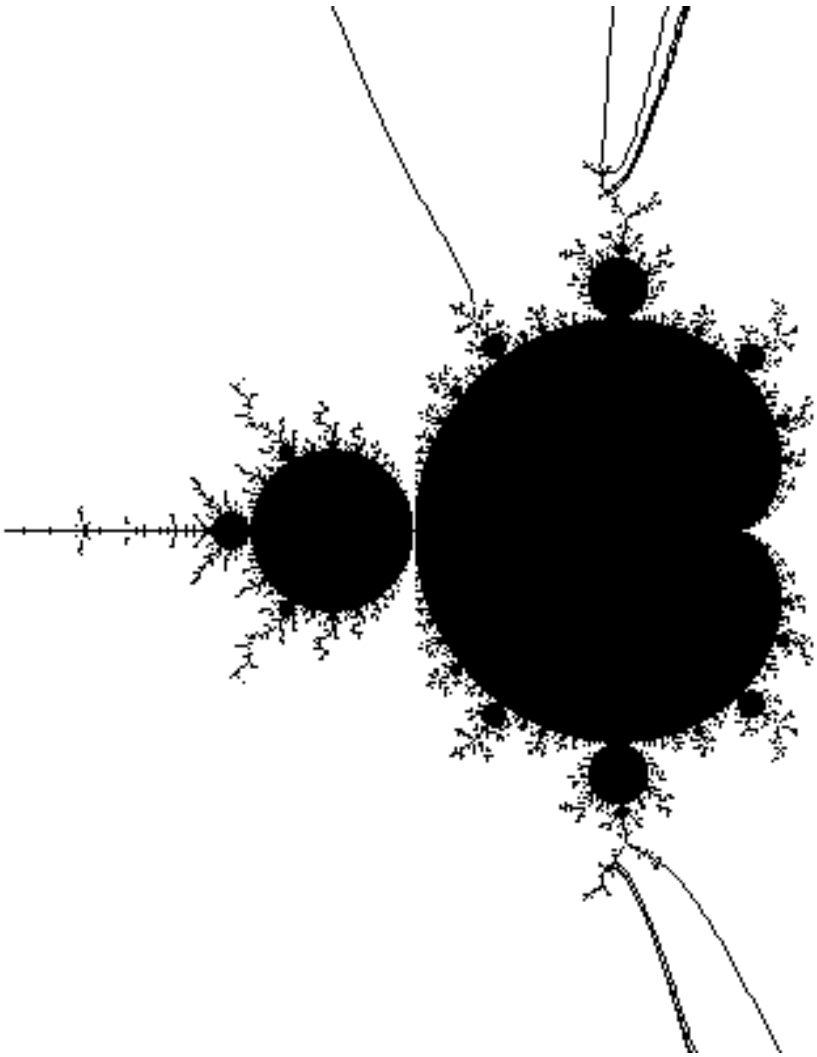

Figure B.21: Period 22, Rotation number 5/11

B.11 Period 24 - denominator 16777215.

Rotation number 1/12.

f_1: $(5592406/16777215, 1398105/16777215)$

g_1: $(1398103/16777215, 1398103/16777215)$

Internal address	f_2 **angles**	**C.d.** f_1	**C.d.** g_1
$1 \to 23 \to 24$	(5592403,5592404)	1	23
$1 \to 21 \to 22 \to 24$	(5592397,5592398)	3	$\times$
$1 \to 19 \to 20 \to 22 \to 24$	(5592373,5592374)	5	$\times$
$1 \to 17 \to 18 \to 20 \to 22 \to 24$	(5592277,5592278)	7	$\times$
$1 \to 15 \to 16 \to 18 \to 20 \to 22 \to 24$	(5591893,5591894)	9	$\times$
$1 \to 13 \to 14 \to 16 \to 18 \to 20$ $\to 22 \to 24$	(5590357,5590358)	11	$\times$
$1 \to 11 \to 12 \to 14 \to 16 \to 18$ $\to 20 \to 22 \to 24$	(5584213,5584214)	13	$\times$
$1 \to 9 \to 10 \to 12 \to 14 \to 16$ $\to 18 \to 20 \to 22 \to 24$	(5559637,5559638)	15	$\times$
$1 \to 7 \to 8 \to 10 \to 12 \to 14$ $\to 16 \to 18 \to 20 \to 22 \to 24$	(5461333,5461334)	17	$\times$
$1 \to 5 \to 6 \to 8 \to 10 \to 12 \to 14$ $\to 16 \to 18 \to 20 \to 22 \to 24$	(5068117,5068118)	19	$\times$
$1 \to 3 \to 4 \to 6 \to 8 \to 10 \to 12$ $\to 14 \to 16 \to 18 \to 20 \to 22 \to 24$	(3495253,3495254)	21	$\times$
$1 \to 3 \to 5 \to 7 \to 9 \to 11 \to 13$ $\to 15 \to 17 \to 19 \to 21 \to 22 \to 24$	(13981012,3981013)	23	1

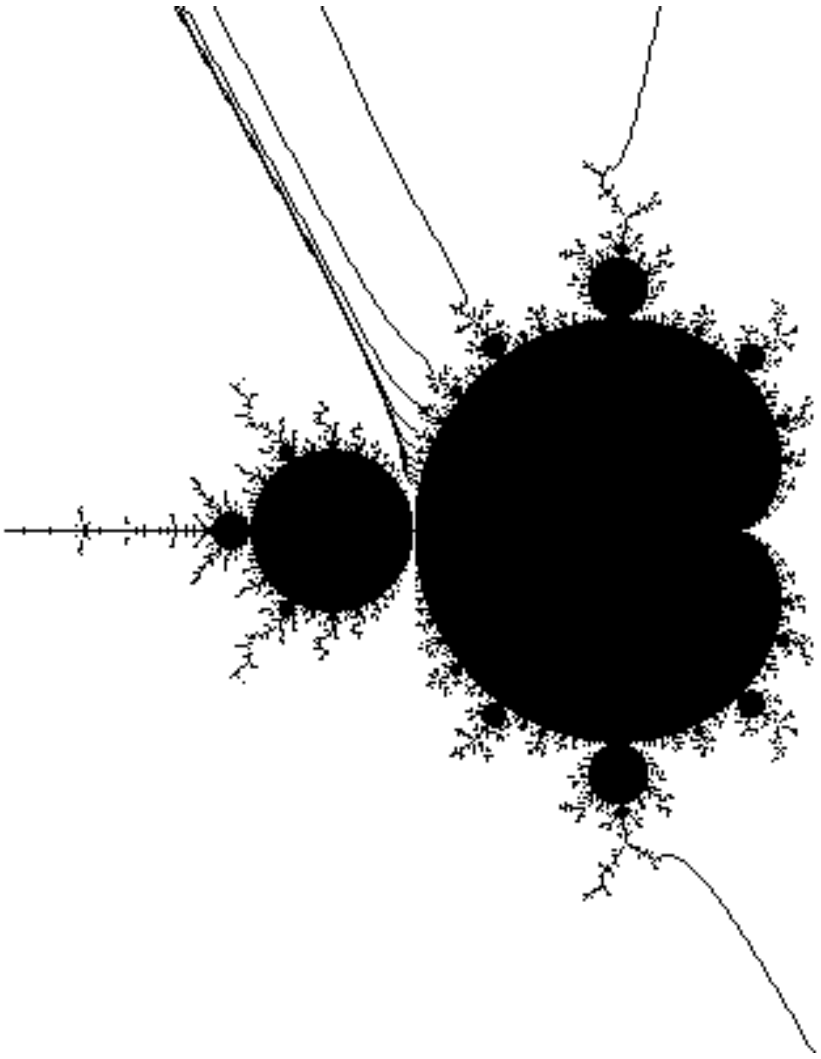

Figure B.22: Period 24, Rotation number 1/12

Rotation number 5/12.

f_1: $(6707606/16777215, 6707609/16777215)$

g_1: $(6707607/16777215, 6707608/16777215)$

Internal address	f_2 **angles**	f_1	g_1
$1 \to 5 \to 9 \to 14 \to 15 \to 19 \to 23 \to 24$	(5034803,5034804)	1	23
$1 \to 5 \to 9 \to 13 \to 14 \to 24$	(5033267,5033268)	3	$\times$
$1 \to 3 \to 4 \to 7 \to 9 \to 12 \to 13 \to 14$ $\to 17 \to 19 \to 22 \to 23 \to 24$	(3460403,3739204)	5	$\times$
$1 \to 3 \to 4 \to 7 \to 9 \to 12 \to 13 \to 14 \to 24$	(3460307,3460324)	7	$\times$
$1 \to 3 \to 4 \to 11 \to 13 \to 14 \to 21 \to 23 \to 24$	(3362003,3378404)	9	$\times$
$1 \to 3 \to 4 \to 11 \to 13 \to 14 \to 24$	(3361997,3361998)	11	$\times$
$1 \to 3 \to 4 \to 14 \to 24$	(3355853,3355854)	13	$\times$
$1 \to 3 \to 5 \to 6 \to 10 \to 24$	(13841611,13841612)	15	$\times$
$1 \to 3 \to 5 \to 6 \to 10 \to 15 \to 17$ $\to 19 \to 20 \to 24$	(13840203,13841228)	17	$\times$
$1 \to 3 \to 6 \to 7 \to 9 \to 10 \to 24$	(13448011,13448012)	19	$\times$
$1 \to 3 \to 6 \to 7 \to 9 \to 10 \to 19$ $\to 21 \to 23 \to 24$	(13446963,13447988)	21	$\times$
$1 \to 3 \to 6 \to 7 \to 10 \to 11 \to 13$ $\to 16 \to 17 \to 20 \to 21 \to 23 \to 24$	(13423411,13423412)	23	1

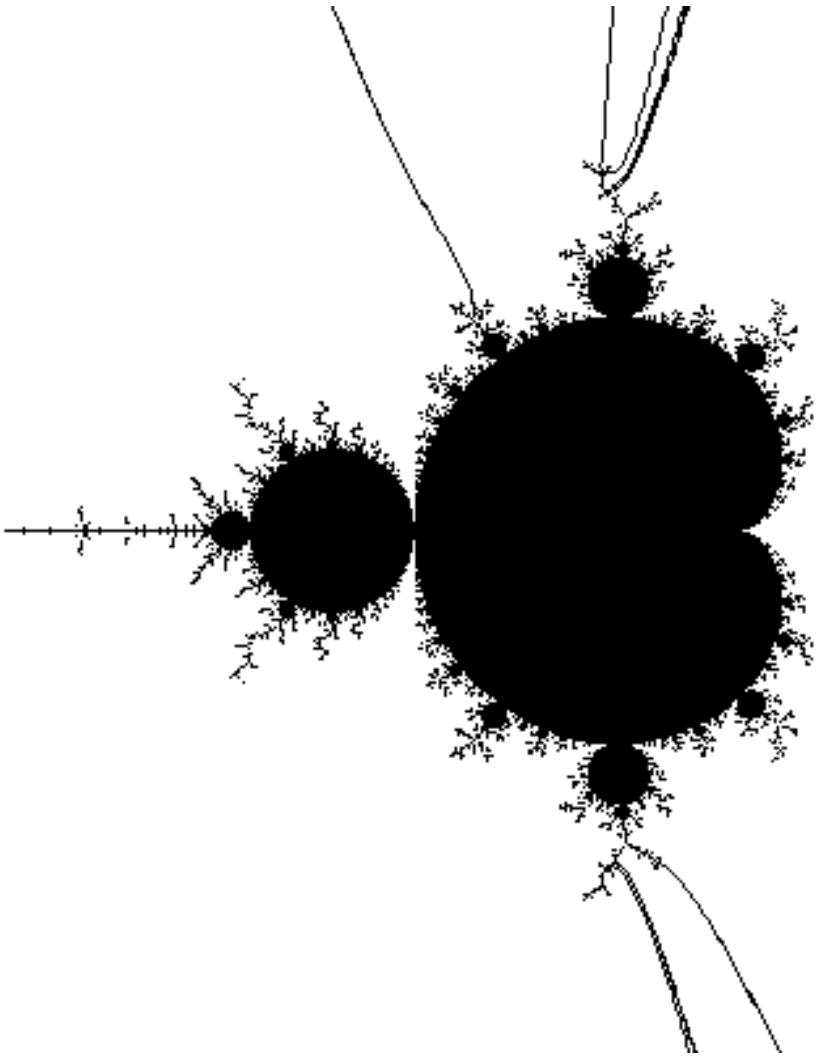

Figure B.23: Period 24, Rotation number 5/12

Appendix C

Hubbard Trees for the Period 1 Cluster Case

C.1 Period 3

C.1.1 Rotation number 1

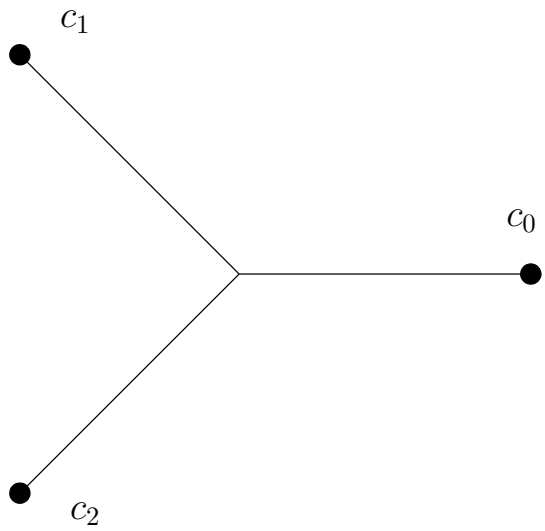

Figure C.1: Hubbard tree for $1 \to 3$, rotation number 1

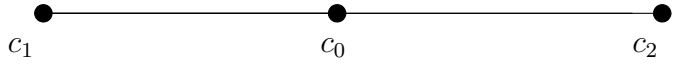

Figure C.2: Hubbard tree for $1 \to 2 \to 3$, c.d $= 3$

C.2 Period 4

C.2.1 Rotation number 1

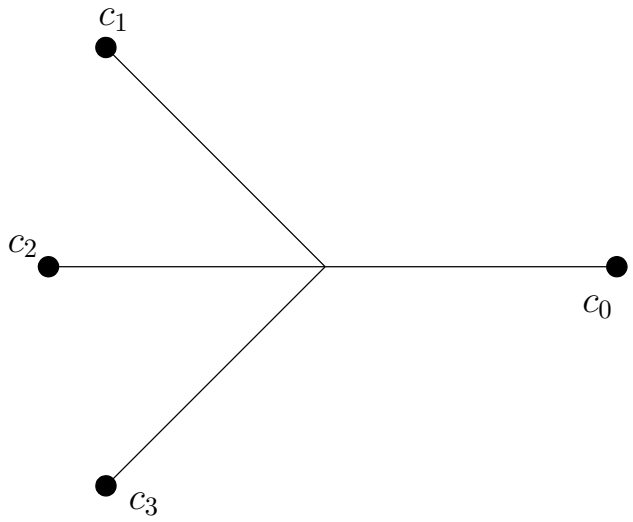

Figure C.3: Hubbard tree for $1 \to 4$, rotation number 1

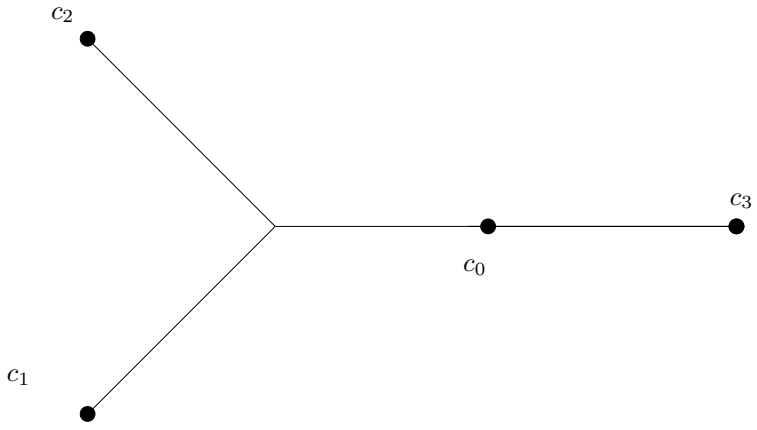

Figure C.4: Hubbard tree for $1 \to 3 \to 4$, c.d = 3

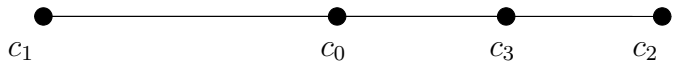

Figure C.5: Hubbard tree for $1 \to 2 \to 3 \to 4$, c.d = 5

C.3 Period 5

C.3.1 Rotation number 1

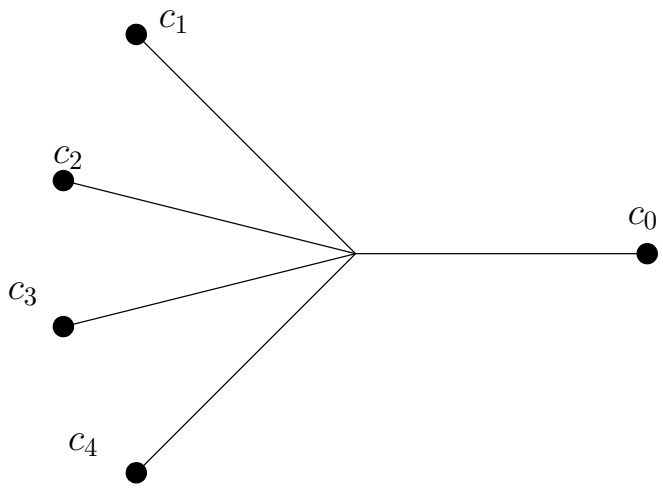

Figure C.6: Hubbard tree for $1 \to 5$, rotation number 1

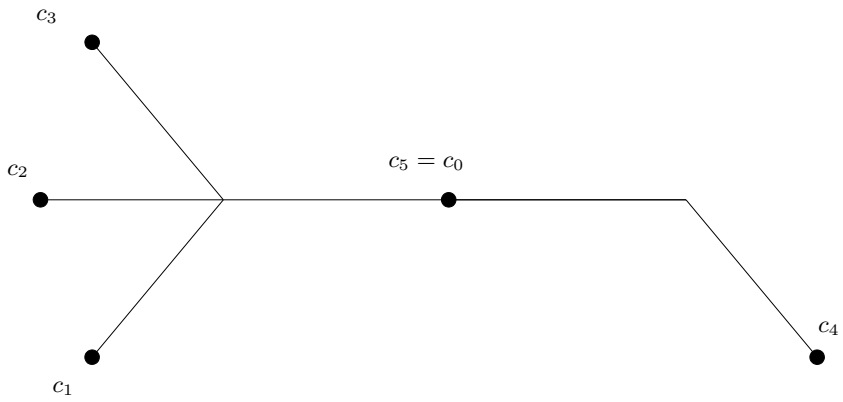

Figure C.7: Hubbard tree for $1 \to 4 \to 5$, c.d = 3

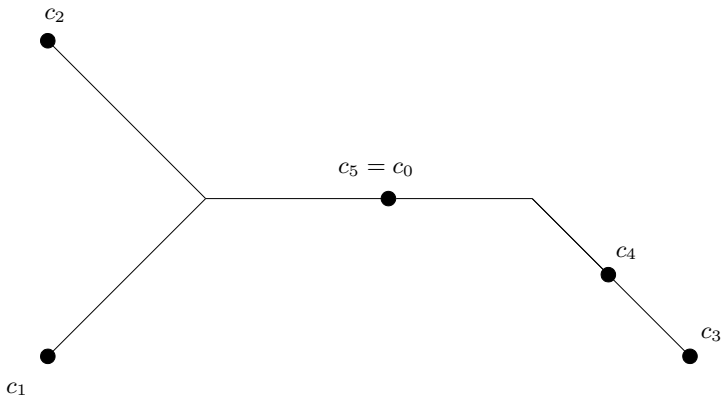

Figure C.8: Hubbard tree for $1 \to 3 \to 4 \to 5$, c.d = 5

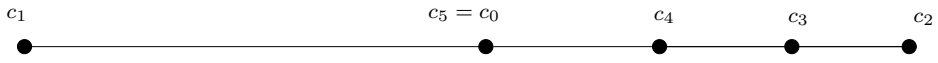

Figure C.9: Hubbard tree for $1 \to 3 \to 4 \to 5$, c.d = 7

C.3.2 Rotation number 2

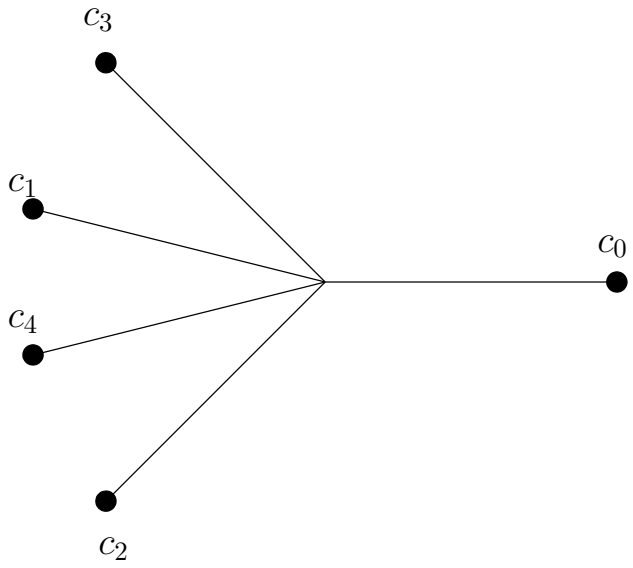

Figure C.10: Hubbard tree for $1 \to 5$, rotation number 2

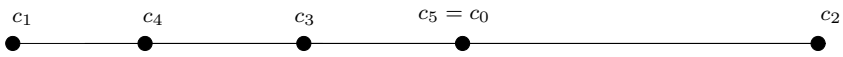

Figure C.11: Hubbard tree for $1 \to 2 \to 4 \to 5$, c.d = 3

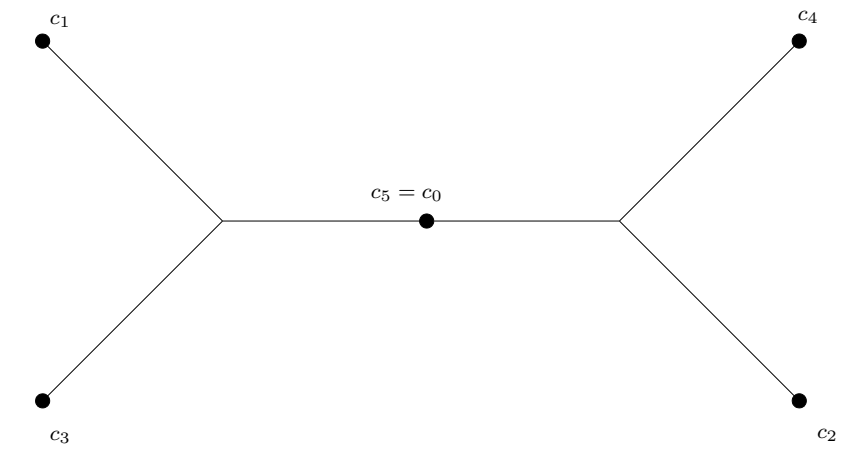

Figure C.12: Hubbard tree for $1 \to 2 \to 5$, c.d $= 5$

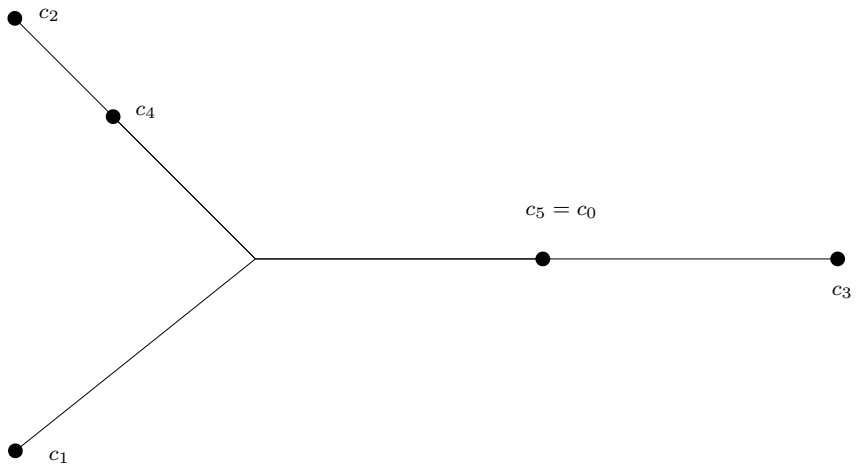

Figure C.13: Hubbard tree for $1 \to 3 \to 5$, c.d $= 7$

C.4 Period 6

C.4.1 Rotation number 1

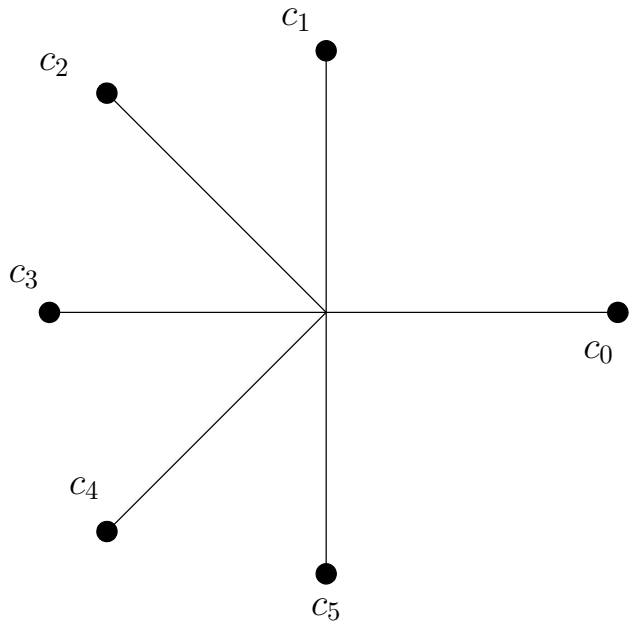

Figure C.14: Hubbard tree for $1 \to 6$, rotation number 1

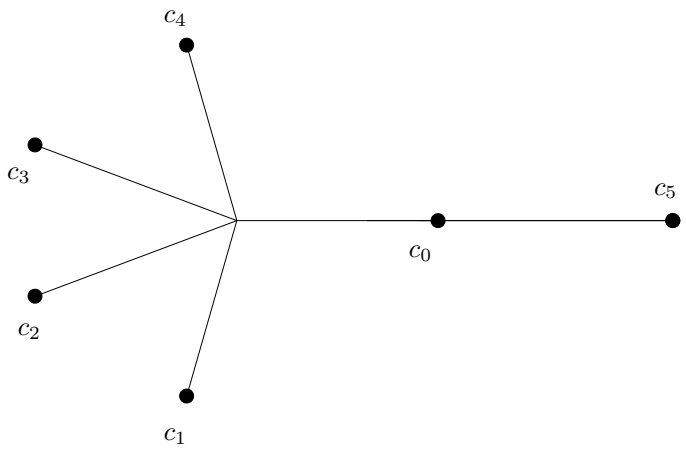

Figure C.15: Hubbard tree for $1 \to 5 \to 6$, c.d = 3

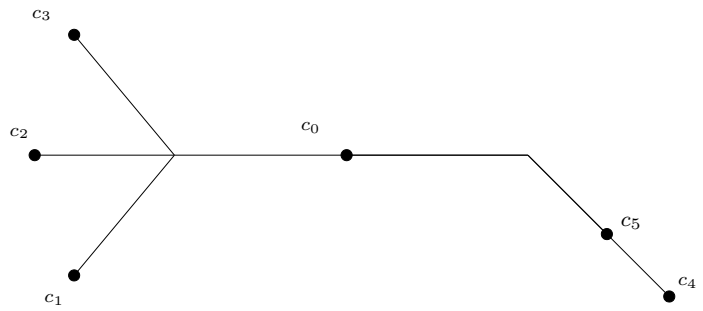

Figure C.16: Hubbard tree for $1 \to 4 \to 5 \to 6$, c.d = 5

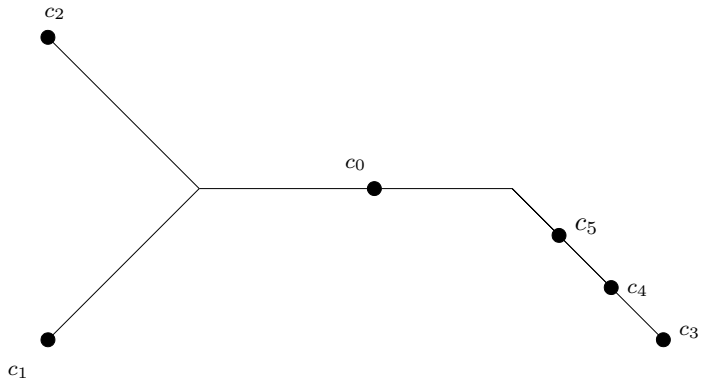

Figure C.17: Hubbard tree for $1 \to 3 \to 4 \to 5 \to 6$, c.d = 7

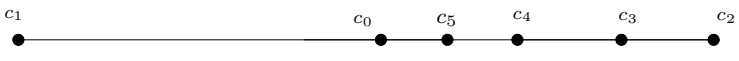

Figure C.18: Hubbard tree for $1 \to 2 \to 3 \to 4 \to 5 \to 6$, c.d = 9

C.5 Period 7

C.5.1 Rotation number 1

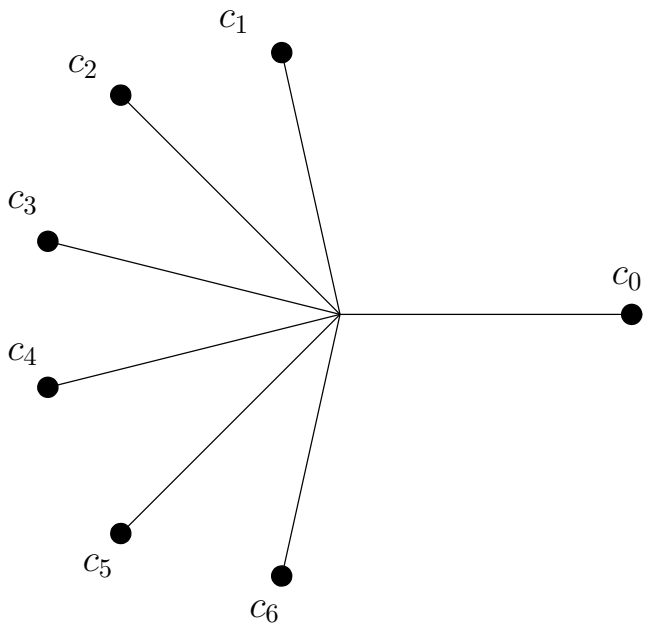

Figure C.19: Hubbard tree for $1 \to 7$, rotation number 1

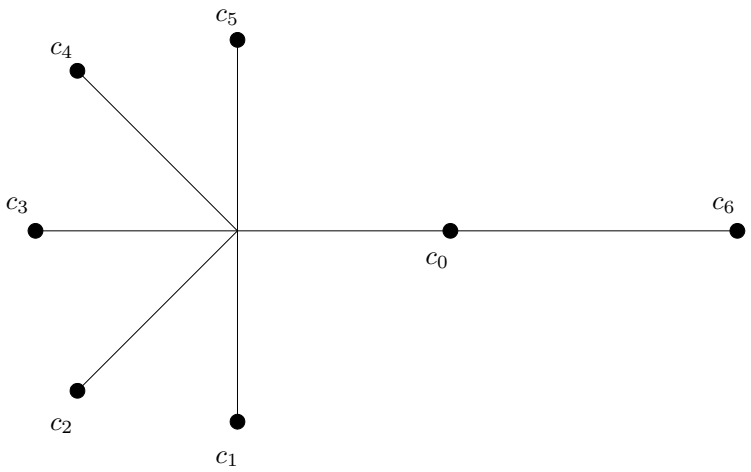

Figure C.20: Hubbard tree for $1 \to 6 \to 7$, c.d = 3

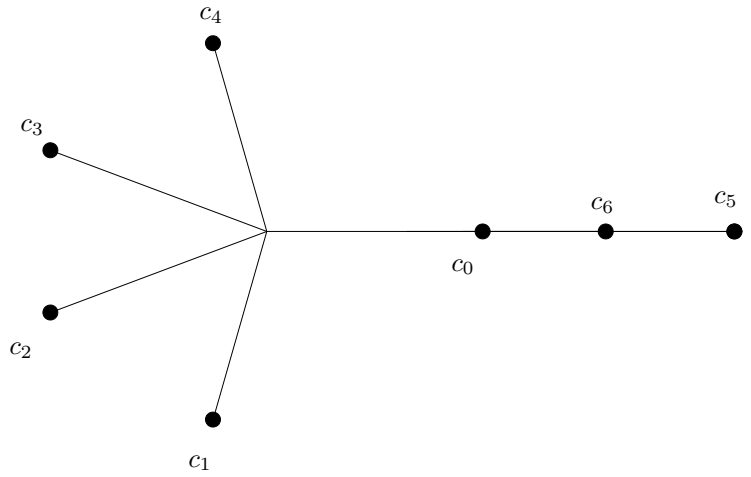

Figure C.21: Hubbard tree for $1 \to 5 \to 6 \to 7$, c.d = 5

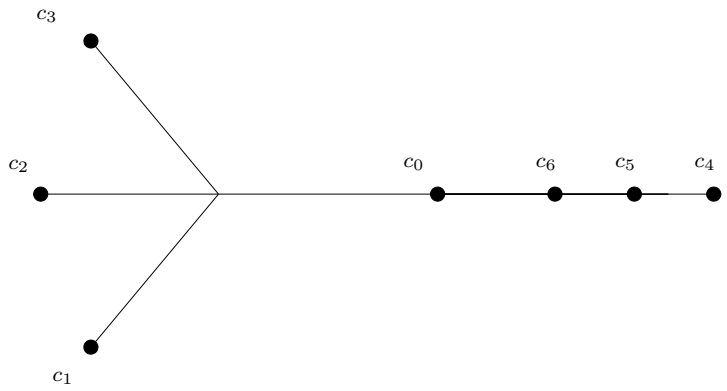

Figure C.22: Hubbard tree for $1 \to 4 \to 5 \to 6 \to 7$, c.d = 7

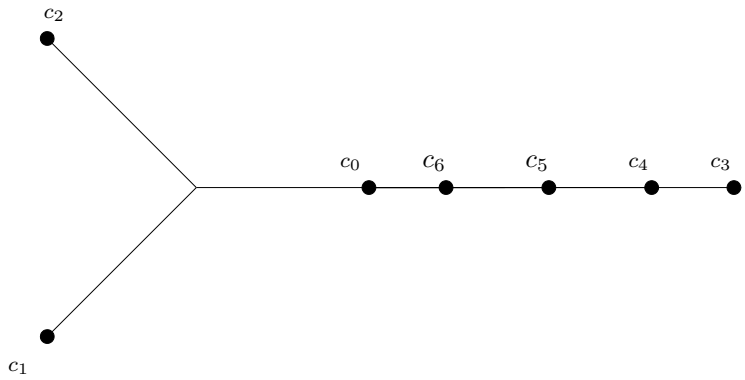

Figure C.23: Hubbard tree for $1 \to 3 \to 4 \to 5 \to 6 \to 7$, c.d = 9

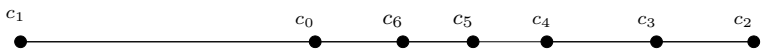

Figure C.24: Hubbard tree for $1 \to 2 \to 3 \to 4 \to 5 \to 6 \to 7$, c.d = 11

C.5.2 Rotation number 2

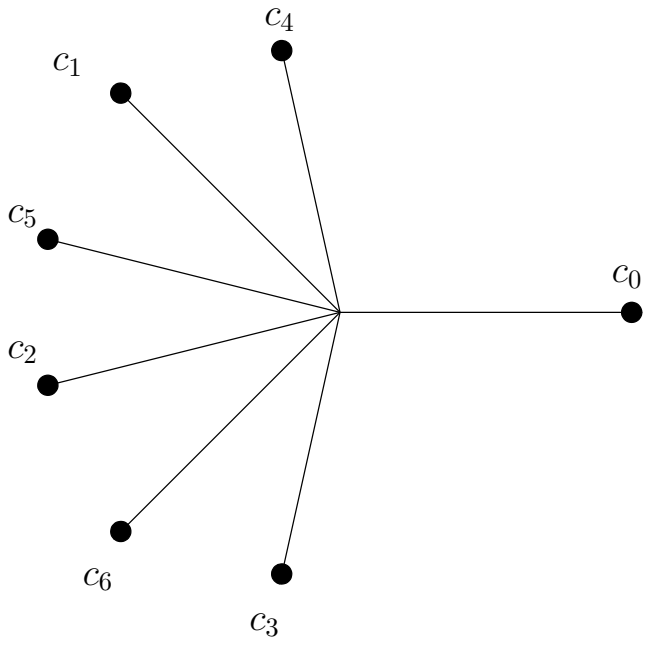

Figure C.25: Hubbard tree for $1 \to 7$, rotation number 2

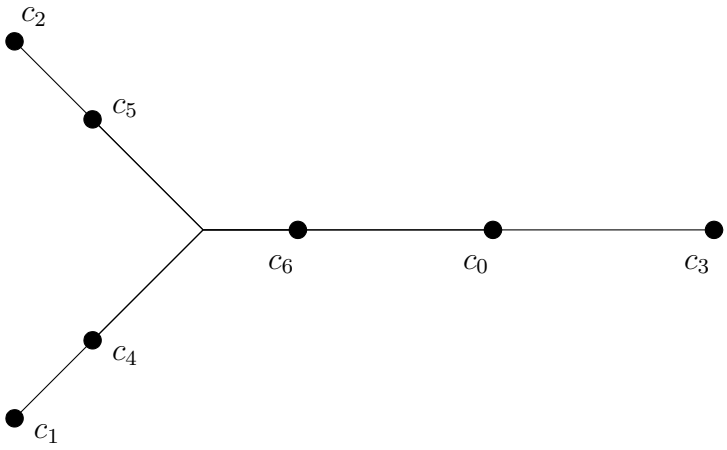

7

Figure C.26: Hubbard tree for $1 \to 3 \to 6 \to 7$, c.d = 3

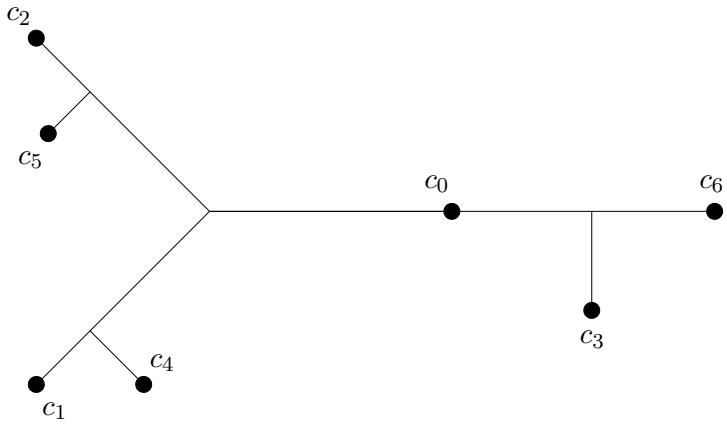

Figure C.27: Hubbard tree for $1 \to 3 \to 7$, c.d = 5

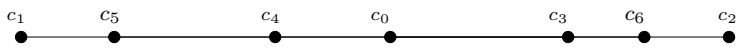

Figure C.28: Hubbard tree for $1 \to 2 \to 3 \to 5 \to 6 \to 7$, c.d = 7

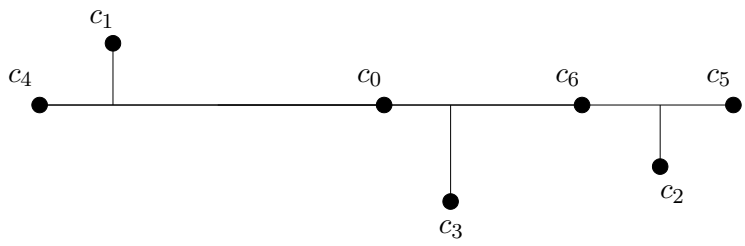

Figure C.29: Hubbard tree for $1 \to 2 \to 3 \to 7$, c.d = 9

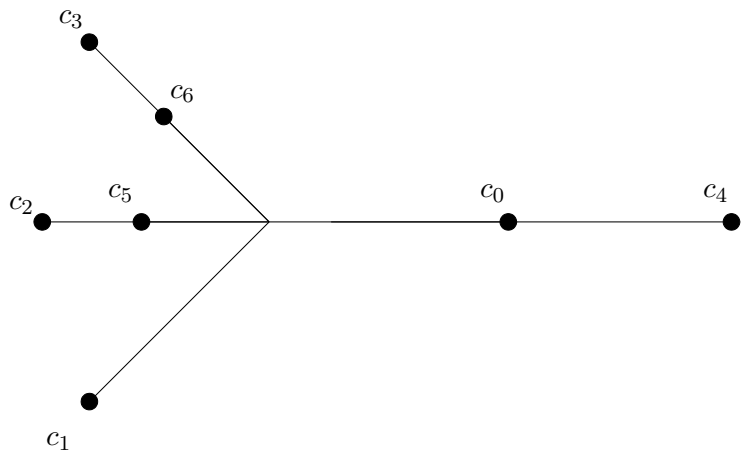

Figure C.30: Hubbard tree for $1 \to 4 \to 7$, c.d = 11

C.5.3 Rotation number 3

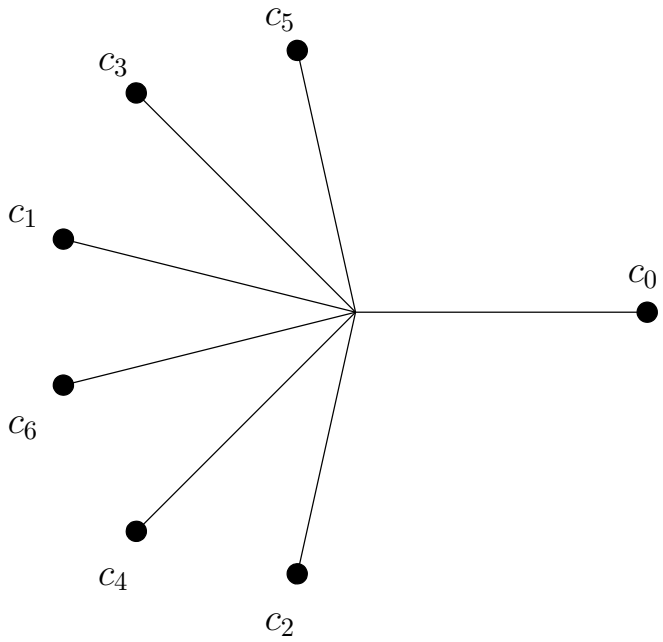

Figure C.31: Hubbard tree for $1 \to 7$, rotation number 3

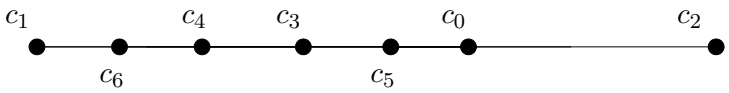

Figure C.32: Hubbard tree for $1 \to 2 \to 4 \to 6 \to 7$, c.d = 3

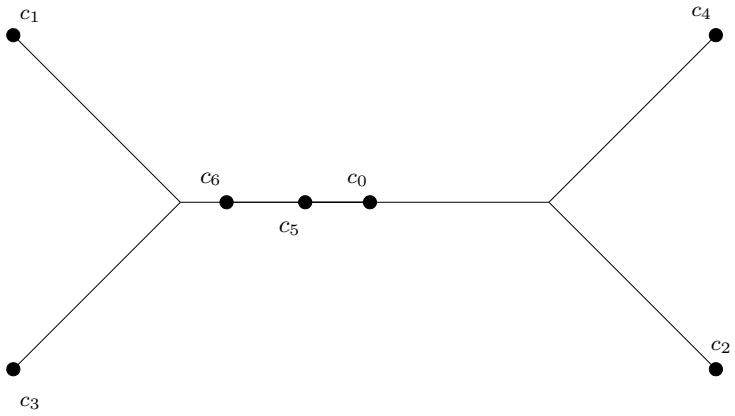

Figure C.33: Hubbard tree for $1 \to 2 \to 6 \to 7$, c.d = 5

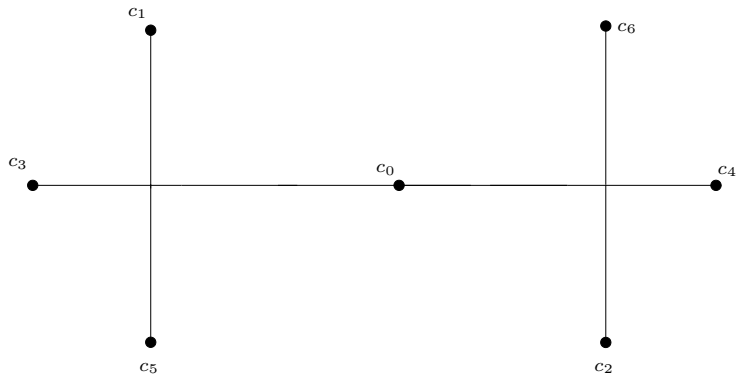

Figure C.34: Hubbard tree for $1 \to 2 \to 7$, c.d = 7

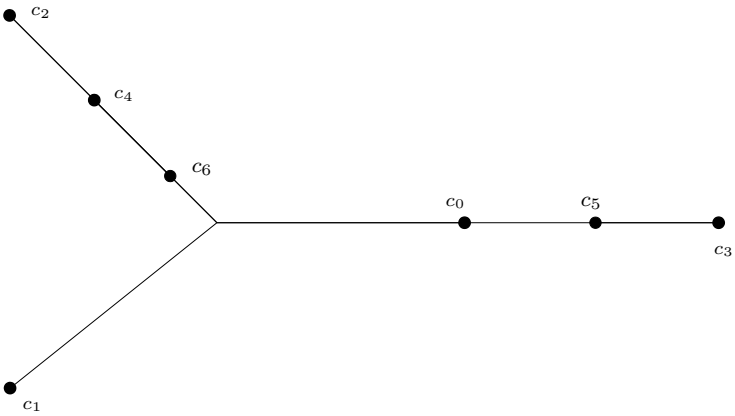

Figure C.35: Hubbard tree for $1 \to 3 \to 5 \to 7$, c.d = 9

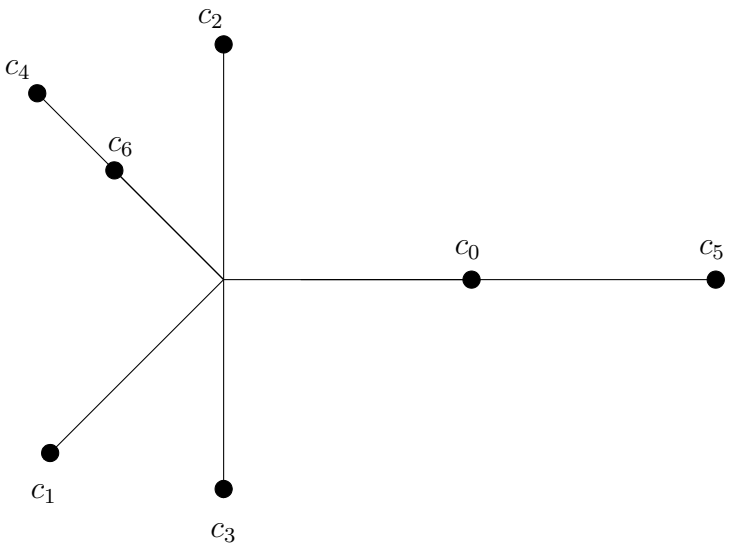

Figure C.36: Hubbard tree for $1 \to 5 \to 7$, c.d = 11

Appendix D

Hubbard trees for the period 2 cluster case

D.1 Period 4

D.1.1 Rotation number 1

Figure D.1: Hubbard tree for $1 \to 2 \to 4$, rotation number 1

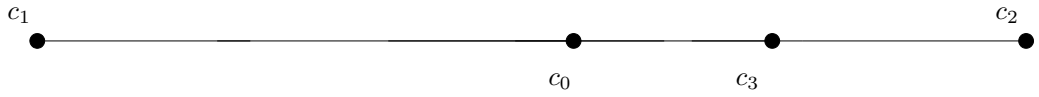

Figure D.2: Hubbard tree for $1 \to 2 \to 3 \to 4$, rotation number 1

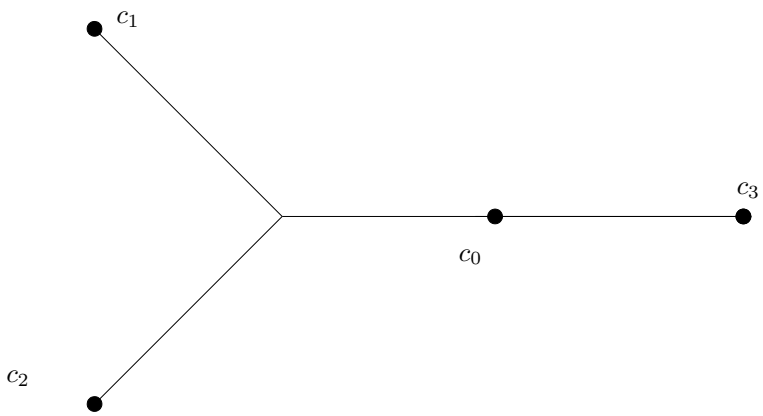

Figure D.3: Hubbard tree for $1_{1/3} \to 3 \to 4$,c.d=1.

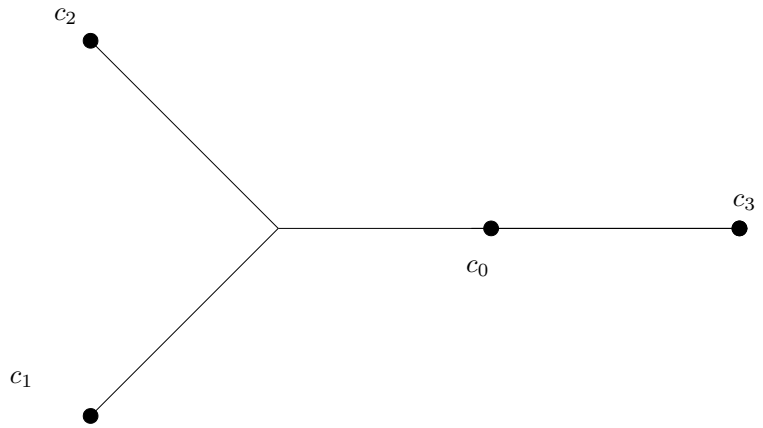

Figure D.4: Hubbard tree for $1_{2/3} \to 3 \to 4$,c.d=3.

D.2 Period 6

D.2.1 Rotation number 1

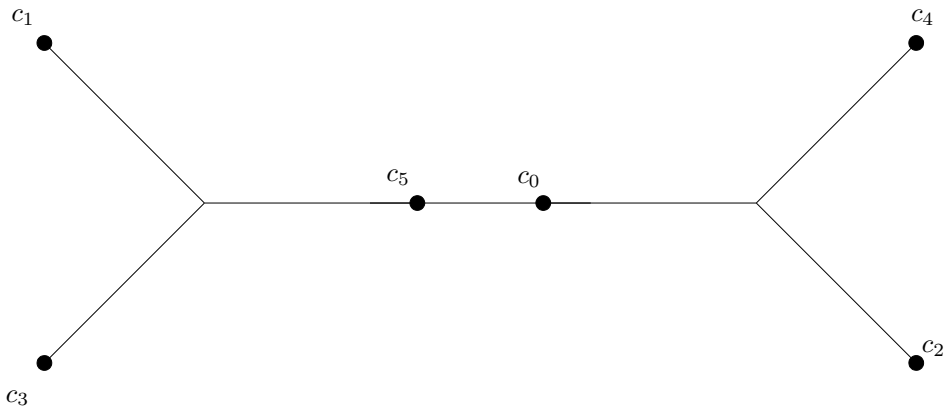

Figure D.5: Hubbard tree for $1 \to 2 \to 6$, rotation number 1

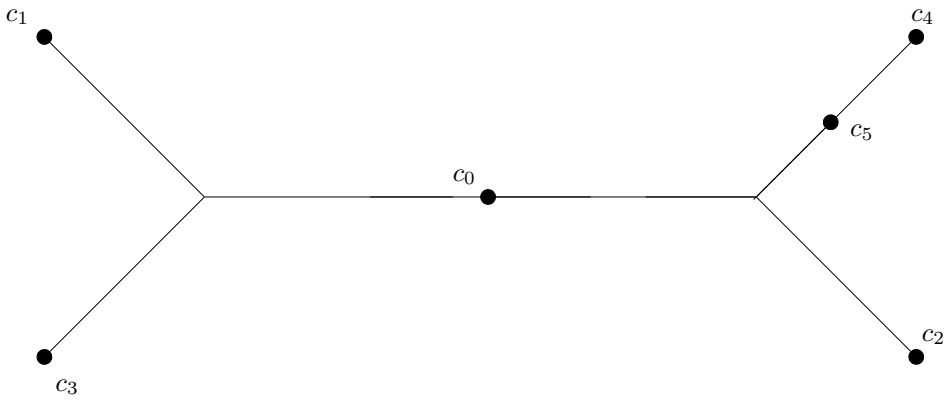

Figure D.6: Hubbard tree for $1 \to 2 \to 5 \to 6$, rotation number 1

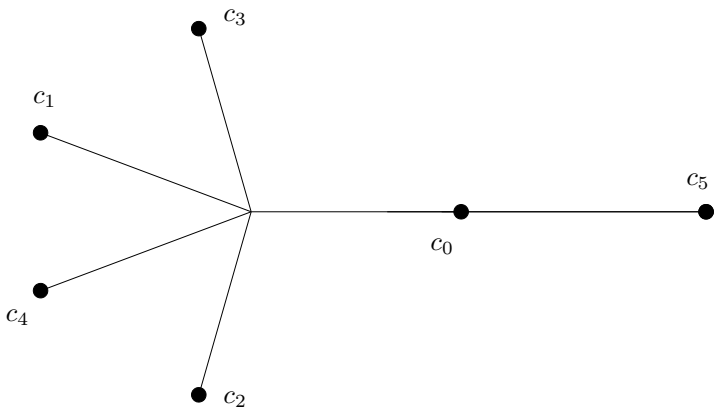

Figure D.7: Hubbard tree for $1 \to 5 \to 6$,c.d=1.

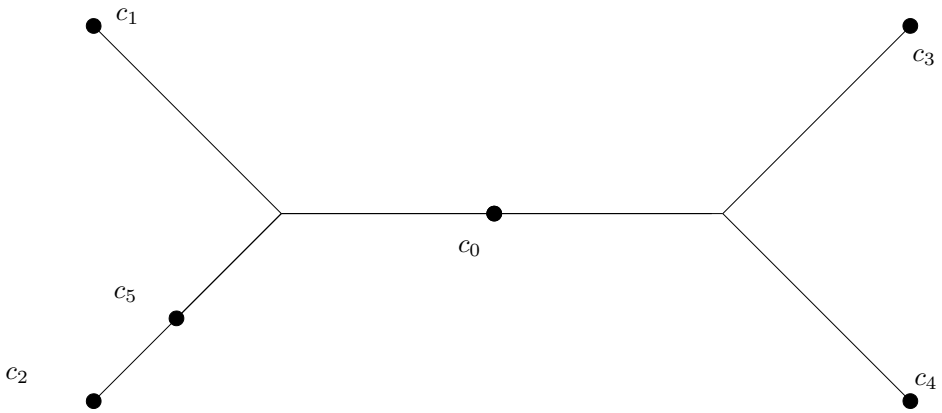

Figure D.8: Hubbard tree for $1 \to 3 \to 4 \to 6$,c.d=3.

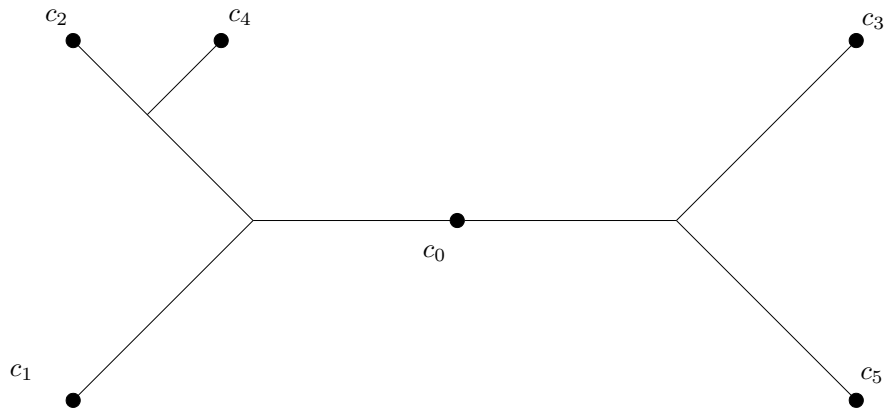

Figure D.9: Hubbard tree for $1 \to 3 \to 5 \to 7 \to 8$,c.d=5.

D.3 Period 8

D.3.1 Rotation number 1

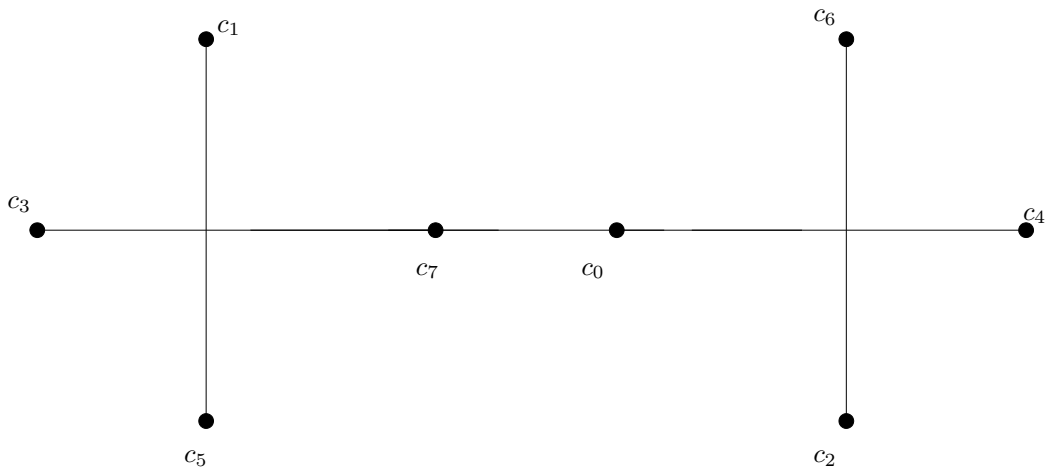

Figure D.10: Hubbard tree for $1 \to 2 \to 8$, rotation number 1

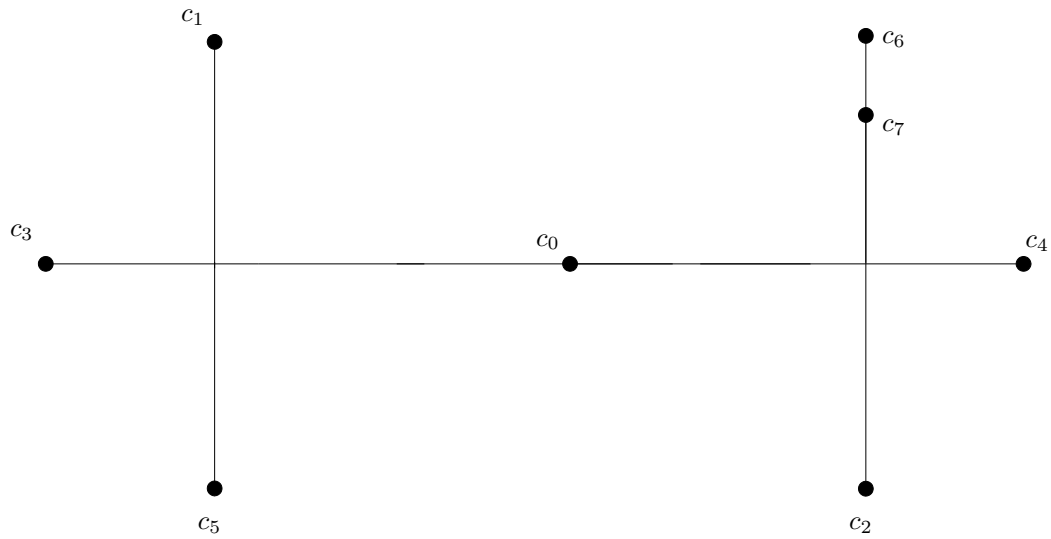

Figure D.11: Hubbard tree for $1 \to 2 \to 7 \to 8$, rotation number 1

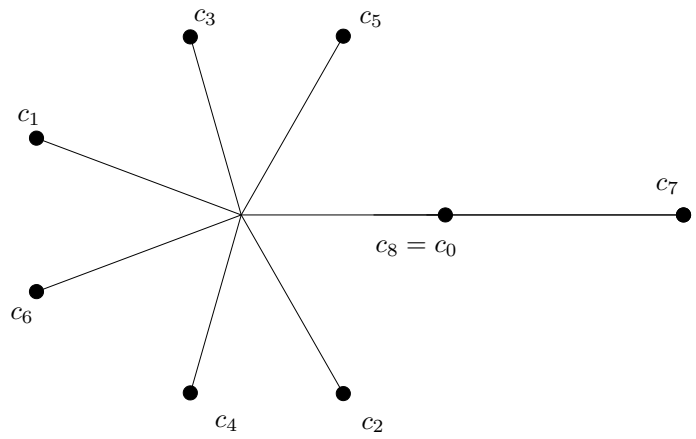

Figure D.12: Hubbard tree for $1 \to 7 \to 8$,c.d=1.

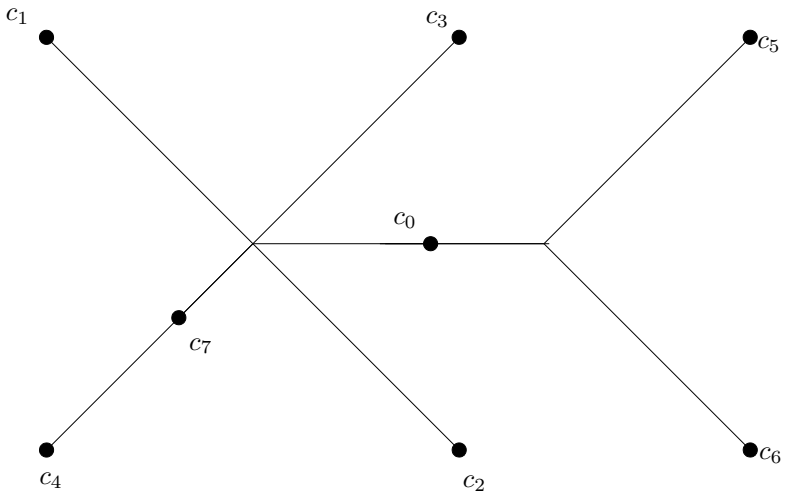

Figure D.13: Hubbard tree for $1 \to 5 \to 6 \to 8$,c.d=3.

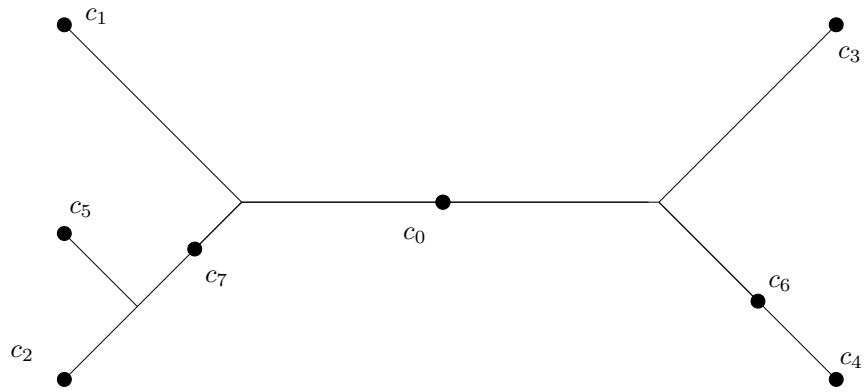

Figure D.14: Hubbard tree for $1 \to 3 \to 4 \to 6 \to 8$,c.d=5.

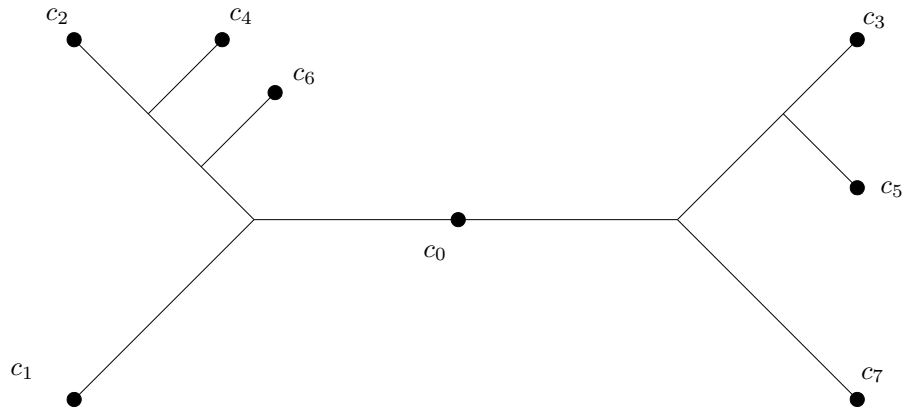

Figure D.15: Hubbard tree for $1 \to 3 \to 5 \to 7 \to 8$,c.d=7.

D.4 Period 10

D.4.1 Rotation number 1

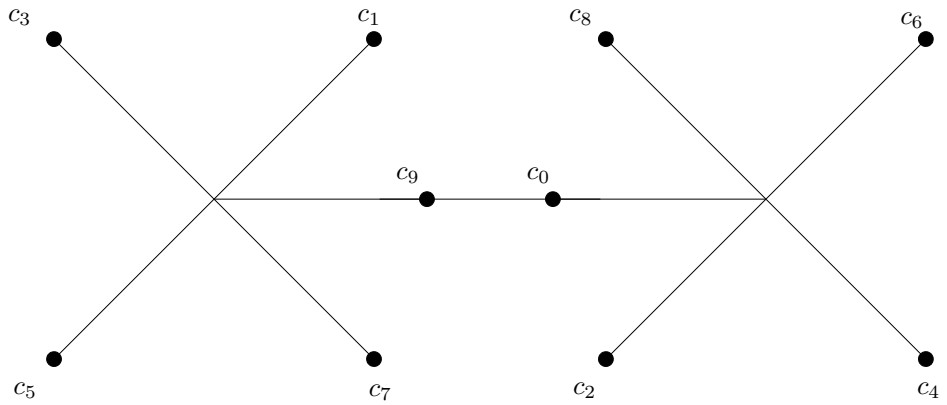

Figure D.16: Hubbard tree for $1 \to 2 \to 10$, rotation number 1

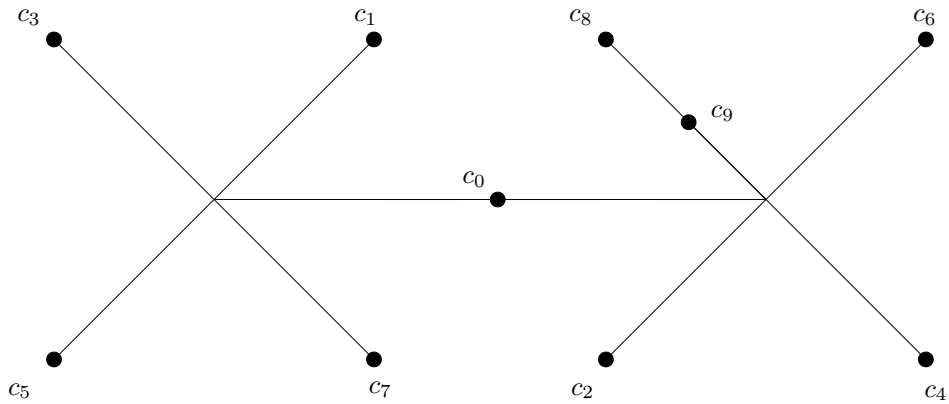

Figure D.17: Hubbard tree for $1 \to 2 \to 9 \to 10$, rotation number 1

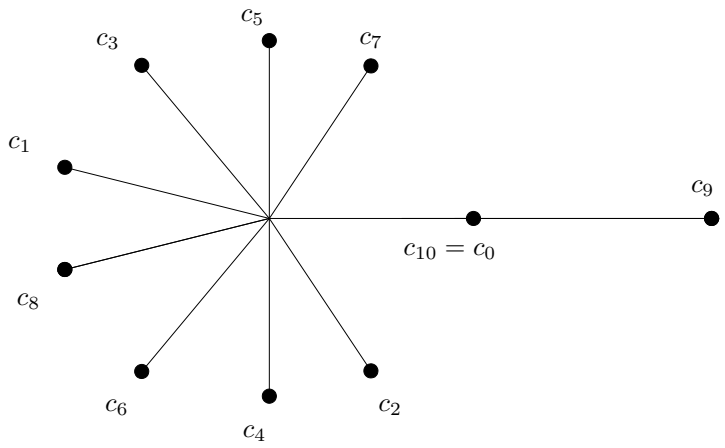

Figure D.18: Hubbard tree for $1 \to 9 \to 10$,c.d=1.

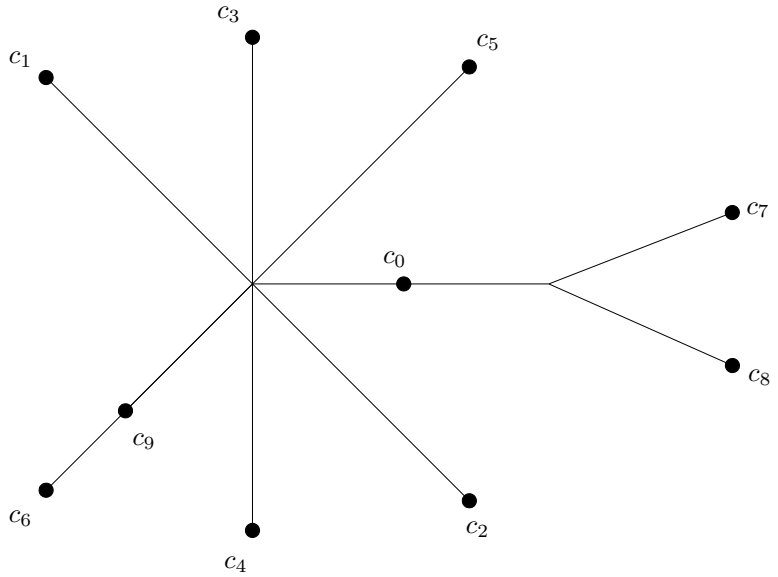

Figure D.19: Hubbard tree for $1 \to 7 \to 8 \to 10$,c.d=3.

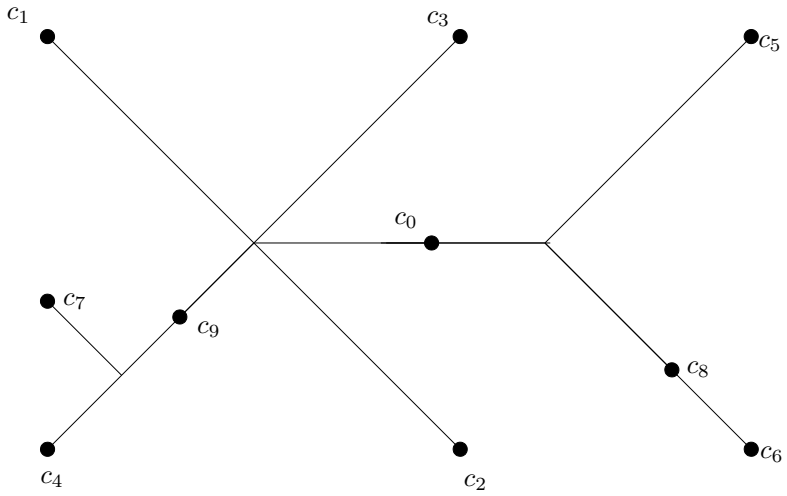

Figure D.20: Hubbard tree for $1 \to 5 \to 6 \to 8 \to 10$,c.d=5.

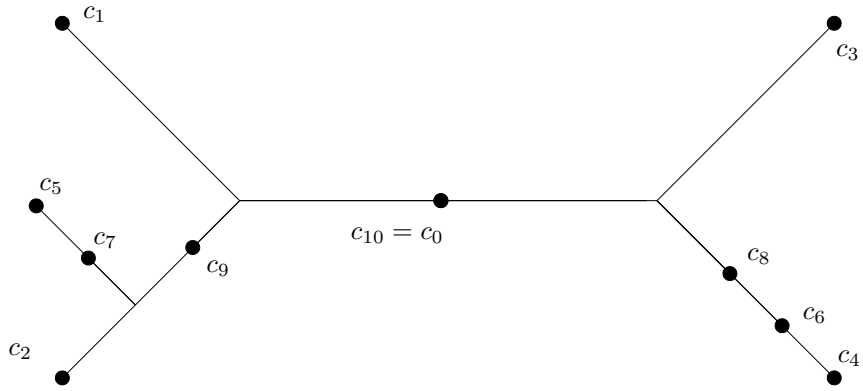

Figure D.21: Hubbard tree for $1 \to 3 \to 4 \to 6 \to 8 \to 10$,c.d=7.

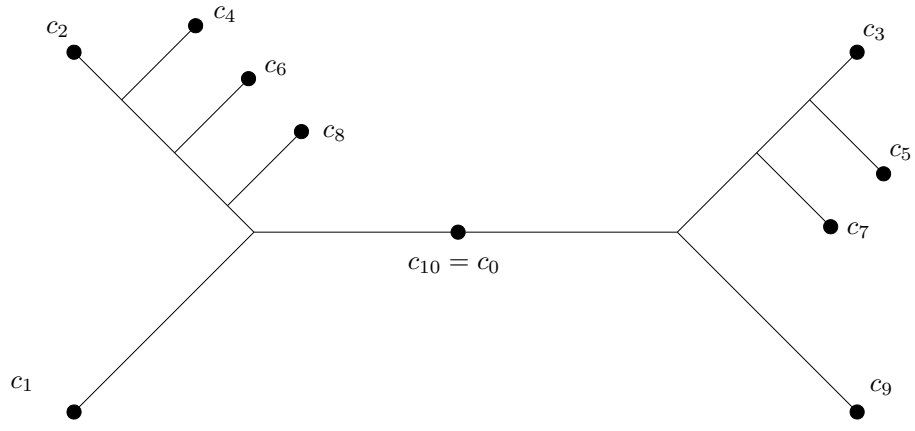

Figure D.22: Hubbard tree for $1 \to 3 \to 5 \to 7 \to 9 \to 10$,c.d=9.

D.4.2 Rotation number 2

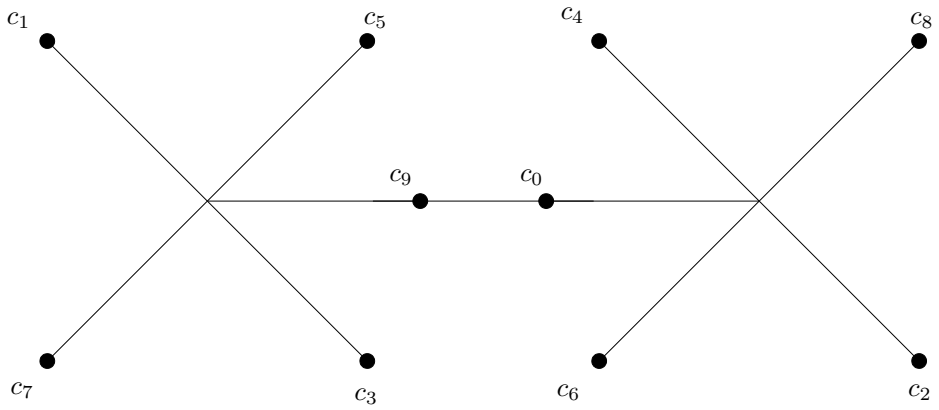

Figure D.23: Hubbard tree for $1 \to 2 \to 10$, rotation number 2

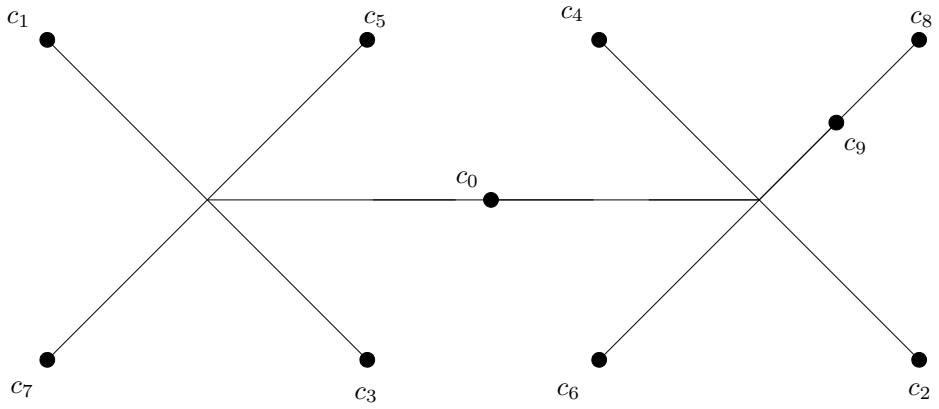

Figure D.24: Hubbard tree for $1 \to 2 \to 9 \to 10$, rotation number 2

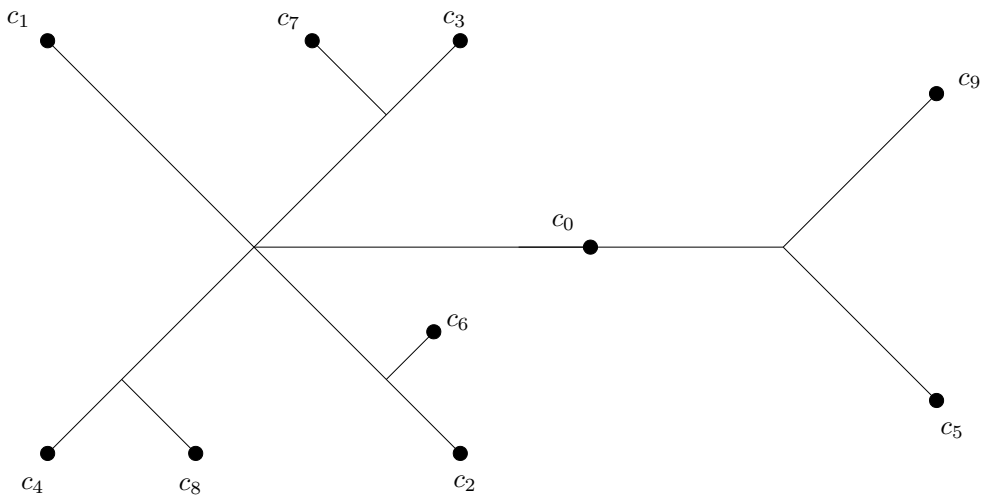

Figure D.25: Hubbard tree for $1 \to 5 \to 9 \to 10$,c.d=1.

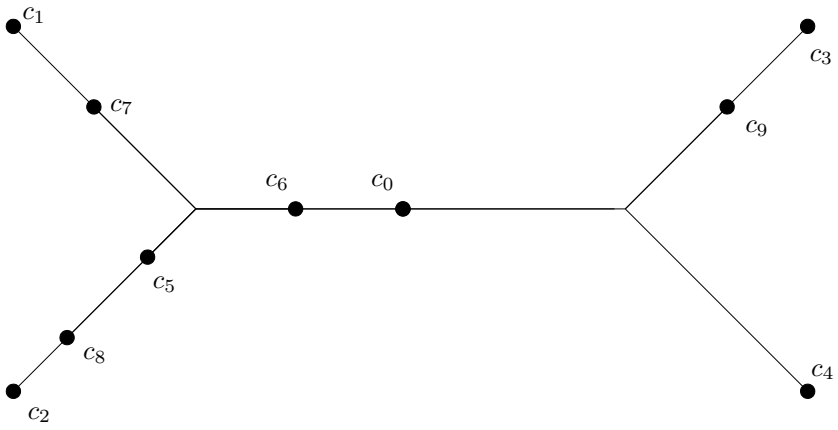

Figure D.26: Hubbard tree for $1 \to 3 \to 4 \to 7 \to 9 \to 10$,c.d=3.

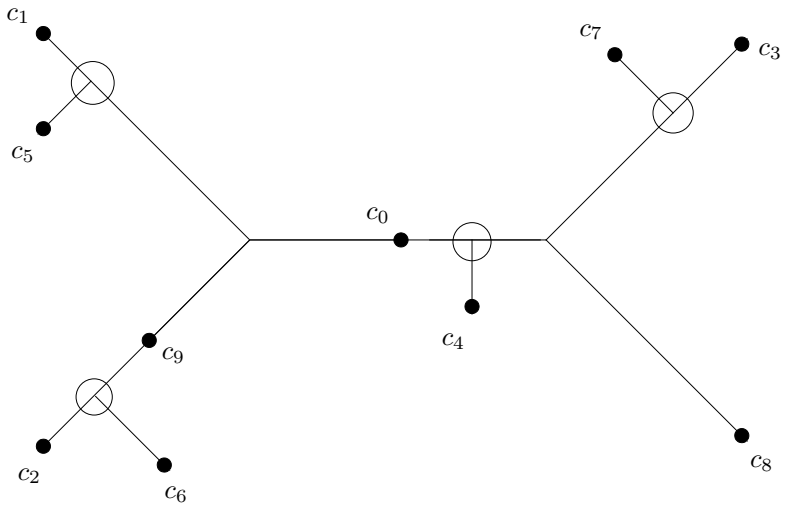

Figure D.27: Hubbard tree for $1 \to 3 \to 4 \to 10$,c.d=5.

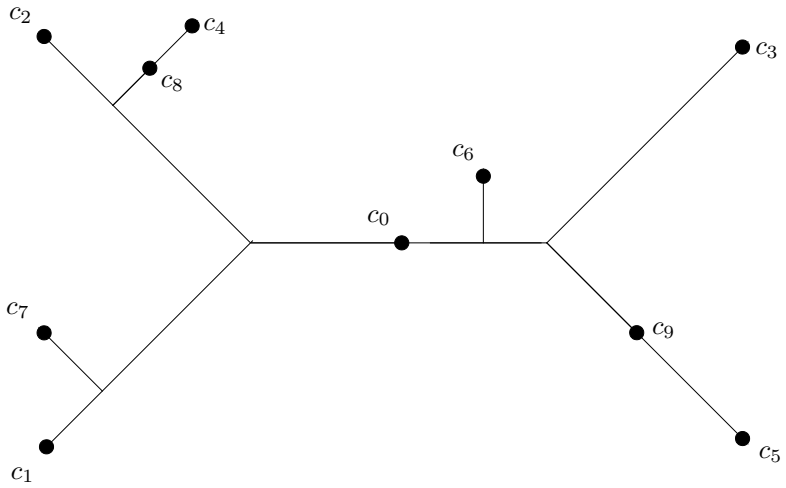

Figure D.28: Hubbard tree for $1 \to 3 \to 5 \to 6 \to 10$,c.d=7.

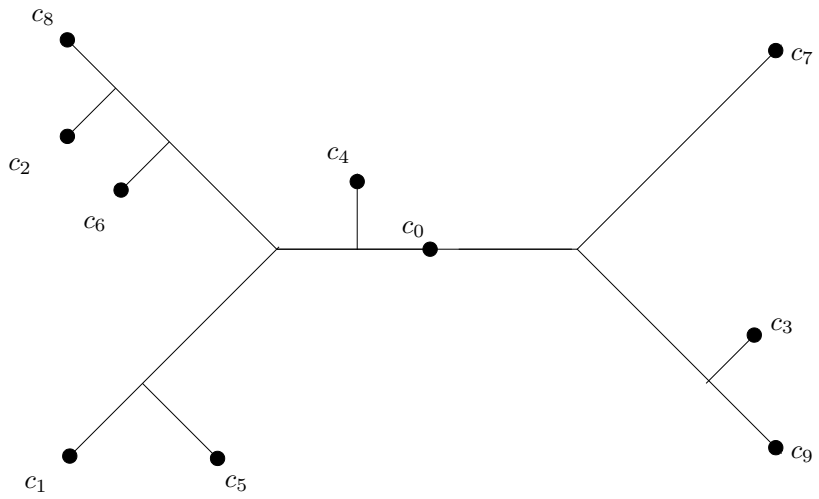

Figure D.29: Hubbard tree for $1 \to 3 \to 6 \to 7 \to 9 \to 10$,c.d=9.

D.5 Period 12

D.5.1 Rotation number 1

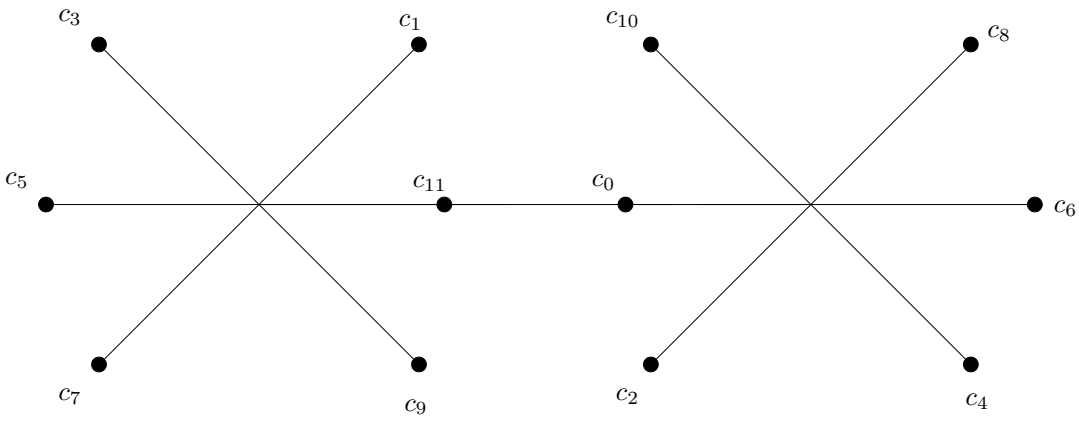

Figure D.30: Hubbard tree for $1 \to 2 \to 12$, rotation number 1

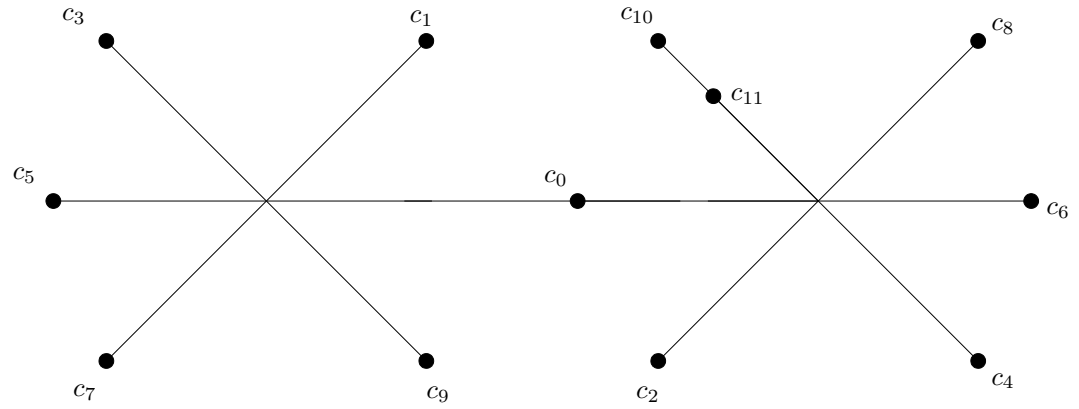

Figure D.31: Hubbard tree for $1 \to 2 \to 11 \to 12$, rotation number 1

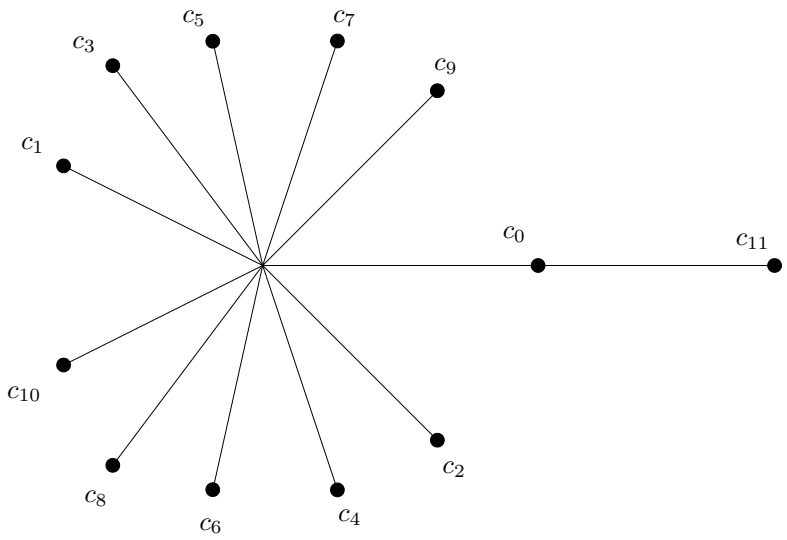

Figure D.32: Hubbard tree for $1 \to 11 \to 12$,c.d=1.

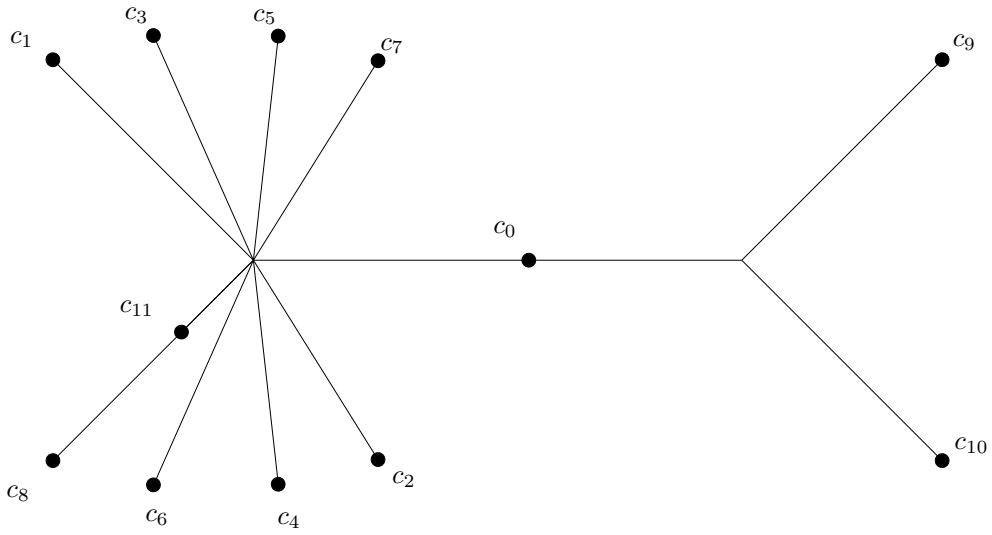

Figure D.33: Hubbard tree for $1 \to 9 \to 10 \to 12$,c.d=3.

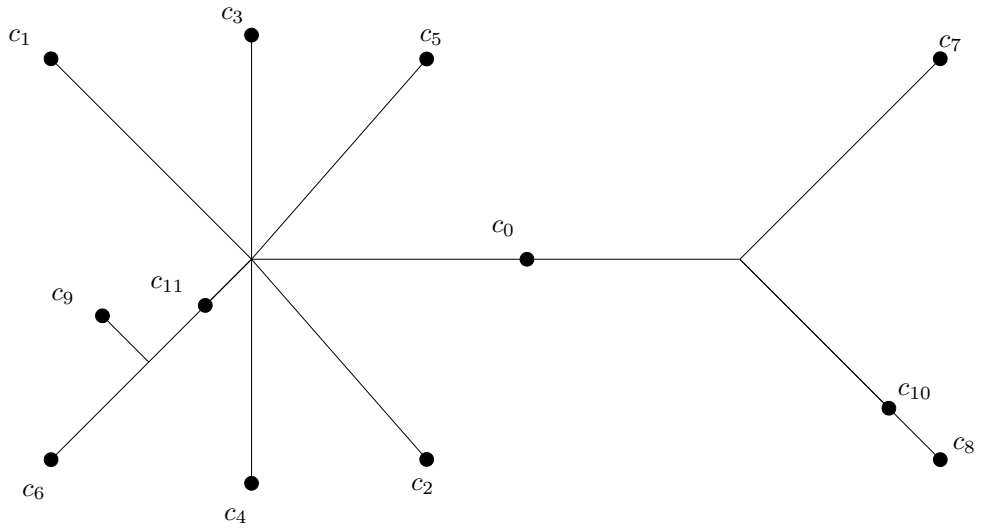

Figure D.34: Hubbard tree for $1 \to 7 \to 8 \to 10 \to 12$,c.d=5.

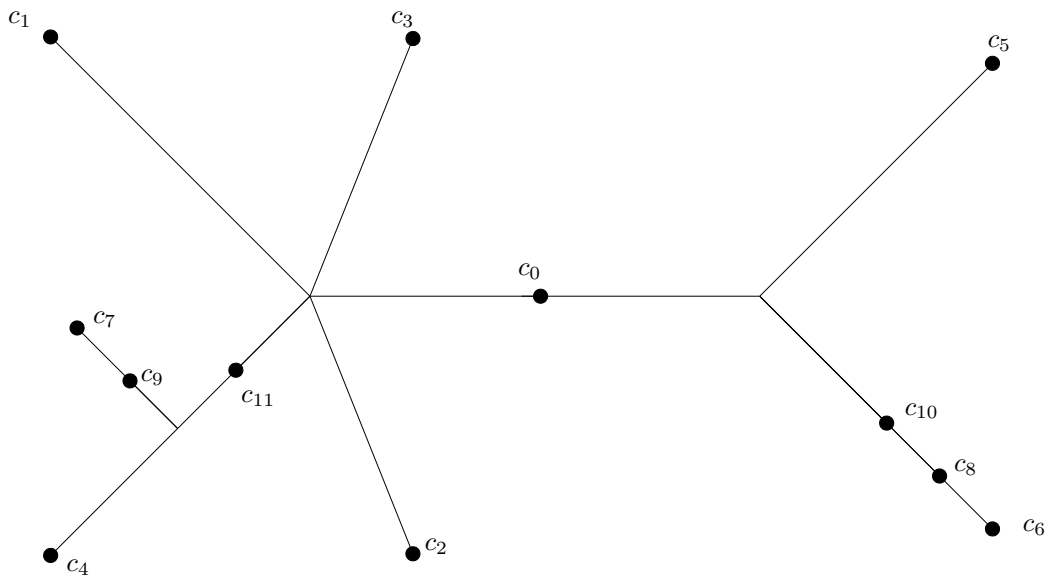

Figure D.35: Hubbard tree for $1 \to 5 \to 6 \to 8 \to 10 \to 12$,c.d=7.

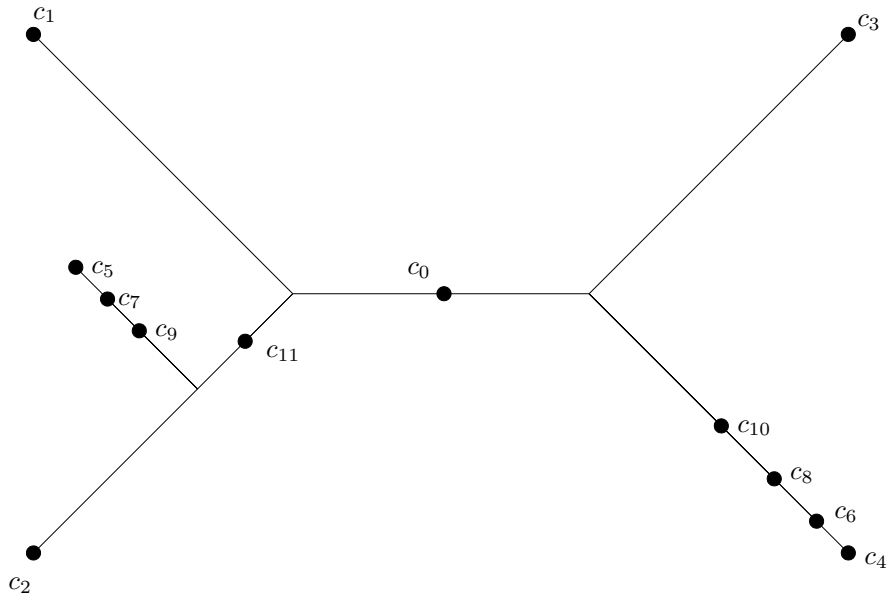

Figure D.36: Hubbard tree for $1 \to 3 \to 4 \to 6 \to 8 \to 10 \to 12$,c.d=9.

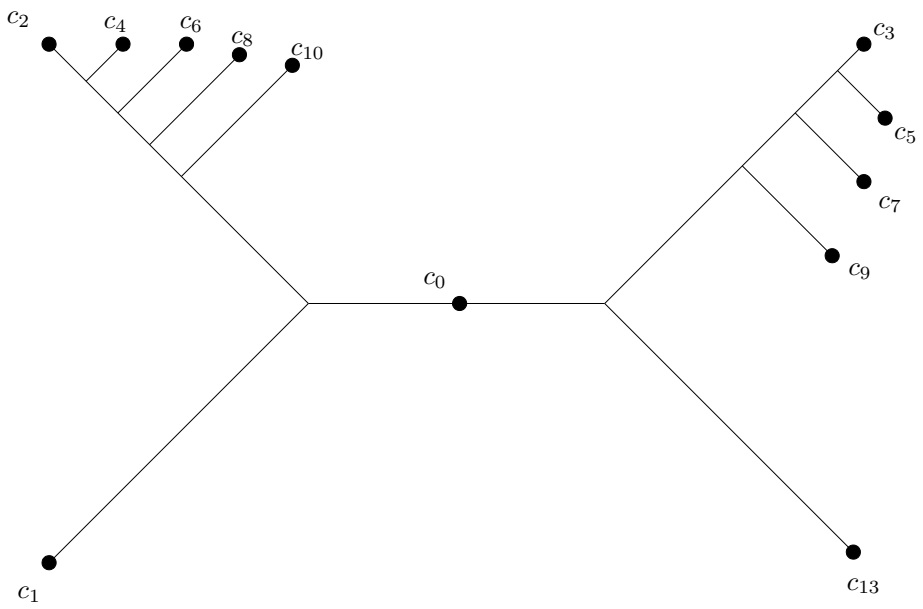

Figure D.37: Hubbard tree for $1 \to 3 \to 5 \to 7 \to 9 \to 11 \to 12$,c.d=11.

D.6 Period 14

D.6.1 Rotation number 1

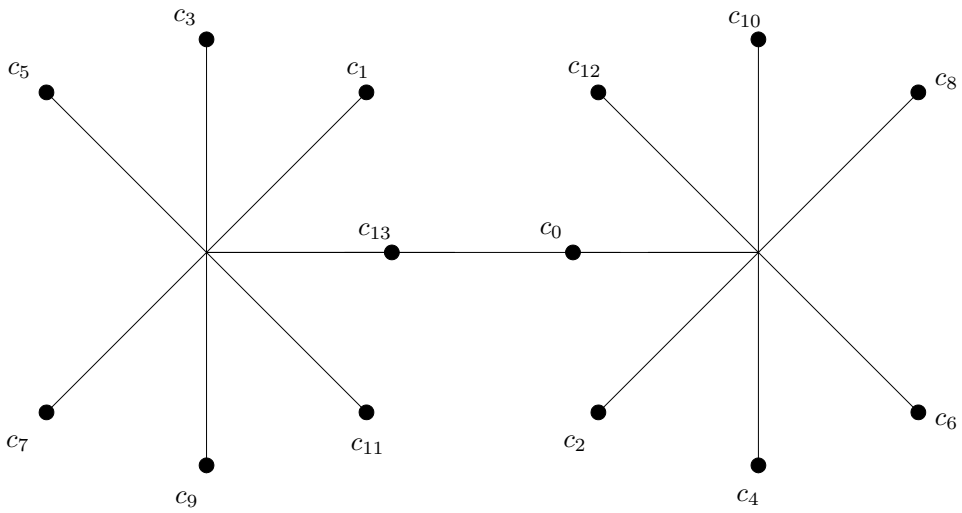

Figure D.38: Hubbard tree for $1 \to 2 \to 14$, rotation number 1

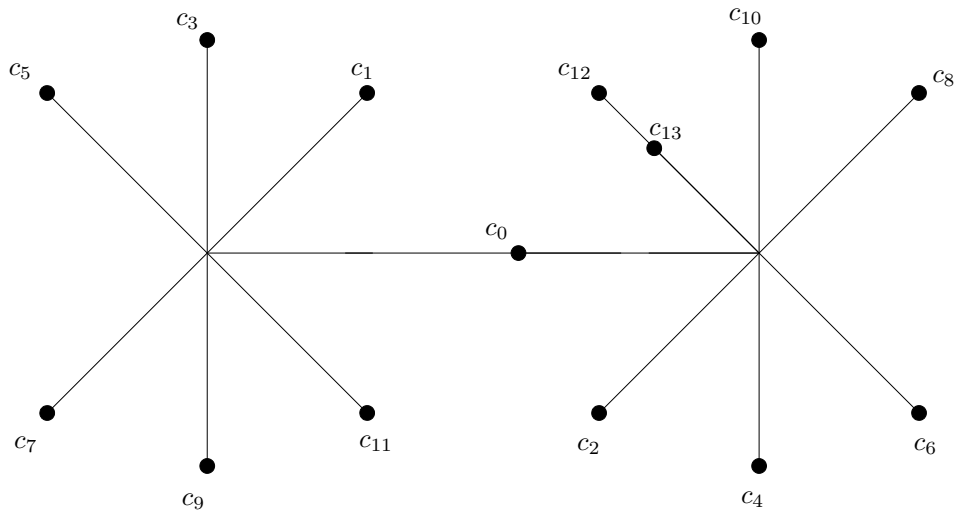

Figure D.39: Hubbard tree for $1 \to 2 \to 13 \to 14$, rotation number 1

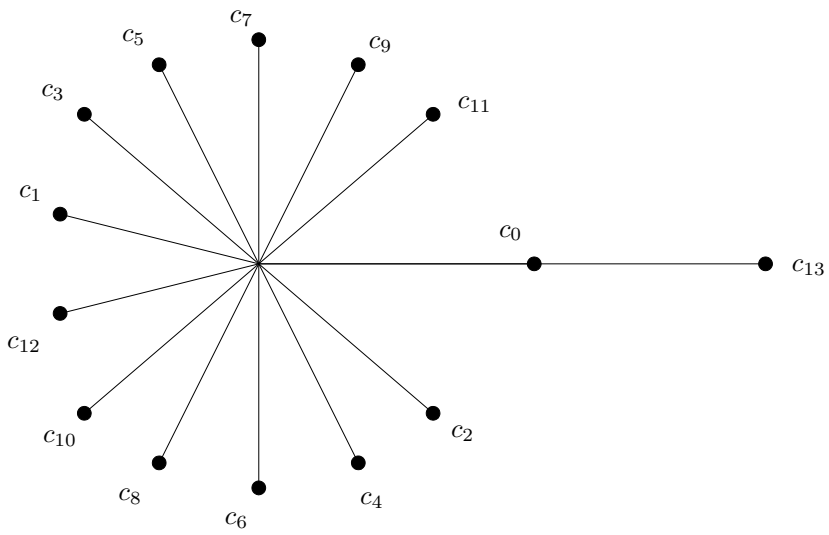

Figure D.40: Hubbard tree for $1 \to 13 \to 14$,c.d=1.

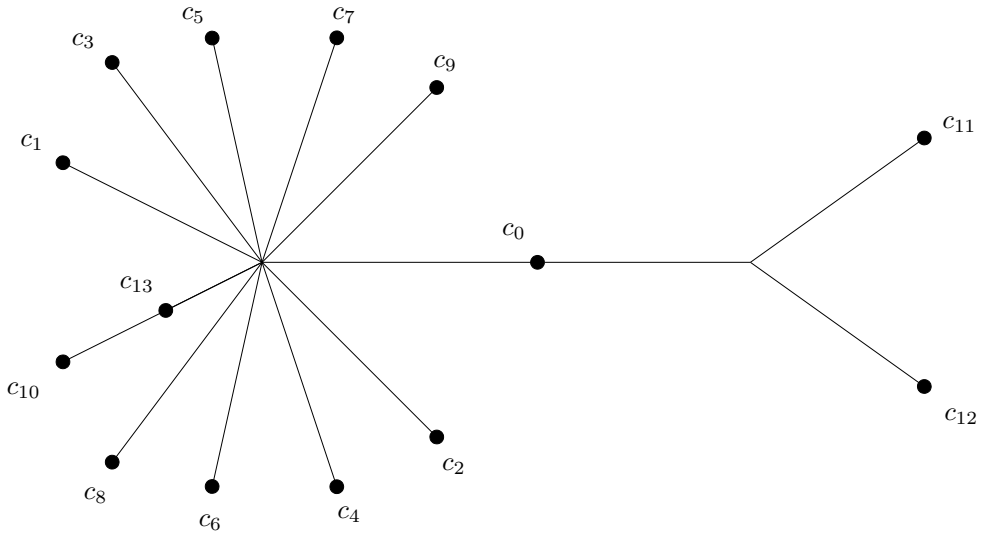

Figure D.41: Hubbard tree for $1 \to 11 \to 12 \to 14$,c.d=3.

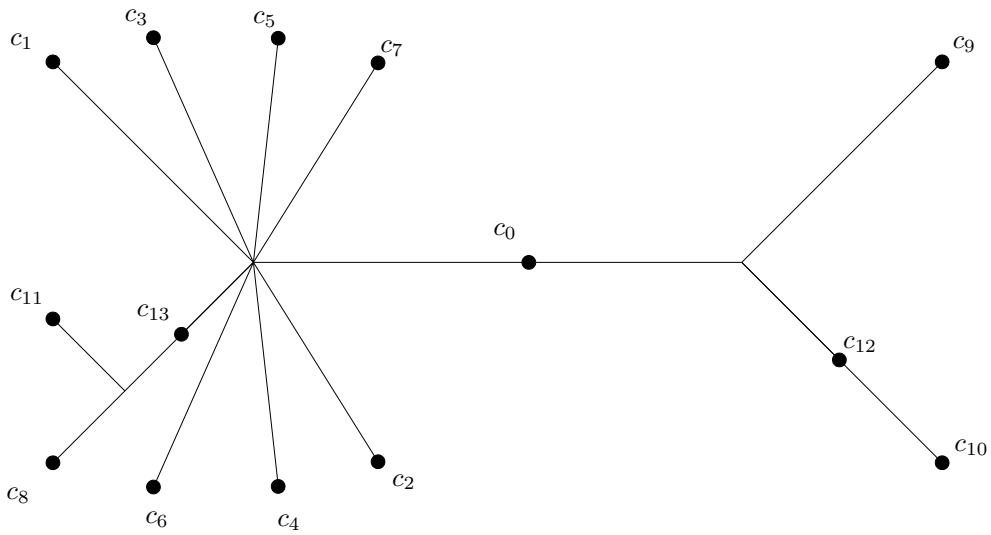

Figure D.42: Hubbard tree for $1 \to 9 \to 10 \to 12 \to 14$,c.d=5.

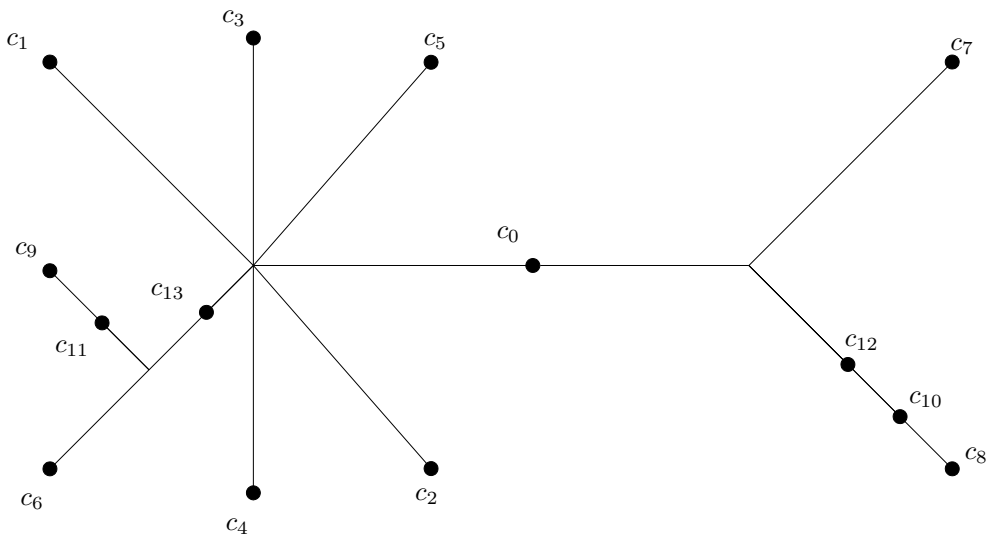

Figure D.43: Hubbard tree for $1 \to 7 \to 8 \to 10 \to 12 \to 14$,c.d=7.

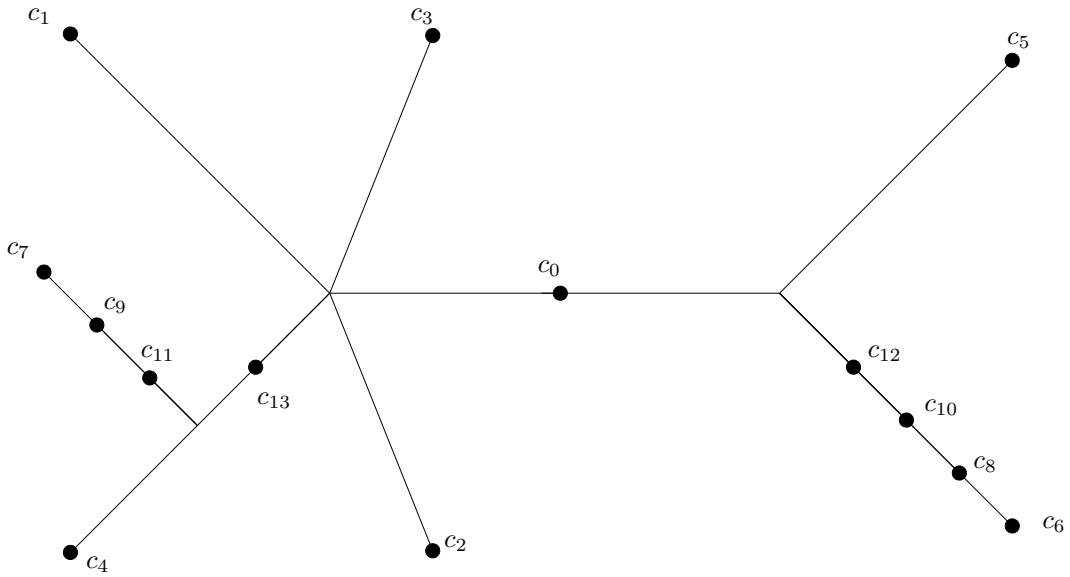

Figure D.44: Hubbard tree for $1 \to 5 \to 6 \to 8 \to 10 \to 12 \to 14$,c.d=9.

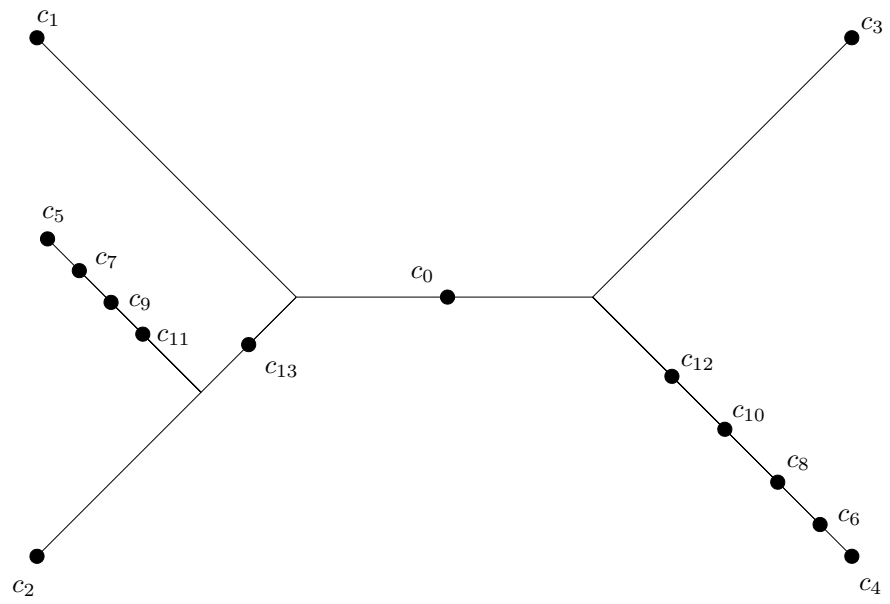

Figure D.45: Hubbard tree for $1 \to 3 \to 4 \to 6 \to 8 \to 10 \to 12 \to 14$,c.d=11.

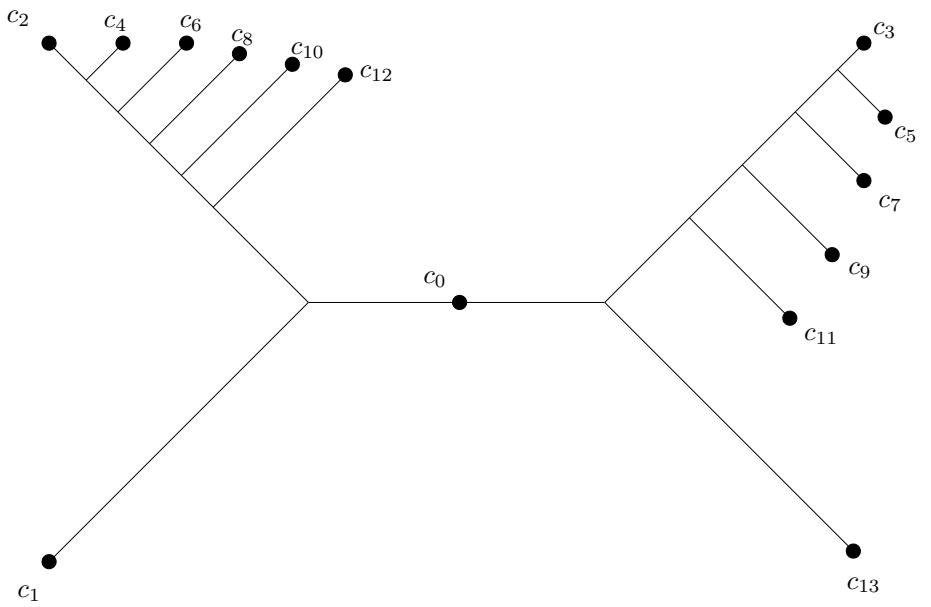

Figure D.46: Hubbard tree for $1 \to 3 \to 5 \to 7 \to 9 \to 11 \to 13 \to 14$,c.d=13.

D.6.2 Rotation number 2

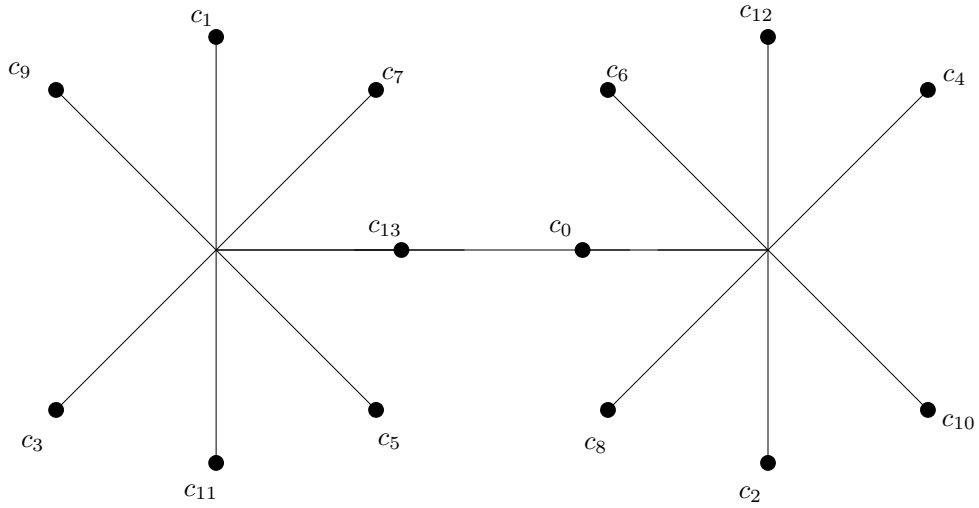

Figure D.47: Hubbard tree for $1 \to 2 \to 14$, rotation number 2

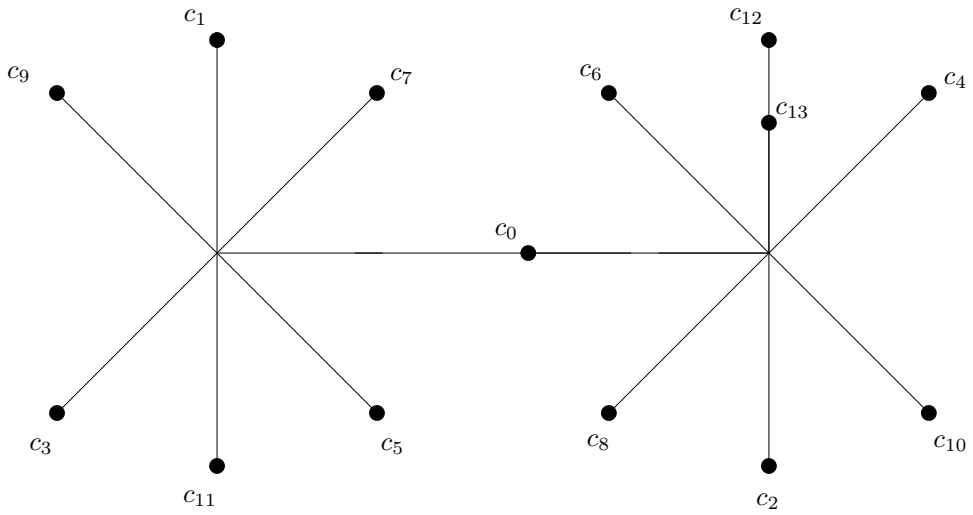

Figure D.48: Hubbard tree for $1 \to 2 \to 13 \to 14$, rotation number 2

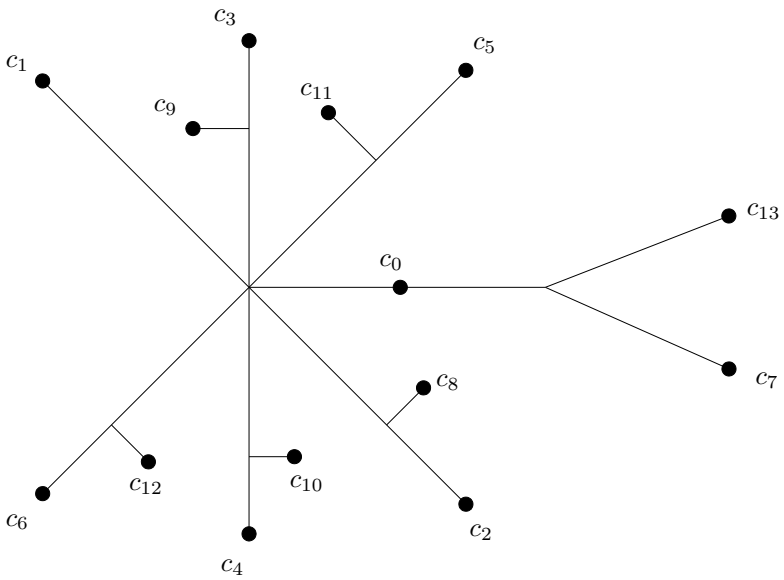

Figure D.49: Hubbard tree for $1 \to 7 \to 13 \to 14$,c.d=1.

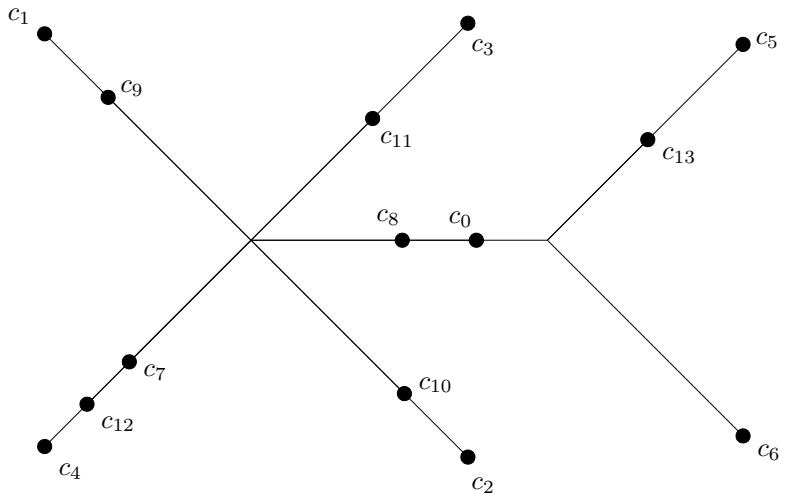

Figure D.50: Hubbard tree for $1 \to 5 \to 6 \to 11 \to 13 \to 14$,c.d=3.

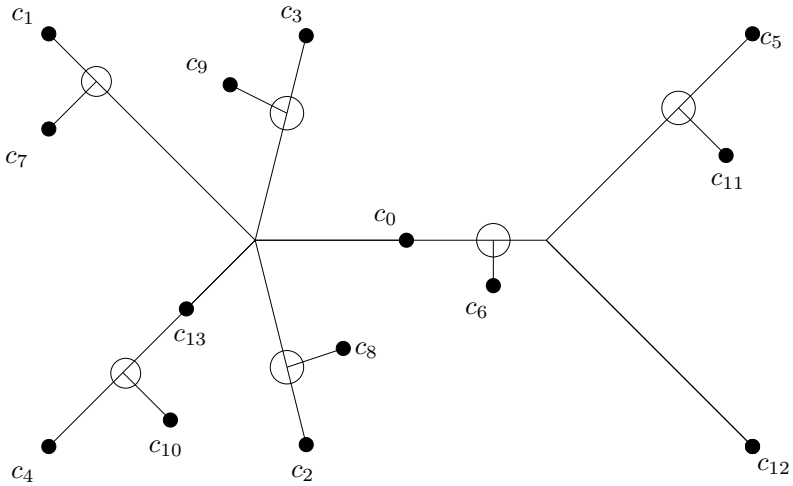

Figure D.51: Hubbard tree for $1 \to 5 \to 6 \to 14$,c.d=5.

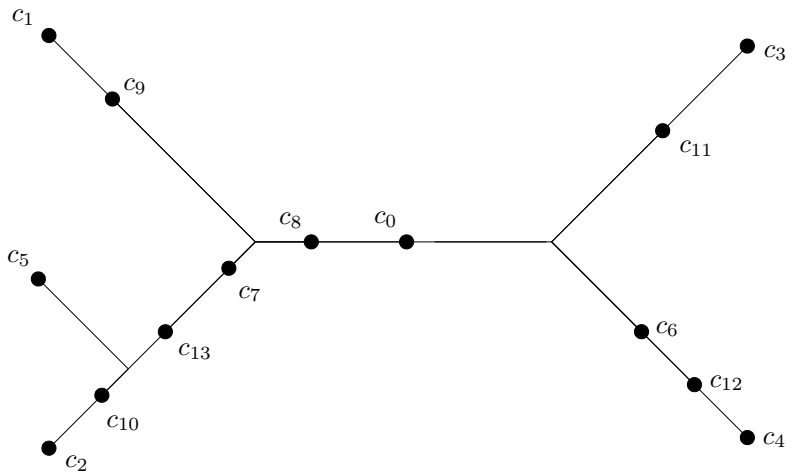

Figure D.52: Hubbard tree for $1 \to 3 \to 4 \to 6 \to 9 \to 11 \to 12 \to 14$,c.d=7.

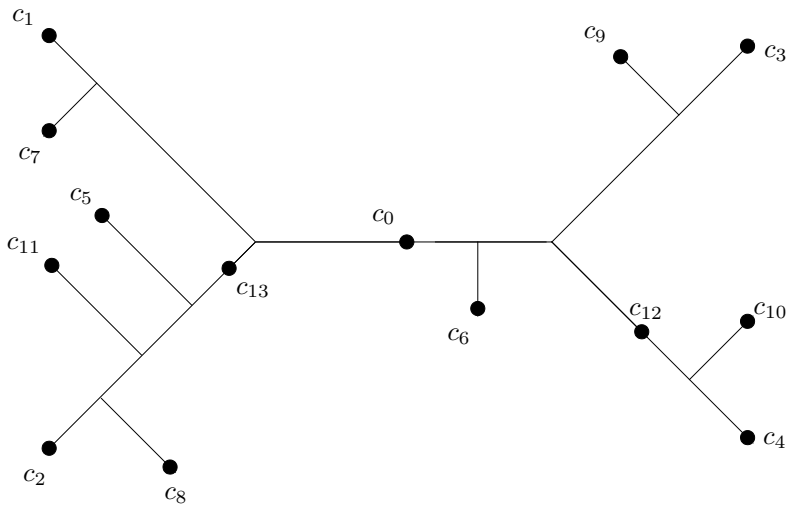

Figure D.53: Hubbard tree for $1 \to 3 \to 4 \to 6 \to 14$,c.d=9.

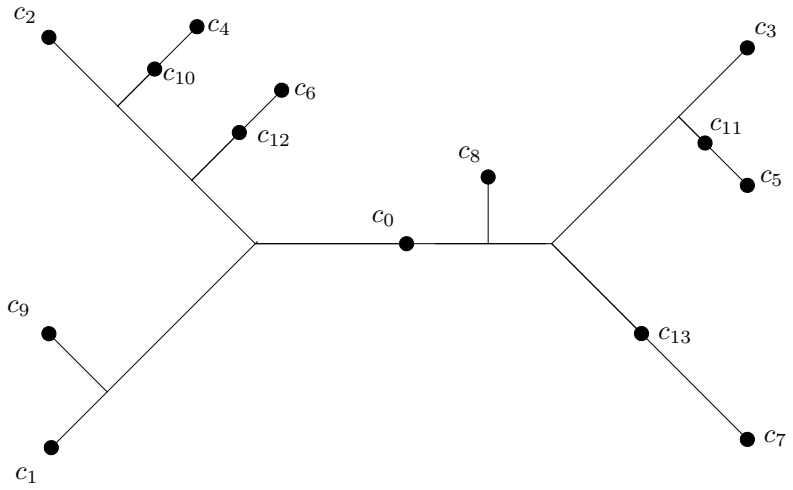

Figure D.54: Hubbard tree for $1 \to 3 \to 5 \to 7 \to 8 \to 14$,c.d=11.

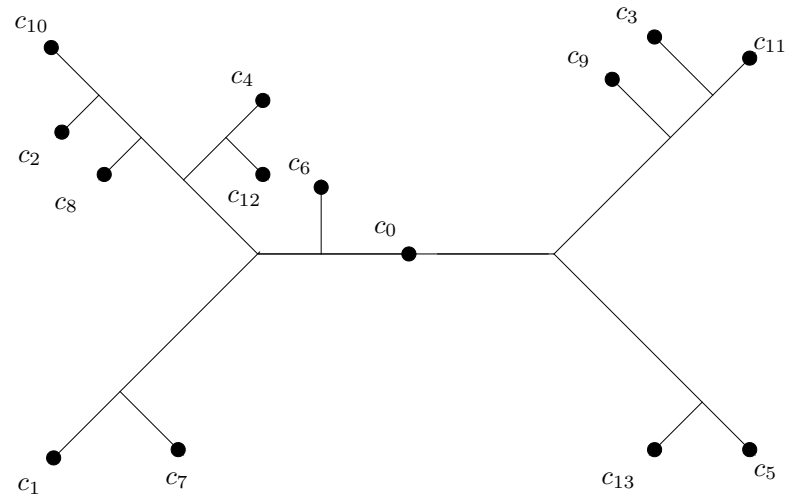

Figure D.55: Hubbard tree for $1 \to 3 \to 5 \to 8 \to 9 \to 11 \to 13 \to 14$,c.d=13.

D.6.3 Rotation number 3

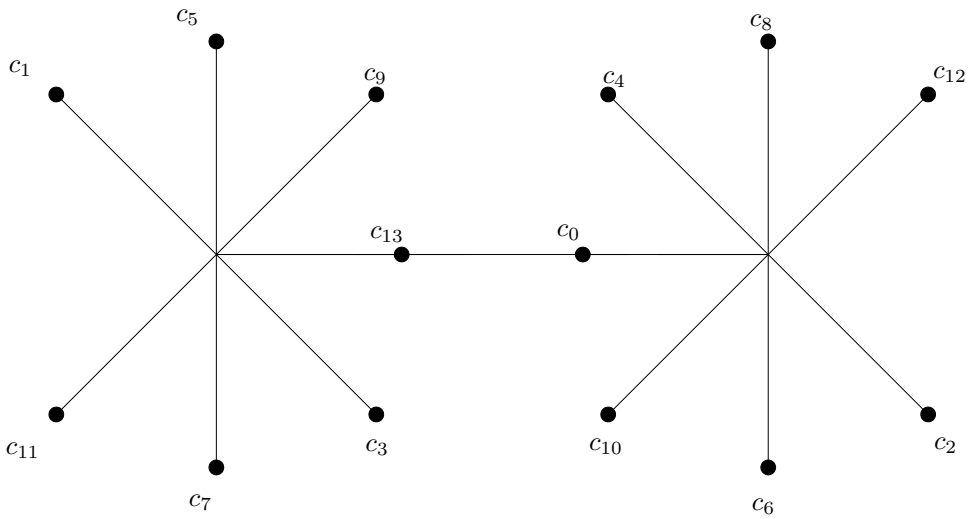

Figure D.56: Hubbard tree for $1 \to 2 \to 14$, rotation number 3

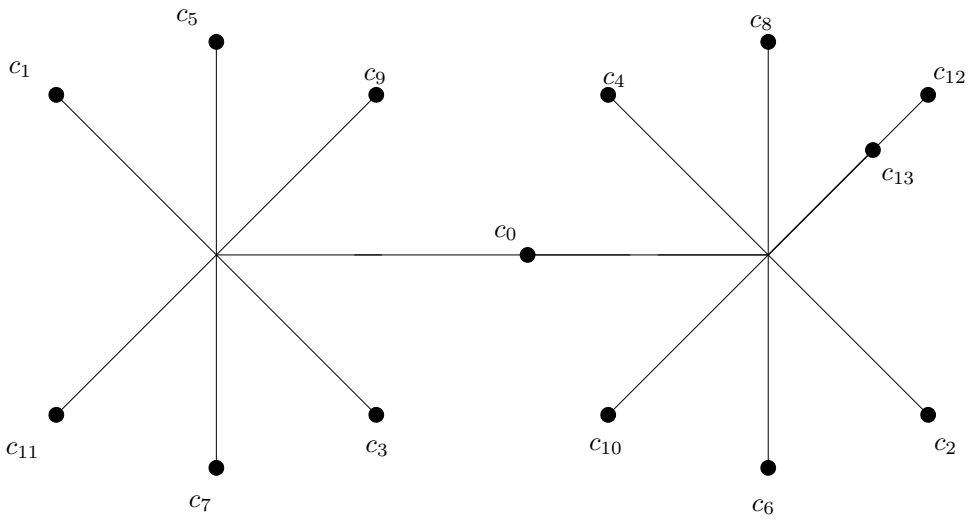

Figure D.57: Hubbard tree for $1 \to 2 \to 13 \to 14$, rotation number 3

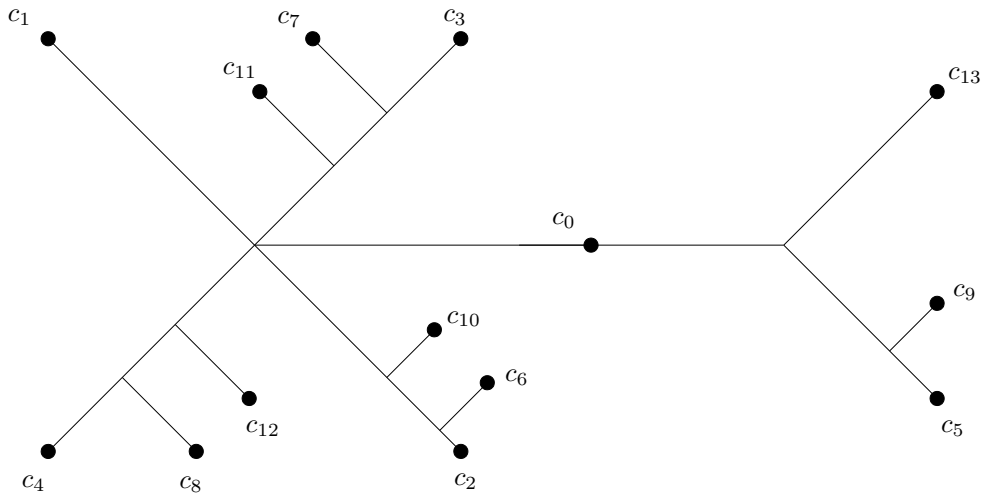

Figure D.58: Hubbard tree for $1 \to 5 \to 9 \to 13 \to 14$,c.d=1.

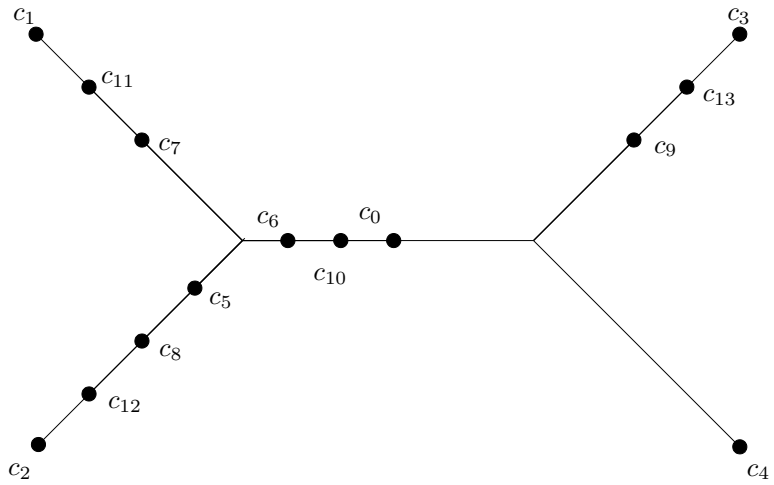

Figure D.59: Hubbard tree for $1 \to 3 \to 4 \to 7 \to 9 \to 12 \to 13 \to 14$,c.d=3.

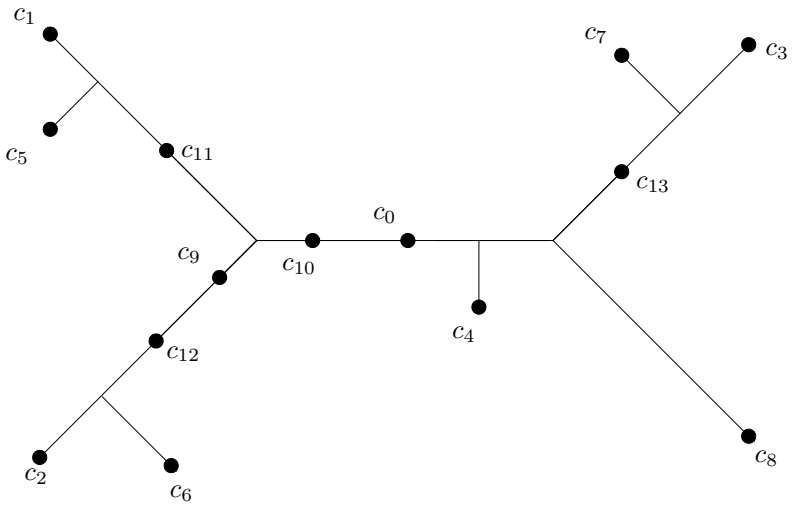

Figure D.60: Hubbard tree for $1 \to 3 \to 4 \to 11 \to 13 \to 14$,c.d=5.

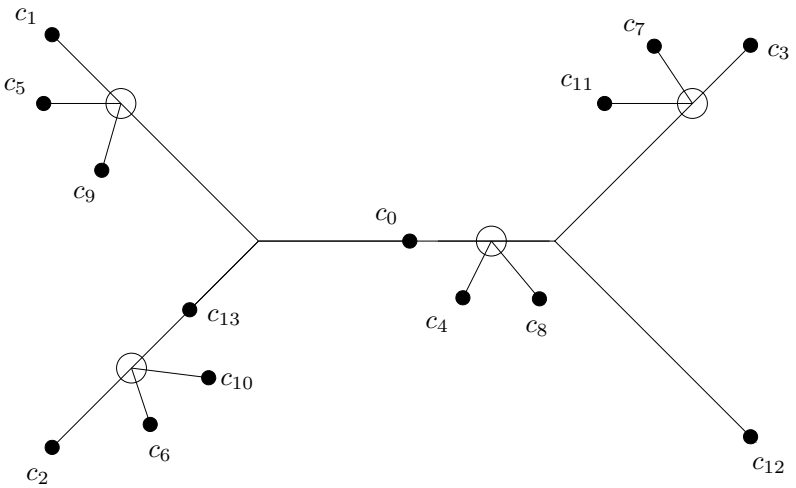

Figure D.61: Hubbard tree for $1 \to 3 \to 4 \to 14$,c.d=7.

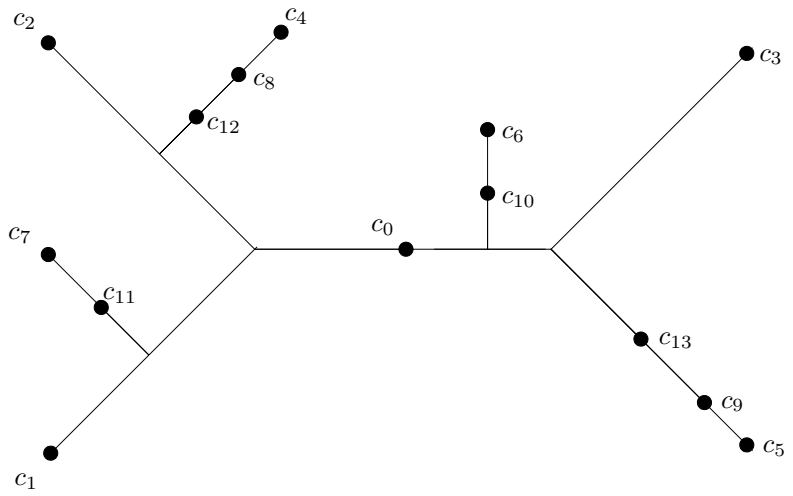

Figure D.62: Hubbard tree for $1 \to 3 \to 5 \to 6 \to 10 \to 14$,c.d=9.

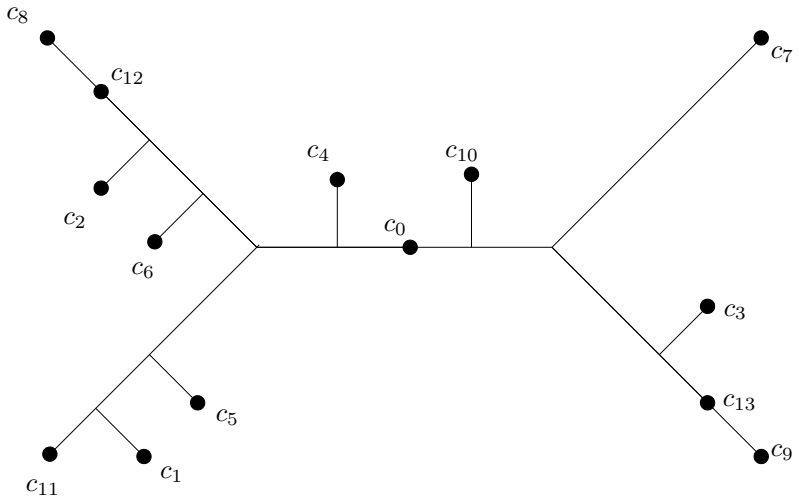

Figure D.63: Hubbard tree for $1 \to 3 \to 6 \to 7 \to 9 \to 10 \to 14$,c.d=11.

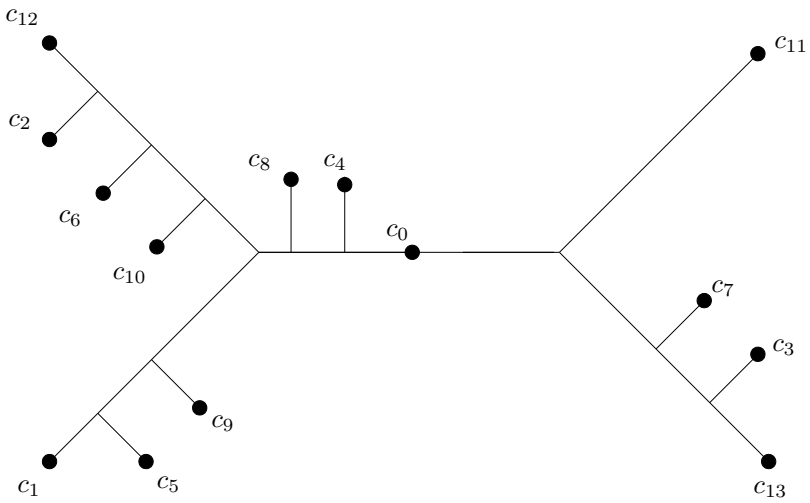

Figure D.64: Hubbard tree for $1 \to 3 \to 6 \to 7 \to 10 \to 11 \to 13 \to 14$,c.d=13.

Appendix E

The Period 2 Case in Higher Degrees

Recall that in Chapter 4, we made no assumptions about the degree of the maps that have fixed cluster points. In constrast, we restricted ourselves to the quadratic case in the period two cluster cycle case in Chapter 5. In this section we will give examples that show that some of the results from Chapter 5 cannot be generalised to higher periods.

Recall that Theorem 5.1.1 stated that, if $F = f_1 \amalg f_2$ has a period two cluster cycle, precisely one of the f_i can belong to $\mathcal{M}_{(1/3,2/3)}$, meaning only one of them lies beyond the period two component. The proof takes advantage of two facts from the quadratic case: firstly, there is only one period two component, and so if both maps lay beyond the period two component then the mating would be obstructed. Secondly, a quadratic rational map has exactly one period two cycle, meaning that the period two cycle has to become the cluster cycle under mating.

We now remark that neither of these two facts is true when the degree is greater than two. Indeed, it is in fact possible that a mating in degree 3 can have both maps lying beyond the same period 2 hyperbolic component.

Example E.0.1. Let f_1 be the map corresponding to the angles $(11/80, 19/80)$ and let f_2 be the map corresponding to the angles $(22/80, 24/80)$. Then f_1 and f_2 both have superattracting orbits of period 4. The critical value component of f_2 has the rays of angle 22/80 and 24/80 landing at its principal root point, and the ray of angle 23/80 lands at its non-principal root. The relevant orbits under angle trebling are

$$11/80 \to 33/80 \to 19/80 \to 57/80 \to 11/80$$

and

$$23/80 \to 69/80 \to 47/80 \to 61/80 \to 23/80.$$

Then we have the following equivalences under the mating $f_1 \amalg f_2$.

$$\gamma_2(69/80) \sim \gamma_1(11/80) = \gamma_1(19/80) \sim \gamma_2(61/80) \tag{E.1}$$

and

$$\gamma_2(47/80) \sim \gamma_1(33/80) = \gamma_1(57/80) \sim \gamma_2(23/80). \tag{E.2}$$

So we see that the ray classes derived from equations (E.1) and (E.2) will give a period two cluster cycle. However, f_1 and f_2 both lie beyond the same period 2 component in the degree 3 multibrot set.

We include the pictures of the two Julia sets, along with the relevant external rays.

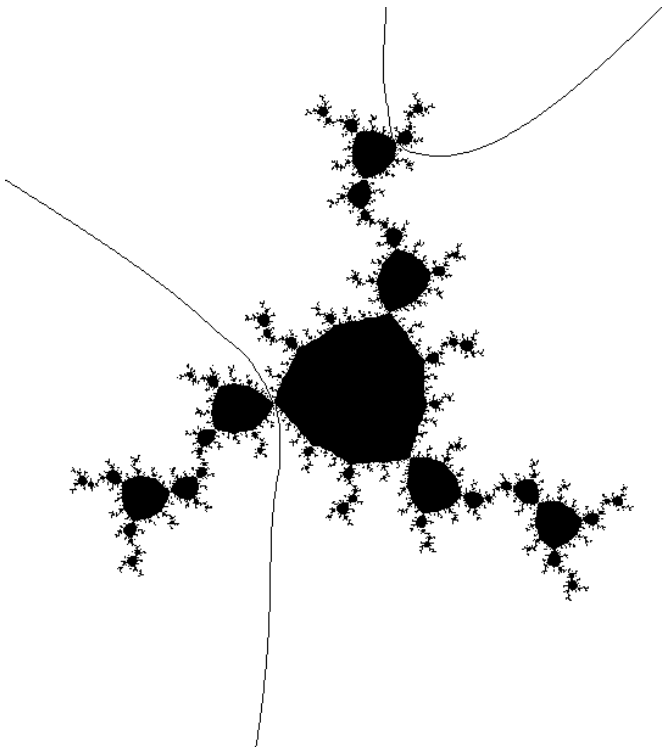

Figure E.1: The Julia set of the map f_1 with the external rays landing on the period two orbit that becomes the cluster cycle.

In the quadratic case, the only root points of critical orbit components are principal root points. Hence there cannot exist matings in the quadratic case where

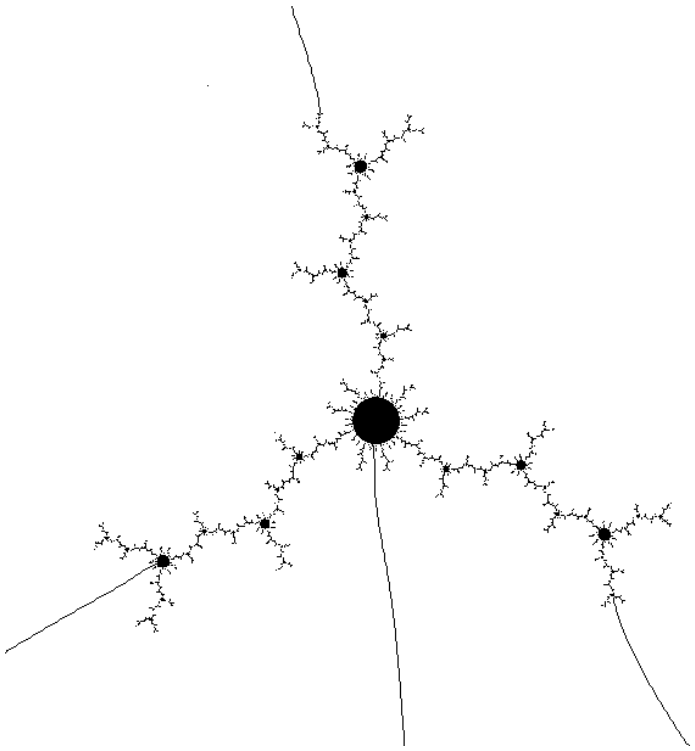

Figure E.2: The Julia set for f_2, the map which mates with f_1 to create a period 2 cycle. Note the external rays that have been drawn land at non-principal root points of the Fatou components.

non-principal root points become cluster points, as is the case in Example E.0.1. However, it is simple to show that at least one of the maps must belong to the wake of some period two component in parameter space, otherwise the resultant rational map will have too many period two cycles.

The combinatorial data for the map constructed in Example E.0.1 is $\rho = 1/2$ and $\delta = 3$. The same combinatorial data can be achieved by the mating $g_1 \perp\!\!\!\perp g_2$ where g_1 is the map corresponding to the angle pair $(21/80, 29/80)$ and g_2 is the map corresponding to the angle pair $(71/80, 73/80)$. In this mating, the cluster point is made up of the ray equivalence classes which is made up of principal root points of critical orbit components for both g_1 and g_2 - in other words it is formed in the same manner as those in Chapter 5. We conjecture that the rational maps $F = f_1 \perp\!\!\!\perp f_2$ and $G = g_1 \perp\!\!\!\perp g_2$ are not be Thurston equivalent. If this conjecture is correct, it would mean that the combinatorial data, as currently defined, would not be enough to classify (in the sense of Thurston) the rational maps with period two cluster cycles in degree 3 or higher. As mentioned in Chapter 5, it would be interesting to

find out what other data is required in order to get Thurston equivalence.

Appendix F

The Higher Period Case

F.1 An overview

In this appendix, we look at the case where the rational map has a cluster cycle of period three. Since this is outside the scope of this thesis, we do not try to prove anything too substantial here, and the general tone will be fairly informal. However, we will endeavour to compare this case with those of the period 1 and 2 cases, and state some questions/conjectures about what can be said in general about rational maps with clusters.

We start off by listing some data of very low periods so we can see if any patterns appear for this case. We also look at what sets of combinatorial data appear, and if any matings are shared.

The first difference we notice is that, even if we pass from period two to period three in the quadratic case, we need to introduce an extra piece of combinatorial data, which tells us the number of times we need to iterate forward from the cluster of the first critical point c_1 to the cluster containing the second critical point c_2. In the one cluster case this was not necessary, since there was only one cluster; in the period 2 cluster cycle case, the result of Proposition 5.1.3 again meant this extra piece of data was not necessary, although we did have to redefine critical displacement.

We give a new definition of the critical displacement below to take into account this new behaviour that is possible for higher periods.

Definition F.1.1. The critical displacement of a period k cluster cycle of a map F is defined as follows. Choose one of the critical points to be the first critical point c_1. Then there exists $j < k$ such that $z_j = F^{\circ j}(c_1)$ is in the same cluster as the second critical point c_2. Then count anticlockwise round the star of this cluster from z_j to

c_2; c_2 will be the $(2\ell+1)$-th endpoint anticlockwise round from z_j in the star. We then say the critical displacement $\delta = (j, 2\ell+1)$.

We define the combinatorial rotation number in the usual way. Below we list some data for the period three cluster cycle case. Afterwards, we will discuss the phenomena and state some questions and conjectures relating to them.

Let f be the map corresponding to the pair of angles $(10/63, 17/63)$. The internal address of this map is $1 \to 3 \to 6$; in other words, f is the tuning of the rabbit by the basilica and the associated parameter is $c \approx -0.11341\ldots+0.86056\ldots i$. There are three period 6 components beyond this component:

- g_1: $(11/63, 12/63)$ has internal address $1 \to 3 \to 5 \to 6$.
- g_2: $(13/63, 14/63)$ has internal address $1 \to 3 \to 4 \to 6$.
- g_3: $(15/63, 16/63)$ has internal address $1 \to 3 \to 4 \to 5 \to 6$.

Figure F.1 shows the position of these components relative to one another. We remark that this structure persists. That is, let $\mathcal{H}$ be a hyperbolic component with internal address $1 \to 3 \to 3k$. Then there are precisely three other components of period $3k$ in the wake of $\mathcal{H}$ (this is an upshot of Proposition 1.8.3).

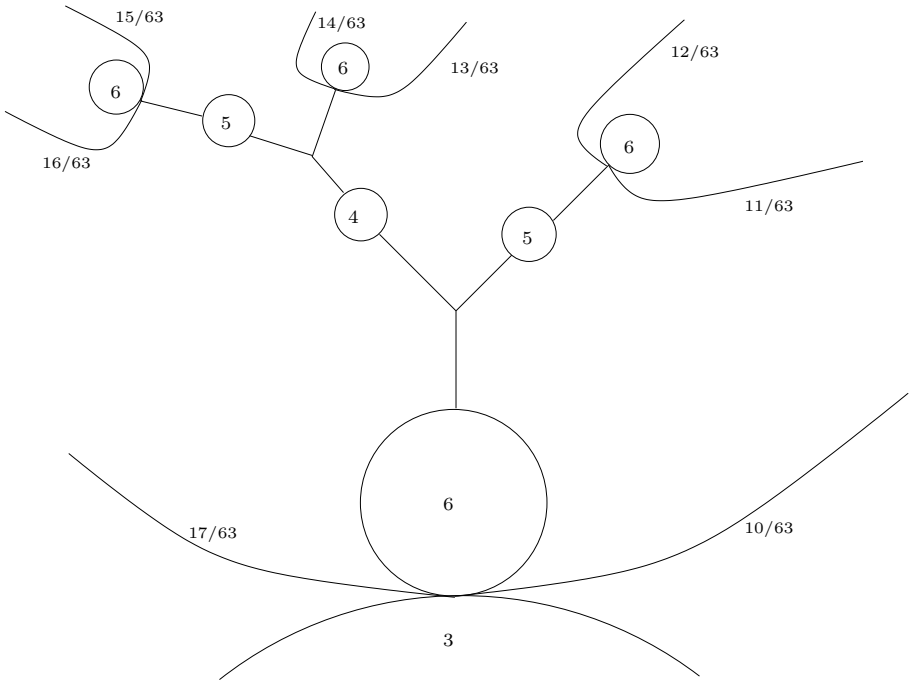

Figure F.1: The position of the period 6 maps in the 1/3-limb of $\mathcal{M}$.

As with the period two case, all combinatorial data can be realised by rational maps apart from the case where the critical points are in the same cluster. It is also possible to create rational maps with cluster cycles by mating with the secondary maps that lie beyond the component corresponding to the angles $(10/63, 17/63)$. We also display whether the map f_2 in the table creates a period three cluster cycle when mated with one of the maps g_i as labelled above.

Crit. disp.	**Angles for f_2**	**Int. add. of f_2**	g_1	g_2	g_3
(1,1)	(29,34)	$1 \to 2 \to 3 \to 5 \to 6$	×	×	×
(1,3)	(43,44)	$1 \to 5 \to 6$	×	✓	×
(2,1)	(57,58)	$1 \to 4 \to 6$	✓	×	×
(2,3)	(23,24)	$1 \to 2 \to 5 \to 6$	×	×	✓

We also include the period 9 examples which are the matings of the map with internal address $1 \to 3 \to 9$, corresponding to the angles $(74/511, 81/511)$. In this case we have

- g_1: $(75/511, 76/511)$ has internal address $1 \to 3 \to 8 \to 9$.
- g_2: $(77/511, 78/511)$ has internal address $1 \to 3 \to 7 \to 9$.
- g_3: $(79/511, 80/511)$ has internal address $1 \to 3 \to 7 \to 8 \to 9$.

The table is then given below.

Crit. disp.	**Angles for f_2**	**Int. add. of f_2**	g_1	g_2	g_3
(1,1)	(349,350)	$1 \to 5 \to 6 \to 9$	×	×	×
(1,3)	(237,274)	$1 \to 2 \to 3 \to 5 \to 6 \to 8 \to 9$	×	×	×
(1,5)	(363,364)	$1 \to 8 \to 9$	×	✓	×
(2,1)	(187,188)	$1 \to 2 \to 5 \to 6 \to 9$	×	×	×
(2,3)	(473,474)	$1 \to 4 \to 7 \to 9$	✓	×	×
(2,5)	(215,216)	$1 \to 2 \to 4 \to 5 \to 8 \to 9$	×	×	✓

Our first observation is to do with the internal addresses of the secondary maps. Using a similar argument to Proposition 1.8.6 we get the following.

Proposition F.1.2. *The internal addresses of the secondary components in the wake of the component with internal address $1 \to 3 \to 3n$ are*

- $1 \to 3 \to 3n-1 \to 3n$.
- $1 \to 3 \to 3n-2 \to 3n$.
- $1 \to 3 \to 3n-2 \to 3n-1 \to 3n$.

We remark that there is a similar pattern for the period 4 case and conjecturally this persists as the periods increase. Furthermore, we conjecture that, for any period, all these secondary components are narrow: that is, they correspond to angles $a/(2^{nk}-1)$ and $(a+1)/(2^{nk}-1)$ for some a.

Returning to the period three case, we see then that we have a certain amount of similarities with the period two case. Again, we see that it is possible that matings with the secondary components (the maps g_i above) can yield maps with period 3 cluster cycles under mating. However, in constrast to the period 2 cluster cycle case, it appears that there is a unique choice of partner map h_i for each of the g_i, such that the $g - i \perp\!\!\!\perp h_i$ has a period three cluster cycle. Again, we conjecture this is true in general, as the period $3n$ of the maps increases.

The question of Thurston equivalence is far more difficult, even in the degree two case. In the one cluster case we see that in retrospect our task was very simple: Alexander's Trick shows that all homeomorphisms of the disk are isotopic. In the period two cluster cycle we had to be more careful, but we were able to take advantage of the fact that the mapping class group of annulus was generated by a single Dehn twist and so, trivially, it is abelian. In higher periods $k > 2$, the complement to the stars of the cluster cycle in the sphere is conformally equivalent to the disk with $k-1$ disks removed. The mapping class group of such an object is far more complicated. Indeed, it is more than likely, in light of the problems found in the higher degree case when the period is two, we would conjecture that the combinatorial data of the clusters is not enough information to get Thurston equivalence in the higher period case, whatever the degrees of the rational maps in question.

Bibliography

[Ahl78] L. Ahlfors, *Complex Analysis*, 3rd ed., McGraw-Hill, 1978.

[BMM+06] Alexander Blokh, James M. Malaugh, John C. Mayer, Lex G. Oversteegen, and Daniel K. Parris, *Rotational subsets of the circle under z^d*, Topology and its Applications **153** (2006), no. 10, 1540–1570.

[Böt04] L. E. Böttcher, *The principal laws of convergence of iterates and their application to analysis*, Izv. Kazan. Fiz.-Mat. Obshch. **14** (1904), 155–234.

[BS94] Shaun Bullett and Pierrette Sentenac, *Ordered orbits of the shift, square roots, and the devil's staircase*, Math. Proc. Camb. Phil. Soc. **115** (1994), 451–481.

[BS01] H. Bruin and D. Schleicher, *Symbolic dynamics of quadratic polynomials*, Mittag-Leffler report. 2001/2 no. 7, 2001.

[Car13] C. Carathéodory, *Über die gegenseitige Beziehung der Ränder bei der Abbildung des Innern einer Jordanschen Kurve auf einen Kreis*, Math. Ann. **73** (1913), 305–320.

[Con78] J. B. Conway, *Functions of One Complex Variable I*, 2nd ed., Springer, 1978.

[Con95] ———, *Functions of One Complex Variable II*, 1st ed., Springer, 1995.

[DH84] A. Douady and J.H. Hubbard, *Etude dynamique des polynômes complexes (part one)*, Publications Math. d'Orsay 84-02, 1984.

[DH85] ———, *Etude dynamique des polynômes complexes (part two)*, Publications Math. d'Orsay 85-04, 1985.

[DH93] ———, *A proof of Thurston's topological characterization of rational functions*, Acta. Math. **171** (1993), 263–297.

[Dou83] A. Douady, *Systèmes dynamiques holomorphes*, Sem. Bourbaki **599** (1983), 39–63.

[Eps99] A. L. Epstein, *Infinitesimal Thurston rigidity and the Fatou-Shishikura inequality*, Can be found at arXiv:math/9902158v1, 1999.

[Fat19] P. Fatou, *Sur les équations fonctionelles*, Bull. Soc. Math. France **47** (1919), 161–271.

[Fat20] ———, *Sur les équations fonctionelles*, Bull. Soc. Math. France **48** (1920), 33–94 & 208–314.

[For81] Otto Forster, *Lectures on Riemann Surfaces*, Springer, 1981.

[HY61] John G. Hocking and Gail S. Young, *Topology*, Dover, 1961.

[Jul18] G. Julia, *Memoire sur l'itération des fonctions rationelles*, J. Math. Pure. Appl. **8** (1918), 47–245.

[Kam01] Atsushi Kameyama, *The Thurston equivalence for postcritically finite branched coverings*, Osaka J. Math **38** (2001), 565–610.

[Lev85] S. Levy, *Critically finite rational maps*, Ph.D. thesis, Princeton University, 1985.

[LS94] Eike Lau and Dierk Schleicher, *Internal addresses of the Mandelbrot set and irreducibilty of polynomials*, Stony Brook Preprint 19, 1994.

[Mil93] J. Milnor, *Geometry and dynamics of quadratic rational maps*, Experimental Math. **2** (1993), 37–83.

[Mil00a] ———, *On rational maps with two critical points*, Experimental Math. **9** (2000), 481–522.

[Mil00b] ———, *Periodic orbits, external rays and the Mandelbrot set: An expository account*, Astérisque **261** (2000), 277–333.

[Mil04] ———, *Pasting together Julia sets: A worked out example of mating*, Experimental Math. **13** (2004), 55–92.

[Mil06] ———, *Dynamics in One Complex Variable*, 3rd ed., Princeton University Press, 2006.

[Moo25] R. L. Moore, *Concerning upper semi-continuous collections of continua*, Trans. Amer. Math. Soc. **27** (1925), 416–428.

[Mun00] James R. Munkres, *Topology*, Prentice Hall, 2000.

[Pil96] Kevin M. Pilgrim, *Rational maps whose Fatou components are Jordan domains*, Ergodic Th. Dyn. Sys. **16** (1996), 1323–1343.

[Pil03] ———, *An algebraic formulation of Thurston's combinatorial equivalence*, Proc. Amer. Math. Soc. **131** (2003), 3527–3534.

[Pom92] Ch. Pommerenke, *Boundary Behaviour of Conformal Maps*, Springer, 1992.

[Ree92] M. Rees, *A partial description of parameter space of rational maps of degree two: Part I*, Acta Math. **168** (1992), 11–87.

[Sch94] Dierk Schleicher, *Internal addresses in the Mandelbrot set and irreducibility of polynomials*, Ph.D. thesis, Cornell University, 1994.

[Sch99] ———, *On fibers and local connectivity of Mandelbrot and multibrot sets*, arXiv:math/9902155v1, 1999.

[Sch08] ———, *Internal addresses of the Mandelbrot set and Galois groups of polynomials (version of 5/2/2008)*, arXiv:math/9411238v2, 2008.

[Sen81] E. Seneta, *Nonnegative Matrices and Markov Chains*, 3rd ed., Springer, 1981.

[Shi87] M. Shishikura, *On the quasiconformal surgery of rational functions*, Ann. Sci. Éc. Norm. Sup. 4ème Ser. **20** (1987), 1–29.

[ST00] M. Shishikura and Tan Lei, *A family of cubic rational maps and matings of cubic polynomials*, Experimental Math. **9** (2000), 29–53.

[Sut81] W. A. Sutherland, *Introduction to Metric and Topological Spaces*, OUP, 1981.

[Tan92] Tan Lei, *Matings of quadratic polynomials*, Ergodic Th. Dyn. Sys. **12** (1992), 589–620.

[Thu83] W. Thurston, *The combinatorics of iterated rational maps*, Preprint, Priceton University, 1983.

[Wit88] Ben Wittner, *On the bifurcation loci of rational maps of degree two*, Ph.D. thesis, Cornell University, 1988.

[You48] J. W. T. Youngs, *The extension of a homeomorphism defined on the boundary of a* 2*-manifold*, Bull. Amer. Math. Soc. **54** (1948), no. 8, 805–808.

[Zak00] S. Zakeri, *Biaccessibility in quadratic Julia sets*, Ergodic Th. Dyn. Sys. **20** (2000), 1859–1883.